JOHANNES KEPLER
UNIVERSITÄT LINZ | JKU

TNF

Technisch-Naturwissenschaftliche
Fakultät

Pair excitations and exchange effects in the dynamics of strongly correlated Fermi–fluids

DISSERTATION

zur Erlangung des akademischen Grades

Doktor

im Doktoratsstudium der

Technischen Wissenschaften

Eingereicht von:

DI Martin Panholzer

Angefertigt am:

Institut für Theoretische Physik

Beurteilung:

o. Univ. Prof. Dr. Eckhard Krotscheck (Betreuung)

Prof. Charles E. Campbell

Linz, August, 2010

Eidesstattliche Erklärung

Ich erkläre an Eides statt, dass ich die vorliegende Dissertation selbstständig und ohne fremde Hilfe verfasst, andere als die angegebenen Quellen und Hilfsmittel nicht benutzt bzw. die wörtlich oder sinngemäß entnommenen Stellen als solche kenntlich gemacht habe.

Martin Panholzer

Abstract

In this thesis a microscopic method for a quantitative determination of the dynamics of strongly correlated Fermion systems is developed. We build upon variational ground state calculations that were carried out in the optimized Jastrow-Feenberg variational method.

Excited states are then treated within the Correlated Basis Functions (CBF) method. A systematic method to improve the description of the dynamics of a correlated system is to derive a hierarchy of equations of motions for n-particle-n-hole excitations. This work contains two important advances of this procedure torwards an accurate *ab initio* method:

In the first part, the equations of motion for single particle-hole excitations (correlated time dependent Hartree-Fock (cTDHF) equations) are derived and solved, including exchange diagrams. Neglecting exchange diagrams, the theory leads to a random phase approximation (RPA) in terms of an effective particle-hole interaction V_{ph}. Going beyond this, we also include exchange diagrams ("xRPA"); these exchange diagrams can also be formulated in terms of an effective interaction V_{ex}, which is *different* from V_{ph}. Additionally, single particle excitation energies are treated consistently at the correlated Hatree-Fock level. Furthermore, an energy dependent interaction appears already at the single particle hole excitation level, which will be derived in the lowest non-vanishing order.

The second part is concerned with the inclusion of pair excitations in the dynamic wave function and, consequently, in the equations of motion. These effects are the key for lowering the collective mode and the roton minimum towards the experimentally observed values. In particular, the lowering of the roton in two dimensional ^{3}He is very pronounced. As a consequence the mode reemerges below the particle hole band as sharp excitation above a certain density. This effect has been seen here for the first time, it has meanwhile been confirmed experimentally.

Finally these two advancements are combined and applied to ^{3}He in three dimensions. The agreement with the experiment is excellent and further Fermi systems await exploration.

Zusammenfassung

In dieser Dissertation wird eine mikroskopische Methode zur quantitativen Bestimmung der Dynamik in stark korrelierten Fermi-Systemen entwickelt. Die Theorie baut auf einer Variations–Grundzustands Rechnung auf, die in der optimierten Jastrow-Feenberg Variationsmethode ausgeführt wird.

Angeregte Zustände werden demnach in der Correlated Basis Functions (CBF) Methode behandelt. Eine systematische Methode um die Beschreibung der Dynamik von korrelierten Systemen zu verbessern wird durch Ableiten einer Hierarchie von Bewegungsgleichungen für n–Teilchen–n–Loch Anregungen erreicht. Diese Arbeit enthält zwei wichtige Verbesserungen dieses Zugangs in Richtung einer präzisen *ab initio* Methode.

Im ersten Teil werden die Bewegungsgleichungen für ein–Teilchen–ein–Loch Anregungen (correlated time dependent Hartree-Fock (cTDHF) Gleichungen) abgeleitet und gelöst, insbesondere unter Berücksichtigung der nicht–lokalen Austauschdiagramme. Vernachlässigen der Austauschdiagramme führt auf die Random Phase Approximation (RPA) mit einer effektiven Teilchen-Loch Wechselwirkung V_{ph}. Darüber hinausgehend, werden nun auch Austauschdiagramme mitgenommen ("xRPA"); diese können in eine effektive Wechselwirkung V_{ex}, verschieden zu V_{ph}, zusammengefasst werden. Zusätzlich werden die ein–Teilchen Anregungsenergien konsistent auf dem korrelierten Hartree–Fock Niveau behandelt. Des Weiteren erhält man eine energieabhänginge Wechselwirkung bereits bei ein-Teilchen ein-Loch Anregungen, welche in der niedrigsten nicht verschwindenden Ordnung abgeleitet werden.

Im zweiten Teil werden Paaranregungen in der dynamischen Wellenfunktion und konsequenterweise in den Bewegungsgleichungen mitgenommen. Diese Effekte sind der Schlüssel zum Absenken der kollektiven Mode und des Roton-Minimums in Richtung der experimentell beobachteten Werte. Das Absenken des Rotons in zweidimensionalem ^{3}He ist stark ausgeprägt. Als Konsequenz taucht die Mode unter dem Teilchen-Loch Band als scharfe Anregung, ab einer bestimmten Dichte, auf. Dieser Effekt wurde hier zum ersten Mal beobachtet und mittlerweile experimentell bestätigt.

Zum Abschluss werden diese zwei Verbesserungen kombiniert und auf ^{3}He in drei Dimensionen angewandt. Die Übereinstimmung mit dem Experiment ist hervorragend, die Anwendung auf weitere Fermi-Systeme daher naheliegend.

Contents

Chapter 1

Introduction

Since ancient times a common paradigm has been, that once we know the fundamental laws of the tiniest building blocks we are able to understand every phenomenon in nature. This is in principle true. We know the fundamental laws that govern our every day life (quantum mechanics and electro-dynamics) since the mid of the last century. But we are far from understanding all the complex behavior of matter, constituted of many particles, from first principles.[5, 15] Solving the corresponding equations is neither possible nor desireable, because of the immense number of variables. Furthermore, in most cases we are not interested in what every particle does, rather we want to predict the new collective behavior of the system, e.g. which structure it forms or when phase transitions occur or the elementary excitations of the system. Here, contrary to many other approaches, the macroscopic behavior is directly calculated from the fundamental laws. More precisely, we try to find the connection between elementary quantum mechanics and the collective behavior of the many body system. The difficulty is to find the balance between simplifying the exact problem and keeping enough flexibility to give quantitative results.

In this thesis the dynamic behavior of the homogeneous ^{3}He liquid at zero temperature is calculated from nothing else than the bare interaction and quantum mechanics. Helium is the ideal test ground for such theories:

- At low temperatures it does not solidify, thus forming a quantum liquid.
- It exists in a boson and fermion version, ^{4}He and ^{3}He, respectively. Therefore one can study the influence of quantum statistics on the many body problem.
- It is one of the most strongly correlated system available in the lab.

As result our theory should be easily applicable to other, less strongly correlated, systems. Indeed we recently applied it successfully to the electron liquid [8].

A popular approach to calculate the dynamic behavior of Fermi-systems is the random phase approximation (RPA)

$$\chi(q,\omega) = \frac{\chi_0(q,\omega)}{1 - V_{\mathrm{p-h}}(q)\chi_0(q,\omega)}\,. \tag{1.1}$$

where χ_0 is the density response of the non interacting system [37] and $V_{\mathrm{p-h}}$ is a suitable effective interaction (more on that later). There are different ways to derive the RPA. Most closely related to our work is the derivation via time-dependent Hartree-Fock theory[28, 29, 40] (TDHF). In doing so, one recognizes that the direct or bare interaction enters the equation. This makes only sense for weakly interacting systems. If the interaction is stronger, as for constituents like helium, the Fourier-transform does not exist. In addition, even for existing (in q-space) but strong interactions this procedure gives results which are far from reality. The reason is that the effective interaction between two particles in the liquid is different from the bare interaction. But how to obtain this effective interaction? The first way is to use certain exact properties of the dynamic structure function, i.e. sumrules, and choose the interaction such that these are fullfiled. This has the advantage that it can be simply implemented, but the disadvantage that it is difficult to improve upon that. The second is to determine the effective interaction from a microscopic calculation[31]. (Microscopic means determined from nothing else than the bare interaction.) At the beginning this approach is related with more work in order to derive a formulation analogue to the RPA, but we are able to improve the result by successive abolition of critical approximations. We choose the second approach in this work.

1.1 Static or ground state properties

In this thesis the properties of a many fermion system at zero temperature are studied. Quantum mechanically this means we are concerned with the ground state and the low energy excitations of the many body problem. We start with a discusion of the ground state.

An important parameter is the number density $\rho = \frac{N}{V}$. Starting at low density the interaction can usually be neglected and the properties of the system are dominated by the Fermi statistics[1]. This means the energy per particle is

$$\frac{E}{N} = \frac{3}{5}E_F = \frac{3}{5}\frac{\hbar^2(3\pi^2\rho)^{2/3}}{2m} \tag{1.2}$$

[1]This is only true for short ranged interactions like hard–core potentials. For the electron gas, which is the basic example for long ranged interaction, the situation is reversed. For small density the interaction is more important than the kinetic energy from the Fermi statistics.

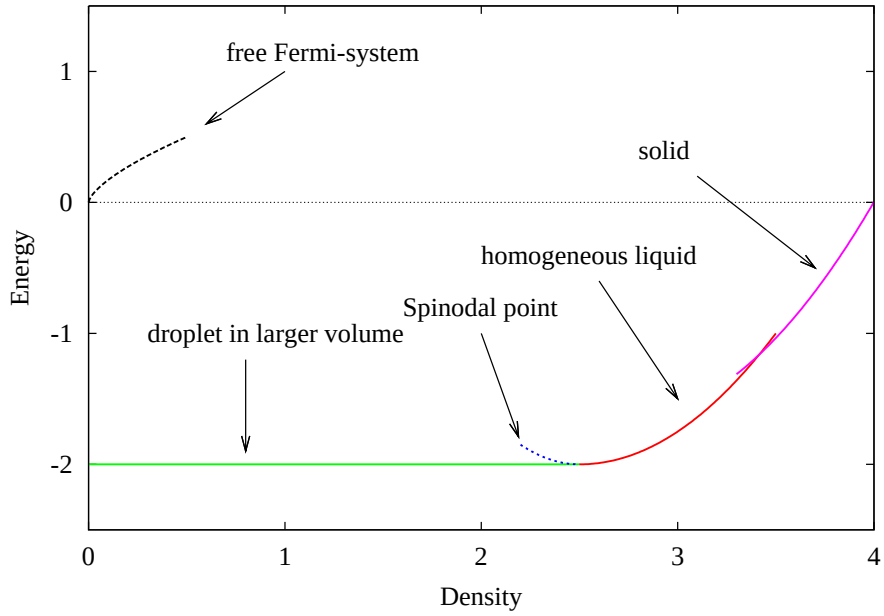

Figure 1.1: A sketch of $E(\rho)$ for a typical selfbonded system. For details see text.

in 3 dimensions. In this regime the system is not self bound since the slope of $E/N(\rho)$ is positive. This implies the system would expand if it is not confined.

The one particle density defined as

$$\rho(\mathbf{r}) = \langle \Psi_0 | \, \hat{\rho}(\mathbf{r}) \, | \Psi_0 \rangle = \rho \tag{1.3}$$

is constant in the whole volume. If one increases the density of the system, something astonishing will happen: suddenly the particles condense to a dense droplet occupying only a fraction of the volume, if the system is self bound.[2] This situation is visualized in figure 1.1. The system is only stable in the state with lowest energy. Thus the homogeneous Fermi gas is only metastable if a system is self bound. Also, there is no continuous transition from the Fermi gas to the strongly correlated Fermi fluid. This is the reason why perturbation theory has to fail in describing such systems.

Fermi-Hyper-Netted-Chain (FHNC) calculations [33] for the fluid state yield very good results for the static properties, which are input to the calculations in this thesis. Furthermore, the self–consistent calculations converge only down to a certain value of the density, i.e. where the compressibility becomes negative. This indicates the approach of a spinodal point. Also indicated in figure 1.1 is the phase transition to the solid. Close to this transition the particles become strongly correlated. The strength of the correlations become visible in the pair distribution function which is defined for the homogen system

[2]It depends on the interaction of the system whether it is self bounded or not. ^{3}He and ^{4}He are self bounded.

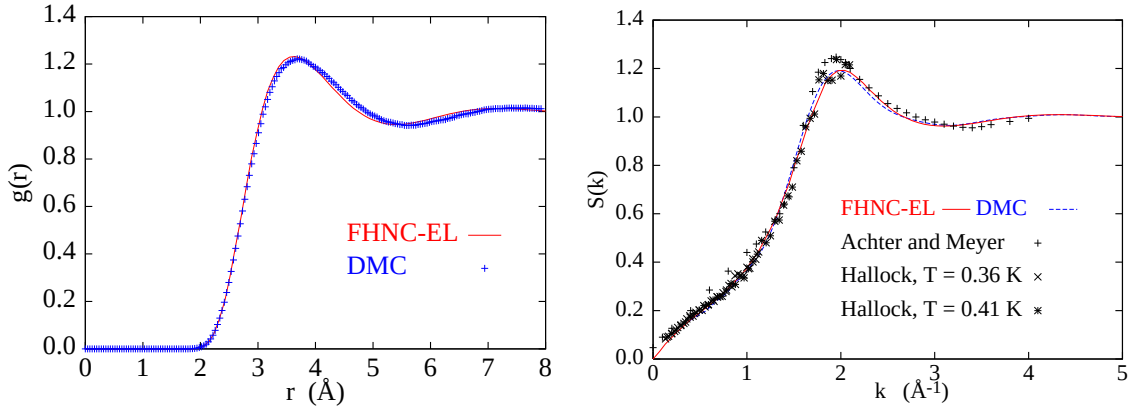

Figure 1.2: The pair distribution and the static structure function for three dimensional ^{3}He at saturation density compared with experiment by Achter and Meyer [1] and Hallock [24] and Diffustion Monte Carlo (DMC) calculations [11].

as

$$g(|\mathbf{r}_1 - \mathbf{r}_2|) = \frac{N(N-1)}{\rho^2} \int d^3r_3 \dots d^3r_N |\Psi(\mathbf{r}_1, \dots, \mathbf{r}_n)|^2 \tag{1.4}$$

where $\Psi(\mathbf{r}_1, \dots, \mathbf{r}_n)$ is the ground state wave function. The pair distribution function describes the probability of finding a particle in $\mathbf{r}_2$ if there is one in $\mathbf{r}_1$. A rough measure for the importance of correlations or the vicinity of the phase transition to the solid state is the height and the sharpness of the first peak, see right pane in figure 1.2. The position of the peak is the nearest neighbor distance. The position of the second peak is the next nearest neighbor distance. For a fluid this one is broader than the first peak. Another view on the same quantity is the static structure function, which is essentially the Fourier transform of the pair distribution function

$$S(q) = 1 + \rho \int d^3r \; e^{i\mathbf{q}\cdot\mathbf{r}}[g(r) - 1] \tag{1.5}$$

This quantity is also peaked at the wave vector corresponding to the periodicity of the particles, left pane in figure 1.2. In proper units, *i.e.* Fermi wave vector k_F, this peak is approximately at constant wave vector for different densities. The height of the peak is related to the closeness of a phase transition to the solid. One could generalize the statement: The position of the maximum is approximately the same for all systems close to a phase transition to the solid, if the solid state has the same lattice. For bulk ^{3}He the peak in the static structure is at $q_{max} \approx 2.5k_F$. For the electron liquid at low densities, which is very different to Helium, the peak is approximately at the same position. This is a very general statement, which has far reaching consequences for the dynamics as we will see in the next section.

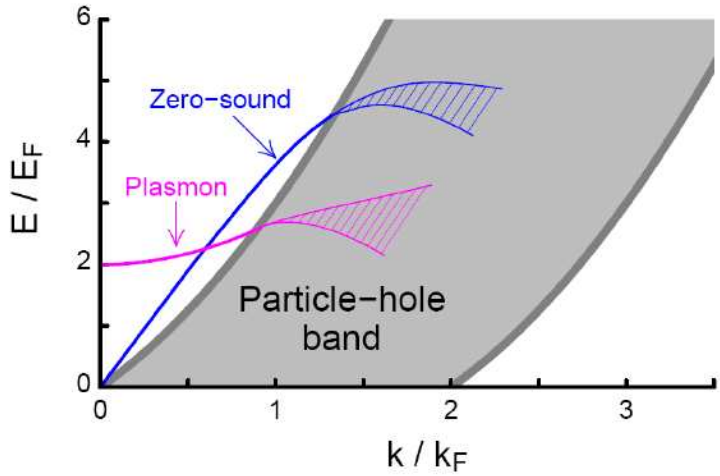

Figure 1.3: The PHB and the collective modes for the electron and Helium fluid are shown. In ^{3}He the collective mode is called zero-sound, because the dispersion starts linear like ordinary sound. For electrons in 3 dimensions the collective mode starts at a finite energy and is called plasmon.

1.2 Qualitative discussion of the dynamics

Our theory is designed to describe the dynamics of the many body system. Specifically we are interested in the excitations of the ground state. Therefore we need, as starting point, a precise theory of the ground state. The accuracy of our dynamic theory depends on the accuracy of the ground state. For the sake of discussion we first study a very simple system, the non interacting Fermi gas. The ground state is a Slater-determinant of plane waves, $|\Phi_0\rangle$. According to the Pauli exclusion principle the momentum distribution constitutes a sphere, the Fermi-sphere. The energy E of a particle with momentum $\hbar k$ is simply $E = \frac{\hbar^2 k^2}{2m}$, the kinetic energy. The elementary particle number conserving excitation is the creation of a particle-hole pair $|\Phi_{ph}\rangle = a_p^\dagger a_h |\Phi_0\rangle$, where p and h denote states outside and inside the Fermi sphere, respectively and $p = h + q$. The energy of this excitation is the kinetic energy difference $e_{ph} = \frac{\hbar^2}{2m}(p^2 - h^2)$. For such a simple system the dynamic structure function is obtained directly by insertion in the definition:

$$S(q,E) = \frac{1}{N}\sum_n |\langle\Psi_n|\rho_q|\Psi_0\rangle|^2 \delta(E - E_{n0}) = \frac{1}{N}\sum_{p,h} |\langle\Phi_{ph}|\rho_q|\Phi_0\rangle|^2 \delta(E - e_{ph}) \quad (1.6)$$

The accessible region in q, E space is a band confined to $\max(0, q^2 - 2q) \leq E \leq q^2 + 2q$, called the particle hole band (PHB).

As soon as we have interaction between the particles we have two additional excitations:

- The collective mode (zero sound, plasmon), which is a sharp excitation with certain momentum and energy. Like ordinary sound, it is a long lived excitation at small

momenta (i.e. outside the PHB). It becomes strongly damped (Landau damping) as it enters the PHB. See figure 1.3.

- Multi-particle excitations, which contribute a weak broad background to the dynamic structure factor.

Details on the dynamic structure function are found in the next chapters, here we want to concentrate on a significant feature, the roton minimum. A first approximation for the collective mode, if we neglect p-h excitations, is the Feynman spectrum $\varepsilon_q = \frac{\hbar^2 q^2}{2mS(q)}$[19]. Altough we know that it is about a factor two to high for the roton minimum in ^{4}He, the spectrum has the qualitatively correct behavior. We immediately see that the peak in $S(q)$ is responsible for the formation of the roton minimum. As we discussed in the previous section this peak is related to the closeness of a liquid to solid phase transition.[38] At the phase transition, which is before the roton minimum becomes zero, rotational and translational symmetry breaking occurs. Among other the excitation spectrum becomes direction dependent. Therefore the momentum of roton minimum, which depends on the direction in the lattice, is at twice the edge of the Brillouin zone. Thus the name "roton" is misleading and it has nothing to do with rotation. Instead it is a very general effect and is visible in many different systems.

1.2.1 Time Dependent Hartree–Fock (TDHF)

The basic method which underlies this work is TDHF. We briefly review the ideas and the derivation of the method. More details can be found in several books [40, 20].

Starting from an optimized HF ground state we generate particle number conserving particle–hole excitations: $|\Phi_{ph}\rangle = a_p^\dagger a_h |\Phi_0\rangle$. These excitations are weighted by a time dependent amplitude $c_{ph}(t)$. In principle we allow arbitrary many independent excitations, thus the trial wave function has the form:

$$|\Psi_0(t)\rangle = e^{\frac{1}{2}\sum_{ph} c_{ph}(t) a_p^\dagger a_h} |\Phi_0\rangle \tag{1.7}$$

The optimal amplitudes are determined by extremizing the action $\mathcal{S}$ if the system is under a small external perturbation $H_{ext}(t)$:

$$\mathcal{S}\left[c_{ph}, c_{ph}^*\right] = \int dt \ \langle\Psi_0(t)| \ H + H_{\text{ext}}(t) - \mathrm{i}\,\hbar\frac{\partial}{\partial t} \ |\Psi_0(t)\rangle = \int dt \ L \tag{1.8}$$

where the Hamiltonian in second quantized form

$$H = \sum_\alpha t_\alpha a_\alpha^\dagger a_\alpha + \frac{1}{2}\sum_{\alpha\beta\gamma\delta} \langle\alpha\beta| \, V \, |\delta\gamma\rangle \, a_\alpha^\dagger a_\beta^\dagger a_\gamma a_\delta. \tag{1.9}$$

enters. As result we obtain the linearized equations of motion

$$0 = i\hbar\dot{c}_{ph} + h^{ext}_{ph} + e_{ph}c_{ph} + \sum_{p'h'} \langle ph'| V |hp'\rangle_a c_{p'h'} + \sum_{p'h'} \langle pp'| V |hh'\rangle_a c^*_{p'h'} \quad (1.10)$$

where $e_{ph} = e_p - e_h$ is the Hartree-Fock single particle energy difference and e_α is the Hartree-Fock energy

$$e_\alpha = t_\alpha + \sum_h \langle \alpha h| V |h\alpha\rangle_a \quad (1.11)$$

and $\langle \alpha h| V |h\alpha\rangle_a = \langle \alpha h| V |h\alpha\rangle - \langle \alpha h| V |\alpha h\rangle$. It consists of the constant Hartree and the momentum dependent Fock energy.

The important point is that the bare interaction $V(r)$ enters the equations in the matrixelement

$$\begin{aligned} \langle ph'| V |hp'\rangle &= \frac{1}{V^2}\int d^3r d^3r' e^{ipr} e^{ih'r'} V(r-r') e^{-ihr} e^{-ip'r'} \quad (1.12)\\ &= \frac{1}{NV^2}\sum_k \int d^3r d^3r' e^{ih_1 r} e^{ih_2 r'} \tilde{V}(k) e^{ik(r-r')} e^{-ip_1 r} e^{-ip_2 r'} \\ &= \frac{1}{N}\delta_{p-h,p'-h'} \tilde{V}(p-h) \end{aligned}$$

where we introduced the dimensionless Fourier transform

$$f(r) = \frac{1}{N}\sum_k e^{ikr}\tilde{f}(k)\,. \quad (1.13)$$

The Fourier transform of a hard core potential, as it is the case for Helium, does not exist. Thus the method is inapplicable for such systems. A possible cure, as mentioned above, is the ad hoc introduction of effective interactions. The introduction is justified by arguing that the particles in the fluid experience a screened interaction instead of the bare interaction. By generalizing this approach to a correlated wave function we are able to derive this effective interaction in a rigorous way.

By neglecting exchange terms and the Fock energy the TDHF equation can be solved analytically. This is yet another way to derive the RPA.

1.3 Organization of the thesis

The thesis is divided in two parts. The first part describes, as a self-contained treatise, the scientific work done during my PhD studies. It also goes into details in issues which are not yet published. If a topic has already been published or submitted it only briefly discussed and referred to the related paper. In the second part are selected publications submitted or published during my PhD studies.

Outline of part I

In chapter 2 the ingredients for the development of a dynamic theory are presented. For that purpose the Fermi hyper-netted chain method (FHNC), which provides a good ground state, is first reviewed. The basis for the excited states are Jastrow correlated Hartree-Fock states. The tool to deal with matrix elements of these states is correlated basis functions theory (CBF). The trial wave function and the theory are formulated in the terms of CBF matrix elements.

In chapter 3 we restrict our selves to one-particle one-hole excitations. Contrary to the common treatment we do not neglect exchange effects. We obtain correlated TDHF equations with exchange. Transforming this equations to a weakly interacting form, eq. (1.10), provides us with an expression for the effective interaction in the direct and the exchange channel (xRPA). Of course these interactions are not the same. At the end we show that inclusion of exchange terms has a significant effect on the dynamics of ^{3}He.

In chapter 4 we take two-particle two-hole excitation into account, but neglect exchange effects temporarily. Only an outline of the derivation is given, since the details are found in [II].

In chapter 5 we combine the results of the previous two chapters. This will give an outstanding agreement of the microscopic many body theory compared with the experiment.

Publications in part II

(I) Henri Godfrin, Matthias Meschke, Hans-Jochen Lauter, Helga M. Böhm, Eckhard Krotscheck and Martin Panholzer. Roton-like collective mode observed in a Fermi liquid beyond the particle-hole continuum, submitted to nature

(II) H. M. Böhm, R. Holler, E. Krotscheck, and M. Panholzer. Dynamic Many-Body Theory. II. Dynamics of Strongly Correlated Fermi Fluids submitted to Phys. Rev. B

(III) M. Panholzer, H. M. Böhm, R. Holler, E. Krotscheck. Exchange Effects and the Dynamics of He-3 *Journal of Low Temperature Physics* , 158:135–140 ,2010

Part I

Thesis

Chapter 2

The basics: FHNC and CBF

In order to develop a dynamic theory for many body systems we need an accurate description of the ground state. For strongly interacting Fermi systems the best starting point is a Jastrow correlated Hartree-Fock ground state. The method to obtain the various ground state properties is the Fermi Hypernetted chain method (FHNC). The basic idea and the simplest approximations are given in the first part of this chapter. The second part is devoted to the problem of determining the matrix-elements of correlated excited Hartree-Fock states, the correlated basis functions (CBF). Altough this all is not new [14, 18, 13, 34], it is necessary to define the language to be used later.

2.1 The FHNC method

To improve upon the HF ground state, which greatly over estimates the energy, we introduce a Jastrow correlated wave function

$$|\psi\rangle = F\,|\Phi_0\rangle \tag{2.1}$$

where, in the case of an infinite homogen system, $|\Phi_0\rangle$ is a Slater-determinant of plane waves and F is the correlation operator. The simplest choice for F is the Jastrow-ansatz

$$F = \prod_{1\le i<j\le N} f(r_{ij}) = e^{\frac{1}{2}\sum_{i<j} u(r_{ij})}. \tag{2.2}$$

The calculation of one and two-body quantities is based on established methods of statistical mechanics [25]. One possible way is to derive all the necessary quantities from the generating functional

$$G_{00}(\beta) = \ln I_{00}(\beta) = \ln \langle\Phi_0|\, e^{\sum_{i<j} u(r_{ij};\beta)}\,|\Phi_0\rangle \tag{2.3}$$

with

$$u(r_{ij};\beta) = u(r_{ij}) + \beta\left[v(r_{ij}) - \frac{\hbar^2}{4m}\nabla^2 u(r_{ij})\right] \tag{2.4}$$

and

$$I_{00} = \int d^3r_1 \dots d^3r_N |\psi|^2 \tag{2.5}$$

the normalization integral. The β dependence is not always explicitly written, which means $\beta = 0$. It will later simplify some calculations.

To derive a cluster expansion we define the short ranged quantity

$$h(r_{ij}) = f^2(r_{ij}) - 1 \; . \tag{2.6}$$

Now we express the generating functional in terms of these correlation functions.

$$\begin{aligned} G_{00} &= \ln \langle \Phi_0 | \prod_{1 \le i < j \le N} [1 + h(r_{ij})] \, | \Phi_0 \rangle & (2.7) \\ &= \sum_{n=0}^{\infty} \frac{1}{n!} \left(\frac{d}{d\alpha} \right)^n \ln \langle \Phi_0 | \prod_{1 \le i < j \le N} [1 + \alpha h(r_{ij})] \, | \Phi_0 \rangle \Big|_{\alpha=0} \\ &= \sum_{n=0}^{\infty} (\Delta G)_n & (2.8) \end{aligned}$$

This is called the power series expansion and $(\Delta G)_n$ is represented by the sum of all diagrams contributing to the generating functional with exactly n correlation lines. The first term is

$$\begin{aligned} (\Delta G)_1 &= \sum_{i<j} \langle \Phi_0 | \, h(r_{ij}) \, | \Phi_0 \rangle = \frac{1}{2} \sum_{m,n<k_F} \langle mn | \, h(r_{12}) \, | mn \rangle_a \\ &= \frac{1}{2} \rho^2 \int d^3r_1 d^3r_2 h(r_{12}) \left[1 - \frac{1}{\nu} l^2(r_{12}k_F) \right] \\ &= \frac{1}{2} N \rho \int d^3r h(r) \left[1 - \frac{1}{\nu} l^2(rk_F) \right] & (2.9) \end{aligned}$$

where ν is the spin degeneracy. The new element that appears is the Slater or exchange function

$$l(r_{12}k_F) = \frac{1}{\rho} \sum_{m<k_F} \phi_m^*(\mathbf{r}_1) \phi_m(\mathbf{r}_2) \tag{2.10}$$

which has the convolution property

$$\frac{\rho}{\nu} \int d^3r l(|\mathbf{r}_1 - \mathbf{r}|k_F) l(|\mathbf{r} - \mathbf{r}_2|k_F) = l(r_{12}k_F) \; . \tag{2.11}$$

It can be simply proven in q-space or by using $\int d^3r \phi_{k_m,\sigma_m}(r) \phi_{k_n,\sigma_n}(r) = \delta_{m,n} \delta_{\sigma_m,\sigma_n}$, where we explicitly wrote the spin quantum number.

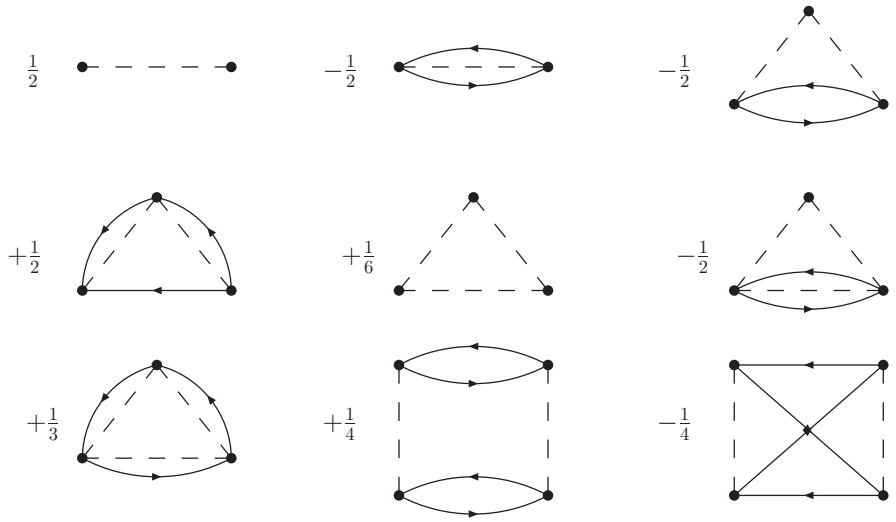

Figure 2.1: Some diagrams of G_{00} are shown. The first two diagrams constitute $(\Delta G)_1$. The third and the forth and the last two diagrams constitute $(\Delta G)_2$ after the cancellation of reducible diagrams.

The next order of the generating functional is

$$(\Delta G)_2 = \frac{1}{2!} \langle \Phi_0 | \, 2 \sum_{i<j<k} h(r_{ij}) h(r_{jk}) + 2 \sum_{i<j,k<l} h(r_{ij}) h(r_{kl}) \, | \Phi_0 \rangle - \left(\sum_{i<j} \langle \Phi_0 | \, h(r_{ij}) \, | \Phi_0 \rangle \right)^2 . \tag{2.12}$$

The interesting observation is that the term in the second line cancels the unconnected part of the first line. Therefore the generating functional is a connected quantity and also has the correct behavior in the thermodynamic limit. At this point it is convenient to introduce a diagrammatic language. The basic elements are closed points, which denote coordinates which are integrated. Every closed point carries a factor ρ. The correlation function $h(r_{ij})$ is represented by a dashed line and the exchange function $l(r_{ij}k_F)$ by an oriented solid line. In figure 2.1 some diagrams contributing to G_{00} are shown. By further analysis it is possible to derive rules, which allow the determination of higher order diagrams. Here we provide only the final rules, instead of the derivation of that rules, which is rather lengthy [30]. For that purpose, we define some topological statements:

- A diagram is *connected* if there is at least one path (consisting of correlation and/or exchange lines) between any two points.

- A diagram is *biconnected* if there are at least two non overlapping path between any two points.

- A diagram is called *irreducible* if it does not factorize in two or more simpler diagrams.

With that we state the following rules for the diagrammatic expansion of G_{00}

1. All diagrams contributing to G_{00} are irreducible.
2. Every n point diagram carries a factor $\frac{1}{n!}$
3. Every point is attached to at least one correlation line, every pair of points is connected by at most one correlation line
4. Exchange lines appear in closed, non-intersecting loops. Each loop consiting of n points contributes a factor $\left(\frac{-1}{\nu}\right)^{n-1}$.

In figure 2.1 some of the lowest order diagrams are shown. The $\left(\frac{1}{\nu}\right)^{n-1}$ factor is usually omitted. The remaining factor in front of each diagram is a combination of a topological factor and a cancellations effect described in the literature[32].

In the next section we also need open points which denote external variables, no density factor is assigned.

2.1.1 The pair distribution function derived from the generating functional

Once we have a diagrammatic expansion of G_{00} it is easy to derive a diagrammatic expansion of the pair distribution function which is defined by

$$g(r) = \frac{N(N-1)}{\rho^2 I_{00}} \int d^3r_3 \dots d^3r_N \psi^*(1,\dots,N)\psi(1,\dots,N) \; . \tag{2.13}$$

It is straight forward to show that

$$g(r_{12}) = \frac{2}{\rho^2}\frac{\delta G_{00}}{\delta u(r_{12})} = \frac{2}{\rho^2}\frac{\delta G_{00}}{\delta h(r_{12})} f^2(r_{12}) \; . \tag{2.14}$$

Diagrammatically the functional derivative of G_{00} with respect to $h(r_{12})$ corresponds to removing one correlation line and opening the points which are connected to this line and give them the labels r_1 and r_2. In figure 2.2 the first few diagrams are shown. The diagrams contributing to the pair distribution function are classified due to the appearance of exchange at the external points:

$$g(r) = 1 + \Gamma_{dd}(r) + 2\Gamma_{de}(r) + \Gamma_{ee}(r) \tag{2.15}$$

where $\Gamma_{dd}(r)$ denotes the set of diagrams with no exchange on the external points, respectively $\Gamma_{ee}(r)$ all diagrams with exchange on both external points and $\Gamma_{de}(r)$ exchange on

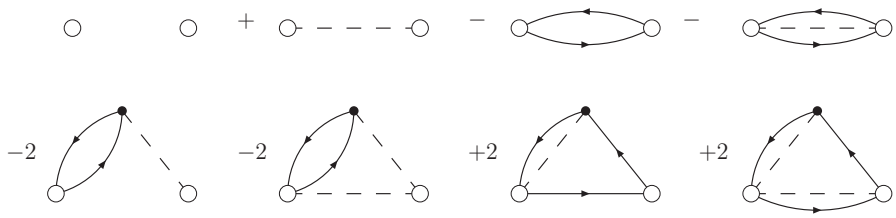

Figure 2.2: Some diagrams of $g(r)$ are shown. These diagrams are derived from the first four diagrams in figure 2.1.

one of the external points. These diagrams are split into nodal[1] and non-nodal diagrams, for example

$$\Gamma_{dd}(r) = N_{dd}(r) + X_{dd}(r) \tag{2.16}$$

Further we split the non-nodal diagrams in composite and elementary diagrams. Composite diagrams can be factorized into two or more independent functions of r_{12}. All diagrams that are non-nodal and not composite are elementary diagrams, denoted for example $E_{dd}(r_{12})$. One kind of exchange structure we have not treated yet are the cyclic chain diagrams (e.g. $X_{cc}(r_{12})$). These appear only as subdiagrams in the cluster expansion of the pair distribution function. With this last piece, we have all subdiagrams necessary to formulate the fermion version of the HNC equations. These are basically chaining and paralleling operations, which are simple multiplications in q- and r-space respectively. This has to be done taking into consideration the statistical restrictions. The FHNC method consists of eight equation which have to be iterated until convergence is reached. (These equations are provided in appendix A for reference.) Thus we have formulated a method to determine the pair distribution function or the static structure function directly from a suitably chosen $u(r)$.

2.1.2 Energy calculation

The energy is

$$E = \frac{1}{I_{00}} \langle\psi| H |\psi\rangle \ . \tag{2.17}$$

The potential energy is simply given by

$$\frac{E_{pot}}{N} = \frac{\rho}{2} \int d^3r g(r) v(r) \ . \tag{2.18}$$

It is convenient to use the Jackson-Feenberg identity

$$F\nabla^2 F = \frac{1}{2}(\nabla^2 F^2 + F^2\nabla^2) + \frac{1}{2}F^2 \left[\nabla, [\nabla, \ln F]\right] - \frac{1}{4}\left[\nabla, \left[\nabla, F^2\right]\right] \tag{2.19}$$

[1] A diagram is called nodal if all paths between the external points must pass through at least one internal point. According to the above definition we can also say, a diagram is nodal if it is not biconnected with respect to the external points.

where the square brackets denote the commutator. With that the kinetic energy is written

$$-\frac{1}{I_{00}}\frac{\hbar^2}{2m}\langle\psi|\sum_i\nabla_i^2|\psi\rangle = T_F - \frac{N\hbar^2\rho}{8m}\int d^3r g(r)\nabla^2 u(r) + T_{JF} \tag{2.20}$$

where T_F is the kinetic energy of the non interacting system and T_{JF} denotes the expectation value of the last term of eq. (2.19). By partial integration we can write it as

$$\begin{aligned} T_{JF} =& \frac{\hbar^2}{8mI_{00}}\sum_i\langle\Phi_0|\left[\nabla_i^2F^2\right]|\Phi_0\rangle \\ =& \frac{\hbar^2}{8mI_{00}}\sum_i\int d^3r_1\ldots d^3r_N F^2\nabla_i^2|\Phi_0(1,\ldots,N)|^2\ . \end{aligned} \tag{2.21}$$

Diagrammatically this quantity is obtained from the cluster expansion of G_{00} by taking one point of a diagram which is involved in exchange. Then let the Laplacian act only on the two exchange lines at this point. The simplest expression obtained this way is

$$-\frac{\hbar^2\rho^2}{8m\nu}\int d^3r_1d^3r_2\Gamma_{dd}(r_{12})\nabla_1^2\left(l(r_{12}k_F)l(r_{21}k_F)\right)\ . \tag{2.22}$$

Thus the energy per particle can be written as

$$\frac{E}{N} = \frac{T_F}{N} + \frac{\rho}{2}\int d^3r g(r)v_{JF}(r) + \frac{T_{JF}}{N}\ . \tag{2.23}$$

2.1.3 Determination of the optimal correlation function

Once we are able to calculate the energy for a certain correlation function, the optimal correlation function is determined by minimizing the energy:

$$\frac{\delta}{\delta u(r)}\frac{\langle\psi|H|\psi\rangle}{I_{00}} = 0\ . \tag{2.24}$$

This was first done with parameterized correlation functions [41, 30]. But it was soon realized that a functional optimization is advantageous. The Euler equation is derived by functional variation of the energy

$$\frac{\hbar^2}{4m}\nabla^2 g(r) = g'(r) \tag{2.25}$$

with

$$g'(r) = \int d^3r' v_{JF}(r')\frac{\delta g(r')}{\delta u(r)} + \frac{2}{N\rho}\frac{\delta T_{JF}}{\delta u(r)} \tag{2.26}$$

This quantity is approximately calculated by another set of equations, the FHNC' equations. The determination of the pair distribution function via the Euler equation is denoted as FHNC-EL. The results of an elaborate version of the theory [33] are in very good agreement with the experiment.

2.2 Correlated basis functions (CBF)

The basic ingredient is the correlated excited state:

$$|\mathbf{m}\rangle = \frac{F\ |\Phi_{\mathbf{m}}\rangle}{\langle\Phi_{\mathbf{m}}|\, F^\dagger F\, |\Phi_{\mathbf{m}}\rangle^{1/2}}\,. \tag{2.27}$$

where we restrict to excited states with the same particle number $|\Phi_{\mathbf{m}}\rangle = a^\dagger_{p_i} a^\dagger_{p_j} \ldots a_{h_j} a_{h_i}\,|\Phi\rangle$ and F is determined previously by e.g. a FHNC calculation. We again use the notion that p and h labels denote particle and hole states, respectively. There are mainly two reasons why we need CBF. First, in order to describe excited states and their dynamics we need such states as starting point. Second, even the Feenberg ansatz for the ground state is, due to the "nodal surface" problem, not exact. To improve it, one uses CBF. It is possible to introduce creation and destruction operators for correlated excited states which are normalized

$$\left|\alpha^\dagger_k\,\Psi_{\mathbf{m}}\right\rangle \equiv F_{N+1} a^\dagger_k\,|\Phi_{\mathbf{m}}\rangle \Big/ \langle\Phi_{\mathbf{m}}|\, a_k F^\dagger_{N+1} F_{N+1} a^\dagger_k\,|\Phi_{\mathbf{m}}\rangle^{1/2} \tag{2.28}$$

$$\left|\alpha_k\,\Psi_{\mathbf{m}}\right\rangle \equiv F_{N-1} a_k\,|\Phi_{\mathbf{m}}\rangle \Big/ \langle\Phi_{\mathbf{m}}|\, a^\dagger_k F^\dagger_{N-1} F_{N-1} a_k\,|\Phi_{\mathbf{m}}\rangle^{1/2}\,. \tag{2.29}$$

These correlated operators obey the same commutation relations as the uncorrelated one (But they are not Hermitian conjugates).

Now we come to the core of CBF, the determination of matrix elements. We have naturally diagonal and off-diagonal elements:

2.2.1 Diagonal matrix elements

$$\begin{aligned} I_{\mathbf{m},\mathbf{m}} &\equiv \langle\Phi_{\mathbf{m}}|F^\dagger F|\Phi_{\mathbf{m}}\rangle\,, \\ H_{\mathbf{m},\mathbf{m}} - H_{\mathbf{o},\mathbf{o}} &= \langle\mathbf{m}|H - H_{\mathbf{o},\mathbf{o}}|\mathbf{m}\rangle \equiv \langle\mathbf{m}|H'|\mathbf{m}\rangle \end{aligned} \tag{2.30}$$

The ratios of normalization integrals can be written, for $|\Phi_{\mathbf{m}}\rangle = a^\dagger_{p_1}\ldots a^\dagger_{p_d} a_{h_d}\ldots a_{h_1}\,|\Phi_0\rangle$

$$z_{p_1\ldots p_d h_1\ldots h_d} \equiv z_{\mathbf{m}} = \sqrt{\frac{I_{\mathbf{m},\mathbf{m}}}{I_{\mathbf{o},\mathbf{o}}}}\,.$$

These normalization integrals are related to the generating functional

$$z_{\mathbf{m}} = e^{\frac{1}{2}(G_{\mathbf{mm}} - G_{00})} \tag{2.31}$$

The only difference of $G_{\mathbf{mm}}$ to the one defined in (2.3) is, that the exchange line is defined as

$$l_m(r) = \frac{1}{N}\sum_{i\in\mathbf{m}} e^{\mathrm{i}\mathbf{k}_i\mathbf{r}}\,. \tag{2.32}$$

The convolution property is also valid for this new exchange line.

For $d \ll N$ the difference between $G_{\mathbf{mm}}$ and G_{00} is of order $1/N$. This is the legitimation to write

$$G_{\mathbf{mm}} - G_{00} = \int d^3r \frac{\delta G_{00}}{\delta l(rk_F)} \left[l_m(r) - l(rk_F) \right] . \tag{2.33}$$

If we assume a definite $m = ph$ we can further write

$$G_{\mathbf{mm}} - G_{00} = \frac{1}{N} \int d^3r \frac{\delta G_{00}}{\delta l(rk_F)} \left[e^{\mathbf{ipr}} - e^{\mathbf{ihr}} \right] \equiv \delta G(p) - \delta G(h) \tag{2.34}$$

An investigation of the diagrams generated by this procedure gives the connection to the FHNC quantity X_{cc}

$$\delta G(k) = -\ln \left[1 - \tilde{X}_{cc}(k) \right] \tag{2.35}$$

From this analysis we see that the normalization integrals factorize, for large particle numbers and $d \ll N$ as

$$z_{p_1 \ldots p_d h_1, \ldots h_d} = \frac{z_{p_1} \ldots z_{p_d}}{z_{h_1} \ldots z_{h_d}} + \mathcal{O}(N^{-1}) .$$

with

$$z_k = \frac{1}{\sqrt{1 - \tilde{X}_{cc}(k)}} \tag{2.36}$$

A similar procedure is also applied to the matrix element of the Hamiltonian and as a result the energy becomes additive

$$\langle p_1, \ldots p_d h_1 \ldots h_d | \, H' \, | p_1, \ldots p_d h_1 \ldots h_d \rangle = \sum_{i=1}^{d} e_{p_i h_i} + \mathcal{O}(N^{-1}) , \tag{2.37}$$

where $e_{ph} = e_p - e_h$. These quantities are also related to FHNC quantities

$$e_k = \frac{1}{N} \int d^3r \frac{\delta H_{00}}{\delta l(rk_F)} e^{\mathbf{ikr}} = \frac{\hbar^2 k^2}{2m} + \frac{\tilde{X}'_{cc}(k)}{1 - \tilde{X}_{cc}(k)} + u_0 \tag{2.38}$$

2.2.2 Off-diagonal quantities

We define the off–diagonal quantities

$$\begin{aligned} M_{\mathbf{m,n}} &= \langle \mathbf{m} | \mathbf{n} \rangle \equiv \delta_{\mathbf{m,n}} + N_{\mathbf{m,n}} , \\ H'_{\mathbf{m,n}} &= \langle \mathbf{m} | H' | \mathbf{n} \rangle (1 - \delta_{\mathbf{m,n}}) , \\ W_{\mathbf{m,n}} &= H'_{\mathbf{m,n}} - \frac{1}{2} \left(H_{\mathbf{m,m}} + H_{\mathbf{n,n}} - 2H_{\mathbf{o,o}} \right) N_{\mathbf{m,n}} . \end{aligned} \tag{2.39}$$

We start with the investigation of the overlap matrix element $N_{\mathbf{m,n}}$. It is evident that for $d \ll N$ this quantity depends only on the orbitals in which the states $\mathbf{m}$ and $\mathbf{n}$ differ and an error of $\mathcal{O}(1/N)$. This means

$$\langle \Phi_m | \, F^\dagger F \, | \Phi_n \rangle = \langle m_1 \ldots m_d | \, \mathcal{N}(1, \ldots, d) \, | n_1 \ldots n_d \rangle_a + \mathcal{O}(1/N) \tag{2.40}$$

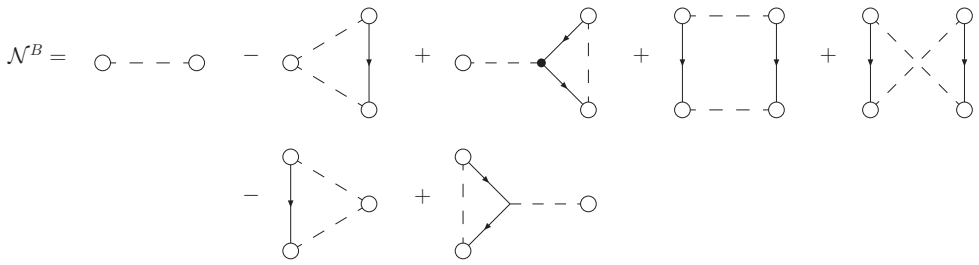

Figure 2.3: The basic diagrams of $\mathcal{N}^B(1,2)$ up to second order are shown. The dashed line represents the renormalized correlation line or sometimes called super-bond Γ_{dd}

To be more definite we restrict ourselves to $d = 2$. For example assume $m = ph$ and $n = p'h'$, then the above matrix element defines a two–body operator $\mathcal{N}$

$$\langle \mathbf{ph} | \, | \mathbf{p'h'} \rangle = \langle ph' | \, \mathcal{N}(1,2) \, | hp' \rangle_a \tag{2.41}$$

All the complexity has been moved to the operator $\mathcal{N}$, which is of course not necessary local. Usually the operator is split in four parts due to the appearance of the non locality

$$\mathcal{N}(1,2) = \mathcal{N}_{dd}(1,2) + \mathcal{N}_{dc}(1,2) + \mathcal{N}_{cd}(1,2) + \mathcal{N}_{cc}(1,2) \tag{2.42}$$

with

$$\begin{aligned} \mathcal{N}_{dd}(1,2) &= \mathcal{N}_{dd}(r_{12})\delta(r_1 - r_1')\delta(r_2 - r_2') \\ \mathcal{N}_{dc}(1,2) &= \mathcal{N}_{d,cc}(r_1, r_2; r_1', r_2')\delta(r_1 - r_1') = \mathcal{N}_{cd}(2,1) \\ \mathcal{N}_{cc}(1,2) &= \mathcal{N}_{cc,cc}(r_1, r_2; r_1', r_2') \end{aligned} \tag{2.43}$$

On a closer inspection one observes that these quantities factorize

$$\langle ij | \, \mathcal{N}(1,2) \, | kl \rangle_a = z_i z_j z_k z_l \, \langle ij | \, \mathcal{N}^B(1,2) \, | kl \rangle_a \tag{2.44}$$

Figure (2.3) shows some diagrams contributing to $\mathcal{N}^B(1,2)$. The simplest approximation is

$$\mathcal{N}^B(1,2) \approx \mathcal{N}^B_{dd}(1,2) = \Gamma_{dd}(r_{12}) \tag{2.45}$$

which is consistent with the simplified FHNC equations (A.17).

The $W_{\mathbf{m},\mathbf{n}}$ term can be calculated from the $N_{\mathbf{m},\mathbf{n}}$ terms by the β derivative method

$$W_{\mathbf{m},\mathbf{n}} = \frac{\partial}{\partial \beta} N_{\mathbf{m},\mathbf{n}}(\beta) \Big|_{\beta=0} . \tag{2.46}$$

Therefore a similar classification as above is possible. The local part, which is a good starting point for the numerical implementation

$$W^B_{dd}(r_{12}) = \Gamma'_{dd}(r_{12}) + \frac{\hbar^2}{4m} \nabla^2 \Gamma_{dd}(r_{12}) \tag{2.47}$$

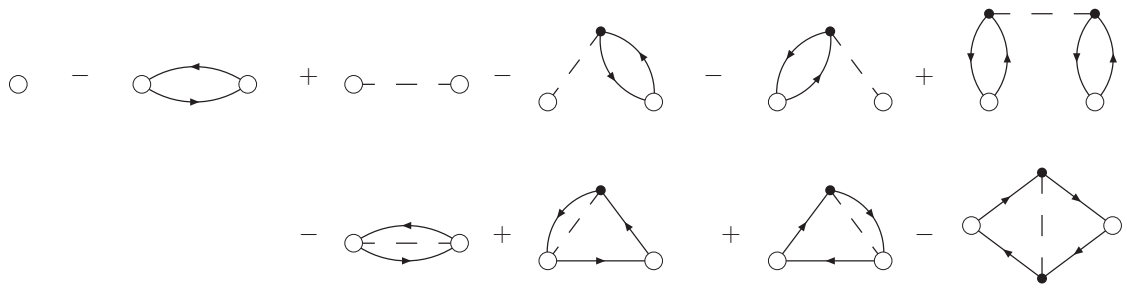

Figure 2.4: The first line shows the direct terms of the last line in eq. (2.48), the second the exchange terms.

2.2.3 Link to the static structure function

It is possible to calculate the static structure function directly from CBF matrix elements. Since the density operator is local we write

$$\begin{aligned}
S(q) =& \langle\psi|\,\rho_{-q}\rho_q\,|\psi\rangle = \sum_{\alpha\alpha'} \langle\Phi_0|\,FFa^\dagger_{\alpha-q}a_\alpha a^\dagger_{\alpha'+q}a_{\alpha'}\,|\Phi_0\rangle \\
=& \sum_{\alpha\alpha'}\left[\delta_{\alpha,\alpha'} + \sqrt{\frac{I_{\alpha-q\,\alpha'+q\,\alpha\,\alpha'}}{I_{00}}}N_{0,\alpha-q\,\alpha'+q\,\alpha\,\alpha'}n(\alpha)\bar{n}(\alpha-q)\right] n(\alpha')\bar{n}(\alpha'+q) \\
=& S_F(q) + \sum_{hh'}\sqrt{\frac{I_{h-q\,h'+q\,h\,h'}}{I_{00}}}\bar{n}(h-q)\bar{n}(h'+q)\,\langle hh'|\,\mathcal{N}(1,2)\,|h-q\,h'+q\rangle_a \\
\approx& S_F(q) + \sum_{hh'}\bar{n}(h-q)\bar{n}(h'+q)\,\langle hh'|\,\tilde{\Gamma}_{\rm dd}(q)\,|h-q\,h'+q\rangle_a
\end{aligned} \tag{2.48}$$

In the last line we kept only terms which are first order in $\tilde{\Gamma}_{\rm dd}$. The diagrams representing the last line are drawn in figure 2.4 and indeed these are the first terms in an cluster expansion of $S(q)$. We also see what we neglect if we approximate $\mathcal{N}(1,2) \approx \tilde{\Gamma}_{\rm dd}(q)$. Interestingly if we omit exchange too (second line in figure 2.4), we obtain the simplified FHNC expression for the static structure function (A.17). This means that the use of simplified FHNC equations is consistent with neglecting exchange in the CBF matrix elements. For our work this means that, if we take exchange into account, we have to use results of the full FHNC equations.

2.2.4 The power $\tilde{\Gamma}_{\rm dd}$ expansion

We have shown in this chapter how the CBF matrix elements can be calculated exactly. In applications we are normally forced to make approximations. Some care is needed in order to properly approximate a matrix element. It is important to incorporate all diagrams of a certain order in $\tilde{\Gamma}_{\rm dd}$. Otherwise it is possible to miss some cancellations of diagrams, which lead to wrong results. A nice example of such cancellations can be observed by reviewing

the derivation of the static structure function in 2.2.3. Since the density operator is local it is legitimate to commute it with the Jastrow correlations. Thus we obtain

$$\begin{aligned} S(q) =& \sum_{hh'} \left[\delta_{h,h'} \frac{I_{h+q\,h}}{I_{00}} + \sqrt{\frac{I_{h+q\,h} I_{h'+q\,h'}}{I_{00}^2}} \bar{n}(h'+q) \left\langle h+qh' \right| \mathcal{N}(1,2) \left| hh'+q \right\rangle_a \right] \bar{n}(h+q) \\ \approx& \sum_h \bar{n}(h+q) \frac{I_{h+q\,h}}{I_{00}} + \sum_{hh'} \bar{n}(h+q) \bar{n}(h'+q) \left\langle h+qh' \right| \tilde{\Gamma}_{\mathrm{dd}}(q) \left| hh'+q \right\rangle_a \end{aligned} \tag{2.49}$$

In order to be consistent we have to expand the normalization $\frac{I_{h+q\,h}}{I_{00}}$ up to first order in $\tilde{\Gamma}_{\mathrm{dd}}$.

$$\begin{aligned} \frac{I_{h+q\,h}}{I_{00}} =& \frac{z_{h+q}^2}{z_h^2} = \frac{1 - X_{cc}(h)}{1 - X_{cc}(h+q)} \approx \frac{1 + \frac{1}{\nu} \sum_{h'} \tilde{\Gamma}_{\mathrm{dd}}(h-h')}{1 + \frac{1}{\nu} \sum_{h'} \tilde{\Gamma}_{\mathrm{dd}}(h+q-h')} \\ =& 1 + \frac{1}{\nu} \sum_{h'} \tilde{\Gamma}_{\mathrm{dd}}(h-h') - \frac{1}{\nu} \sum_{h'} \tilde{\Gamma}_{\mathrm{dd}}(h+q-h') + \mathcal{O}(\tilde{\Gamma}_{\mathrm{dd}}^2) \end{aligned} \tag{2.50}$$

The second term in the last line cancels with a part of the exchange term in eq. (2.49) and thus gives the same $S(q)$ as in (2.48).

Successive inclusion of higher orders in $\tilde{\Gamma}_{\mathrm{dd}}$ will generally improve the results.

2.2.5 Generalization to $d > 2$

In the literature cluster expansions are only given for $d = 2$, with the additional information that the generalization to higher d is straight forward. This is true, but for a better understanding of the following chapters it is advantageous to write down the matrix-elements we need later. Indeed the generalization of the factorization given in eq. (2.44) is straight forward

$$\left\langle ijk \right| \mathcal{N}(1,2,3) \left| lmn \right\rangle_a = z_i z_j z_k z_l z_m z_n \left\langle ijk \right| \mathcal{N}^B(1,2,3) \left| lmn \right\rangle_a \tag{2.51}$$

Further the classification of diagrams according the exchange structure of the external points is obvious

$$\mathcal{N}(1,2,3) = \mathcal{N}_{ddd}(1,2,3) + 3\mathcal{N}_{cc,dd}(1,2,3) + 3\mathcal{N}_{cc,cc,d}(1,2,3) + \mathcal{N}_{cc,cc,cc}(1,2,3) \tag{2.52}$$

with the constraint that every external point is at least touched by one correlation line. Figure 2.5 shows some of the lowest order diagrams of the overlap matrix element for $d = 3$.

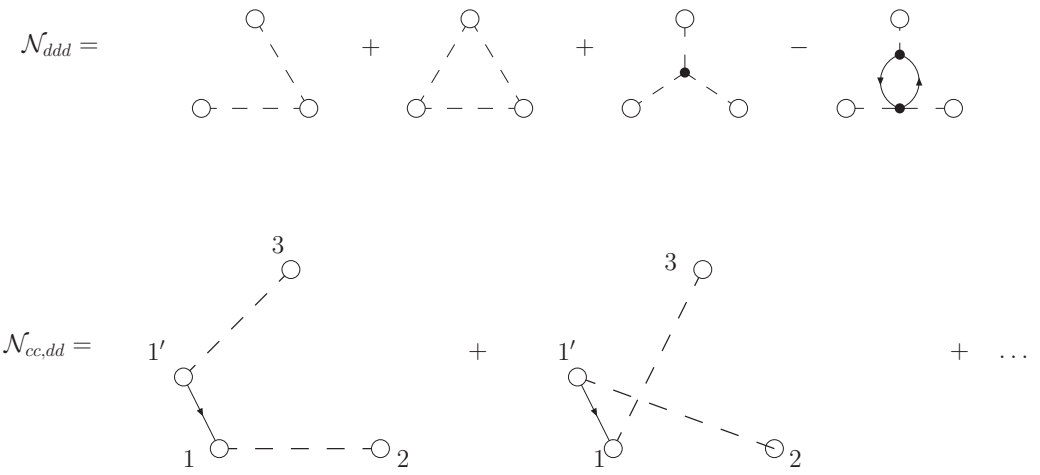

Figure 2.5: The first line shows the first few diagrams of the direct part of $\mathcal{N}^{(3)}$. The second line shows the lowest order of the nonlocal diagrams.

Four body coupling

We will also need the simplest four body diagram, which factorize in the lowest order

$$\begin{aligned} M_{pp'hh',p''p'''h''h'''} \approx\ & \delta_{pp''}\delta_{p'p'''}\delta_{hh''}\delta_{h'h'''} + \delta_{pp''}\delta_{hh''}\left\langle p'h'''\right|\tilde{\Gamma}_{\mathrm{dd}}\left|h'p'''\right\rangle \\ & +\delta_{p'p'''}\delta_{h'h'''}\left\langle ph''\right|\tilde{\Gamma}_{\mathrm{dd}}\left|hp''\right\rangle + \left\langle p'h'''\right|\tilde{\Gamma}_{\mathrm{dd}}\left|h'p'''\right\rangle\left\langle ph''\right|\tilde{\Gamma}_{\mathrm{dd}}\left|hp''\right\rangle \end{aligned} \tag{2.53}$$

Chapter 3

Exchange in correlated RPA

The simple RPA uses an effective or screened interaction, which have to be determined in a separate calculation. Only for systems with an interaction that has a Fourier transform, the use of the bare interaction is possible. In fact, for the most interesting systems in nature this is not the case. Therefore one has to find a procedure to determine this effective interaction. There are several ways to find such an effective interaction, one is to require the fulfilment of the m_0 and m_1 sumrule, another is to apply phenomenological considerations [3, 4, 27]. In this thesis a different approach is chosen, we start from an accurate microscopic description of the ground state which incorporates the important Jastrow correlations. Thus we formulate the TDHF in a correlated basis [12] (cTDHF). By transforming this equations to a form identical to (1.10), we obtain a clear description of how to determine the effective interaction out of CBF matrix elements [31]. Thus we end up with a microscopic description of the effective interaction in terms of FHNC quantities.

In this chapter a description how to perform this transformation and which approximations are necessary is presented. At the end numerical results for the different approximations are shown. A part of the work presented in this chapter has already been published [III], but the treatment here is more up to date and detailed.

3.1 The trial wave function

In this chapter we will use a stationary principle in order to derive equations of motion. Therefore we need a trial wave function which is flexible enough to describe the important physical effects. One can use the theory applied for Bosons as guide line for our calculations for Fermions. It has been shown that pair excitations play an important role for Bosons[6].

The generalization to Fermions have the form

$$\begin{aligned} |\Psi(t)\rangle &= \exp\left[-\mathrm{i}H_{oo}t/\hbar\right]|\Psi_0(t)\rangle\ , \\ |\Psi_0(t)\rangle &= \frac{1}{I^{1/2}(t)}\exp\frac{1}{2}U(t)\,|\psi\rangle\,, \\ I(t) &= \left\langle \psi\ \exp\frac{1}{2}U^\dagger(t)\right|\exp\frac{1}{2}U(t)\,\psi\Big\rangle\,. \end{aligned} \tag{3.1}$$

where

$$U(t) = \sum_{ph}\delta u^{(1)}_{ph}(t)\ \alpha^\dagger_p\alpha_h + \sum_{php'h'}\delta u^{(2)}_{pp'hh'}(t)\ \alpha^\dagger_p\alpha^\dagger_{p'}\alpha_{h'}\alpha_h \tag{3.2}$$

$\delta u^{(1)}_{ph}(t)$ is the time-dependent correlated particle hole excitation amplitude and similar $\delta u^{(2)}_{pp'hh'}(t)$ the two particle two hole excitation amplitude. In this chapter we restrict ourselves to single particle hole excitations in order to derive the RPA equations.

In using this definition of the trial function, a normalization factor has been absorbed in $\delta u^{(1)}_{ph}$ in contrast to [12].

3.2 The cTDHF equations

The particle–hole amplitudes $\delta u^{(1)}_{ph}(t)$ are determined by the stationarity principles [28]

$$\mathcal{S}\left[\delta u^{(1)}_{ph}, \delta u^{(1*)}_{ph}\right] = \int dt\ \mathcal{L}(t)\ , \tag{3.3}$$

from the Lagrangian

$$\begin{aligned} \mathcal{L}(t) &= \langle\Psi(t)|\ H + H_{\mathrm{ext}}(t) - \mathrm{i}\,\hbar\frac{\partial}{\partial t}\ |\Psi(t)\rangle \\ &= \langle\Psi_0(t)|\ H' + H_{\mathrm{ext}}(t) - \mathrm{i}\,\hbar\frac{\partial}{\partial t}\ |\Psi_0(t)\rangle\ . \end{aligned} \tag{3.4}$$

where the external potential enters via

$$H_{\mathrm{ext}}(t) \equiv \int d^3r\, h_{\mathrm{ext}}(\mathbf{r};t)\,\hat\rho(\mathbf{r}) \tag{3.5}$$

and thus couples to the density, since we are interested in the density–density response. (If we would be interested in spinfluctuations the external perturbation has to couple to the spin density.) By minimizing the action, equations of motion are derived, where we keep only the first order in the particle–hole amplitudes, since we investigate linear response in this thesis. The result is the cTDHF equation

$$-2\int \rho_{ph,0}(\mathbf{r})h_{\mathrm{ext}}(\mathbf{r},t) = \sum\left[H_{ph,p'h'} - \mathrm{i}\hbar M_{ph,p'h'}\frac{\partial}{\partial t}\right]\delta u^{(1)}_{p'h'} + \sum H_{pp'hh',0}\delta u^{*(1)}_{p'h'}\,. \tag{3.6}$$

The procedure outlined above is known as time–dependent Hartree–Fock (TDHF) theory [28, 29, 40], generalized to strongly interacting systems [12, 31].

We assume harmonic time dependence of the external potential

$$h_{\rm ext}(\mathbf{r},t) = h_{\rm ext}(\mathbf{r};\omega)\left[e^{\mathrm{i}\omega t} + e^{-\mathrm{i}\omega t}\right] e^{\eta t} \tag{3.7}$$

where the infinitesimal η ensures the adiabatic switching on of the potential. This imposes the time dependence

$$\delta u_{ph}^{(1)}(t) \;=\; \left[\delta u_{ph}^{(1+)}(\omega)e^{-\mathrm{i}\omega t} + \delta u_{ph}^{*(1-)}e^{\mathrm{i}\omega t}\right] e^{\eta t}\,. \tag{3.8}$$

With this we can write the above equation in super matrix form

$$\begin{bmatrix} \mathbf{A}-\hbar\omega\mathbf{M}-\mathrm{i}\eta & \mathbf{B} \\ \mathbf{B}^* & \mathbf{A}^*+\hbar\omega\mathbf{M}^*+\mathrm{i}\eta \end{bmatrix} \begin{pmatrix} \delta u^{(1+)} \\ \delta u^{(1-)} \end{pmatrix} = \begin{pmatrix} \rho_{ph,0} \\ \rho_{0,ph} \end{pmatrix} h_{ext}(q,\omega) \tag{3.9}$$

where A, B and M are matrices with components

$$\begin{aligned} A_{ph,p'h'} &= e_{ph}\delta_{pp'}\delta_{hh'} + H_{ph,p'h'} \\ B_{ph,p'h'} &= H_{php'h',0} \\ M_{ph,p'h'} &= \delta_{pp'}\delta_{hh'} + N_{ph,p'h'} \end{aligned} \tag{3.10}$$

and

$$\delta u^{(1+)} = \begin{pmatrix} \delta u^{(1+)}_{h_1+qh_1} \\ \delta u^{(1+)}_{h_2+qh_2} \\ \vdots \end{pmatrix} \qquad . \tag{3.11}$$

where we introduced the momentum transfer $q = p - h$. We also defined the matrix element of the density operator $\hat{\rho}(\mathbf{r}) = \sum_i \delta(\mathbf{r}-\mathbf{r}_i)$:

$$\rho_{ph,0} = \langle \mathbf{ph}|\,\hat{\rho}\,|\mathbf{0}\rangle\ . \tag{3.12}$$

The density matrix element can be written in two ways. Since the density operator is a function of the position only, it commutes with the Jastrow correlations due to its locality(see 2.2.3):

$$\langle \mathbf{ph}|\,\hat{\rho}\,|\mathbf{0}\rangle = \sum_\alpha \frac{\langle\Phi_{ph}|\,FFa^\dagger_{\alpha-q}a_\alpha\,|\Phi_0\rangle}{\langle\Phi_{ph}|\,FF\,|\Phi_{ph}\rangle^{1/2}} = \sum_\alpha \frac{\langle\Phi_{ph}|\,a^\dagger_{\alpha-q}a_\alpha FF\,|\Phi_0\rangle}{\langle\Phi_{ph}|\,FF\,|\Phi_{ph}\rangle^{1/2}} \tag{3.13}$$

which directly yields to

$$\begin{aligned}
\begin{pmatrix} \rho_{ph,0} \\ \rho_{0,ph} \end{pmatrix} &= \begin{pmatrix} z_{ph} + N_{ph,p'h'} z_{p'h'} & 0 \\ 0 & z_{ph} + N_{p'h',ph} z_{p'h'} \end{pmatrix} \begin{pmatrix} \rho^F_{p'h',0} \\ \rho^F_{0,p'h'} \end{pmatrix} \\
&= \begin{pmatrix} \mathbf{1} + N_{ph,p'h'} & 0 \\ 0 & \mathbf{1} + N_{p'h',ph} \end{pmatrix} \begin{pmatrix} \tilde{\rho}^F_{p'h',0} \\ \tilde{\rho}^F_{0,p'h'} \end{pmatrix} \qquad (3.14) \\
&= \begin{pmatrix} \frac{1}{z^2_{ph}} & N_{pp'hh',0} \\ N_{0,pp'hh'} & \frac{1}{z^2_{ph}} \end{pmatrix} \begin{pmatrix} \tilde{\rho}^F_{p'h',0} \\ \tilde{\rho}^F_{0,p'h'} \end{pmatrix} \qquad (3.15)
\end{aligned}$$

where $\rho^F_{ph,0} = \langle \Phi_{ph} | \, \hat{\rho} \, | \Phi_0 \rangle = \langle p | \, \hat{\rho} \, | h \rangle$, the matrix element of the density operator of the non-interacting system, has been defined. Additionally we have defined the quantity $\tilde{\rho}^F_{p'h',0} = z_{ph} \rho^F_{p'h',0}$. Now we invert the cTDHF-matrix

$$\begin{pmatrix} \delta u^{(1+)} \\ \delta u^{(1-)} \end{pmatrix} = \begin{bmatrix} \mathbf{A} - (\hbar\omega + \mathrm{i}\eta)\mathbf{M} & \mathbf{B} \\ \mathbf{B}^* & \mathbf{A}^* + (\hbar\omega + \mathrm{i}\eta)\mathbf{M}^* \end{bmatrix}^{-1} \begin{pmatrix} \rho_{ph,0} \\ \rho_{0,ph} \end{pmatrix} h_{ext}(q,\omega) \, . \qquad (3.16)$$

The density fluctuation expressed in this matrix notation is

$$\delta\rho(q,\omega) = \langle \Psi | \, \hat{\rho}(q) - \rho_0 \, | \Psi \rangle = \begin{pmatrix} \rho_{0,ph} & \rho_{ph,0} \end{pmatrix} \begin{pmatrix} \delta u^{(1+)} \\ \delta u^{(1-)} \end{pmatrix} \, . \qquad (3.17)$$

From that we directly obtain the linear response

$$\chi(q,\omega) = \begin{pmatrix} \rho_{0,ph} & \rho_{ph,0} \end{pmatrix} \begin{bmatrix} \mathbf{A} - (\hbar\omega + \mathrm{i}\eta)\mathbf{M} & \mathbf{B} \\ \mathbf{B}^* & \mathbf{A}^* + (\hbar\omega + \mathrm{i}\eta)\mathbf{M}^* \end{bmatrix}^{-1} \begin{pmatrix} \rho_{0,ph} \\ \rho_{ph,0} \end{pmatrix} \, . \qquad (3.18)$$

The idea is now that the cTDHF matrix can be simplified by absorbing the correlated density matrix elements. The result is a RPA like equation with an effective interaction. First we define the supermatrices

$$\Omega = \begin{pmatrix} e_{ph} - \hbar\omega - \mathrm{i}\eta & 0 \\ 0 & e_{ph} + \hbar\omega + \mathrm{i}\eta \end{pmatrix} \, , \qquad \mathbf{W} = \begin{pmatrix} W_{ph,p'h'} & W_{pp'hh',0} \\ W_{0,pp'hh'} & W_{p'h',ph} \end{pmatrix} \qquad (3.19)$$

$$\mathbf{N} = \begin{pmatrix} N_{ph,p'h'} & N_{pp'hh',0} \\ N_{0,pp'hh'} & N_{p'h',ph} \end{pmatrix} \, . \qquad (3.20)$$

Then the xRPA matrix equation assumes the form

$$\begin{aligned}
&\begin{bmatrix} \mathbf{A} - (\hbar\omega + \mathrm{i}\eta)\mathbf{M} & \mathbf{B} \\ \mathbf{B}^* & \mathbf{A}^* + (\hbar\omega + \mathrm{i}\eta)\mathbf{M}^* \end{bmatrix} = \left[\Omega + \frac{1}{2}\Omega\mathbf{N} + \frac{1}{2}\mathbf{N}\Omega + \mathbf{W} \right] \\
&= \left[\mathbf{1} + \frac{1}{2}\tilde{\mathbf{N}} \right] \left[\Omega + \mathbf{V}_{\mathrm{p-h}}(\omega) \right] \left[\mathbf{1} + \frac{1}{2}\tilde{\mathbf{N}} \right] , \qquad (3.21)
\end{aligned}$$

using $\tilde{\mathbf{N}} = \mathbf{N} + \mathbf{\Delta N}$ this defines a new, energy–dependent interaction matrix

$$\mathbf{V}_{\mathrm{p-h}}(\omega) = \left[1 + \frac{1}{2}\tilde{\mathbf{N}}\right]^{-1} \left[\mathbf{W} - \frac{1}{2}\mathbf{\Delta N}\Omega - \frac{1}{2}\Omega\mathbf{\Delta N} - \frac{1}{4}\tilde{\mathbf{N}}\Omega\tilde{\mathbf{N}}\right] \left[1 + \frac{1}{2}\tilde{\mathbf{N}}\right]^{-1} . \tag{3.22}$$

In doing so we deviate from the transformation in [31], in order to obtain exactly the noninteracting density matrix element. Using the mean of the two representations of the density matrix element (3.14) and (3.15) yields the definition of $\tilde{\mathbf{N}}$:

$$\begin{pmatrix} \rho_{0,ph}(r) \\ \rho_{ph,0}(r) \end{pmatrix} = \left[\mathbf{1} + \frac{1}{2}\mathbf{N} + \frac{1}{2}\mathbf{\Delta N}\right] \begin{pmatrix} \tilde{\rho}^F_{0,p'h'}(r) \\ \tilde{\rho}^F_{p'h',0}(r) \end{pmatrix} \tag{3.23}$$

with

$$\mathbf{\Delta N} = \begin{pmatrix} \left(\frac{1}{z^2_{ph}} - 1\right)\delta_{pp'}\delta_{hh'} & 0 \\ 0 & \left(\frac{1}{z^2_{ph}} - 1\right)\delta_{pp'}\delta_{hh'} \end{pmatrix} . \tag{3.24}$$

With the definition

$$\mathbf{c} \equiv \begin{pmatrix} c^{(1+)}_{ph} \\ c^{(1-)}_{ph} \end{pmatrix} = \left[\mathbf{1} + \frac{1}{2}\tilde{\mathbf{N}}\right] \begin{pmatrix} \delta u^{(1+)}_{p'h'} \\ \delta u^{(1-)}_{p'h'} \end{pmatrix} \tag{3.25}$$

our response equation assumes the simple and familiar form

$$\left[\Omega + \mathbf{V}_{\mathrm{p-h}}(\omega)\right]\mathbf{c} = 2\mathbf{h} \tag{3.26}$$

where, in fact, the $\delta\rho(\mathbf{r};\omega) = \Re e \sum_{ph} c^{(1+)}_{ph}(\omega)\tilde{\rho}^F_{0,ph}(\mathbf{r}) + c^{(1-)}_{ph}(\omega)\tilde{\rho}^F_{ph,0}(\mathbf{r})$, *i.e.* we have the ordinary RPA relationship.

3.3 Diagrammatic reduction of the equations

On the first sight the transformation defined in the previous section looks only like a formal simplification, where some of the complexity has been moved to the interaction matrix. This is true to some extent, but if we take only diagrams of first order in $\tilde{\Gamma}_{\mathrm{dd}}$ into account, the problem indeed simplifies. In figure 3.1 the N-matrix in this approximation is shown. This approximation also implies $\Delta N = 0$. Performing the transformation we end up with a microscopic derivation of the effective interaction $\mathbf{V}_{\mathrm{p-h}}$, which is a diagrammatic subset of $\mathbf{W}$. We start our investigation in the direct channel, because here it is easier to see what happens. Later we also take the exchange channel into account. To distinguish the direct and the exchange channel we introduce the following notion:

$$\mathbf{N} = \begin{pmatrix} \langle ph'|\, N\, |hp'\rangle_a & \langle pp'|\, N\, |hh'\rangle_a \\ \langle hh'|\, N\, |pp'\rangle_a & \langle p'h|\, N\, |h'p\rangle_a \end{pmatrix} = \mathbf{N}^{(d)} + \mathbf{N}^{(ex)} \tag{3.27}$$

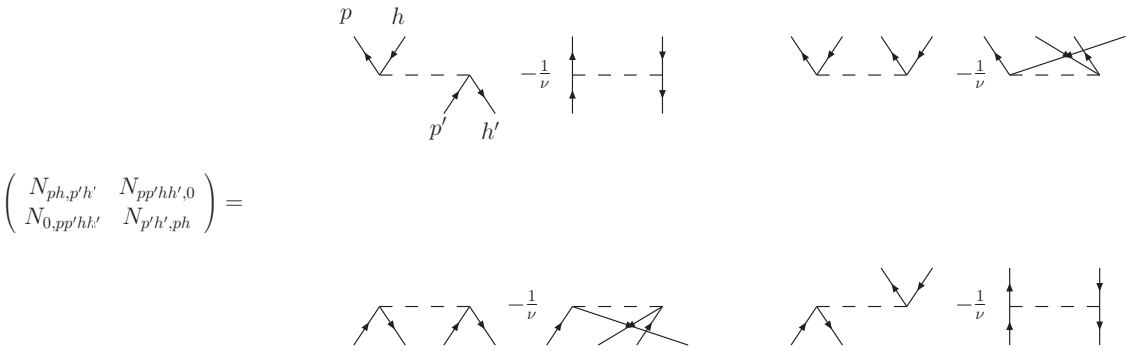

Figure 3.1: The figure shows the N-matrix in the approximation given in (2.45). The dashed line represents $\tilde{\Gamma}_{\rm dd}$. The lines with arrows indicate the Hartree-Fock single particle orbitals.

and accordingly the other quantities.

It is important to visualize the diagrams generated by matrix multiplication. For instance let us examine the result of $(\mathbf{N}\cdot\mathbf{N})_{ph,p'h'} = \sum_{p''h''} N_{ph,p''h''}N_{p''h'',ph} + N_{pp''hh'',0}N_{0,p''p'h''h'}$: This produces diagrams with two $\tilde{\Gamma}_{\rm dd}$ lines connected by p'' and h''. The summation over h'' becomes a Slater exchange line and the summation over p'' a delta-function minus an exchange line. Thus in the direct part the matrix multiplication simply reduces to a multiplication with $2S_F(q)$ in momentum space.

3.3.1 Direct channel

We define the irreducible matrix $\mathbf{X}$ by

$$\mathbf{N}^{(d)} = \left(1 + \frac{1}{2}\mathbf{N}^{(d)}\right)\mathbf{X}^{(d)} \tag{3.28}$$

In the direct channel the matrix multiplication is easily performed. Therefore this matrix equation can be written as ordinary equation

$$\tilde{\Gamma}_{\rm dd}(q) = \tilde{X}_{\rm dd}(q) + \tilde{\Gamma}_{\rm dd}(q)S_F(q)\tilde{X}_{\rm dd}(q) \tag{3.29}$$

where we used

$$\mathbf{X}^{(d)} = \begin{pmatrix} \langle ph'|\,\tilde{X}_{\rm dd}\,|hp'\rangle & \langle pp'|\,\tilde{X}_{\rm dd}\,|hh'\rangle \\ \langle hh'|\,\tilde{X}_{\rm dd}\,|pp'\rangle & \langle p'h|\,\tilde{X}_{\rm dd}\,|h'p\rangle \end{pmatrix} = \begin{pmatrix} \tilde{X}_{\rm dd}(p-h) & \tilde{X}_{\rm dd}(p-h) \\ \tilde{X}_{\rm dd}(h-p) & \tilde{X}_{\rm dd}(h-p) \end{pmatrix} \tag{3.30}$$

and $\tilde{X}_{\rm dd}(q)$ is indeed the non nodal FHNC quantity. This is easily proven by inserting the simplified FHNC equations (A.17). A deeper understanding is gained by investigating this operation in the diagrammatic language. In that language we see that $\tilde{\Gamma}_{\rm dd}$ is the infinite chain of the non-nodal quantity $\tilde{X}_{\rm dd}$.

Now we examine the interaction-part. We define the quantity $\mathbf{X}'$

$$\mathbf{W}^{(d)} = \left(1 + \frac{1}{2}\mathbf{N}^{(d)}\right) \mathbf{X}'^{(d)} \left(1 + \frac{1}{2}\mathbf{N}^{(d)}\right) \tag{3.31}$$

in $\mathbf{W}$ we use the simplest approximation for the matrix elements

$$\langle ij| W |kl\rangle = \delta_{i-k,l-j} W(i-k) = \Gamma'_{dd}(i-k) - \frac{\hbar^2(i-k)^2}{4m}\Gamma_{dd}(i-k) \tag{3.32}$$

We anticipate that $\mathbf{X}'^{(d)}$ is given by

$$\mathbf{X}'^{(d)} = \begin{pmatrix} X'_{dd} & X'_{dd} \\ X'_{dd} & X'_{dd} \end{pmatrix} - \frac{\hbar^2 q^2}{4m} \begin{pmatrix} X_{dd} & X_{dd} \\ X_{dd} & X_{dd} \end{pmatrix} + \frac{1}{4} \begin{pmatrix} X_{dd} & X_{dd} \\ X_{dd} & X_{dd} \end{pmatrix} \begin{pmatrix} t_{ph} & 0 \\ 0 & t_{ph} \end{pmatrix} \begin{pmatrix} X_{dd} & X_{dd} \\ X_{dd} & X_{dd} \end{pmatrix} \tag{3.33}$$

where we omitted the momentum dependence of the matrix elements for brevity. Performing all matrix multiplications we are again able to write eq. (3.31) as ordinary equation. We obtain

$$\begin{aligned} W(q) &= (1 + S_F\tilde{\Gamma}_{\rm dd})\tilde{X}'_{\rm dd}(1 + S_F\tilde{\Gamma}_{\rm dd}) - \frac{\hbar^2 q^2}{4m}(1 + S_F\tilde{\Gamma}_{\rm dd}) \left[\tilde{X}_{\rm dd} - \tilde{X}^2_{\rm dd}\right] (1 + S_F\tilde{\Gamma}_{\rm dd}) \\ &= \tilde{X}'_{\rm dd}(1 + 2S_F\tilde{\Gamma}_{\rm dd} + S_F^2\tilde{\Gamma}^2_{\rm dd}) - \frac{\hbar^2 q^2}{4m}\left[\tilde{\Gamma}_{\rm dd}(1 + S_F\tilde{\Gamma}_{\rm dd}) - \tilde{\Gamma}^2_{\rm dd}\right] \\ &= \tilde{X}'_{\rm dd}(1 + 2S_F\tilde{\Gamma}_{\rm dd} + S_F^2\tilde{\Gamma}^2_{\rm dd}) - \frac{\hbar^2 q^2}{4m}\tilde{\Gamma}^2_{\rm dd}\left[S_F - 1\right] - \frac{\hbar^2 q^2}{4m}\tilde{\Gamma}_{\rm dd} \\ &= \tilde{X}'_{\rm dd} + N'_{dd} - \frac{\hbar^2 q^2}{4m}\tilde{\Gamma}_{\rm dd} = \tilde{\Gamma}'_{\rm dd} - \frac{\hbar^2 q^2}{4m}\tilde{\Gamma}_{\rm dd}\,, \end{aligned} \tag{3.34}$$

where we used the simplified FHNC' equation

$$N'_{dd} = 2S_F\tilde{\Gamma}_{\rm dd}\tilde{X}'_{\rm dd} + S_F^2\tilde{\Gamma}^2_{\rm dd}\tilde{X}'_{\rm dd} - \frac{\hbar^2 q^2}{4m}\tilde{\Gamma}^2_{\rm dd}\left[S_F - 1\right] \tag{3.35}$$

which is obtained from (A.11) by application of the method described in section A.2.1. Thus we have shown that the expression for $\mathbf{X}'^{(d)}$ although looking complicated, leads to the correct $W(q)$ as defined in (2.47). Now we insert all this into the equation for the effective interaction and express it with the irreducible quantities

$$\mathbf{V}^{(d)}_{p-h} = \mathbf{X}'^{(d)} - \frac{1}{4}\mathbf{X}^{(d)}\Omega\mathbf{X}^{(d)}\,. \tag{3.36}$$

The local function entering the matrix become

$$V_{ph}(q) = \tilde{X}'_{\rm dd}(q) - \frac{\hbar^2 q^2}{4m}\left[\tilde{X}_{\rm dd}(q) - \tilde{X}^2_{\rm dd}(q)\right] - \frac{1}{2}\sum_{ph}\tilde{X}^2_{\rm dd}(q)e_{ph}\,. \tag{3.37}$$

It is important to note that the ω-dependence vanish in the direct part. Further simplification is possible if we neglect the Fock-term in the single particle-hole energy

$$e_{ph} = t(p) + u(p) - t(h) - u(h) \approx \frac{\hbar^2(p^2 - h^2)}{2m}. \tag{3.38}$$

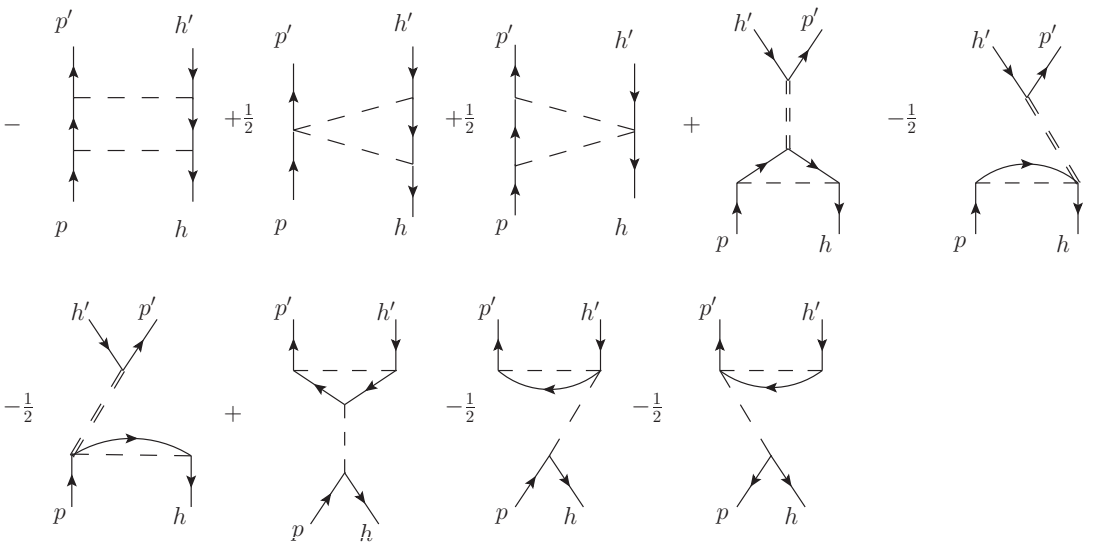

Figure 3.2: The second order of the $\mathbf{N}^{(\text{non d})}$ matrix is shown whereas the trivial first oder part is omitted. The non nodal quantity $\tilde{X}_{\text{dd}}$ is represented by a double dashed line.

This is consistent with neglecting the exchange terms, since the Fock-energy is the exchange term of the Hartree-energy. Therefore the effective interaction reduces to

$$V_{ph}(q) = \tilde{X}'_{\text{dd}}(q) - \frac{\hbar^2 q^2}{4m}\tilde{X}_{\text{dd}}(q)\,. \tag{3.39}$$

3.3.2 Determination of the exchange matrix element in xRPA

First we have to find the exchange analog of (3.28):

$$\mathbf{N}^{(\text{non d})} = \left(1 + \frac{1}{2}\mathbf{N}^{(ex)}\right)\mathbf{X}^{(ex)} + \frac{1}{2}\mathbf{N}^{(ex)}\mathbf{X}^{(d)} + \frac{1}{2}\mathbf{N}^{(d)}\mathbf{X}^{(ex)}\,. \tag{3.40}$$

In that expression no simple chaining operation appears, therefore we choose

$$\mathbf{X}^{(ex)} = \begin{pmatrix} \langle ph'|\,\Gamma_{dd}\,|p'h\rangle & \langle pp'|\,\Gamma_{dd}\,|h'h\rangle \\ \langle hh'|\,\Gamma_{dd}\,|p'p\rangle & \langle hp'|\,\Gamma_{dd}\,|h'p\rangle \end{pmatrix} \tag{3.41}$$

Executing the matrix multiplications results in second order diagrams. These second order diagrams are a part of the complete second order contribution to $\mathcal{N}$. Therefore we assign this quantity with a different name, $\mathbf{N}^{(\text{non d})}$. The second order part of $\mathbf{N}^{(\text{non d})}$ is shown in figure 3.2. The interesting point is that first order in the effective interaction leads to some second order contributions in the correlated equations. Or the other way round: To obtain the same approximation in the cTDHF equations as in the reduced equations, one has to calculate some second order diagrams.

$\mathbf{X}'^{(ex)}$ is obtained by generalization of (3.33).

$$\mathbf{X}'^{(ex)} = \begin{pmatrix} \langle ph'|\,\Gamma'_{dd}\,|p'h\rangle & \langle pp'|\,\Gamma'_{dd}\,|h'h\rangle \\ \langle hh'|\,\Gamma'_{dd}\,|p'p\rangle & \langle hp'|\,\Gamma'_{dd}\,|h'p\rangle \end{pmatrix} - \frac{\hbar^2 q^2}{4m}\mathbf{X}^{(ex)} \\ - \frac{1}{4}\left[\mathbf{X}^{(d)} - \mathbf{X}^{(ex)}\right]\begin{pmatrix} t_{ph} & 0 \\ 0 & t_{ph} \end{pmatrix}\left[\mathbf{X}^{(d)} - \mathbf{X}^{(ex)}\right] + \frac{1}{4}\mathbf{X}^{(d)}\begin{pmatrix} t_{ph} & 0 \\ 0 & t_{ph} \end{pmatrix}\mathbf{X}^{(d)} \quad (3.42)$$

We insert this all into the expression for the effective interaction

$$\mathbf{V}^{(ex)}_{p-h} = (\mathbf{X}' - \frac{1}{4}\mathbf{X}\Omega\mathbf{X})_{ex} = \mathbf{X}'^{(ex)} - \frac{1}{4}\left[\mathbf{X}^{(d)}\Omega\mathbf{X}^{(ex)} + \mathbf{X}^{(ex)}\Omega\mathbf{X}^{(d)} + \mathbf{X}^{(ex)}\Omega\mathbf{X}^{(ex)}\right] \quad (3.43)$$

In the simplest approximation we keep only first order terms. This leads to the result of [33], which is a local exchange potential:

$$\langle ph'|\,V_{ex}(r-r')\,|p'h\rangle \quad (3.44)$$

with

$$V_{ex}(q) = \Gamma'_{dd}(q) - \frac{\hbar^2 q^2}{4m}\Gamma_{dd}(q) = W(q)\,. \quad (3.45)$$

It remains to show whether

$$\mathbf{W}^{(\text{non d})} = \frac{1}{4}\left[\mathbf{N}^{(ex)}\mathbf{X}'^{(d)}\mathbf{N}^{(d)} + \mathbf{N}^{(d)}\mathbf{X}'^{(d)}\mathbf{N}^{(ex)} + \mathbf{N}^{(ex)}\mathbf{X}'^{(d)}\mathbf{N}^{(ex)}\right] \\ +(1+\frac{1}{2}\mathbf{N})\mathbf{X}'^{(ex)}(1+\frac{1}{2}\mathbf{N}) \quad (3.46)$$

is a good approximation of $\mathbf{W}^{(ex)}$. Indeed, this produces additionally to the first order contribution, some of the second and third order diagrams. Hence the situation is similar to the above one. In the effective equations we calculate more diagrams than in the cTDHF equations. Altough the treatment of exchange effects is very demanding and not exact, it seems to be essential in obtaining quantitative agreement with the experiment.

3.4 The numerical method

In the simple RPA the response equation can be solved analytically. This is no longer possible if we include exchange terms. Therefore we have to resort to purely numerical means. There are in principle two methods which tackle the problem at the same point, inverting the xRPA matrix. The first method is finding the eigenvalues and eigenvectors of the matrix. Once we found the spectrum we are able to solve this equation for arbitrary ω without much computational effort. The disadvantage of this approach is that for energy dependent potentials this is no longer possible. Energy dependent potentials appear already in an advanced treatment of the exchange, but at latest if we want to include

two-particle two-hole excitations we can not avoid the energy dependence. The second method is the numerical inversion of the xRPA matrix for every ω. This is much slower but one is not restricted to the eigenvalue problem.

To properly discretize the problem one first rewrite the summations occurring in the matrix multiplications as integrals. These integrals are then discretized and written as matrix multiplications. Due to the finite number of discretization points we obtain discrete excitation energies. A small imaginary part η is added to artificially broaden the appearing δ functions. η has to be adjusted such that it is large enough to obtain a smooth response and not to large in order to keep the details of the respone. The calculations in figure 3.6 and 3.7 where performed with $N = 32 \times 32$ integration points. More details about the numerical method can be found in Ref. [36].

3.5 The long wavelength behavior

As pointed out in [39] the RPA becomes valid in the limit $q \to 0$. We investigate now this limit for the case studied above, i.e. CBF single p-h excitations, including exchange diagrams. We write the relevant part of the xRPA equations with restriction to $[\mathbf{V}_{p-h}]_{ph,p'h'} = \langle ph'|\, V_{ph}\, |hp'\rangle - \langle ph'|\, V_{ex}\, |p'h\rangle$:

$$e_{h+q,h}c_{h+q,h} - \frac{1}{\nu}\sum_{h'} n(h')\bar{n}(h'+q)V_{ex}(h-h')c_{h'+q,h'} + [\dots] = 0\ . \tag{3.47}$$

We approximate the particle-hole amplitude by its Fermi-sea average and the single particle hole energy difference by the Hartree-Fock energy difference, where we have to use the same level of approximation as for the matrix elements: $e_k = t(k) - \frac{1}{\nu}\sum_h n(h)V_{ex}(k-h)$. Thus

$$\left[2hq + q^2 - \frac{1}{\nu}\sum_{h'} n(h')\left(V_{ex}(h+q-h') - V_{ex}(h-h') + \bar{n}(h'+q)V_{ex}(h-h')\right)\right] c_q + [\dots] = 0\ , \tag{3.48}$$

using $\bar{n}(h'+q) = 1 - n(h'+q)$ we obtain

$$\left[2hq + q^2 - \frac{1}{\nu}\sum_{h'} n(h')\left(V_{ex}(h+q-h') - n(h'+q)V_{ex}(h-h')\right)\right] c_q + [\dots] = 0\ . \tag{3.49}$$

By renaming the summation variables we end up with a form that is identical to the exchange term in the B-channel

$$\left[2hq + q^2 - \frac{1}{\nu}\sum_{h'} n(h')\bar{n}(h'-q)V_{ex}(h+q-h')\right] c_q + [\dots] = 0\ . \tag{3.50}$$

Thus we see that the exchange diagrams do not vanish in the limes $q \to 0$. In that approximation the contribution from the exchange term is only local, thus

$$\tilde{V}_{\rm ex}(q) \equiv -\frac{1}{\nu}\sum_{h'} n(h')\bar{n}(h'-q)V_{ex}(h+q-h') \tag{3.51}$$

This means that in the long wave length limit the equations of motion assume the RPA form with an effective interaction of the form:

$$V_{\rm ph}^{\rm RPA}(q) = V_{\rm ph}(q) + \tilde{V}_{\rm ex}(q) \tag{3.52}$$

It is important to note that the exchange interaction and the Fock energy are related. If they are not chosen properly, a wrong $q \to 0$ behavior for the response is obtained.

3.6 Sumrules and how to estimate the error

Sumrules relate properties of excitations to ground state quantities, known from experiments or ground state calculations. Of course we use approximations for the matrix elements entering our theory and therefore the sumrules do not necessary reproduce the known ground state quantities exactly. Thus we are able to use these rules to estimate the error of our theory. In order to be able to compare with other results and to justify the approximations made for the matrix elements it is important that these sumrules are as accurate as possible fullfiled.

Define the n-th moment:

$$m_n = \int_0^\infty d\omega\ \omega^n S(q,\omega). \tag{3.53}$$

In our case the zeroth and the first moment sumrule are important:

$$m_0 = S(q) = \int_0^\infty d\omega\ S(q,\omega), \tag{3.54}$$

$$m_1 = \frac{\hbar^2 q^2}{2m} = \int_0^\infty d\omega\ \omega S(q,\omega). \tag{3.55}$$

Calculating the response from the CBF matrix elements we have three possible sources for errors:

- The difference of the Jastrow Feenberg wave function to the exact ground state wavefunction.
- The difference of our approximation of the CBF matrix element, which mainly consists of first order in $\tilde{\Gamma}_{\rm dd}$, to the exact one.
- Discretisation errors.

Note that in our approach multipair excitations do not effect the sumrules. Fortunately we are able to estimate the error of the CBF matrix elements, since we know their relation to ground state properties.

The static structure:

$$\langle 0|\, \rho_q \rho_{-q}\, |0\rangle = S(q)\,. \tag{3.56}$$

This is directly related to

$$\sum_{h,h'} \frac{\sqrt{I_{h+qh} I_{h'+qh'}}}{I_{00}} M_{h+qh,h'+qh'} = \sum_{h} \frac{I_{h+qh}}{I_{00}} + \sum_{h,h'} \frac{\sqrt{I_{h+qh} I_{h'+qh'}}}{I_{00}} N_{h+qh,h'+qh'}. \tag{3.57}$$

Free kinetic energy

$$\langle 0|\, \rho_q (H - H_{00}) \rho_{-q}\, |0\rangle = \sum_{k,k'} \langle 0|\, a_k^\dagger a_{k+q} (H - H_{00}) a_{k'+q}^\dagger a_{k'}\, |0\rangle = \frac{\hbar^2 q^2}{2m} \tag{3.58}$$

which is equivalent to

$$\sum_{h,h'} \frac{\sqrt{I_{h+qh} I_{h'+qh'}}}{I_{00}} A_{h+qh,h'+qh'} = \sum_{h} \frac{I_{h+qh}}{I_{00}} e_{h+qh} + \sum_{h,h'} \frac{\sqrt{I_{h+qh} I_{h'+qh'}}}{I_{00}} H_{h+qh,h'+qh'}. \tag{3.59}$$

Fermi sea average of the Brillouin condition

$$\langle 0|\, (H - H_{00}) \rho_q \rho_{-q}\, |0\rangle = 0 \tag{3.60}$$

equivalent to

$$\sum_{h,h'} \sqrt{\frac{I_{h+q\, h'+q\, hh'}}{I_{00}}} B_{h+qh,h'+qh'} = \sum_{h,h'} \sqrt{\frac{I_{h+q\, h'+q\, hh'}}{I_{00}}} H_{0,h+qhh'-qh'}. \tag{3.61}$$

These properties lead to exact fulfilment of the m_0 and m_1 sumrule in the collective approximation. In most cases[31, 12] one uses this three conditions as defining equations for the matrix elements of CBF. This approach is only reasonable if local approximations are made for the CBF matrix elements and thus exchange and other nonlocal diagrams are neglected. The approach is then consistent with the simplified FHNC method, defined in A.2.1. We do not make these simplifications and thus this method become ambiguous. Our input quantities are obtained from an elaborated FHNC calculation[33]. As result the above mentioned properties are no longer exactly fullfiled since we use approximations for the CBF matrix elements, thus they are fulfilled approximately. But we are sure that the difference becomes smaller if we calculate the CBF matrix elements to higher order. Thus it is legitimate to abort this procedure at sufficient accuracy. In figure 3.4 we show the result of eq. (3.59) and (3.61) which give reasonable results. (Notice that the relative

error of eq. (3.59) is about 3 persent.) The error of eq. (3.57) shown in figure 3.3 is also of the expected order.

Actually we do not solve the cTDHF equations, instead we solve the transformed equations (xRPA) which take additional diagrams into account. Thus, in order to estimate the error made in the matrix elements, we should check how well the sumrules are fulfilled in the collective approximation. It is easy to solve the collective equations analytically.The collective approximation of the xRPA response is

$$\chi^{\rm coll}(q,\omega) = \begin{pmatrix} S_F & S_F \end{pmatrix} \begin{pmatrix} -\hbar\omega S_F + \varepsilon_q + S_F^2 V_A & S_F^2 V_B \\ S_F^2 V_B & +\hbar\omega S_F + \varepsilon_q + S_F^2 V_A \end{pmatrix}^{-1} \begin{pmatrix} S_F \\ S_F \end{pmatrix} \tag{3.62}$$

where we omitted the q dependence in order to keep clarity and abbreviated the average Hartree–Fock single particle hole energy difference by ε_q. It is straight forward to invert the matrix

$$\chi^{\rm coll}(q,\omega) = \frac{2S_F\left(\frac{\varepsilon_q}{S_F} + S_F(V_A - V_B)\right)}{-(\hbar\omega)^2 + \frac{\varepsilon_q^2}{S_F^2} + 2\varepsilon_q V_A + S_F^2(V_A^2 - V_B^2)} \tag{3.63}$$

Of particular interest is the imaginary part of the response for positive energies

$$\Im m\left[\chi^{\rm coll}(q,\omega>0)\right] = \\ -\frac{\pi S_F\left(\frac{\varepsilon_q}{S_F} + S_F(V_A - V_B)\right)}{\sqrt{\frac{\varepsilon_q^2}{S_F^2} + 2\varepsilon_q V_A + S_F^2(V_A^2 - V_B^2)}}\,\delta\left(\hbar\omega - \sqrt{\frac{\varepsilon_q^2}{S_F^2} + 2\varepsilon_q V_A + S_F^2(V_A^2 - V_B^2)}\right) \tag{3.64}$$

The m_1 sumrule yield

$$S_F\left(\frac{\varepsilon_q}{S_F} + S_F(V_A - V_B)\right) \equiv \frac{\hbar^2 q^2}{2m} \tag{3.65}$$

and the m_0 sumrule

$$\frac{S_F\left(\frac{\varepsilon_q}{S_F} + S_F(V_A - V_B)\right)}{\sqrt{\frac{\varepsilon_q^2}{S_F^2} + 2\varepsilon_q V_A + S_F^2(V_A^2 - V_B^2)}} \equiv S(q)\,. \tag{3.66}$$

In figure 3.3 we compare the m_0 sumrule in the collective approximation with the FHNC $S(q)$. More interesting is the comparison of the m_1 sumrule (3.65) and the expected value as shown in figure 3.4. The remaining very small difference is due to discretisation errors, because it is analytically exact, as shown in the previous section.

3.7 Results in different approximations

Due to the complicated nature of the exchange channel, we have many different possibilities for approximations. Therefore it is necessary to approach the problem systematically.

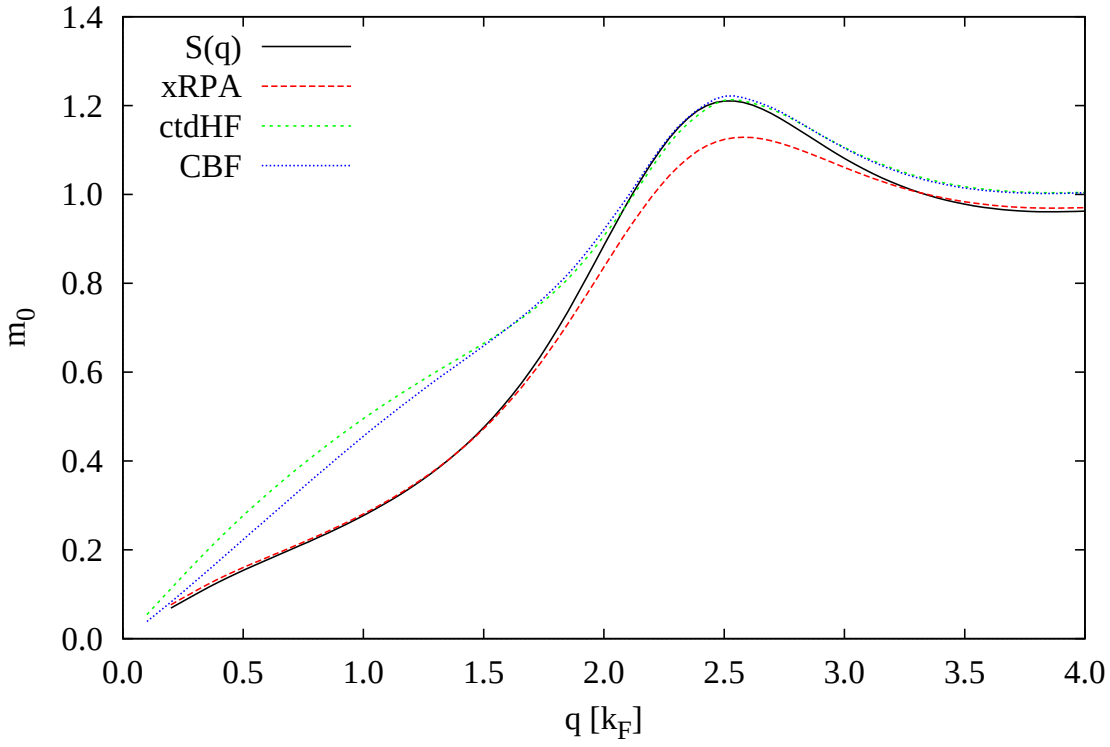

Figure 3.3: The result of different approximations for the m_0 sumrule are shown. Solid black is the reference static structure functions obtained from FHNC calculations [33]. Dashed red is the result of the m_0 sumrule in xRPA in the collective approximation (3.66). Short dashed green is the same for cTDHF. Dotted blue is the result of eq. (3.57).

First we split the effective interaction in different parts:

$$\mathbf{V}_{p-h} = \mathbf{V}^{(d)}_{p-h} + \mathbf{V}_{ex} + \mathbf{V}_E + \mathbf{V}_F \tag{3.67}$$

The first term is explained above. The second is the simplest exchange contribution

$$\mathbf{V}_{ex} = \begin{pmatrix} \langle ph'|\, V_{ex}\, |p'h\rangle & \langle pp'|\, V_{ex}\, |h'h\rangle \\ \langle hh'|\, V_{ex}\, |p'p\rangle & \langle hp'|\, V_{ex}\, |h'p\rangle \end{pmatrix} \tag{3.68}$$

The first two are of first order in $\tilde{\Gamma}_{\rm dd}$. The third one is the energy dependent contribution:

$$V_E = -\frac{1}{4}\mathbf{X}\begin{pmatrix} \hbar\omega & 0 \\ 0 & -\hbar\omega \end{pmatrix}\mathbf{X} \tag{3.69}$$

which is of second order. The last one comes from the Fock-term in the energy and is therefore of third order

$$V_F = -\frac{1}{4}\mathbf{X}\begin{pmatrix} u(p)-u(h) & 0 \\ 0 & u(p)-u(h) \end{pmatrix}\mathbf{X} \tag{3.70}$$

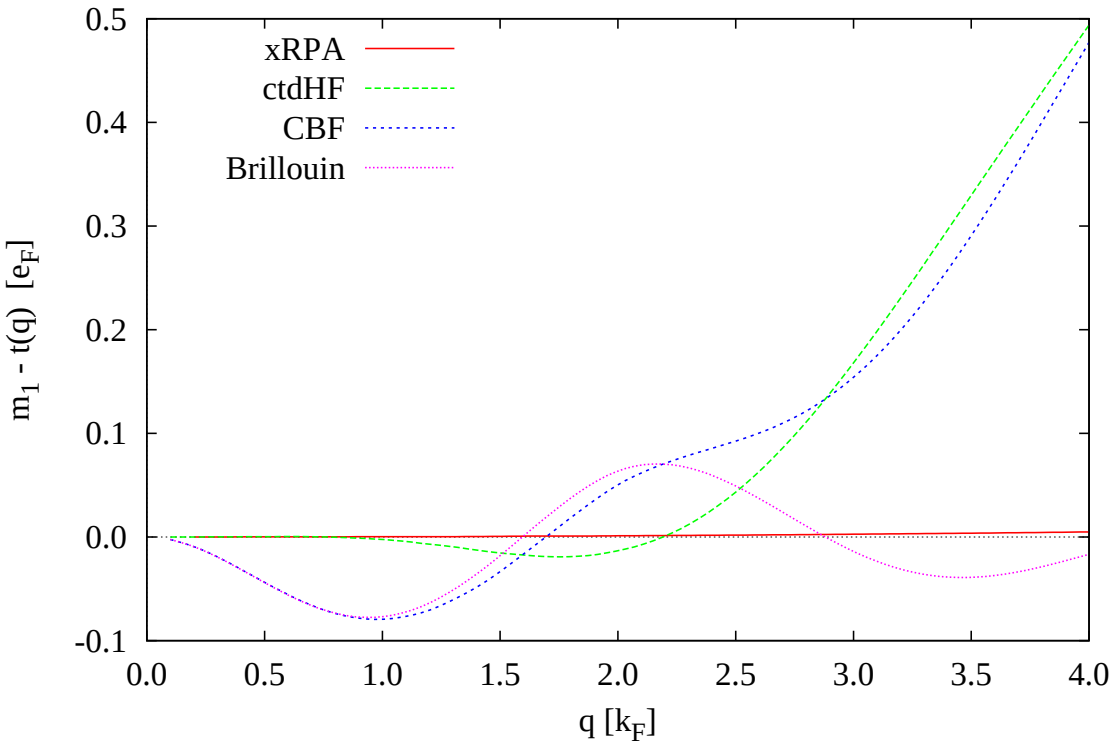

Figure 3.4: The difference of different approximations for the m_1 sumrule to the exact result are shown. Solid red is the result of the m_1 sumrule (3.65) which is practical identical with the zero axis. Dashed green is the same for cTDHF. Short dashed blue is the result of (3.59), and dotted magenta is the result of (3.61) in units of the Fermi-energy, which should be zero.

Before we consider the effects of the individual terms, we have to discuss the input quantities. In the simplest approximation, as shown above, we are consistent with the simplified FHNC scheme. Thus the effective interaction is a function of the static structure function only and the m_0 sumrule is fulfilled by construction. This changes as soon as we take exchange into account. Because by including exchange terms, we calculate additional FHNC diagrams, which are not contained in the simplified FHNC scheme. This means the more diagrams we calculate additional to the direct diagrams the less justified is the use of simplified FHNC quantities. On the other hand using the quantities ($\tilde{\Gamma}_{\mathrm{dd}}$, $\tilde{X}_{\mathrm{dd}}$, etc.) out of the full FHNC equations will not give the exact $S(q)$, since in general we will not sum all diagrams. But we are assured that including more diagrams will lead to a better fulfilment of the m_0 sumrule.

In figure 3.5 the described behavior can be seen. All the calculations where performed for the three dimensional ^{3}He at a density of $\rho = 0.0166\mathring{A}^{-3}$. The red lines correspond to calculations with simplified FHNC quantities. The red full line is the result of the

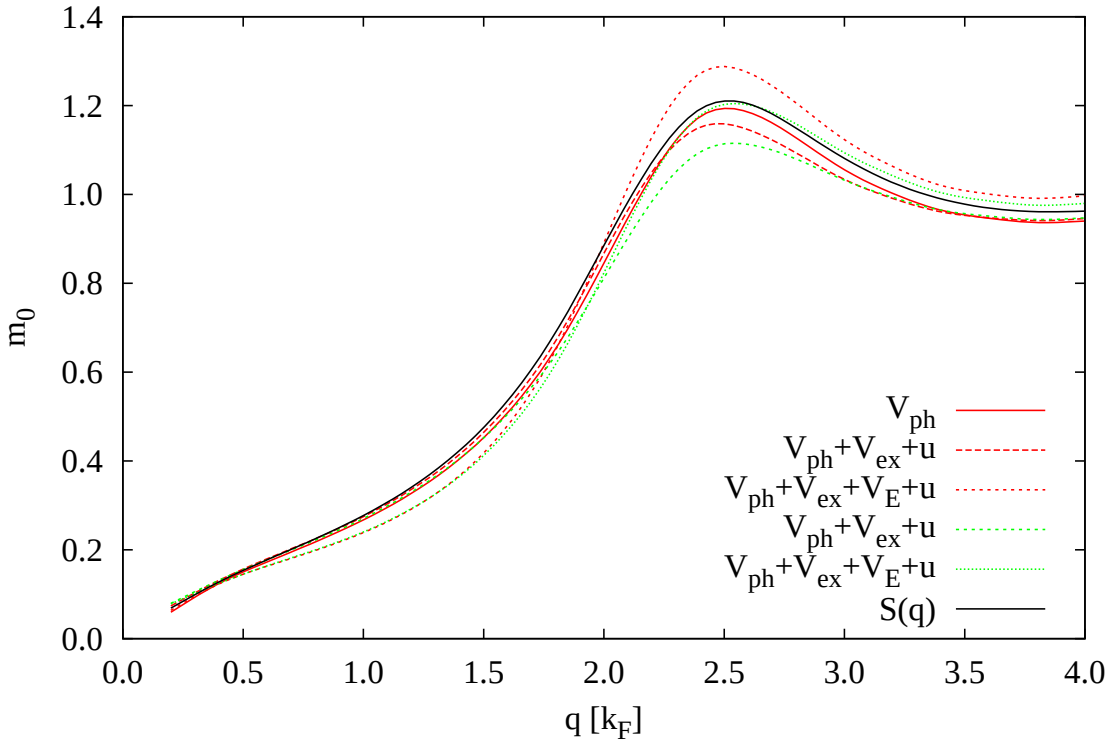

Figure 3.5: The plot shows the m_0 sumrule in different approximations. The black line shows the static structure function calculated via FHNC [33]. The red lines show different approximations for the xRPA matrix, but all input quantities are taken from simplified FHNC. In green are different approximations for the xRPA matrix, but all input quantities are taken from full FHNC.

simple RPA, where V_{ph} is the local effective interaction. This gives the best agreement with $S(q)$ as expected. If one adds simply the exchange term V_{ex} one obtains a much worse result (red long dashed line). This is to some extent an effect of the inconsistency of the approximations. In one quantity, the interaction, we take the exchange into account and in the other, the Hartree-Fock energy difference, we still neglect the Fock-term $u(k)$. Including the Fock-energy leads to a small improvement to the sumrule. Including next the energy dependent part of the interaction V_E again worsens the agreement, as expected. The green lines show the result with input quantities taken from the full FHNC equations. One sees that, when V_E is included, it is advantageous to use the FHNC quantities.

In figure 3.6 and 3.7 one can see the result of the different approximations for the dynamic structure factor. The starting point or the reference in both figures is the ordinary RPA result with the effective interaction V_{ph} (red line). In figure 3.6 the green line is the result with simplest exchange term V_{ex} and without the Fock-energy $u(k)$. The more accurate should be the calculation with the Fock-energy (blue line). The magenta line

corresponds to the blue line, but is instead calculated with quantities out of the FHNC equations. In figure 3.7 we compare the results with the energy dependent part of the effective interaction V_E. The green line is calculated with simplified FHNC quantities and the blue line with the full FHNC quantities. To conclude this section we summarize the effect of the exchange terms. We observe that inclusion of exchange lowers the position of the collective mode slightly. This is in agreement with the experiment, which gives a collective mode significantly below the RPA one [21, 2]. The strong damping of the collective mode starts at lower momentum transfer, compared to RPA. This is the result of two effects, first the lowering of the collective mode torward the p-h continuum due to exchange effects. Second the up shift of the p-h continuum due to the inclusion of the Fock-energy, which can be modeled by a effective mass of $m = 0.84$ in the kinetic energy.

3.8 An alternative transformation of the cTDHF equation

The transformation given above is not mandatory. Rather we have a few possibilities to transform the cTDHF equations. The difficulty is to find the best and what are the criteria which determine the best. Here we propose a transformation that yields an energy independent effective interaction. Let's write the cTDHF matrix in the form

$$\left[\Omega + \frac{1}{2}\Omega\underline{\mathbf{N}} + \frac{1}{2}\underline{\mathbf{N}}\Omega + \begin{pmatrix} W_{ph,p'h'} & B \\ B^* & W_{p'h',ph} \end{pmatrix}\right] = \left[\mathbf{1}+\underline{\mathbf{N}}\right]^{\frac{1}{2}}\left[\Omega+\widetilde{\mathbf{V}}_{\mathrm{p-h}}\right]\left[\mathbf{1}+\underline{\mathbf{N}}\right]^{\frac{1}{2}}, \quad (3.71)$$

with

$$\underline{\mathbf{N}} = \begin{pmatrix} N_{ph,p'h'} & 0 \\ 0 & N_{p'h',ph} \end{pmatrix} \quad (3.72)$$

and

$$\overline{\mathbf{N}} = \mathbf{N} - \underline{\mathbf{N}} \quad (3.73)$$

The effective interaction is then

$$\begin{aligned} \widetilde{\mathbf{V}}_{\mathrm{p-h}} \;=\; & (\mathbf{1}+\underline{\mathbf{N}})^{-\frac{1}{2}}\left[\left(1+\frac{1}{2}\underline{\mathbf{N}}\right)\begin{pmatrix} e_{ph} & 0 \\ 0 & e_{ph}\end{pmatrix}\left(1+\frac{1}{2}\underline{\mathbf{N}}\right) - \frac{1}{4}\underline{\mathbf{N}}\begin{pmatrix} e_{ph} & 0 \\ 0 & e_{ph}\end{pmatrix}\underline{\mathbf{N}}\right. \\ & \left. + \begin{pmatrix} W_{ph,p'h'} & B \\ B^* & W_{p'h',ph} \end{pmatrix}\right](\mathbf{1}+\underline{\mathbf{N}})^{-\frac{1}{2}} - \begin{pmatrix} e_{ph} & 0 \\ 0 & e_{ph}\end{pmatrix} \end{aligned} \quad (3.74)$$

This effective interaction is less appealing than in (3.22) due to the explicit appearance of the single particle hole energies and due to the separate treatment of the B-channel. But up to first order in $\underline{\mathbf{N}}$ the dependence on the particle hole energy vanishes. An

important advantage is that with this transformation the effective interaction is not energy dependent. Omitting the B-matrix leads to a nice relation for the m_0 sumrule. Note that the B-matrix is zero anyhow for a good enough ground state theory. This leads immediately to a decomposition of the response in $\delta u_{ph}^{(1+)}$ and $\delta u_{ph}^{(1-)}$. Consequently the final result is of the form

$$\chi(q,\omega) = \tilde{\chi}(q,\omega) + \tilde{\chi}^*(q,-\omega) \tag{3.75}$$

which is an analytic property of the exact response, as derived in [39]. In that form the sumrule is evaluated analytically. Since

$$\tilde{\chi}(q,\omega) = \mathbf{1_R}\,(\mathbf{1}+N_{p_1h_1,ph})^{\frac{1}{2}}\left[e_{ph}-\hbar\omega-\mathrm{i}\eta+V^A_{ph,p'h'}\right]^{-1}(\mathbf{1}+N_{p'h',p_2h_2})^{\frac{1}{2}}\,\mathbf{1_C}\ , \tag{3.76}$$

it is easy to show that[1]

$$\int d\hbar\omega\Im m\left[e_{ph}-\hbar\omega-\mathrm{i}\eta+V^A_{ph,p'h'}\right]^{-1} = \pi\mathbf{1} \tag{3.77}$$

With that the sumrule is cast into a form analog to eq. (3.57). It is now difficult to decide whether this or the other transformation is better. If no approximations where made, both forms are equivalent. Finally we summarize the pros and cons of the discussed transformation.

+ Effective interaction is energy independent

+ If the B matrix is set to zero, this transformation keeps the 'diagonal' form.

+ Compared to the previous transformation, a nice relation for the m_0 sumrule is obtained

– Diagrammatically not that rich as the original one (This becomes less important as CBF matrix elements are calculated more accurately.)

The last point makes it less attractive for a numerical application. On the other hand, its formal properties are very convincing. Once we have a good enough ground state, such that the B-matrix is zero, one does not want to destroy this property by the transformation, not at least to keep numerical speed. It is worth to put more time in determining the CBF matrix elements, because once we have the matrices we only need one inversion for the transformation and an eigenvalue decomposition for the determination of the spectrum for a definite momentum transfer.

[1] First one needs the spectral decomposition of the matrix. The inversion is then simply done by taking the reciprocal value of the eigenvalues. Since η is infinitesimal the imaginary part gives only a δ-function. The integration is then easily performed.

We are able to go one step further, in order to obtain an approximation of similar simplicity than RPA. This is done by omitting exchange terms and Fock energies and set the B-channel to zero (as would be the case for the exact ground state). We obtain

$$\chi^{(\mathrm{TDAa})}(q,\omega) = \frac{\frac{S}{S_F}\kappa_0^{(+)}(q,\omega)}{1+V_{scRPA}(q)\kappa_0^{(+)}(q,\omega)} + \frac{\frac{S}{S_F}\kappa_0^{(-)}(q,\omega)}{1+V_{scRPA}(q)\kappa_0^{(-)}(q,\omega)} \tag{3.78}$$

with

$$V_{scRPA}(q) = \frac{t(q)}{S_F(q)}\left(\frac{1}{S_F(q)} - \frac{1}{S(q)}\right). \tag{3.79}$$

Consequently and in order to be consistent we should also neglect the off diagonal part of H in the A-channel i.e. $H_{ph,p'h'} = \delta_{p,p'}\delta_{h,h'}e_{ph}$. The result for the response function is

$$\chi^{(\mathrm{TDAb})}(q,\omega) = \frac{\frac{S^2}{S_F^2}\kappa_0^{(+)}(q,\omega)}{1+\hbar\omega\tilde{\Gamma}_{\mathrm{dd}}(q)\kappa_0^{(+)}(q,\omega)} + \frac{\frac{S^2}{S_F^2}\kappa_0^{(-)}(q,\omega)}{1+\hbar\omega\tilde{\Gamma}_{\mathrm{dd}}(q)\kappa_0^{(-)}(q,\omega)} \tag{3.80}$$

This response function, a type of a correlated Tamm-Dancoff approximation (cTDA), fulfils the m_0 and the m_1 sumrule by definition. As in RPA there is no place for fitting parameters, but this is expected, since the two sumrules are very restricting conditions for the response function. For example if one want to lower the position of the collective mode one has to add strength above the collective mode in order to fulfill both sumrules. Thus this can only be done consistently by introducing multi pair excitations, which yield a broad continuum at higher energies. In other words, the overestimation of the energy of the collective mode is a result of the restriction to single p-h excitations. From that we conclude that not an effective mass is the dominant effect for lowering the position of the collective mode, it would rather be multi pair excitations which are responsible. Therefore not an effective mass should be modified in order to fit an experiment but rather the multi-pair continuum.

3.9 Overview and concluding remarks

In figure 3.8 a diagram is provided which gives a survey over the different approximations and transformations given in this chapter. Starting from the equations of motion derived in the Jastrow-correlated basis (cTDHF) we are already in a position to derive the density response function. At this level pair excitations can be included by changing the CBF matrix elements to energy dependent effectvie matrix elements. But more on that in the next chapter.

RPA type equations are obtained by transformation to the density matrix elements of the non interacting system, eq. (3.21). If no further approximations are made, we obtain

expressions for the effective interaction in the direct and the exchange channel (xRPA). By neglection of the Fock energy and the exchange interaction the ordinary RPA is obtained.

But there is no need to stick to the transformation (3.21). It is possible to find a transformation in which the energy dependence is exactly diagonal, eq. (3.71). Making the analog approximations that led to RPA, we end up with cTDA (3.78).

Finally replacing the particle hole band by its collective approximation, in both the RPA and cTDA, the well known Feynman spectrum is obtained.

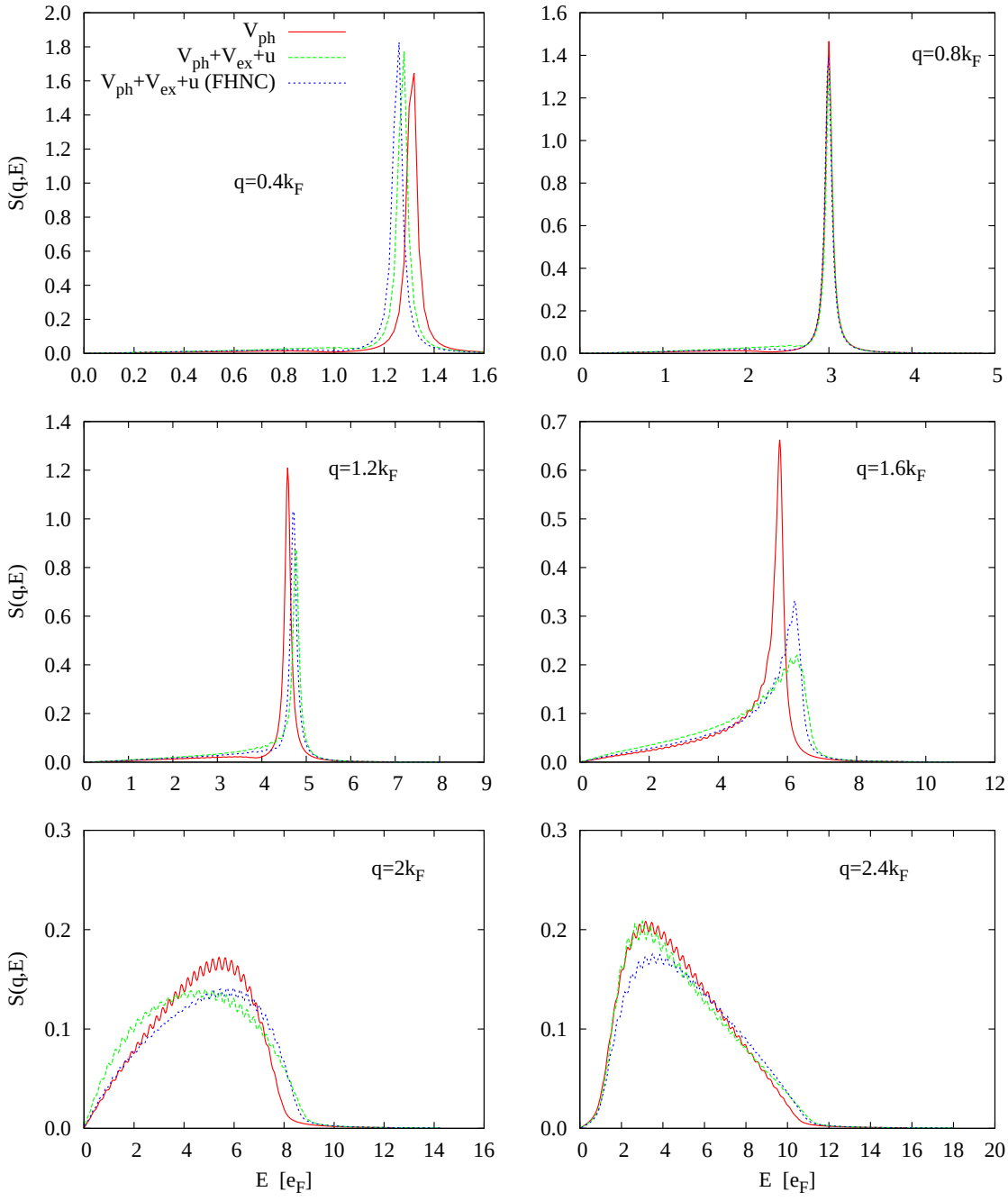

Figure 3.6: The dynamic structure function at momentum transfers $q = 0.4$, 0.8, 1.2, 1.6, 2 and $2.4k_F$ is plotted. See text for details.

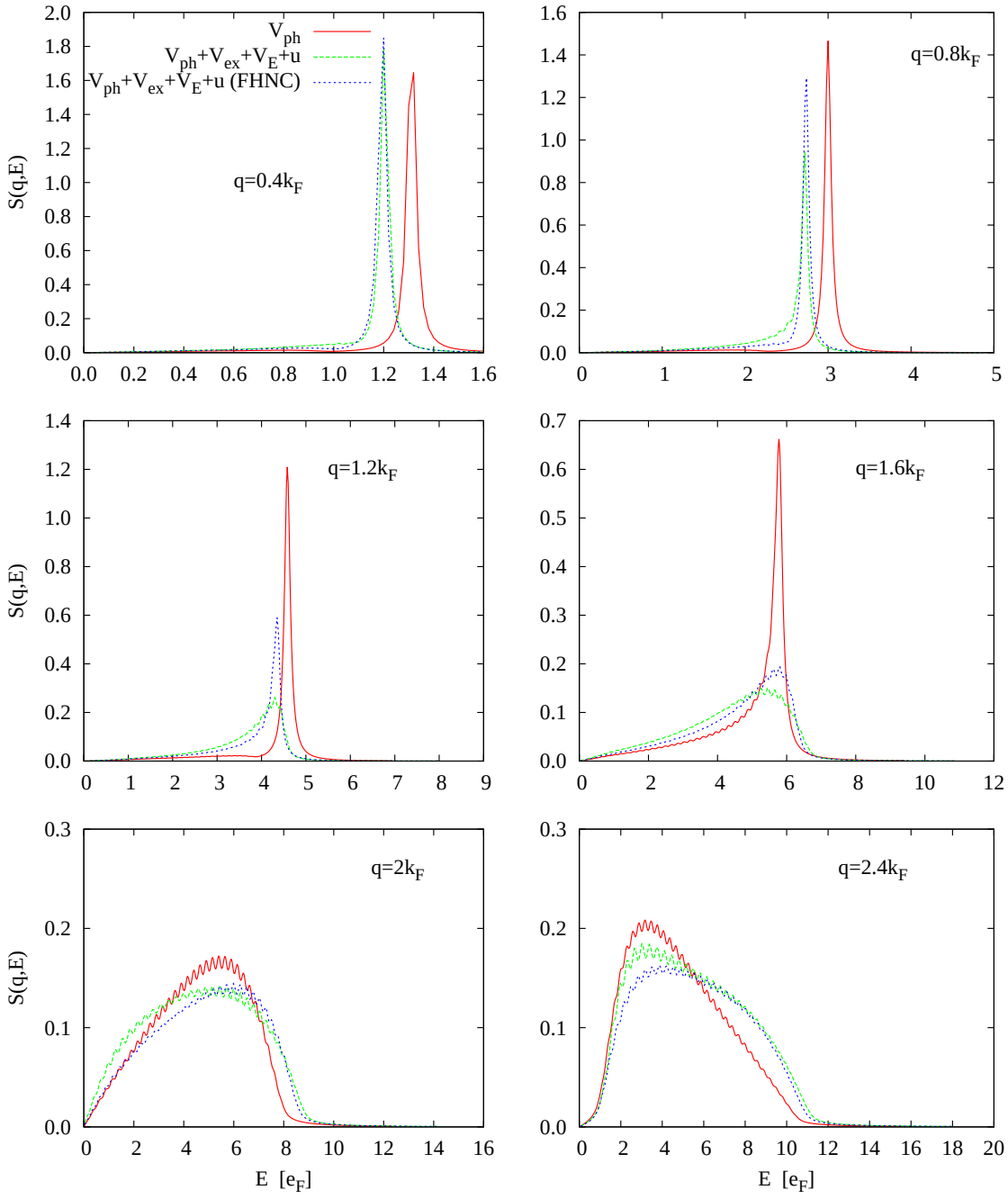

Figure 3.7: The basically same as in figure 3.6, only different approximations. See text for details.

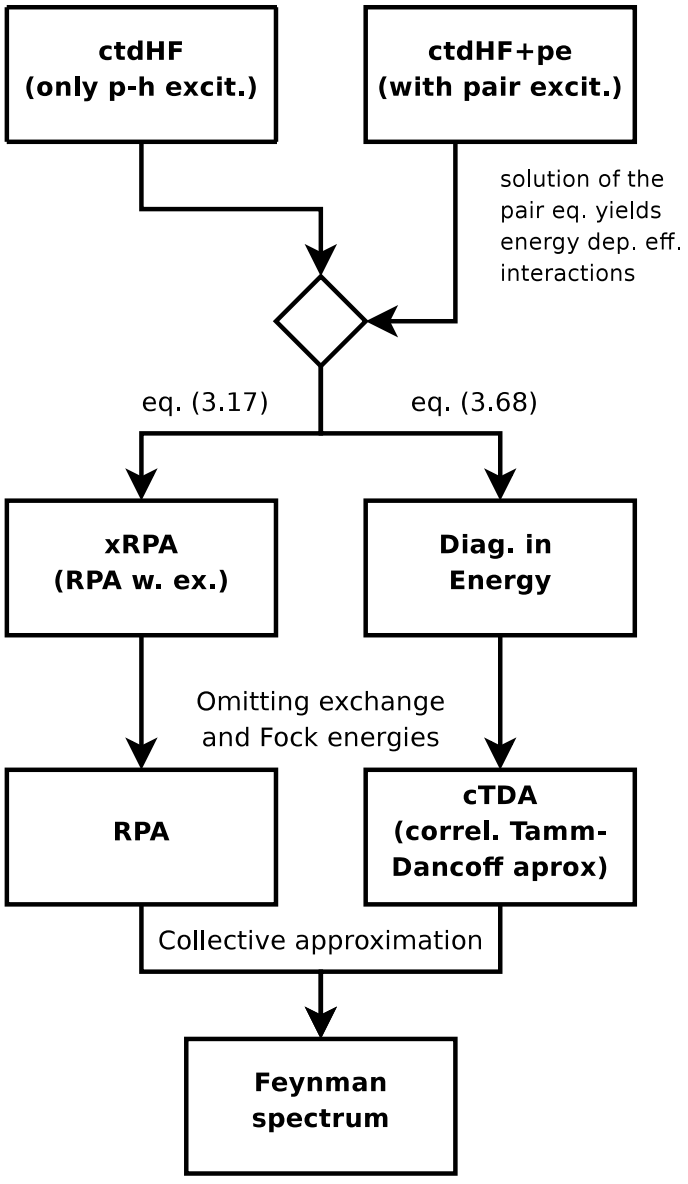

Figure 3.8: Overview of the different approximations and transformations given in this chapter.

Chapter 4

Pair-excitations without exchange

In resent publications we showed that pair excitations play a crucial role in strongly correlated Fermi-fluids [7, 9]. The main effects are a lowering of the collective mode towards the experimental value and a natural broadening of the collective mode. The broadening is result of the possible decay of the collective mode into pair excitations. Further more the roton minimum is significantly lowered. This effect is especially pronounced in two dimensional ^{3}He, where the roton resharpens at the lower border of the PHB. This observation has been confirmed experimentally [I].

In this chapter we only give an outline of the derivation. All the details and more results are found in the publications [I, II].

4.1 Outline of the derivation

4.1.1 Transition density

The transition density as given in chapter 2 is easily extended to include pair fluctuations:

$$\begin{aligned}\delta\rho(\mathbf{r};t) &= \sum_{ph}\rho_{0,ph}(\mathbf{r})\delta u^{(1)}_{ph}(t) + \frac{1}{2}\sum_{pp'hh'}\rho_{0,pp'hh'}(\mathbf{r})\delta u^{(2)}_{pp'hh'}(t) \\ &= \sum_{ph}\tilde{\rho}^{F}_{0,ph}(\mathbf{r})\left[\sum_{p'h'}M_{ph,p'h'}\delta u^{(1)}_{p'h'}(t) + \frac{1}{2}\sum_{p'p''h'h''}M_{ph,p'p''h'h''}\delta u^{(2)}_{p'p''h'h''}(t)\right] \quad (4.1)\end{aligned}$$

Defining a new one-particle one-hole amplitude

$$\delta v^{(1)}_{ph}(t) = \delta u^{(1)}_{ph}(t) + \frac{1}{2}\sum_{p'p''h'h''}M^{(I)}_{ph,p'p''h'h''}\ \delta u^{(2)}_{p'p''h'h''}(t)\,. \quad (4.2)$$

with

$$M^{(I)}_{ph,p'p''h'h''} = \sum_{p_1h_1}M^{-1}_{ph,p_1h_1}M_{p_1h_1,p'p''h'h''} \quad (4.3)$$

Inserting this into the expression for the transition density gives

$$\delta\rho(\mathbf{r};t) = \sum_{php'h'} \tilde{\rho}^{F}_{0,ph}(\mathbf{r}) M_{ph,p'h'} \delta v^{(1)}_{p'h'}(t)\,. \tag{4.4}$$

The definition of the renormalized one-particle one-hole amplitude is vital for the derivation of the Euler-Lagrange equations. It leads to decoupled equations for the single pair and double pair fluctuations.

4.1.2 The equations of motion including pair fluctuations

In the equation of motion for the single pair fluctuations an additional term, which describes the coupling to pair fluctuations, appears:

$$\begin{aligned} & \sum \left[H'_{ph,p'h'} \mp (\hbar\omega + \mathrm{i}\eta) M_{ph,p'h'}\right] \delta v^{(1\pm)}_{p'h'} + \sum H'_{pp'hh',0}\, \delta v^{(1\mp)}_{p'h'} \\ + \;& \frac{1}{2} \sum \left[K^{(ph)}_{p'p''h'h'',0}\, \delta u^{(2\mp)}_{p'p''h'h''} + K_{ph,p'p''h'h''}\, \delta u^{(2\pm)}_{p'p''h'h''}\right] = -2 \int d^3r\, \rho_{0,ph}(\mathbf{r})\, h_{\mathrm{ext}}(\mathbf{r};\omega)\,. \end{aligned} \tag{4.5}$$

The equations of motion in the pair channel are

$$\begin{aligned} - \;& \sum \left[K_{pp'hh',p''p'''h''h'''} \mp (\hbar\omega + \mathrm{i}\eta) M^{(I)}_{pp'hh',p''p'''h''h'''}\right] \delta u^{(2\pm)}_{p''p'''h''h'''} \\ = \;& 2 \sum \left[K^{(p''h'')}_{pp'hh',0} \delta v^{(1\mp)}_{p''h''} + K_{pp'hh',p''h''} \delta v^{(1\pm)}_{p''h''}\right]\,. \end{aligned} \tag{4.6}$$

In convolution approximation we obtain

$$\begin{aligned} M^{(I)}_{pp'hh',p''p'''h''h'''} \;\approx\; & \delta_{pp''}\delta_{p'p'''}\delta_{hh''}\delta_{h'h'''} + \delta_{pp''}\delta_{hh''} \langle p'h'''|\, \tilde{\Gamma}_{\mathrm{dd}}\, |h'p'''\rangle \\ + \;& \delta_{p'p'''}\delta_{h'h'''} \langle ph''|\, \tilde{\Gamma}_{\mathrm{dd}}\, |hp''\rangle + \langle p'h'''|\, \tilde{\Gamma}_{\mathrm{dd}}\, |h'p'''\rangle \langle ph''|\, \tilde{\Gamma}_{\mathrm{dd}}\, |hp''\rangle \end{aligned} \tag{4.7}$$

and

$$\begin{aligned} K_{pp'hh',p''p'''h''h'''} \;\approx\; & \delta_{pp''}\delta_{p'p'''}\delta_{hh''}\delta_{h'h'''}(e_{ph} + e_{p'h'}) \\ + \;& \delta_{pp''}\delta_{hh''} \left[e_{ph} \langle p'h'''|\, \tilde{\Gamma}_{\mathrm{dd}}\, |h'p'''\rangle\right] \\ + \;& \{pp''hh'' \leftrightarrow p'p'''h'h'''\}\,. \end{aligned} \tag{4.8}$$

The coupling to pair fluctuations is described on the one hand by the off diagonal three body vertex $K^{(ph)}_{p'p''h'h'',0}$ which vanishes for $q > 2$ and can safely be neglected as shown in [II]. Concentrating on the important physics and keeping the results compact we omit this term in the following derivation. The other is the important three body vertex, which is in the localized form

$$K_{q,q'q''} \;=\; \frac{S(q')S(q'')}{S_F(q)S_F(q')S_F(q'')} \frac{\hbar^2}{2m\,N^2} \left[\mathbf{q}\cdot(\mathbf{q}'\tilde{X}_{\mathrm{dd}}(q') + \mathbf{q}''\tilde{X}_{\mathrm{dd}}(q''))\right]\,. \tag{4.9}$$

4.1.3 Solution of the pair equation

The exact solution of the two-pair equation is presented in [II]. Here we present an approximate solution which captures the important physics.

The pair equation is simplified by convoluting the whole equation with

$$M^{-1}_{ph,p''h''}M^{-1}_{p'h',p'''h'''} = \left[\delta_{p,p''}\delta_{h,h''} - \langle ph''|\,\tilde{X}_{dd}\,|hp''\rangle\right]\left[\delta_{p',p'''}\delta_{h',h'''} - \langle p'h'''|\,\tilde{X}_{dd}\,|h'p'''\rangle\right]$$

which is the inverse of $M^{(I)}_{pp'hh',p''p'''h''h'''}$. As result the pair equation becomes diagonal in the energy

$$\begin{aligned} & E_{pp'hh',p''p'''h''h'''}(\omega)\delta u^{(2\pm)}_{p''p'''h''h'''} \\ \equiv\ & \left[-e_{ph} - e_{p'h'} \pm (\hbar\omega + \mathrm{i}\eta)\right]\delta u^{(2\pm)}_{pp'hh'} \\ & + \sum e_{p''h''}\left[\langle ph''|\,X_{dd}\,|hp''\rangle\,\delta u^{(2\pm)}_{p''p'h''h'} + \langle p'h''|\,X_{dd}\,|h'p''\rangle\,\delta u^{(2\pm)}_{pp''hh''}\right] \\ =\ & \sum M^{-1}_{ph,p''h''}M^{-1}_{p'h',p'''h'''}K_{p''p'''h''h''',p_4h_4}\delta v^{(1\pm)}_{p_4h_4}\,. \end{aligned} \tag{4.10}$$

Here the factor 2 cancels due to symmetry of the pair amplitude $\delta u^{(2\pm)}_{pp'hh'} = \delta u^{(2\pm)}_{p'ph'h}$. An approximation which captures the right physics is obtained by expanding the pair equation in a perturbation series, whose zeroth order is the collective approximation:

$$E^{(0)}_{pp'hh',p''p'''h''h'''}(\omega) = \delta_{p,p''}\delta_{p',p'''}\delta_{h,h''}\delta_{h',h'''}\left[-\varepsilon(q) - \varepsilon(q') \pm (\hbar\omega + \mathrm{i}\eta)\right] \tag{4.11}$$

The first order perturbation

$$\begin{aligned} E^{(1)}_{pp'hh',p''p'''h''h'''}(\omega) = {} & \delta_{p,p''}\delta_{p',p'''}\delta_{h,h''}\delta_{h',h'''} \\ & \times\left[-e_{ph} + \frac{\hbar^2q^2}{2mS_F(q)} - e_{p'h'} + \frac{\hbar^2q'^2}{2mS_F(q')} \pm (\hbar\omega + \mathrm{i}\eta)\right] \end{aligned} \tag{4.12}$$

gives then the two particle two hole continuum. Combining these two terms leads to a two particle two hole continuum centered around the Feynman dispersion. We are able to invert the operator (up to first order) acting on the pair amplitudes

$$\delta u^{(2\pm)}_{qq'} \;=\; \frac{S_F(q'')\mu^{(+)}_0\left(q,q',\pm\omega + \frac{\hbar}{2m}\left[q^2X(q) + q'^2X(q')\right]\right)}{S(q)S(q')}NK_{qq',q''}\delta v^{(1\pm)}_{q''}\,.$$

Where we introduced the pair analog of the partial Linhard function $\mu^{(+)}_0$

$$\mu^{(+)}_0(q,q',\omega) = \frac{1}{N^2}\sum_{hh'}\frac{n(h)n(h')\bar{n}(h+q)\bar{n}(h'+q')}{\hbar\omega - e_{ph} - e_{p'h'} + i\eta}\,. \tag{4.13}$$

This solution is inserted in the single pair equation and thus removes the explicit dependence on the pair fluctuations. At the end one arrives at a form identical to (3.21).

The only difference is a new definition of $\mathbf{W}$, which is now ω dependent. Thus the final equation of motion:

$$\begin{aligned} & -2\int \rho_{0,ph}(\mathbf{r})h_{\rm ext}(\mathbf{r},\omega) - \sum \left[H'_{ph,p'h'} \mp (\hbar\omega + \mathrm{i}\eta)M_{ph,p'h'}\right]\delta v^{(1\pm)}_{p'h'} - \sum H_{pp'hh',0}\delta v^{(1\mp)}_{p'h'} \\ + & \sum K^2_{q,q'q''}\frac{S_F(q)^2 S_F(q')S_F(q'')\mu_0^{(+)}\left(q',q'',\pm\omega+\frac{\hbar}{2m}\left[q'^2X(q')+q''^2X(q'')\right]\right)}{2S(q')S(q'')}N^3\delta v^{(1\pm)}_q \\ = & \; S_F(q)\Delta W_A(q,\pm\omega)\delta v^{(1\pm)}_q \end{aligned} \tag{4.14}$$

In matrix notation this changes (3.19) to

$$\begin{aligned} \mathbf{W}(\omega) &= \begin{pmatrix} W_{ph,p'h'}(\omega) & W_{pp'hh',0}(-\omega) \\ W_{0,pp'hh'}(\omega) & W_{p'h',ph}(-\omega) \end{pmatrix} \\ &= \begin{pmatrix} W_{ph,p'h'}+\Delta W_A(q,\omega) & W_{pp'hh',0}+\Delta W_B(q,\omega) \\ W_{0,pp'hh'}+\Delta W_B(q,-\omega) & W_{p'h',ph}+\Delta W_A(q,-\omega) \end{pmatrix} \end{aligned} \tag{4.15}$$

The approximation $K^{(ph)}_{p'p''h'h'',0} = 0$ implies $\Delta W_B(q,\omega) = 0$. The transformation to the RPA form is completely analog to (3.21), except that the effective interaction matrix has no longer identical entry's.

$$\mathbf{V}_{p-h} = \begin{pmatrix} V_A(q,\omega) & V_B(q,-\omega) \\ V_B(q,\omega) & V_A(q,-\omega) \end{pmatrix} \tag{4.16}$$

4.1.4 Response function

This makes the response function only a little more complicated than in RPA. We obtain

$$\begin{aligned} \chi(q;\omega) &= N(q;\omega)/D(q;\omega) \\ N(q;\omega) &= \kappa_0(q;\omega) + \kappa_0^*(q;-\omega) \\ &- \kappa_0(q;\omega)\kappa_0^*(q;-\omega)\left[\tilde{V}_{\rm A}(q;\omega) + \tilde{V}^*_{\rm A}(q;-\omega) - \tilde{V}_{\rm B}(q;\omega) - \tilde{V}^*_{\rm B}(q;-\omega)\right] \\ D(q;\omega) &= 1 - \kappa_0(q;\omega)\tilde{V}_{\rm A}(q;\omega) - \kappa_0^*(q;-\omega)\tilde{V}^*_{\rm A}(q;-\omega) \\ &+ \kappa_0(q;\omega)\kappa_0^*(q;-\omega)\left[\tilde{V}_{\rm A}(q;\omega)\tilde{V}^*_{\rm A}(q;-\omega) - \tilde{V}_{\rm B}(q;\omega)\tilde{V}^*_{\rm B}(q;-\omega)\right] . \end{aligned} \tag{4.17}$$

with the partial Lindhard functions

$$\kappa_0(q;\omega) \equiv \frac{1}{N}\sum_h \frac{\bar{n}_{\mathbf{p}} n_{\mathbf{h}}}{\hbar\omega - e_{ph} + \mathrm{i}\eta} \tag{4.18}$$

which relate to the full Lindhard function

$$\chi_0(q;\omega) = \kappa_0(q;\omega) + \kappa_0^*(q;-\omega)\,. \tag{4.19}$$

It is spelled out explicitly and extensively discussed in appendix B.2.

Chapter 5

The full theory: Pair-excitations and exchange

Now we are able to combine the results of the last two chapters, which means taking exchange and double pair excitations into account. First we show how to properly include double pair excitations in the xRPA formalism. After that we apply the theory to ^{3}He in three dimensions. (The generalization to 2D systems is no problem.) Then we make the postphoned comparison with the experiment[21, 17].

5.1 The transition density

The expression for the transition density given in eq. (4.1) is exact. In the last chapter we neglected all exchange diagrams. Now we want to investigate what changes if we include exchanges. In principle it is possible to include all exchange diagrams. But we argue that since the effect of double pair excitations and the effect of exchange diagrams alone is small, the effect of exchanges in the double pair channel is negligible. Therefore we can safely neglect exchange diagrams in the double pair channel. We show now that with this approximation the explicit expression for $M^{(I)}_{ph,p'p''h'h''}$ is unchanged, regardless of whether we take exchange in $M_{ph,p'h'}$ into account or not. For that reason we have to execute

$$M_{ph,p'p''h'h''} = \sum_{p_1h_1} M_{ph,p_1h_1} M^{(I)}_{p_1h_1,p'p''h'h''} \tag{5.1}$$

and see what diagrams are generated if we include exchange diagrams in M_{ph,p_1h_1}. The result of this operation is shown in figure 5.1. We see that all diagrams generated are indeed part of $M_{ph,p'p''h'h''}$.

If we look at the single pair – double pair coupling

$$K_{ph,p'p''h'h''} = H_{ph,p'p''h'h''} - \sum_{p_1h_1} H_{ph,p_1h_1} M^{(I)}_{p_1h_1,p'p''h'h''}\,, \tag{5.2}$$

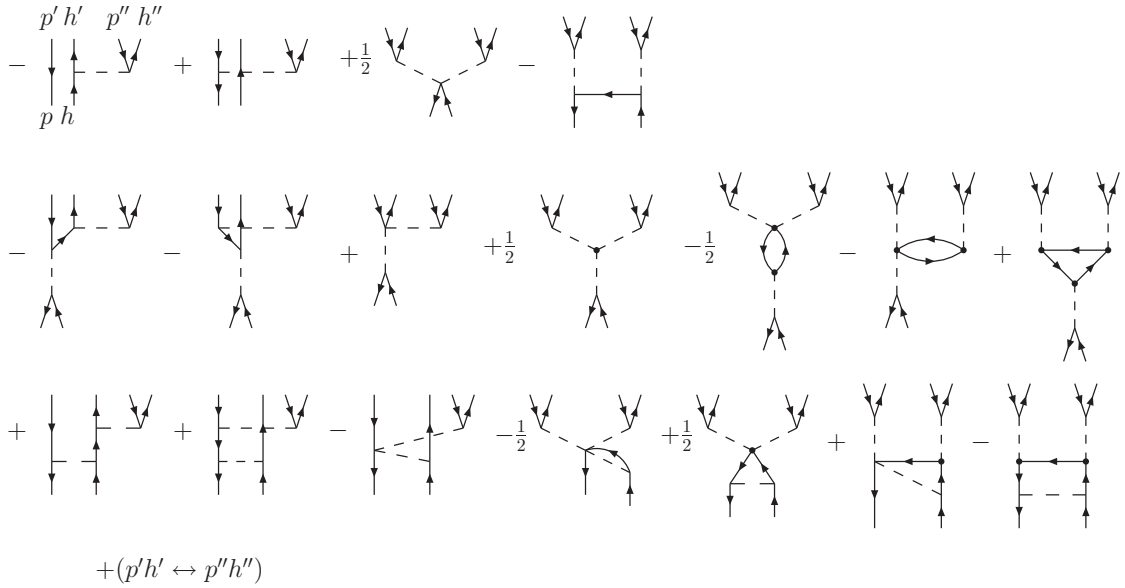

Figure 5.1: The figure shows the diagrams generated by eq. (5.1).The first line is $M^{(I)}_{ph,p'p''h'h''}$. The second line is generated by multiplying all direct diagrams in M_{ph,p_1h_1}. The last line is the result of multiplication of exchange diagrams. We observe that in doing so we generate some exchange diagrams of $M_{ph,p'p''h'h''}$.

we observe that the single pair quantity H_{ph,p_1h_1} enters. To be rigorous one has to take the exchange in that quantity into account, but as we mentioned earlier it will only give a small effect on the response, since two small quantities come together. Therefore we neglect it in the numerical evaluation. (Altough it should be no big problem to include it.) Thus we end up with the same vertex as in the previous chapter (4.9).

Using the notation introduced in chapter 3 we obtain

$$\mathbf{V}_{p-h} = \mathbf{V}^{(d)}_{p-h} + \mathbf{V}_{ex} + \mathbf{V}_E + \mathbf{V}_F + \mathbf{V}_{pair}(\omega) \tag{5.3}$$

with

$$\mathbf{V}_{pair}(\omega) = \left[\mathbf{1} + \frac{1}{2}\mathbf{N}\right]^{-1} \begin{pmatrix} \Delta W_A(q,\omega) & \Delta W_B(q,-\omega) \\ \Delta W_B(q,\omega) & \Delta W_A(q,-\omega) \end{pmatrix} \left[\mathbf{1} + \frac{1}{2}\mathbf{N}\right]^{-1} \tag{5.4}$$

The inclusion of exchanges is possible as long as they don't affect the solution of the pair equation. In a next step it is possible to include the exchange terms in the transformation. This is possible without much computational effort. If one wants to include further exchange diagrams, this is only possible with enormous additional computational effort. This has to be balanced against the gain in accuracy of the result. As mentioned earlier, not much change in the result is expected. Nevertheless we want to show how in principle this can be done. In a first step exchanges are taken into account in the various elements of the tree body vertex $K_{ph,p'p''h'h''}$. As a consequence this quantity becomes non local. (Of

course one can localize it again by calculating the Fermi sea average. But this will have a negligible effect on $K_{q,q'q''}$, e.g. $H_{q,q'q''}$ is totally unchanged, since it is already exact.) The non locality of the part that couples to the one body quantity δv_{ph} is no problem, because this is treated in the same way as the other parts of the interaction. The time consuming part is the numerical solution of the pair equation, which is beyond current possibilities.

One thing left to mention is that, if we want to include exchanges in $\Delta W_A(q,\omega)$ and $\Delta W_B(q,\omega)$ these terms become non local and can not be written as antisymmetrized matrix elements. For example

$$\Delta W_{A,php'h'} \neq \langle ph'| \Delta W_A |hp'\rangle_a \tag{5.5}$$

5.2 Results and comparison with the experiment

We applied the procedure described above to ^{3}He in 3 dimensions at saturation density. In fig. 5.2 we compare the different approximations. The modification of the spectrum due to the inclusion of exchange is most interesting in the low momentum transfer region $q < 2k_F$. In this region we can compare with the experiment [21, 17, 2] as shown in figure 5.3 and 5.4. For the interaction we took the most important terms in the interaction matrix into account:

$$\mathbf{V}_{p-h} = \mathbf{V}^{(d)}_{p-h} + \mathbf{V}_{ex} + \mathbf{V}_E + \mathbf{V}_{pair}(\omega) \tag{5.6}$$

The agreement is very exciting. Most interestingly is the effect of the inclusion of the Fock-term in the single particle excitations. It moves the upper border of the PHB to higher energies (fig. 5.4), which results in an earlier appearance of Landau-damping, as indicated by the width of the collective mode observed in experiments [17, 21]. (Fore more details see applications chapter in [II].)

We know about the weakness of the Fock-energy, which should be viewed as an average over the real excitation energies, which are of course dependent on the starting point in the Fermi-sphere. In [10, 35, 23, 22] it has been shown that the effective mass of the excitation energy is strongly peaked close to the surface of the Fermi-sphere. The ansatz made in [10, 35] for the calculation of the effective mass, suggests that with the inclusion of pair excitations we are able to properly account for this effect. Work in that direction is in progress. It remains to mention that the ad hoc introduction of a constant effective mass of the order of the Fermi-surface effective mass is clearly oversimplified and inconsistent, not only with the first two sumrules, but also with experiments.

Despite the excellent agreement with the experiment some words of caution are in order. The energy dependent correction of the effective interaction $\mathbf{V}_E$ includes some additional diagrams of higher order (second order), but not all diagrams. This means

while the inclusion of $\mathbf{V}_E$ is an apparently good approximation for Helium it may not be that good for electrons. Due to the long range of the Coulomb interaction the limiting behavior has to be checked very carefully in order to be precise.

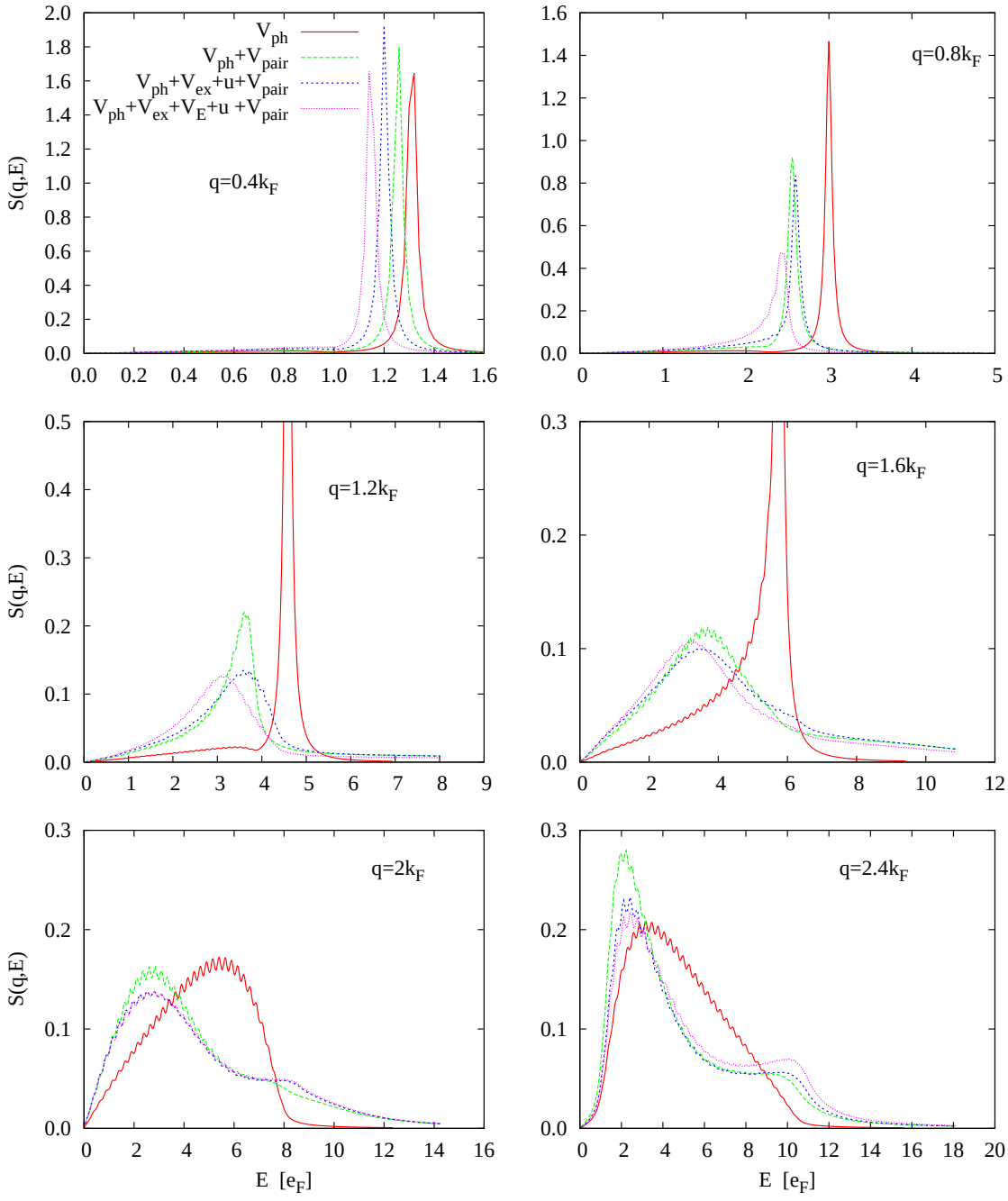

Figure 5.2: Comparison of different levels of implementation of our theory at momentum transfers $q = 0.4;\ 0.8;\ 1.2;\ 1.6;\ 2.0;\ 2.4\, k_F$.

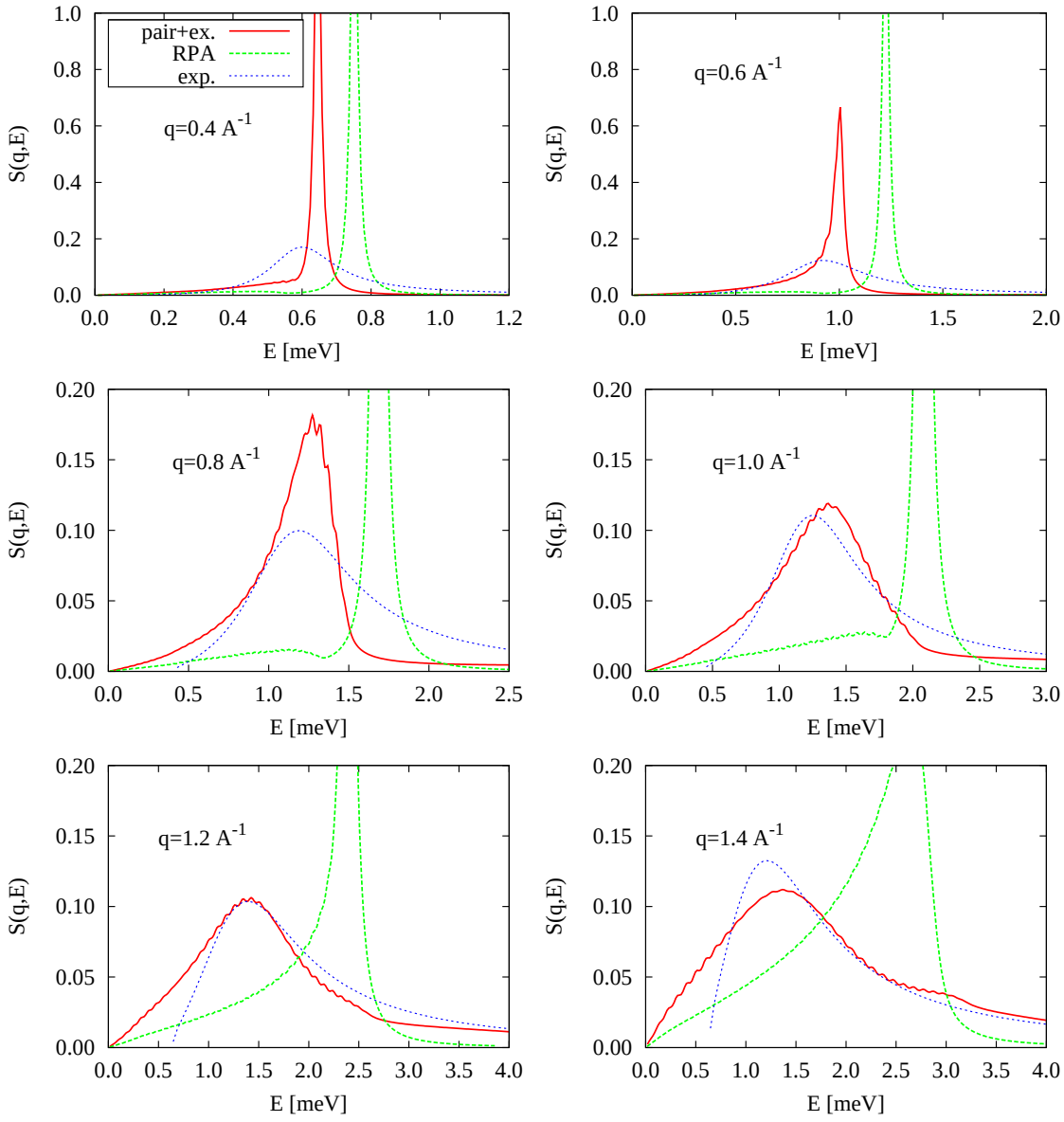

Figure 5.3: Comparison of the experiment[21, 17] and theory at momentum transfers $q = 0.4;\ 0.6;\ 0.8;\ 1.0;\ 1.2;\ 1.4\,\text{Å}^{-1}$.

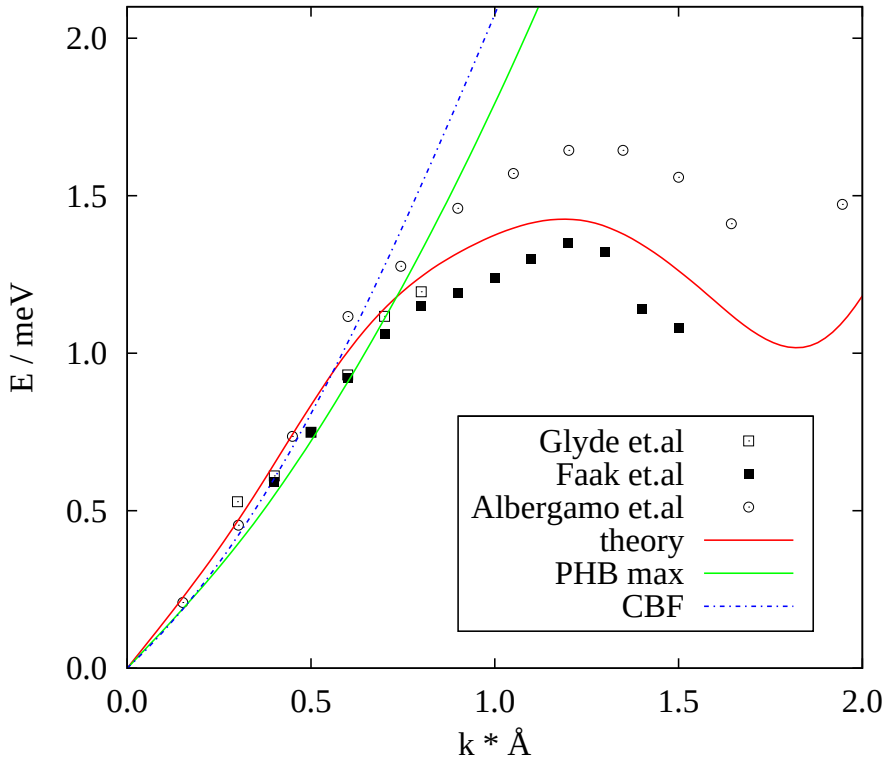

Figure 5.4: Comparison of the position of the collective mode in experiments by [21] (squares), [17] (solid squares) and [2] (circles) with the theory (red line). The upper border of the non interacting PHB is indicated by the green line. The cained blue line is the upper border of the PHB calculated with CBF theory.

Chapter 6

Conclusions and future prospects

The work on this thesis was started with the objective to investigate the influence of exchange effects on the density-density response function. It was expected that the inclusion of exchange terms has no big influence on the result, which would justify their omission. However we have shown that exchange effects modify the excitation spectrum in a way which is in accordance with the experiment and that their inclusion lead to a better understaning of the physics.

It has been shown that a change in the single particle excitation energies needs to be balanced with exchange terms in order to give the correct $q \to 0$ behavior and to keep the fulfilment of the sumrules. Equally important is the insight into the weakness of the simple RPA treatment in describing the dynamics of strongly correlated systems like ^{3}He. We have rigorously shown that including exchange terms at the cTDHF level leads to energy dependent interactions in the RPA equations. With this understanding it becomes clear that the introduction of a constant effective mass of the order of $m^* = 3m$ in order to fit the experimentally observed position of the collective mode, in the standard RPA is physically meaningless and any other fitting function is as well justified.

A different part of my thesis was to appropriately account for pair excitations. The work on this topic has been developed and successfully applied to different systems during the last years. It turned out that this is the most important part in arriving at a quantitative microscopic theory. Beside the expected lowering of the collective mode it also predicts a new phenomena, the reemerging of the collective mode below the PHB. Experimental results support this finding, which will have far reaching consequences and which await further investigation. Our results in [II] also show that the collective mode, when entering the PHB, becomes strongly damped, known as Landau damping. Additionally, we observed a slight kink in the dispersion of the collective mode. Application of these findings to the experimental results [17, 21] suggests that the collective mode is always close to the PHB and enters the PHB at relatively low momentum transfer, which

could simply be explained by an effective mass slightly lower than the bare mass $m^* < m$ contrary to common belief.

Finally, we combined these two approaches. It is remarkable that the CBF single particle energies can be fitted by an effective mass of $m^* = 0.84m$, which is in accordance with the argumentation above.

The agreement with the experiment is satisfactory and makes us self-confident for further investigations. The most obvious extension is the inclusion of selfenergy corrections in the excitations spectrum.[26] As already mentioned, this has to be done in a proper way in adjustment with the exchange channel. Work in this direction is in progress.

Future prospects

The results show that we have a powerful tool to describe quantum fluids on a microscopic basis. The question now is in which direction we want to develop this tool. We are at the crossroads with many different possibilities. The most promising are:

- Spin-density response: Neutron scattering experiments are sensitive to the relative spin-orientation too. This means that the spin-density response is also measured. But up to now no microscopic theory exists which is able to describe these excitations in a quantitative way. We believe that inclusion of exchange terms is the key, which allows us to make progress in this direction. Ideally, one should start from a spin-dependent FHNC calculation. Unfortunately this is a very demanding task and it is not yet clear if it can be done within the FHNC formalism [16]. If this is not possible one has to derive a new set of equations and see whether these can be solved in reasonable time. Work in this direction is in progress.

- Magnetic excitations: This point is closely related to the previous one. It should be possible to describe spin-waves, which are elementary excitations in an external magnetic field.

- Electrons in a solid: Instead of using a plane wave slater determinant one could also use a Slater determinant of band structure functions as starting point. It remains to show whether these need to be Jastrow correlated or not. However, the extension of FHNC theory to electrons in a lattice is a demanding task.

- Application to nuclear interactions: Exchange effects are especially important in nuclear matter. N.-H. Kwong has investigated this topic in his PhD thesis [36]. It would be interesting to extend the FHNC approach to nuclear interactions and consequently apply the theory developed in this thesis to this challenging problem.

Appendix A

The FHNC and FHNC' equations

A.1 The FHNC equations

The full set of equations are shown here for reference. The equations for the non-nodal quantities are expressed in coordinate space:

$$\begin{aligned}
X_{dd}(r) &= \exp\left[u(r)+N_{dd}(r)+E_{dd}(r)\right]-1-N_{dd}(r) \\
X_{de}(r) &= \left[1+\Gamma_{dd}(r)\right]\left[N_{de}(r)+E_{de}(r)\right]-N_{de}(r) \\
X_{ee}(r) &= \left[1+\Gamma_{dd}(r)\right]\left[-\frac{1}{\nu}L^2(r)+N_{ee}(r)+E_{ee}(r)\right]-N_{ee}(r) \\
&\quad +\left[1+\Gamma_{dd}(r)\right]\left[N_{de}(r)+E_{de}(r)\right]^2 \\
X_{cc}(r) &= -\frac{1}{\nu}L(r)\Gamma_{dd}(r)+E_{cc}(r)\,.
\end{aligned} \tag{A.1}$$

The four nodal quantities are calculated in momentum space:

$$\begin{aligned}
\tilde{N}_{dd}(k) &= \tilde{\Gamma}_{dd}(k)-\tilde{X}_{dd}(k) \\
&= \left[\tilde{\Gamma}_{dd}(k)+\tilde{\Gamma}_{de}(k)\right]\tilde{X}_{dd}(k)+\tilde{\Gamma}_{dd}(k)\tilde{X}_{de}(k) \\
\tilde{N}_{de}(k) &= \tilde{\Gamma}_{de}(k)-\tilde{X}_{de}(k) \\
&= S_d(k)-1-\tilde{\Gamma}_{dd}(k)-\tilde{X}_{de}(k) \\
\tilde{N}_{ee}(k) &= \tilde{\Gamma}_{ee}(k)-\tilde{X}_{ee}(k) \\
&= S(k)-2S_d(k)+1-\tilde{X}_{ee}(k)+\tilde{\Gamma}_{dd}(k) \\
\tilde{N}_{cc}(k) &= -\tilde{X}_{cc}(k)\left[\frac{\frac{1}{\nu}\tilde{l}(k)-\tilde{X}_{cc}(k)}{1-\tilde{X}_{cc}(k)}\right],
\end{aligned} \tag{A.2}$$

where we used

$$\begin{aligned} S_d(k) &= \frac{1-\tilde{X}_{de}(k)}{\left[1-\tilde{X}_{de}(k)\right]^2-\left[1+\tilde{X}_{ee}(k)\right]\tilde{X}_{dd}(k)} \\ \tilde{\Gamma}_{dd}(k) &= \frac{\tilde{X}_{dd}(k)}{\left[1-\tilde{X}_{de}(k)\right]^2-\left[1+\tilde{X}_{ee}(k)\right]\tilde{X}_{dd}(k)} \\ \tilde{\Gamma}_{de}(k) &= S_d(k)-1-\tilde{\Gamma}_{dd}(k) \\ \tilde{\Gamma}_{ee}(k) &= S(k)-1-\tilde{\Gamma}_{dd}(k)-2\tilde{\Gamma}_{de}(k) \end{aligned} \tag{A.3}$$

and in coordinate space

$$\begin{aligned} L(r) &= l(rk_F)-\nu\left[N_{cc}(r)+E_{cc}(r)\right] \\ \Gamma_{dd}(r) &= \exp\left[u(r)+N_{dd}(r)+E_{dd}(r)\right]-1\,. \end{aligned} \tag{A.4}$$

The radial distribution function expressed in terms of FHNC quantities is

$$\begin{aligned} g(r) &= 1+X_{dd}(r)+N_{dd}(r)+2X_{de}(r)+2N_{de}(r)+X_{ee}(r)+N_{ee}(r) \\ &= \left[1+\Gamma_{dd}(r)\right]\left\{-\frac{1}{\nu}L^2(r)+N_{ee}(r)+E_{ee}(r)+\left[1+N_{de}(r)+E_{de}(r)\right]^2\right\}. \end{aligned} \tag{A.5}$$

and the static structure factor assumes the form

$$S(k)=\frac{1+\tilde{X}_{ee}(k)}{\left[1-\tilde{X}_{de}(k)\right]^2-\left[1+\tilde{X}_{ee}(k)\right]\tilde{X}_{dd}(k)} \tag{A.6}$$

A.2 The FHNC' equations

Now $X'_{dd}(r)$ is obtained by replacing one of the parallel connections by a primed quantity:

$$X'_{dd}(r)=e^{u(r)+N_{dd}(r)+E_{dd}(r)}[v_{JF}(r)+N'_{dd}(r)+E'_{dd}(r)]-N'_{dd}(r) \tag{A.7}$$

This is the only equation were the potential enters. Next we have to consider the diagrammatic contribution from the T_{JF} term. This is obtained by replacing, in turn, every connected pair of exchange lines $l(r_{ij}k_F)l(r_{ik}k_F)$ by $\frac{\hbar^2}{4m}\nabla^2 l(r_{ij}k_F)l(r_{ik}k_F)$ in the cluster expansion of $g(r)$. This means that the FHNC equations have to be modified at places where $l(rk_F)$ appears. For example in the last equation in (A.1)

$$X'_{cc}(r)=-\frac{1}{\nu}L(r)\Gamma'_{dd}(r)+[1+\Gamma_{dd}(r)]E'_{cc}(r)+\Gamma_{dd}(r)\left[N'_{cc}(r)-\frac{\hbar^2}{4m\nu}\nabla^2 l(rk_F)\right] \tag{A.8}$$

For reference the remaining two non-nodal equations are

$$\begin{aligned}
X'_{de}(r) &= \Gamma'_{dd}(r)\left[N_{de}(r)+E_{de}(r)\right]+\left[1+\Gamma_{dd}(r)\right]E'_{de}(r)+\Gamma_{dd}(r)N'_{de}(r)\\
X'_{ee}(r) &= \Gamma'_{dd}(r)\left[-\frac{1}{\nu}L^2(r)+N_{ee}(r)+E_{ee}(r)+\left[N_{de}(r)+E_{de}(r)\right]^2\right]\\
&\quad +2\left[1+\Gamma_{dd}(r)\right]\left[L(r)\left[N'_{cc}(r)+E'_{cc}(r)\right]+\left[N_{de}(r)+E_{de}(r)\right]\left[N'_{de}(r)+E'_{de}(r)\right]\right]\\
&\quad +\left[1+\Gamma_{dd}(r)\right]E'_{de}(r)+\Gamma_{dd}(r)N'_{de}(r)\\
&\quad -\frac{\hbar^2}{2m\nu}\left[1+\Gamma_{dd}(r)\right]\left[L(r)\nabla^2 l(rk_F)+|\nabla l(rk_F)|^2\right] \qquad \text{(A.9)}
\end{aligned}$$

The nodal equations are obtained by a linearization[1] of the corresponding FHNC equations:

$$\tilde{N}'_{ij}(k)=\sum_{kl}\frac{\delta\tilde{N}_{ij}(k)}{\delta\tilde{X}_{kl}(k)}\tilde{X}'_{kl}(k) \qquad \text{(A.10)}$$

This leads directly to

$$\begin{aligned}
\tilde{N}'_{dd}(k) &= \left[S_d^2(k)-1\right]\tilde{X}'_{dd}(k)+2\tilde{\Gamma}_{dd}(k)S_d(k)\tilde{X}'_{de}(k)+\tilde{\Gamma}^2_{dd}(k)\tilde{X}'_{ee}(k)\\
\tilde{N}'_{de}(k) &= S_d(k)\left[S(k)-S_d(k)\right]\tilde{X}'_{dd}(k)\\
&\quad +\left[\tilde{\Gamma}_{dd}(k)\left[S(k)-S_d(k)\right]+S_d(k)\left[S_d(k)-\tilde{\Gamma}_{dd}(k)\right]\right]\tilde{X}'_{de}(k)\\
&\quad +\tilde{\Gamma}_{dd}(k)\left[S_d(k)-\tilde{\Gamma}_{dd}(k)\right]\tilde{X}'_{ee}(k)\\
\tilde{N}'_{ee}(k) &= \left[S(k)-S_d(k)\right]^2\tilde{X}'_{dd}(k)\\
&\quad +\left[\tilde{\Gamma}_{dd}(k)\left[S(k)-S_d(k)\right]+S_d(k)\left[S_d(k)-\tilde{\Gamma}_{dd}(k)\right]\right]\tilde{X}'_{de}(k)\\
&\quad +\left[\left[S_d(k)-\tilde{\Gamma}_{dd}(k)\right]^2-1\right]\tilde{X}'_{ee}(k)\\
\tilde{N}'_{cc}(k) &= \left[\frac{1-\frac{1}{\nu}\tilde{l}(k)}{\left[1-\tilde{X}_{cc}(k)\right]^2-1}\right]\tilde{X}'_{cc}(k) \qquad \text{(A.11)}
\end{aligned}$$

The only thing that is left is the connection

$$\Gamma'_{dd}(r)=X'_{dd}(r)+N'_{dd}(r) \qquad \text{(A.12)}$$

With this we derived the FHNC' equations. Finally the Euler-Lagrange equation in momentum space is

$$\frac{\hbar^2 k}{4m}[S(k)-1]+S'(k)=0 \qquad \text{(A.13)}$$

with

$$S'(k)=\sum_{i\in\{dd,de,ee\}}\frac{\partial S(k)}{\partial\tilde{X}_i(k)}\tilde{X}'_i(k)\,. \qquad \text{(A.14)}$$

[1]This means not that this is an approximation, rather it is a consequence of the β-derivative algorithm. (chain rule)

A.2.1 Simplified FHNC

Sometimes a simplified version of the FHNC-EL equations is useful. The simplified version yields the correct long wave length behavior by definition. In this limit we have

$$\tilde{X}_{de}(k) = \mathcal{O}(k) \quad \text{as} \quad k \to 0 \tag{A.15}$$

$$1 + \tilde{X}_{ee}(k) = S_F(k) + \mathcal{O}(k^2) \quad \text{as} \quad k \to 0 \tag{A.16}$$

as shown in [33]. Thus we obtain for the static structure factor

$$S(k) = \frac{S_F(k)}{1 - S_F(k)\tilde{X}_{\mathrm{dd}}(k)} = S_F(k)\left[1 + \tilde{\Gamma}_{\mathrm{dd}}(k)S_F(k)\right] \tag{A.17}$$

in the simplified FHNC. The other quantities are obtained by using the above mentioned long wave length properties. In the determination of CBF matrix elements it is sometimes opportune to use the static structure as input quantity[2] and calculate with the above equation the corresponding simplified FHNC quantities.

[2]Obtained for example from the experiment[24], FHNC or Monte Carlo calculations[11].

Appendix B

The partial Lindhard function and its pair analog

B.1 k-space integration

In this thesis we often have to sum over $\frac{1}{N}\sum_h n(h)\bar{n}(h+q)f(\mathbf{h},\mathbf{q})$. We can transform the sum to an integral

$$\frac{1}{N}\sum_h = \frac{\nu V}{8\pi^3 N}\int d^3h = \frac{\nu}{8\pi^3\rho}\int d^3h = \frac{6\pi^2}{8\pi^3 k_F^3}\int d^3h = \frac{1}{V_F}\int d^3h, \tag{B.1}$$

here we used $\rho = \frac{N}{V} = \frac{\nu k_F^3}{6\pi^2}$ where ν is the number of spin states and that $V_F = \frac{4\pi k_F^3}{3}$ is the volume of the Fermi-sphere. It is convenient to represent the momenta in units of k_F.

If $f(\mathbf{h},\mathbf{q})$ depends only on the dot product $\mathbf{hq}$ and $\mathbf{q}$, which is often the case, we can map the three dimensional integral to a one dimensional in the following way:

- introduce polarcoordinates, with the z-axis in direction of $\mathbf{q}$

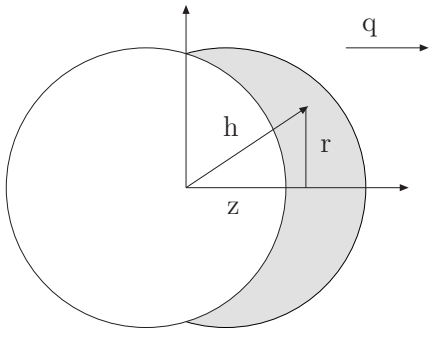

Figure B.1: The grey marked region indicates the integration range. The new coordinate system is also drawn.

- shift the origin about $-\mathbf{q}/2$. This delivers $\mathbf{h} \to \tilde{\mathbf{h}} + \frac{\mathbf{q}}{2}$
- then integrate over ϕ and r. This is possible because now f depends only on z, the projection of h on q

Now it is possible to write the integral in the following form

$$2\pi q \int_{L_q} dz N(z) f(z, \mathbf{q}) \tag{B.2}$$

with

$$N(z) = \begin{cases} \frac{1}{2q}\left(1 - (z - \frac{q}{2})^2\right) & -1 + \frac{q}{2} < z < 1 + \frac{q}{2}, \quad q > 2 \\ \frac{1}{2q}\left(1 - (z - \frac{q}{2})^2\right) & 1 - \frac{q}{2} < z < 1 + \frac{q}{2}, \quad q < 2 \\ z & 0 < z < 1 - \frac{q}{2}, \quad q < 2 \end{cases} \tag{B.3}$$

and

$$L_q = \begin{cases} \left\{z : -1 + \frac{q}{2} < z < 1 + \frac{q}{2}\right\} & q > 2 \\ \left\{z : 0 < z < 1 + \frac{q}{2}\right\} & q < 2 \end{cases} . \tag{B.4}$$

We test the upper procedure with the simplest function one can imagine, namely $f = 1$. The result is well known and gives:

$$S_F(q) = \frac{3q}{4} - \frac{q^3}{16} \qquad \text{for} \quad q < 2 \tag{B.5}$$

and otherwise one.

B.2 The Lindhard function

The Lindhardfunction is defined as

$$\chi_0(q,\omega) = \frac{1}{N}\sum_h \left(\frac{n(h)\bar{n}(h+q)}{\hbar\omega - e_{h+q,h} + i\eta} - \frac{n(h)\bar{n}(h+q)}{\hbar\omega + e_{h+q,h} + i\eta} \right). \tag{B.6}$$

It can be divided into two parts:

$$\kappa_0^{(+)}(q,\omega) = \frac{1}{N}\sum_h \frac{n(h)\bar{n}(h+q)}{\hbar\omega - e_{h+q,h} + i\eta} \tag{B.7}$$

and

$$\kappa_0^{(-)}(q,\omega) = -\frac{1}{N}\sum_h \frac{n(h)\bar{n}(h+q)}{\hbar\omega + e_{h+q,h} + i\eta} \tag{B.8}$$

with $\chi_0 = \kappa_0^{(+)} + \kappa_0^{(-)}$. To calculate χ_0 we need Dirac's relation

$$\frac{1}{\omega - e \pm i\eta} = P\frac{1}{\omega - e} \mp i\pi\delta(\omega - e). \tag{B.9}$$

Here P indicates the principal value of the integral. There are some ways to calculate χ_0, one possibility is to introduce cylindrical polar coordinates as mentioned above. The calculation is now straight forward and yields for $q < 2$:

$$\begin{aligned} \Re e\kappa_0^{(+)}(q,\omega) &= \frac{3}{4e_F}\left\{ -\frac{1}{2} + \frac{\omega}{4q}\left(1 + 2\ln\omega - 2\ln|-2q+q^2+\omega|\right) \right. \\ &+ \left. \frac{1}{2q}\left(-1 + \left(\frac{\omega}{2q} - \frac{q}{2}\right)^2\right)\ln\left|\frac{1+\frac{q}{2}-\frac{\omega}{2q}}{1-\frac{q}{2}-\frac{\omega}{2q}}\right| \right\} \end{aligned} \tag{B.10}$$

and for $q > 2$

$$\Re e\kappa_0^{(+)}(q,\omega) = \frac{3}{4e_F}\left(-\frac{1}{2} + \frac{\omega}{2q^2} - \frac{1}{2q}(-1+\nu_+^2)\ln\left|\frac{1+\nu_+}{1-\nu_+}\right| \right). \tag{B.11}$$

It is now easy to calculate $\Re e\chi_0(q,\omega)$ when one uses the symmetry relation $\Re e\kappa_0^{(-)}(q,\omega) = \Re\kappa_0^{(+)}(q,-\omega)$. We have also introduced the quantity $\nu_\pm = -\frac{q}{2} \pm \frac{\omega}{2q}$.

$$\Re e\chi_0(q,\omega) = \frac{3}{4e_F}\left(-1 + \frac{1}{2q}(1-\nu_+^2)\ln\left|\frac{1+\nu_+}{1-\nu_+}\right| - \frac{1}{2q}(1-\nu_-^2)\ln\left|\frac{1-\nu_-}{1+\nu_-}\right| \right) \tag{B.12}$$

and

$$\Im m\chi_0(q,\omega) = -\frac{1}{e_F}\frac{3\pi}{8q}\begin{cases} 1-\nu_+^2 & q>2, \quad q^2-2q<\omega<q^2+2q \\ 1-\nu_+^2 & q<2, \quad -q^2+2q<\omega<q^2+2q \\ \omega & q<2, \quad 0<\omega<2q-q^2 \end{cases}. \tag{B.13}$$

Finally we want to list some usefull properties of the Lindhard-function:

$$\begin{aligned}
\chi_0(q,\omega) &= \chi_0^*(q,-\omega) && \text{(B.14)}\\
\Re e\kappa_0^{(+)}(q,-\omega) &= \Re e\kappa_0^{(-)}(q,\omega) && \text{(B.15)}\\
\Im m\kappa_0^{(+)}(q,-\omega) &= -\Im m\kappa_0^{(-)}(q,\omega) && \text{(B.16)}\\
\Im m\kappa_0^{(+)}(q,\omega) &= \Im m\kappa_0^{(+)}(q,\omega)\Theta(\omega) && \text{(B.17)}\\
\Im m\kappa_0^{(-)}(q,\omega) &= \Im m\kappa_0^{(-)}(q,\omega)\Theta(-\omega). && \text{(B.18)}
\end{aligned}$$

B.3 The pair analog of the partial Lindhard function

The calculation of μ proceeds along the same lines as for the partial Lindhard function.

B.3.1 Guidance for calculation

Let's recall the definition of $\mu_0^{(+)}$

$$\mu_0^{(+)}(q,q',\omega) = \frac{1}{N^2}\sum_{hh'} \frac{n(h)\bar{n}(h+q)n(h')\bar{n}(h'+q')}{\hbar\omega - e_{ph} - e_{p'h'} + i\eta}. \tag{B.19}$$

Summation over h' gives

$$\mu_0^{(+)}(q,q',\omega) = \frac{1}{N}\sum_{h} n(h)\bar{n}(h+q)\kappa_0^{(+)}(q',\omega - 2hq - q^2), \tag{B.20}$$

where we used the definition (B.7). Following the instructions given in B.1 we can write (B.20) as

$$\mu_0^{(+)}(q,q',\omega) = \frac{3q}{2}\int_{L_q} dz N(z)\kappa_0^{(+)}(q',\omega - 2zq). \tag{B.21}$$

We can divide the integration in two parts:

- $\Re e\kappa_0^{(+)}$: We have to distinguish four regions of the q, q' plane for the integration. This reduces to three, if one uses the symmetry $q \leftrightarrow q'$. Since $N(z)$ is only a polynomial in z and $\Re e\kappa_0^{(+)}$ some ln-function the basic integral we have to solve is

$$\int dz z^n \ln(z+a) = \frac{z^{n+1}}{(n+1)^2}\left(-1 +_2 F_1\left[n+1, 1, 2+n, -\frac{z}{a}\right] + \ln(z+a)\right), \tag{B.22}$$

  where ${}_2F_1$ is the Hypergeometric function. Now we collect all terms together and get a real long expression.

- $\Im m\kappa_0^{(+)}$: Here we choose a different approach, because we have only four different integrals of a polynomial function. So they are easy to calculate, but the integration range makes some problem. Hence, we get many distinctions of cases.

B.3.2 Useful properties

It is sometimes usefull to know the behavior of μ for small q. From equation (B.20) we obtain for $q << 1$

$$\mu_0^{(+)}(q,q',\omega) \approx \kappa_0^{(+)}(q',\omega)\frac{1}{N}\sum_{h} = \kappa_0^{(+)}(q',\omega)S_F(q). \tag{B.23}$$

The sumrule for $\mu_0^{(+)}$ looks like

$$\int d\omega \Im m \mu_0^{(+)}(q, q', \omega) = -\pi S_F(q) S_F(q'), \tag{B.24}$$

where we have to use

$$\int d\omega \Im m \kappa_0^{+}(q, \omega) = -\pi S_F(q). \tag{B.25}$$

Bibliography

[1] E. K. Achter and L. Meyer. X-ray scattering from liquid helium. *Phys. Rev.*, 188:291–300, 1969.

[2] F. Albergamo, R. Verbeni, S. Huotari, G. Vankó, and G. Monaco. Zero sound mode in normal liquid ^{3}He. *Phys. Rev. Lett.*, 99:205301–205305, 2007.

[3] C. H. Aldrich and D. Pines. Polarization potentials and elementary excitations in he II at low temperatures. *J. Low Temp. Phys.*, 25:677–690, 1976.

[4] C. H. Aldrich III and David Pines. Polarization potentials and elementary excitations in liquid ^{3}He. *J. Low Temp. Phys.*, 31(5/6):689–715, 1978.

[5] P.W. Anderson. More Is Different - Broken Symmetry and Nature of Hierarchical Structure of Science. *Science*, 177(4047):393–&, 1972.

[6] V. Apaja, J. Halinen, V. Halonen, E. Krotscheck, and M. Saarela. Charged-boson fluid in two and three dimensions. *Phys. Rev. B*, 55:12925–12945, 1997.

[7] H. M. Böhm, H. Godfrin, E. Krotscheck, H. J. Lauter, M. Meschke, and M. Panholzer. Pair excitations and vertex corrections in Fermi fluids and the dynamic structure function of two-dimensional ^{3}He. *International Journal of Modern Physics B*, 21:2055, 2007.

[8] H. M. Böhm, R. Holler, E. Krotscheck, and M. Panholzer. Dynamic pair excitations in aluminium. *International Journal of Modern Physics B*, 22:4655–4665, 2008.

[9] H. M. Böhm, E. Krotscheck, and M. Panholzer. Pair excitations and vertex corrections in Fermi fluids. *J. Low Temp. Phys.*, 148:139, 2007.

[10] J. Boronat, J. Casulleras, V. Grau, E. Krotscheck, and J. Springer. The effective mass of two–dimensional ^{3}He. *Phys. Rev. Lett.*, 91:085302–085305, 2003.

[11] J. Casulleras and J. Boronat. Progress in monte Carlo calculations of Fermi systems: Normal liquid ^{3}He. *Phys. Rev. Lett.*, 84(14):3121–3124, 2000.

[12] J. M. C. Chen, J. W. Clark, and D. G. Sandler. An extension of RPA theory to strongly- interacting system. *Z. Physik A*, 305:223–229, 1982.

[13] J. W. Clark, L. Mead, E. Krotscheck, K. E. Kürten, and L. M. Ristig. *Nucl. Phys. A*, 328:45, 1979.

[14] J. W. Clark and P. Westhaus. Method of correlated basis functions. *Phys. Rev.*, 141(3):833–857, 1966.

[15] P Coleman. Many body physics: Unfinished revolution. *ANNALES HENRI POINCARE*, 4(Suppl. 2):S559–S580, 2003.

[16] J. Egger, 2010. (private communication).

[17] B. Fåk, K. Guckelsberger, R. Scherm, and A. Stunault. Spin fluctuations and zero sound in normal ^{3}He studied by neutron scattering. *J. Low Temp. Phys.*, 97(5/6):445–487, 1994.

[18] E. Feenberg. *Theory of Quantum Fluids.* Academic, New York, 1969.

[19] R. P. Feynman and M. Cohen. Energy spectrum of the excitations in liquid helium. *Phys. Rev.*, 102:1189–1204, 1956.

[20] Gabriele Giuliani and Giovanni Vignale. *Quantum Theory of the Electron Liquid.* Cambridge University Press, Cambridge, 2005.

[21] H. R. Glyde, B. Fåk, N. H. van Dijk, H. Godfrin, K. Guckelsberger, and R. Scherm. Effective mass, spin fluctuations, and zero sound in liquid ^{3}He. *Phys. Rev. B*, 61:1421–1432, 2000.

[22] D. S. Greywall. ^{3}He specific heat and thermometry at millikelvin temperatures. *Phys. Rev. B*, 33(11):7520–7538, 1986.

[23] Dennis S. Greywall. Specific heat of normal liquid ^{3}He. *Phys. Rev. B*, 27(5):2747–2766, 1983.

[24] Robert B. Hallock. Liquid structure factor measurements on ^{3}He. *J. Low Temp. Phys.*, 9(1/2):109–121, 1972.

[25] J. P. Hansen and I. R. McDonald. *Theory of Simple Liquids.* Academic Press, New York, 1976.

[26] R. Holler, 2010. (private communication).

[27] W. Hsu and D. Pines. Effective interactions in dilute mixtures of ^{3}He in ^{4}He. *J. Stat. Phys.*, 38:273–312, 1985.

[28] A. K. Kerman and S. E. Koonin. Hamiltonian formulation of time-dependent variational principles for the many-body system. *Ann. Phys. (NY)*, 100:332–358, 1976.

[29] P. Kramer and M. Saraceno. *Geometry of the time-dependent variational principle in quantum mechanics*, volume 140 of *Lecture Notes in Physics*. Springer, Berlin, Heidelberg, and New York, 1981.

[30] E. Krotscheck. Variational method for liquid ^{3}He: I. the Fermi hypernetted-chain approach. *J. Low Temp. Phys.*, 27:199–215, 1977.

[31] E. Krotscheck. Effective interactions, linear response, and correlated rings: A study of chain diagrams in correlated basis functions. *Phys. Rev. A*, 26:3536–3556, 1982.

[32] E. Krotscheck. Variations on the electron gas. *Ann. Phys. (NY)*, 155:1–55, 1984.

[33] E. Krotscheck. Fermi–hypernetted chain theory for liquid ^{3}He: A reassessment. *J. Low Temp. Phys.*, 119:103–145, 2000.

[34] E. Krotscheck and J. W. Clark. Studies in the method of correlated basis functions. ii. diagrammatic analysis and integral equation methods. *Nucl. Phys. A*, 328:73–103, 1979.

[35] E. Krotscheck and J. Springer. Physical mechanisms for effective mass enhancement in ^{3}He. *J. Low Temp. Phys.*, 132(5/6):281–295, 2003.

[36] N.-H. Kwong. *Realistic calculations of excitations in nuclear matter*. PhD thesis, California Institute of Technology, 1982.

[37] J. Lindhard. *K. Dan. Vidensk. Selk. Mat.-Fys. Med.*, 8:28, 1954.

[38] P. Nozières. Is the roton in superfluid ^{4}He the ghost of a Bragg spot ? *J. Low Temp. Phys.*, 137:45–67, 2004.

[39] D. Pines and P. Nozieres. *The Theory of Quantum Liquids*, volume I. Benjamin, New York, 1966.

[40] D. J. Thouless. *The quantum mechanics of many-body systems*. Academic Press, New York, 2 edition, 1972.

[41] J. G. Zabolitzky. Fermi-hypernetted-chain methods and the ground state of fermion matter. *Phys. Rev. A*, 16:1258–1283, 1977.

Acknowledgement

This dissertation would not have been possible without the guidance and the help of several individuals who in one way or another contributed and valuably assisted in the preparation and completion of this study. I want to express my gratitude to the following people:

First and foremost Prof. Eckhard Krotscheck for supporting me in carrying out this work and for his invaluable guidance through the depths of many particle theory. His inestimable input and encouragement have driven me to produce quality research.

Prof. Helga Böhm and Robert Holler, who were always available for fruitful discussions and gave a helping hand in any kind of problem.

Prof. Henri Godfrin for his hospitality during my stay in Grenoble, and for showing a theorist the flavor of the experimentalists' world. The discussions with him further detailed my understanding of fermion dynamics.

Prof. Charles E. Campbell for his excellent introduction into the field of many body physics and critically reading this thesis and many helpful discussions.

The friends and colleagues at this institute and Daniel Primetzhofer from the Institute of Experimental Physics for creating very friendly working conditions and the various illuminating interdisciplinary discussions during the "Teichrunden" and various coffees.

And last but not least all the other friends, my family and my partner Martina and our son Tobias, who accompanied me through all the hassle and who were important for the life besides physics. They endured living with a PhD student of theoretical physics with admirable patience.

Curriculum Vitae

Name: Martin Panholzer

Date and Place of Birth: February 5, 1980, Linz

Nationality: Austria

Home Address: Gutauer Straße 58 4283 Bad Zell Austria

Employment and education:

1995-1999	Apprenticeship at voestalpine
1999	Military Service
2000-2002	Employment at voestalpine; evening school at HTBLA Linz
2002	High School Diploma (Matura); Graduation passed with distinction
2002-2007	Technical Physics at Johannes Kepler University Linz; Graduation passed with distinction
since 2007	PhD studies at Johannes Kepler University Linz

Prizes:

2007	Wilhelm Macke Prize for Diplomathesis: Dynamic response in liquid ^{3}He

Conferences:

Apr. 2008	Meco 33 in Puchberg/Wels, Austria (poster)
Sep. 2008	Cryocourse in Miraflores, Spain (talk and poster)
Aug. 2009	QFS in Evanston, US (poster)

Invited research stay:

Nov. 2009	coexperimentator at Institut Laue-Langevin (ILL): Zero-sound in a liquid 3He monolayer at atomic wave-vectors; Proposal: 6-01-306

Teaching:

2005-2007	Tutorials in Theoretical Physics
2007-2010	Teaching assistant for the courses Theoretical Physics I, II and III

Publications:

[1] M. Panholzer, H. M. Boehm, R. Holler, and E. Krotscheck. Exchange Effects and the Dynamics of He-3. *JOURNAL OF LOW TEMPERATURE PHYSICS*, 158(1-2, Sp.

Iss. SI):135–140, JAN 2010. 17th International Conference on Quantum Fluids and Soilds, Evanston, IL, AUG 05-11, 2009.

[2] H. Godfrin, M. Meschke, H. J. Lauter, H. M. Boehm, E. Krotscheck, and M. Panholzer. Observation of Zero-Sound at Atomic Wave-Vectors in a Monolayer of Liquid He-3. *JOURNAL OF LOW TEMPERATURE PHYSICS*, 158(1-2, Sp. Iss. SI):147–154, JAN 2010. 17th International Conference on Quantum Fluids and Soilds, Evanston, IL, AUG 05-11, 2009.

[3] H. M. Boehm, E. Krotscheck, M. Panholzer, H. Godfrin, H. J. Lauter, and M. Meschke. Two-Dimensional He-3: A Crucial System for Understanding Fermion Dynamics. *JOURNAL OF LOW TEMPERATURE PHYSICS*, 158(1-2, Sp. Iss. SI):194–200, JAN 2010. 17th International Conference on Quantum Fluids and Soilds, Evanston, IL, AUG 05-11, 2009.

[4] H. M. Boehm, R. Holler, E. Krotscheck, and M. Panholzer. Double-plasmon excitations in the alkali metals. *JOURNAL OF PHYSICS A-MATHEMATICAL AND THEORETICAL*, 42(21), MAY 29 2009. International Conference on Strongly Coupled Coulomb Systems, Camerino, ITALY, JUL 29-AUG 02, 2008.

[5] H. M. Boehm, R. Holler, E. Krotscheck, and M. Panholzer. Dynamic pair excitations in 2D Fermi fluids. *JOURNAL OF PHYSICS A-MATHEMATICAL AND THEORETICAL*, 42(21), MAY 29 2009. International Conference on Strongly Coupled Coulomb Systems, Camerino, ITALY, JUL 29-AUG 02, 2008.

[6] Helga M. Boehm, Robert Holler, Eckhard Krotscheck, and Martin Panholzer. DYNAMIC PAIR EXCITATIONS IN ALUMINUM. *INTERNATIONAL JOURNAL OF MODERN PHYSICS B*, 22(25-26):4655–4665, OCT 20 2008. 31st International Workshop on Congensed Matter Theories, Bangkok, THAILAND, DEC 03-08, 2007.

[7] H. M. Boehm, H. Godfrin, E. Krotscheck, H. J. Lauter, M. Meschke, and M. Panholzer. Pair excitations and vertex corrections in fermi fluids and the dynamic structure function of two-dimensional He-3. *INTERNATIONAL JOURNAL OF MODERN PHYSICS B*, 21(13-14):2055–2066, MAY 30 2007. 30th International Workshop on Condensed Matter Theories (CMT30), Dresden, GERMANY, JUN 05-10, 2006.

[8] Helga M. Boehm, Eckhard Krotscheck, and Martin Panholzer. Pair excitations and vertex corrections in fermi fluids. *JOURNAL OF LOW TEMPERATURE PHYSICS*, 148(3-4):139–143, AUG 2007. International Symposium on Quantum Fluids and Solids (QFS-2006), Kyoto, JAPAN, JUL 31-AUG 06, 2006.

Part II

Publications

Roton-like collective mode observed in a Fermi liquid beyond the particle-hole continuum

Henri Godfrin[1], Matthias Meschke[1,§], Hans-Jochen Lauter[2], Helga M. Böhm[3], Eckhard Krotscheck[3] & Martin Panholzer[3]

[1] *Institut Néel, CNRS et Université Joseph Fourier, BP 166, F-38042 Grenoble Cedex 9, France*

[2] *Institut Laue-Langevin, BP 156, 38042 Grenoble Cedex 9, France*

[3] *Institute for Theoretical Physics, Johannes Kepler University, A-4040 Linz, Austria*

§ Present address: Low Temperature Laboratory, Helsinki University of Technology P.O. Box 3500, FIN-02015 TKK, Finland

Understanding the quantum properties of many-body systems is a major goal of present Science, and significant advances have been made in the description of the ground state of interacting particles obeying Bose or Fermi statistics. Bose-Einstein condensates, the Fermi liquid state, and superconductivity, are examples of general interest. The concept of elementary excitations, introduced by Landau, provides an elegant and powerful tool for unveiling the structure of strongly interacting matter. For this reason, many studies have been devoted to the dynamics of the strongly interacting quantum fluids: liquid ^{4}He (bosons) and ^{3}He (fermions). A milestone for understanding correlated bosons was the observation of the "phonon-roton" collective mode of liquid ^{4}He, predicted by Landau[1] to explain the system's thermodynamics. For fermions, the situation is more complicated, since the spectrum hosts two types of modes: collective ("zero-sound" in ^{3}He, or "plasmon" in charged systems), and incoherent particle-hole (PH) excitations. Both are described by Landau's theory of Fermi liquids[2] in the small wave-vector/ low energy region of the spectrum. At higher wave-vectors/energies, the collective mode enters the PH band, where it is strongly damped[2,3]. So far, it was thus believed that the dynamics at high wave-vectors is essentially incoherent. Using a monolayer of liquid ^{3}He, we report here the first observation of a roton-like minimum in a Fermi liquid. We find that the collective mode reappears as a well defined excitation beyond the PH band. Moreover, we provide a new theoretical framework where we introduce intermediate states that are not describable by the quantum numbers of a single (quasi-)particle, leading to an accurate interpretation of the spectra measured for ^{3}He films. By exploring the dynamics of Fermi many-body systems in the region outside the scope of Landau's theory, we open new perspectives in the understanding of highly correlated fermions.

Quantum many-body systems are ubiquitous in nature. The identification of their ground state and the description of their quantised elementary excitations is a cornerstone of modern Physics[1,4]. Nuclei, metals, semiconductors, and neutron stars, are examples of quantum liquids. Their properties depend, among others, on the quantum statistics obeyed by the particles (electrons, nucleons, atoms), leading to the classification in terms of Bose or Fermi systems. The road from the Bose or Fermi gas to their strongly interacting analogue, however, was not smoothly paved, and considerable attention has been devoted to correlated quantum systems[1-4]. The interplay between quantum statistics and interactions in many-body quantum systems is the central theme of this Letter.

Our work is concerned with the helium liquids, the canonical examples of quantum fluids. ^{4}He is a boson, while ^{3}He is, due to its nuclear spin ½, a fermion. At 2.17 K, ^{4}He undergoes a Bose-Einstein condensation to the superfluid state. Liquid ^{3}He, however, remains a normal Fermi liquid down to millikelvin temperatures, where Cooper pairs are formed and Bose-Einstein condense into several superfluid phases. It is neutral, but otherwise analogous to the conduction electrons in a metal. Clearly, Bose and Fermi liquids behave differently, and are thus expected to sustain very different excitations.

The elementary excitations of a Bose liquid have been described by Landau[1]. Their dispersion relation (Figure 1) shows a linear "phonon" mode, which evolves continuously as a function of the wave-vector, displaying a pronounced "roton" minimum[1,5]. The excitations remain well defined even at atomic wave-vectors. The physical origin of the roton minimum is the incipient localisation of the particles under the effect of the interactions[6]. Modern many-body theories have been successful in describing the dynamics of Bose fluids under different conditions of density and dimensionality: bulk, films, or droplets[7-9].

The elementary excitations of liquid ^{3}He are described, at small wave-vectors, by Landau's Fermi liquid theory[2,10]. A "particle-hole" (PH) elementary excitation is created, at zero temperature, by removing a particle from the Fermi sphere, thus creating a hole, and placing it in an empty state outside the Fermi sphere, according to Pauli's exclusion principle. PH states are confined in the spectrum (Figure 2) within the particle-hole band (PHB). The boundaries of the PHB for a non-interacting system (the Fermi "gas") are $E_{max,min} / E_F = (k/k_F)^2 \pm 2 (k/k_F)$ where $E_F = \hbar^2 k_F^2 / 2m$ is the Fermi energy, k the excitation wave-vector, k_F the Fermi wave-vector, and m the (bare) mass of a particle.

Landau's theory predicts that an *interacting* system will behave as a Fermi gas with renormalized parameters. In particular, an effective mass m^* is assigned to the fermionic "quasi-particles". The theory describes well[10] the low temperature properties of bulk liquid ^{3}He, where m^*, depending on the liquid pressure, varies from 3 to 6 times m, the bare mass of a ^{3}He atom. Therefore, the PHB is expected to shift to energies well below those calculated for the non-interacting system. This picture, as discussed later, does not apply at high wave-vectors: substantial mass enhancement is limited to the vicinity of the Fermi surface[10-14].

Fermi liquids also sustain a density collective mode, zero-sound, described by Landau as an oscillation of the whole Fermi sphere[2,10]. Contrarily to ordinary sound, its frequency is higher than the collision rate. First detected by ultrasonic techniques, it has been investigated in detail by neutron scattering[10,14-16]. Zero-sound has a linear dispersion relation, above the PHB, then a negative deviation at intermediate wave-vectors, and finally enters the PHB, where this mode was believed to disappear, due to Landau-damping (decay into PH excitations).

The corresponding excitation in electron fluids is the plasmon. In spite of differences due to charge (a gap is observed at zero wave-vector), the physics is the same[2]. In particular, the plasmon dispersion curve is observed to enter the PHB, and to disappear, as shown in Figure 2.

Not surprisingly, the description of the dynamics of Fermi many-body systems has evolved along a very different route than that of bosons. However, there is no fundamental reason for this. A very elegant discussion of this problem is given in a review article by Pines[3]. It is argued that the phonon-roton mode of liquid ^{4}He and the zero-sound mode of liquid ^{3}He have *strong interactions*, rather than *quantum statistics*, as common origin. Using a phenomenological approach (pseudo-potentials), Pines and co-workers predicted successfully the downturn of the zero-sound mode dispersion in liquid ^{3}He at intermediate wave-vectors. Obtaining a unified theory of the excitations of Bose and Fermi systems was already considered as the Holy Grail of this field[3]. In the following we provide unambiguous experimental and theoretical evidence supporting this point of view, as well as theoretical advances towards this unified description.

In the present experiment, we have determined the dynamic structure factor of a monolayer of liquid ^{3}He, essentially at zero temperature. Two-dimensional Fermi liquids have been extensively investigated by thermodynamic techniques[17-22]; we present here the first direct investigation of their elementary excitations by neutron scattering. We observe a collective mode, which not only remains well defined throughout the whole PHB, but even re-emerges as a sharp mode at large wave-vectors, as shown schematically in Figure 3.

The He film is made at low temperatures by the controlled adsorption of He gas onto a substrate, a high quality ZYX exfoliated graphite (surface area 60 m^2) with large coherence length (190 nm) and low mosaic spread (10°), essential for obtaining good

resolution neutron spectra[22,23]. The substrate was first pre-plated by a complete monolayer of ^{4}He. This high density solid provides a smoother adsorption potential than bare graphite. A monolayer of liquid ^{3}He is then deposited onto the ^{4}He pre-plated substrate. Its density, determined by adsorption isotherm techniques using a coverage scale developed earlier[22], is 4.9 atoms/nm^2. The corresponding effective mass[17-21] is $m^*/m_3 \sim 4$, similar to that of bulk liquid ^{3}He at a pressure of 2 MPa. An aluminium sample cell confines the gas during the adsorption process, performed through a filling capillary. Measurements are made in a dilution refrigerator, at temperatures below 100 mK.

The experiments have been performed at the Institut Laue-Langevin on the time-of-flight spectrometer IN6, using an incident wavelength of 0.512 nm. The measured dynamic structure factor *S(k,E)* contains all the relevant information on the elementary excitations of a system; it essentially gives the probability for creating such an excitation with wave-vector *k* and energy *E*. The main features revealed by our data, shown in Figure 4, are: 1) the zero-sound mode is seen at low wave-vectors; given the limited experimental range, its definite identification requires theoretical support, to be presented later. 2) The mode is broadened as it enters the PHB. 3) It emerges beyond the limits of the PHB as an intense mode, displaying a minimum as a function of energy; its energy increases rapidly beyond this minimum. 4) The high intensity region of *S(k,E)* closely resembles the phonon-maxon-roton dispersion relation of liquid ^{4}He. 5) At low wave-vectors, significant intensity is present at high energies *above* the PHB, indicating the existence of multi-pair excitations. As shown below, the latter play an essential role in explaining the observed position of the roton and the emergence of the collective mode beyond the PHB.

The results of our theoretical calculation of the dynamic structure factor for the density of the experimental system are shown in Figure 5. Adopting the view that the

physical mechanisms that determine the short-wavelength spectrum are the same in ^{4}He and in ^{3}He, we have developed the fermion generalization of the multi-particle fluctuation theory of Jackson, Feenberg, and Campbell[7,9], that has been successful for bosonic quantum fluids. The theory supersedes the intuitive "backflow" theory of Feynman, it allows to avoid the Random Phase Approximation[2] (RPA), which is not applicable at atomic wave-vectors.

The boson theory has by now been developed to a level where a consistent description of the dynamics of ^{4}He in the whole *(k,E)* plane is reached. The derivation of the equations of motion for the Fermi system proceeds along the same lines[9], with additional complications due to the multitude of exchange diagrams; input to the calculations is the static structure function *S(k)* obtained from microscopic Fermi-hypernetted-chain calculations. The main results of the pair-fluctuation theory (Figure 5) are: 1) At low wave-vectors, the existence of a long-lived zero-sound collective mode, close to the PHB upper limit. 2) The mode is broadened, but clearly visible, within the PHB. 3) It emerges from the PHB as a well defined, intense excitation. 4) A phonon-maxon-roton type of dispersion relation is clearly seen. 5) Multi-pair excitations are present at low wave-vectors above the PHB. 6) In addition to an excellent description of the spectrum, a good quantitative agreement with the experiment is obtained, without adjustable parameters.

We have observed for the first time the elementary excitations of two-dimensional liquid ^{3}He. Using the favourable conditions displayed by this system, we demonstrated that a strongly interacting quantum many-body system sustains collective density excitations which are largely independent from the quantum statistics: the fermionic ^{3}He collective mode is found essentially identical to the phonon-roton curve of the bosonic ^{4}He. The current view of Fermi liquids, based on Landau's theory and RPA long-wavelength approximations, is therefore misleading when applied at large wave-vectors.

Despite the additional particle-hole excitations present in Fermi liquids, the high wave-vector dynamics can be dominated by zero-sound (plasmon) coherent excitations. This is certainly the case in the strongly correlated two-dimensional system investigated here. Consequently, opening the scope of plasmonics, these collective modes could be present as high energy excitations in strongly correlated electronic systems, where they could induce coherence effects (superconductivity) at relatively high temperatures. The consequences of the presence of such collective modes at high wave-vectors and their coupling to other collective excitations (phonons, magnons), on the dynamics of electronic systems[24-28] like high Tc superconductors, heavy fermions, metals, graphene, and others, deserve being explored.

References

1. Landau, L.D. On the theory of superfluidity of helium II. *J. of Phys. Moscow* **11**, 91 (1947).

2. Pines, D. & Nozières, P. *The Theory of Quantum Liquids*. Benjamin, New York (1966).

3. Pines, D. Elementary excitations in quantum liquids. *Physics Today* **34**, 106 (Nov. 1981).

4. Thouless, D.J. *The Quantum Mechanics of Many-body Systems*. 2nd ed. Academic Press, New York (1972).

5. Feynman, R.P. & Cohen, M. Energy spectrum of the excitations in liquid helium. *Phys. Rev.* **102**, 1189 (1956).

6. Nozières, P. Is the roton in superfluid ^{4}He the ghost of a Bragg spot? *J. of Low. Temp. Phys.* **137**, 45 (2004).

7. Jackson, H. W. Perturbative form of $S(k,\omega)$ for liquid He^4: basic calculation and results. *Phys. Rev*. A **8,** 1529 (1973).

8. Clements, B.E., Krotscheck E. & Tymczak, C.J. Multiphonon excitations in boson quantum films. *Phys. Rev. B* **53**, 12253 (1996).

9. Campbell, C.E. & Krotscheck, E. Dynamic many-body theory: pair fluctuations in bulk ^{4}He. *Phys. Rev. B*. B**80**, 174501 (2009).

10. Glyde, H.R. *Excitations in Liquid and Solid Helium*. Clarendon Press, Oxford (1994).

11. Friman, B.L. & Krotscheck, E.K. Zero sound, spin fluctuations, and effective mass in liquid ^{3}He. *Phys. Rev. Lett.* **49**, 1705 (1982).

12. Boronat, J., Casulleras, J., Grau, V. Krotscheck, E. & Springer, J. Effective mass of two-dimensional ^{3}He. *Phys. Rev. Lett.* **91**, 085302 (2003).

13. Krotscheck, E. & Springer, J. Physical mechanisms for effective mass enhancement in ^{3}He. *J. of Low Temp. Phys.* **132**, 281 (2003).

14. Glyde, H.R., Fak, B., van Dijk, N.H., Godfrin, H., Guckelsberger K. & Scherm, R. Effective mass, spin fluctuations and zero sound in liquid ^{3}He. *Phys. Rev. B* **61**, 1421 (2000).

15. Sköld, K., Pelizzari, C.A., Kleb, R. & Ostrowski, G.E. Neutron scattering study of elementary excitations in liquid helium-3. *Phys. Rev. Lett.* **37**, 842 (1976).

16. Scherm, R., Gluckelsberger, K., Fak, B., Sköld, K., Dianoux, A.J., Godfrin, H. & Stirling, W.G. Pressure dependence of elementary excitations in normal liquid helium-3. *Phys. Rev. Lett.* **59**, 217 (1987).

17. Greywall, D.S. Heat capacity of multilayers of ^{3}He adsorbed on graphite at low millikelvin temperatures. *Phys. Rev. B* **41**, 1842 (1990).

18. Morhard, K.D., Bäuerle, C., Bossy, J., Bunkov, Yu.M., Fisher, S.N. & Godfrin, H. Two-dimensional Fermi liquid in the highly correlated regime: the second layer of ^{3}He adsorbed on graphite. *Phys. Rev. B* **53**, 2658 (1996).

19. Bäuerle, C., Bunkov, Yu.M., Chen, A.S., Fisher, S.N. & Godfrin, H. Ultra-low temperature magnetic properties of liquid ^{3}He films. *J. of Low Temp. Phys.* **110**, 333 (1998).

20. Casey, A., Patel, H., Nyéki, J., Cowan, B.P. & Saunders, J. Strongly correlated two dimensional fluid ^{3}He. *J. of Low Temp. Phys.* **113**, 293 (1998).

21. Neumann, M., Nyéki, J., Cowan, B.P. & Saunders, J. Bilayer ^{3}He: a simple two-dimensional heavy-fermion system with quantum criticality. *Science* **317**, 1356 (2007).

22. Godfrin H. & Lauter, H.J. *Progress in Low Temp. Physics*, **Vol.XIV**, Chapter 4, p.213-320, ed. W.P. Halperin, Elsevier Science B.V., Amsterdam (1995).

23. Lauter, H.J., Godfrin, H., Frank,V.L.P. & Leiderer, P. Ripplons in ^{4}He films observed by neutron scattering. *Phys. Rev. Lett.* **68**, 2484 (1992).

24. Ruvalds, J. Are plasmons the key to superconducting oxides? *Nature* **328**, 299 (1987).

25. Bostwick, A., Ohta, T., Seyller, T., Horn, K. & Rotenberg, E. Quasiparticle dynamics in graphene. *Nature Physics* **3**, 36 (2007).

26. Diaconescu et al. Low-energy acoustic plasmons at metal surfaces. *Nature* **448**, 57 (2007).

27. Uemura, Y.J. et al. Phase separation and suppression of critical dynamics at quantum phase transitions of MnSi and $(Sr_{1-x}Ca_x)RuO_3$, *Nature Physics* **3**, 29 (2007).

28. Kohsaka, Y. et al. How Cooper pairs vanish approaching the Mott insulator in $Bi_2Sr_2CaCu_2O_{8+\delta}$. *Nature* **454**, 1072 (2008).

Acknowledgements We acknowledge financial support from the Partenariat Hubert Curien "Amadeus" and from the Austrian Science Fund. The experiments could be made in Grenoble thanks to the support of Institut Laue-Langevin and Microkelvin, the EU FRP7 low temperature infrastructure.

Author contributions H.G, M.M and H.-J. L. performed the experiments; H.B., E.K. and M.P. developed the theory. All authors analysed and discussed the results, and contributed to the work.

Author information Reprints and permissions information is available at npg.nature.com/reprintsandpermissions. Correspondence and requests for materials should be addressed to H. G (henri.godfrin@grenoble.cnrs.fr) or E.K. (Eckhard.Krotscheck@jku.at)

Figure captions

Figure 1. Elementary excitations of a model Bose liquid, superfluid ^{4}He. The solid line is the dispersion relation predicted by L.D. Landau. Crosses correspond to the excitation energy as a function of wave-vector determined by neutron scattering (see ref. 10). At low wave-vectors, the dispersion relation is linear, and the excitations are quantised sound waves (phonons). At higher wave-vectors, the spectrum evolves continuously, displaying a maximum and then a characteristic minimum. The corresponding excitations are called respectively *maxons* and *rotons*; the latter play an essential role in the thermodynamic properties of superfluid ^{4}He. Rotons are characteristic of highly interacting systems, and can be viewed as the consequence of an incipient localisation due to interactions.

Figure 2. Elementary excitations of a Fermi liquid. The broad shaded area corresponds to the particle-hole band, i.e., to the excitation energy range as a function of wave-vector accessible by promoting a particle occupying a state inside the Fermi surface, to an empty state outside it. The particle-hole band is an essential feature of a Fermi liquid, associated to the existence of a Fermi surface. In addition, an interacting Fermi system displays collective density modes, called “plasmons” in charged, and “zero-sound” in neutral systems. With increasing wave-vectors, the collective modes enter the particle-hole band, where they decay (Landau damping) into incoherent particle-hole excitations, as depicted by the broad, hatched regions, believed up to now to end the collective modes dispersion curves.

Figure 3. Elementary excitations of a neutral Fermi liquid. Depending on the strength of the interactions and the system's dimensionality, the phonon-roton collective mode may be Landau damped at high wave-vectors (upper curve), or reappear as a well defined collective mode beyond the particle-hole continuum (lower curve). In the latter case, collective dynamic effects at high wave-vectors are allowed. We demonstrate here that this effect is realized in two-dimensional ^{3}He.The underlying physics is applicable to any interacting Fermi system (as in Figure 2).

Figure 4. The dynamic structure factor *S(k,E)*, determined by inelastic neutron scattering for a monolayer of liquid ^{3}He of areal density 4.9 atoms/nm^2, is shown as a function of the neutron momentum transfer *k* and energy transfer *E*. The colour scale of this contour plot evolves from white to red, with 9 contour lines corresponding to intensities 0 to 10 (in arbitrary units proportional to neutron counts). White colour is also used for clarity in the lower part of the graph, where data cannot be exploited due to the presence of a large quasi-elastic background, and in the limits of low and high *k* determined by the angular range covered by the detectors. Solid lines indicate the particle-hole band limits calculated for a Fermi gas with the bare ^{3}He atomic mass. High intensity (red and orange) regions indicate the existence of modes with wave-vector *k* and energy *E*, eventually broadened by the experimental resolution (Δk = 1 nm^{-1}, ΔE = 0.03 meV). The zero-sound collective mode is visible at low wave-vectors, around $k \sim 5$ nm^{-1} and $E \sim 0.7$ meV. It is broadened inside the particle-hole band, but it emerges beyond the particle-hole band limits as a well defined mode, displaying a minimum as a function of energy at $k = 15.5$ nm^{-1} and $E = 0.4$ meV. The collective mode of this Fermi liquid closely resembles the phonon-maxon-roton dispersion relation of liquid ^{4}He (see Figure1).

Figure 5. The dynamic structure factor *S(k,E)*, calculated for a monolayer of liquid ^{3}He of areal density 4.9 atoms/nm^2, is shown as a function of the wave-vector *k* and energy *E*. At this areal density, corresponding to the experimental data shown in Figure 4, the Fermi wave-vector is $k_F = 5.55$ nm^{-1} and the Fermi energy $E_F = 0.213$ meV. Solid lines indicate the particle-hole band limits calculated for a Fermi gas with the bare ^{3}He atomic mass. High intensity (red and orange) regions indicate the existence of modes with wave-vector *k* and energy *E*. The theoretical spectrum has been slightly broadened to make the sharp collective modes visible. The zero-sound collective mode, well defined at low wave-vectors, enters the particle-hole continuum, is broadened, and finally emerges beyond the lower limit of the particle-hole band, displaying a minimum as a function of energy. A phonon-maxon-roton type of dispersion relation is clearly seen.

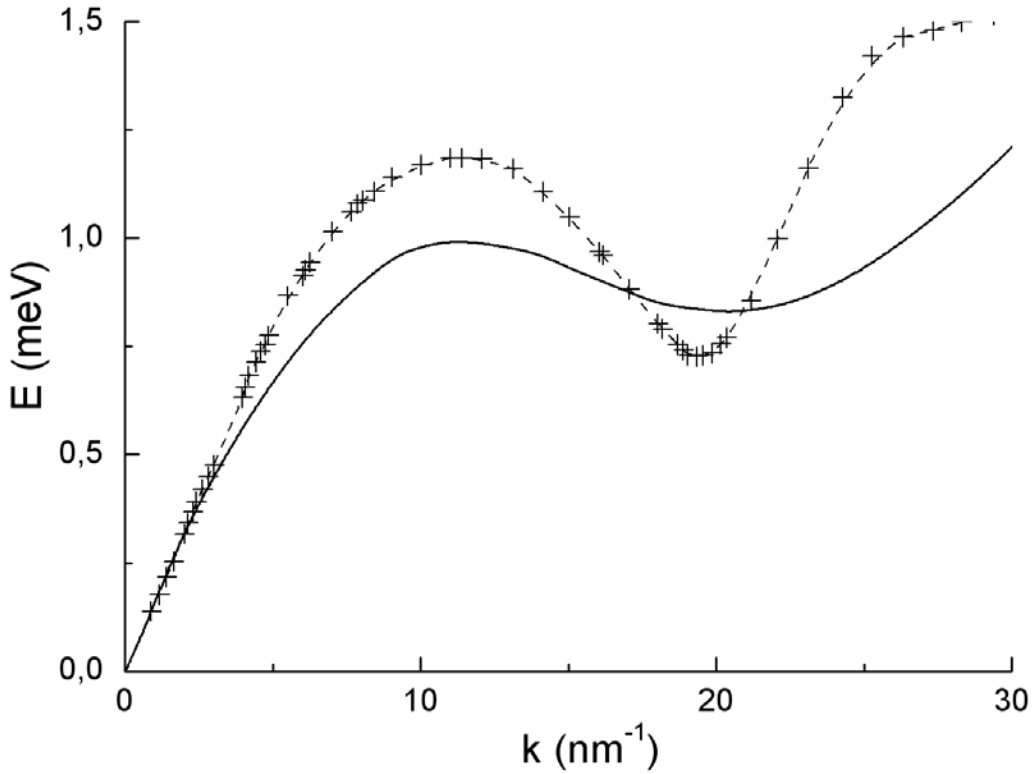

Figure 1

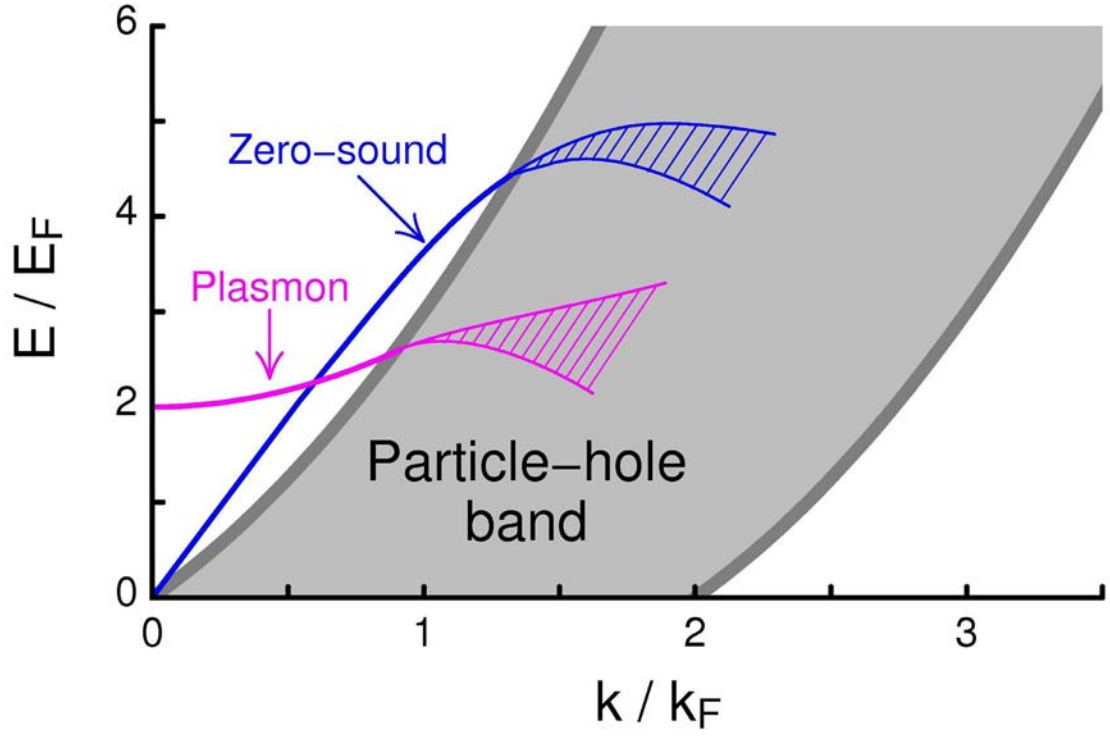

Figure 2

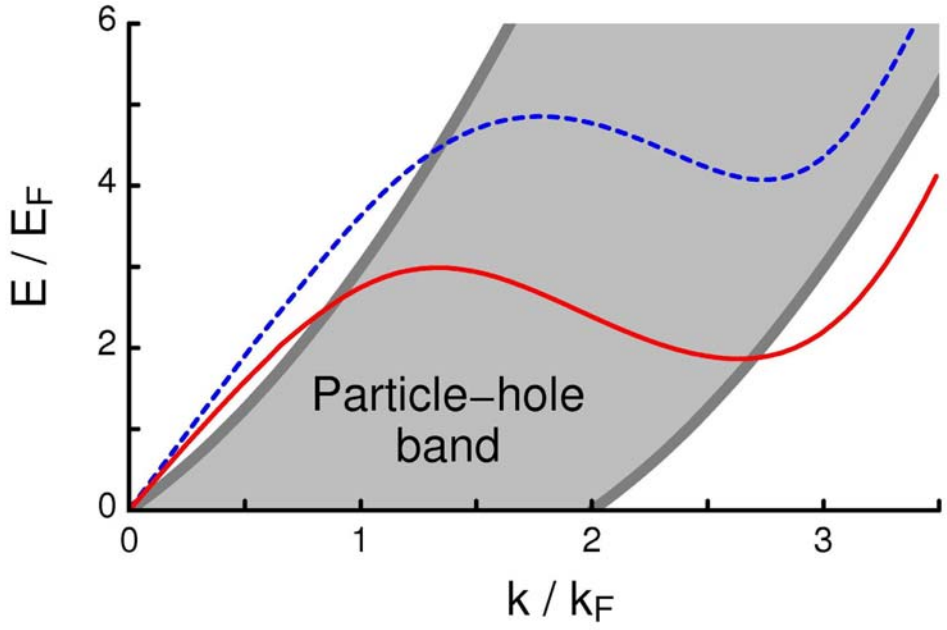

Figure 3

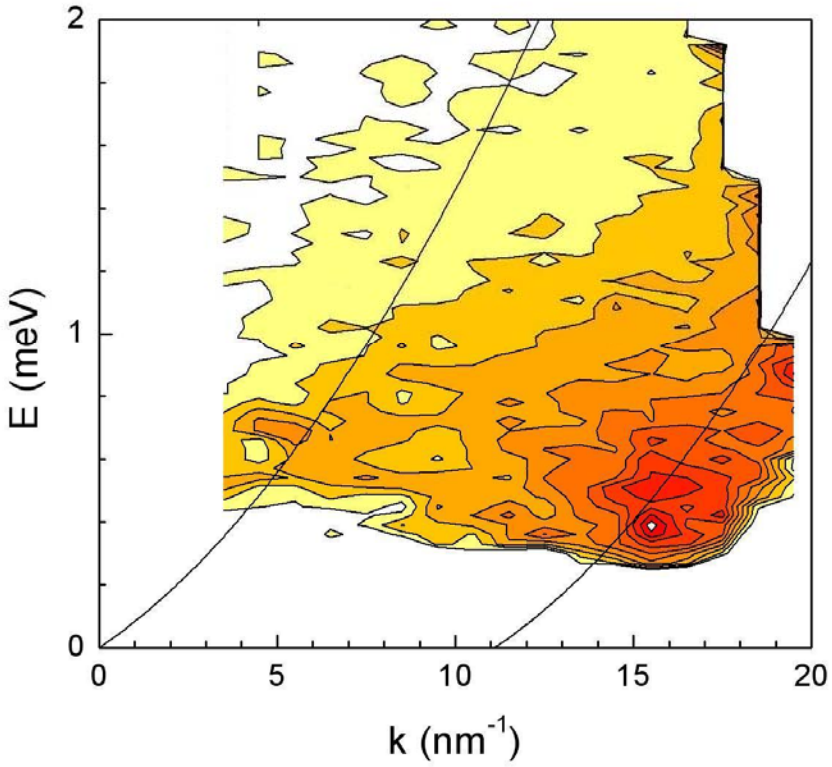

Figure 4

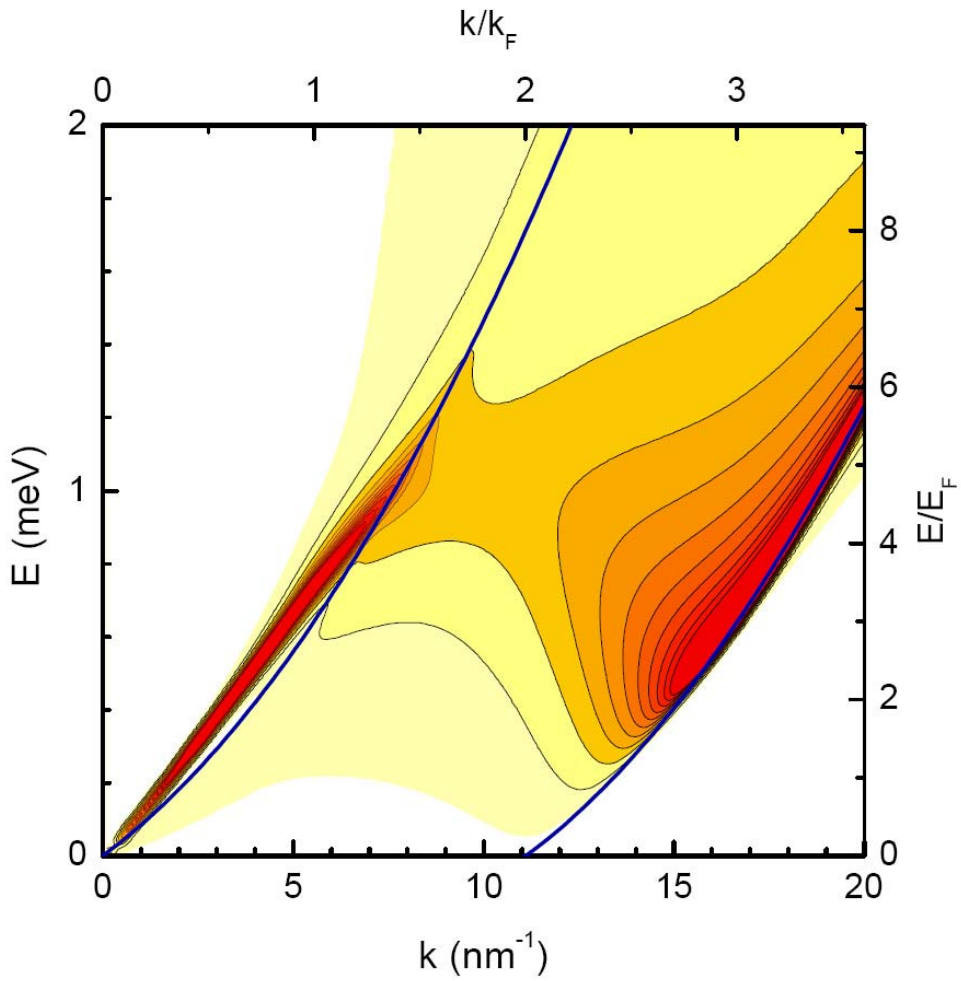

Figure 5

Dynamic Many-Body Theory. II. Dynamics of Strongly Correlated Fermi Fluids

H. M. Böhm[†], R. Holler[†], E. Krotscheck[†+] and M. Panholzer[†]

[†]*Institut für Theoretische Physik, Johannes Kepler Universität, A 4040 Linz, Austria and*

[+]*Department of Physics, University at Buffalo, SUNY Buffalo NY 14260*

Abstract

We develop a systematic theory of multi-particle excitations in strongly interacting Fermi systems. Our work is the generalization of the time-honored work by Jackson, Feenberg, and Campbell for bosons, that provides, in its most advanced implementation, quantitative predictions for the dynamic structure function in the whole experimentally accessible energy/momentum regime. Our view is that the same physical effects – namely fluctuations of the wave function at an atomic length scale – are responsible for the correct energetics of the excitations in both Bose and Fermi fluids. Besides a comprehensive derivation of the fermion version of the theory and discussion of the approximations made, we present results for homogeneous ^{3}He and electrons in three dimensions. We find indeed a significant lowering of the zero sound mode in ^{3}He and a broadening of the collective mode due to the coupling to particle-hole excitations in good agreement with experiments. The most visible effect in electronic systems is the appearance of a "double-plasmon" excitation.

PACS numbers: 67.30.-n, 67.30.em, 71.10.Ca, 71.15.Qe, 71.45.Gm

I. INTRODUCTION

This paper is concerned with a systematic theory of multi-particle excitations in Fermi systems. We utilize an equations of motion method that has been used in the past as a vehicle for many purposes: the derivation of the time–dependent Hartree–Fock (TDHF) theory [1–3], its analog for strongly interacting systems [4, 5], and for studying single– and multi–particle correlations in strongly interacting Bose liquids [6, 7].

The simplest way to deal with excitations is to assume that the low–lying excited states of a quantum fluid can be characterized by the quantum numbers of a single particle. This is the core idea of Landau's quasiparticle picture of "normal" quantum fluids [8, 9] as well as of Feynman's theory of collective modes in the helium liquids [10]. It is appropriate for many long wavelengths excitations such as sound waves in Bose fluids or plasmons in an electron liquid.

Already Feynman realized that this concept is insufficient to describe higher–lying excitations, most prominently the "roton" in ^{4}He. Intuitively appealing, he introduced "backflow" correlations [11]. These are recognizable as a new type of excitations, depending on two particles: *pair fluctuations*. The notion is plausible: For excitations at wavelengths comparable to the interparticle distance, the time–dependence of a system's *short–ranged* structure is expected to be relevant.

The presently state-of-the-art theory for Bose liquids originates from pioneering studies by Jackson, Feenberg [6, 12–16], and Campbell and collaborators [17]. Recently, a complete solution of the pair equation of motion has been accomplished in ^{4}He [7], showing that the "uniform limit approximation" of Refs. 6, 12–17 is surprisingly good. Consequently, theoretical improvement must be sought in three-body and higher-order fluctuations [18].

Although quite successful for bosons, there exists to-date no fermion version of the theory. We therefore develop here the generalization of the equation of motion method for pair fluctuations to fermions. We calculate the fermionic density–density response function $\chi(\mathbf{r}-\mathbf{r}';\, t-t')$, relating the induced density fluctuation $\delta\rho(\mathbf{r};t)$ to a weak external perturbation $h_{\rm ext}(\mathbf{r};t)$. In a homogeneous system this is written in momentum space as

$$\delta\rho(\mathbf{q};\omega) = \rho\,\chi(q;\omega)\,\tilde{h}_{\rm ext}(\mathbf{q};\omega)\,, \tag{1.1}$$

where ρ is the particle number N per volume Ω. We choose Fourier transforms

$$f(\mathbf{r};\omega) \equiv \frac{1}{N}\sum_{\mathbf{q}} e^{-\mathrm{i}\mathbf{q}\cdot\mathbf{r}}\,\tilde{f}(\mathbf{q};\omega) \tag{1.2}$$

to have the same dimension in $\mathbf{q}$- and in $\mathbf{r}$-space.

The imaginary part of $\chi(q;\omega)$ is the experimentally accessible dynamic structure factor,

$$S(q;\omega) = -\frac{\hbar}{\pi}\Im m[\chi(q;\omega)]\,\theta(\omega)\,. \tag{1.3}$$

The dynamic structure factor satisfies, amongst others, the sum rules

$$m_0 = S(q) \;=\; \int_0^\infty d\hbar\omega\; S(q;\omega), \tag{1.4}$$

$$m_1 = \frac{\hbar^2 q^2}{2m} \;=\; \int_0^\infty d\hbar\omega\;\hbar\omega\, S(q;\omega)\,, \tag{1.5}$$

where $S(q)$ is the static structure factor.

We develop our theory with the following objectives:

- Technically, the extension of the Jackson–Feenberg–Campbell theory to Fermi systems amounts to including time–dependent *two–particle–two–hole* excitations. We require that the fermionic $\chi(q;\omega)$ reduces to that of the boson theory in the appropriate limit.

- For bosons, neglecting pair- and higher order fluctuations yields the famous Bijl-Feynman spectrum [10]
$$\varepsilon(q) = \frac{\hbar^2 q^2}{2mS(q)} \equiv \frac{t(q)}{S(q)}\,. \tag{1.6}$$
Its fermionic counterpart is the random–phase approximation (RPA), formulated in terms of effective interactions [19]. We require that our theory reduces to the RPA if pair fluctuations are ignored. This implies, in particular, that we obtain in this case a response function of the form
$$\chi(q;\omega) = \frac{\chi_0(q;\omega)}{1-\widetilde{V}_{\text{p-h}}(q)\,\chi_0(q;\omega)}\,. \tag{1.7}$$
Here, $\chi_0(q;\omega)$ is the Lindhard function and $\widetilde{V}_{\text{p-h}}(q)$ an appropriately defined static "particle–hole interaction" or "pseudo-potential".

One of the tasks of microscopic many–body theory is to justify and calculate effective interactions such as $\widetilde{V}_{\text{p-h}}(q)$, as far as this is possible. Using Jastrow–Feenberg correlation

functions [13] to tame the microscopic hard–core repulsion, it has been shown [5] under what assumptions a density response function of the RPA form (1.7) can be obtained, and a microscopic expression for the static effective interaction $\widetilde{V}_{\text{p-h}}(q)$ was derived. Under what conditions a form (1.7) is meaningful at all will be discussed in depth below.

A phenomenological approach to define a particle-hole interaction or "pseudo-potential" for ^{3}He and electrons was introduced by Aldrich, Iwamoto, and Pines [19, 20]. They determined the physically intuitive and necessary requirements for $\widetilde{V}_{\text{p-h}}(q)$, postulating that the dynamic response is given by the RPA form (1.7). Reflecting the same physics, the $\widetilde{V}_{\text{p-h}}(q)$ derived from microscopic many-body theory [5] is very similar to the Aldrich-Iwamoto-Pines pseudopotentials. The microscopic derivation leads to a $\widetilde{V}_{\text{p-h}}(q)$ that is uniquely determined from the static structure function by the two sum rules (1.4)-(1.5). Defining the RPA this way leads for bosons to the Feynman approximation (1.6) for the spectrum of collective excitations. From here on, we will use the term "RPA" and "Feynman spectrum" in this sense.

Our work is organized as follows: Section II introduces the basic quantities and the most important tools of variational and correlated basis function (CBF) theory. For details, the reader is referred to review articles [21] and pedagogical material [22]; a brief outline of our notations and definitions is given in appendix A. Section III is the core of our work; it provides the derivation of the equations of motion, including pair fluctuations. We show that the theory can be mapped onto a set of TDHF equations [3] with *energy-dependent, effective* interactions. Thus, our work provides the logical generalization of Ref. 5, where single-particle fluctuations led to a TDHF theory with *static* effective interactions.

Section IV focuses on the practical implementation of our theory. We formulate, among others, the "convolution approximation" for fermions. In Section V we derive the density-density response function $\chi(q;\omega)$ and discuss its features.

Modern techniques of many-body theory are robust against the details of the interparticle interaction. We can therefore use the methods developed here to examine the dynamics of two very different systems: The very strongly interacting ^{3}He whose interaction is characterized by a repulsive hard core and a short-ranged attraction, and electrons with their rather tame but long-ranged Coulomb interaction. Section VI implements our method for bulk ^{3}He and the electron liquid. In ^{3}He, we compare with neutron scattering experiments carried out at the Institut Laue Langevin (ILL) in the group led by R. Scherm [23–25]. The

energetics of the collective mode as well as the width of the spectrum at high momentum transfers are significantly improved compared to RPA predictions. In the homogeneous electron liquid the pair-excitation theory predicts plasmon damping as well as double-plasmon excitations. Experimental verification of the double-plasmon excitation in recent inelastic X-ray scattering measurements [26, 27] has added new interest in studying the dynamics of electrons.

Our results are summarized in Sec. VII where we also discuss the directions of future work.

Appendices A–E give further details on the derivations, and Appendix F a very brief summary of the minimal implementation of our theory.

II. THEORY FOR STRONGLY INTERACTING FERMIONS

A. Variational theory

Microscopic many-body theory starts with a phenomenological Hamiltonian for N interacting fermions,

$$H = -\sum_i \frac{\hbar^2}{2m}\nabla_i^2 + \sum_{i<j} v\left(|\mathbf{r}_i - \mathbf{r}_j|\right) \ . \tag{2.1}$$

For strong interactions, CBF theory [13] has proved to be an efficient and accurate method for obtaining ground state properties. It starts with a variational wave function of the form

$$|\Psi_{\mathbf{o}}\rangle = \frac{F\,|\Phi_{\mathbf{o}}\rangle}{\langle\Phi_{\mathbf{o}}|\,F^\dagger F\,|\Phi_{\mathbf{o}}\rangle^{1/2}} \ , \tag{2.2}$$

where $\Phi_{\mathbf{o}}(1,\ldots,i,\ldots,N)$ is a model state, normally a Slater–determinant, and "i" is short for both spatial and ν discrete (spin and/or isospin) degrees of freedom. The *correlation operator* $F(1,\ldots,N)$ is suitably chosen to describe the important features of the interacting system. Most practical and highly successful is the Jastrow–Feenberg [13] form

$$F(1,\ldots,N) \ = \ \exp\left\{\frac{1}{2}\left[\sum_{1\le i<j\le N} u_2(\mathbf{r}_i,\mathbf{r}_j) + \sum_{1\le i<j<k\le N} u_3(\mathbf{r}_i,\mathbf{r}_j,\mathbf{r}_k) + \ldots\right]\right\} . \tag{2.3}$$

The $u_n(\mathbf{r}_1,\ldots,\mathbf{r}_n)$ are made unique by requiring them to vanish for $|\mathbf{r}_i - \mathbf{r}_j| \to \infty$ ("cluster property").

From the wave function (2.2), (2.3), the energy expectation value

$$H_{\mathbf{o},\mathbf{o}} \equiv \langle\Psi_{\mathbf{o}}|\,H\,|\Psi_{\mathbf{o}}\rangle \tag{2.4}$$

can be calculated either by simulation or by integral equation methods. The hierarchy of Fermi-Hypernetted-Chain (FHNC) approximations is compatible with the optimization problem, *i.e.* with determining the optimal *correlation functions* $u_n(\mathbf{r}_1, \ldots, \mathbf{r}_n)$ through functionally minimizing the energy

$$\frac{\delta H_{\mathbf{o},\mathbf{o}}}{\delta u_n(\mathbf{r}_1, \ldots, \mathbf{r}_n)} = 0\,. \tag{2.5}$$

Due to the multitude of exchange diagrams, the Fermi-HNC (FHNC) and corresponding Euler equations can be quite complicated [28]; the simplest approximation of the Euler equations (2.5) that contains the important physics is spelled out in App. A 1.

The optimization of the correlations also facilitates making connections with other types of many-body theories, such as Feynman-diagram based expansions and summations [29].

B. Correlated Basis Functions

Although quite successful in predicting ground state properties of strongly interacting systems, the Jastrow-Feenberg form (2.3) of the correlation operator F has some deficiencies. The most obvious problem is that the nodes of the wave function (2.2) are identical to those of the model state $|\Phi_{\mathbf{o}}\rangle$. To improve upon the description of physics, CBF theory [21, 22, 28] uses the correlation operator F to generate a complete set of correlated and normalized N-particle basis states through

$$|\Psi_{\mathbf{m}}\rangle = \frac{F\,|\Phi_{\mathbf{m}}\rangle}{\langle\Phi_{\mathbf{m}}|F^\dagger F|\Phi_{\mathbf{m}}\rangle^{1/2}}\,, \tag{2.6}$$

where the $\{|\Phi_{\mathbf{m}}\rangle\}$ form a complete basis of model states. Although the $|\Psi_{\mathbf{m}}\rangle$ are not orthogonal, perturbation theory can be formulated in terms of these states [13, 30]. We review here this method only very briefly, details may be found in Refs. 21 and 22; the diagrammatic construction of the relevant ingredients is given in Ref. 31.

For economy of notation, we introduce a "second–quantized" formulation of the correlated states. The Jastrow–Feenberg correlation operator in (2.3) explicitly depends on the particle number, *i.e.* $F = F_N(1, \ldots, N)$ (whenever unambiguous, we omit the corresponding subscript). Starting from the conventional $a_k^\dagger, a_k$, creation and annihilation operators $\alpha_k^\dagger, \alpha_k$ of *correlated states* are defined by their action on the basis states:

$$|\alpha_k^\dagger\,\Psi_{\mathbf{m}}\rangle \;\equiv\; F_{N+1}a_k^\dagger\,|\Phi_{\mathbf{m}}\rangle \Big/ \langle\Phi_{\mathbf{m}}|a_k F_{N+1}^\dagger F_{N+1}a_k^\dagger|\Phi_{\mathbf{m}}\rangle^{1/2}\,, \tag{2.7}$$

$$|\alpha_k\,\Psi_{\mathbf{m}}\rangle \;\equiv\; F_{N-1}a_k\,|\Phi_{\mathbf{m}}\rangle\,\Big/\langle\Phi_{\mathbf{m}}|a_k^\dagger F_{N-1}^\dagger F_{N-1}a_k|\Phi_{\mathbf{m}}\rangle^{1/2}\,. \tag{2.8}$$

According to these definitions, $\alpha_k^\dagger$ and α_k obey the same (anti–) commutation rules as their uncorrelated cousins, *but they are not Hermitian conjugates.* If $|\Psi_{\mathbf{m}}\rangle$ is an N–particle state, then the state in Eq. (2.7) must carry an $(N{+}1)$-particle correlation operator, while that in Eq. (2.8) must be formed with an $(N{-}1)$–particle correlation operator.

In general, we label "hole" states, which are occupied in $|\Phi_{\mathbf{o}}\rangle$, by h, h', h_i , ..., and unoccupied "particle" states by p, p', p_i , *etc.* To display the particle-hole pairs explicitly, we will use alternatively to $|\Psi_{\mathbf{m}}\rangle$ the notation $|\Psi_{p_1\ldots p_d\,h_1\ldots h_d}\rangle$. A basis state with d particle-hole pairs is then

$$|\Psi_{p_1\ldots p_d\,h_1\ldots h_d}\rangle = \alpha_{p_1}^\dagger\cdots\alpha_{p_d}^\dagger\alpha_{h_d}\cdots\alpha_{h_1}|\Psi_{\mathbf{o}}\rangle\,. \tag{2.9}$$

The execution of the theory needs the matrix elements of the Hamiltonian, the unit operator, and the density operator. Key quantities are diagonal and off-diagonal matrix elements of unity and $H'\equiv H-H_{\mathbf{o},\mathbf{o}}$

$$M_{\mathbf{m},\mathbf{n}} \;=\; \langle\Psi_{\mathbf{m}}|\Psi_{\mathbf{n}}\rangle \equiv \delta_{\mathbf{m},\mathbf{n}} + N_{\mathbf{m},\mathbf{n}}\;, \tag{2.10}$$

$$H'_{\mathbf{m},\mathbf{n}} \;\equiv\; W_{\mathbf{m},\mathbf{n}} + \frac{1}{2}\,(H_{\mathbf{m},\mathbf{m}} + H_{\mathbf{n},\mathbf{n}} - 2H_{\mathbf{o},\mathbf{o}})\,N_{\mathbf{m},\mathbf{n}}\,. \tag{2.11}$$

Eq. (2.11) defines a natural decomposition [31, 32] of the matrix elements of $H'_{\mathbf{m},\mathbf{n}}$.

The ratios of normalization integrals, $I_{\mathbf{m},\mathbf{m}} \equiv \langle\Phi_{\mathbf{m}}|F^\dagger F|\Phi_{\mathbf{m}}\rangle$, define the factors

$$z_{p_1\ldots p_d\,h_1\ldots h_d} \equiv\; z_{\mathbf{m}} \;\equiv \sqrt{I_{\mathbf{m},\mathbf{m}}/I_{\mathbf{o},\mathbf{o}}}\;. \tag{2.12}$$

For large particle numbers and $d\ll N$ these factorize as

$$z_{\mathbf{m}} \;=\; \frac{z_{p_1}\cdots z_{p_d}}{z_{h_1}\cdots z_{h_d}} + \mathcal{O}(N^{-1})\,. \tag{2.13}$$

Likewise, to leading order in the particle number, the *diagonal* matrix elements of $H'\equiv H-H_{\mathbf{o},\mathbf{o}}$ become additive, so that for the above d-pair state we can define the CBF single particle energies

$$\langle\Psi_{\mathbf{m}}|H'|\Psi_{\mathbf{m}}\rangle \;\equiv\; \sum_{i=1}^{d} e_{p_ih_i} + \mathcal{O}(N^{-1})\;, \tag{2.14}$$

with $e_{ph} = e_p - e_h$.

For the off–diagonal elements $O_{\mathbf{m},\mathbf{n}}$ of an operator O (specifically the Hamiltonian, the unit-, density- and current-operator) we sort the quantum numbers m_i and n_i such that

$|\Psi_{\mathbf{m}}\rangle$ is mapped onto $|\Psi_{\mathbf{n}}\rangle$ by

$$|\Psi_{\mathbf{m}}\rangle = \alpha^\dagger_{m_1}\alpha^\dagger_{m_2}\cdots\alpha^\dagger_{m_d}\,\alpha_{n_d}\cdots\alpha_{n_2}\alpha_{n_1}\,|\Psi_{\mathbf{n}}\rangle\ . \tag{2.15}$$

From this we recognize that, to leading order in N, any $O_{\mathbf{m},\mathbf{n}}$ depends only on the *difference* between the states $|\Psi_{\mathbf{m}}\rangle$ and $|\Psi_{\mathbf{n}}\rangle$ and *not* on the states as a whole. Consequently, $O_{\mathbf{m},\mathbf{n}}$ can be written as matrix element of a d-body operator

$$O_{\mathbf{m},\mathbf{n}} \equiv \langle m_1\, m_2\, \ldots m_d\,|\mathcal{O}(1,2,\ldots d)\,|n_1\, n_2\, \ldots n_d\rangle_a\ . \tag{2.16}$$

(The index a indicates antisymmetrization.) According to (2.16), $W_{\mathbf{m},\mathbf{n}}$ and $N_{\mathbf{m},\mathbf{n}}$ define $d-$particle operators $\mathcal{N}$ and $\mathcal{W}$, *e.g.*

$$\begin{aligned} N_{\mathbf{m},\mathbf{o}} &\equiv N_{p_1p_2\ldots p_d\,h_1h_2\ldots h_d,0} \equiv \langle p_1p_2\ldots p_d\,|\,\mathcal{N}(1,2,\ldots,d)\,|\,h_1h_2\ldots h_d\rangle_a\ , \\ W_{\mathbf{m},\mathbf{o}} &\equiv W_{p_1p_2\ldots p_d\,h_1h_2\ldots h_d,0} \equiv \langle p_1p_2\ldots p_d\,|\,\mathcal{W}(1,2,\ldots,d)\,|\,h_1h_2\ldots h_d\rangle_a\ . \end{aligned} \tag{2.17}$$

Diagrammatic representations of $\mathcal{N}(1,2,\ldots,d)$ and $\mathcal{W}(1,2,\ldots,d)$ have the same topology [31]. In homogeneous systems, the continuous parts of the p_i, h_i are wave numbers $\mathbf{p}_i, \mathbf{h}_i$; we abbreviate their difference as $\mathbf{q}_i$. The highest occupied momentum is $\hbar k_{\rm F}$.

An important consideration is, for our purposes, the connection between CBF matrix elements, the static structure function, and the optimization conditions for the ground state. The static structure function $S(q) = \frac{1}{N}\langle\Psi_{\mathbf{o}}|\hat\rho_{\mathbf{q}}\hat\rho_{-\mathbf{q}}|\Psi_{\mathbf{o}}\rangle$ is routinely obtained in ground state calculations; for some systems it is also available from experiments. We can also write $S(q)$ as the weighted average of the matrix elements (2.17),

$$S(q)\ =\ S_{\rm F}(q) + \frac{1}{N}\sum_{hh'} z_{pp'hh'}N_{pp'hh',0}\,. \tag{2.18}$$

where $S_{\rm F}(q)$ is the static structure function of non-interacting fermions.

Similarly, the optimization conditions (2.5) for the pair correlation function can, in momentum space, be written in terms of off-diagonal matrix elements of the Hamiltonian:

$$\begin{aligned} 0 = \frac{\delta E}{\delta\tilde u_2(\mathbf{q},\mathbf{q}')} &= \frac{\langle\Phi_{\mathbf{o}}|\,F^\dagger H'F\,[\hat\rho_{\mathbf{q}}\hat\rho_{\mathbf{q}'} - \hat\rho_{\mathbf{q}+\mathbf{q}'}]\,|\Phi_{\mathbf{o}}\rangle}{\langle\Phi_{\mathbf{o}}|F^\dagger F|\Phi_{\mathbf{o}}\rangle} \\ &= \sum_{hh'}\frac{\langle\Phi_{\mathbf{o}}|\,F^\dagger H'F\,\left|a^\dagger_{p'}a^\dagger_p a_h a_{h'}\Phi_{\mathbf{o}}\right\rangle}{\langle\Phi_{\mathbf{o}}|F^\dagger F|\Phi_{\mathbf{o}}\rangle} = \sum_{hh'} z_{pp'hh'}H'_{pp'hh',0} \end{aligned} \tag{2.19}$$

i.e. the weighted average of the off-diagonal matrix elements $H'_{0,pp'hh'}$ vanishes for optimized pair correlations. Both features will provide rules for systematic and consistent approximation schemes for the operators $\mathcal{N}(1,2,\ldots,d)$ and $\mathcal{W}(1,2,\ldots,d)$.

III. EQUATIONS OF MOTION

A. Excitation operator and action principle

To formulate a theory of excited states for strongly interacting fermions we generalize the ansatz (2.2) in analogy to the pair fluctuations theory for strongly interacting bosons [6, 7, 12, 14–17]. We restrict ourselves here to uniform systems. The system is subjected to a small external perturbation

$$H_{\rm ext}(t) \equiv \int d^3r\, h_{\rm ext}(\mathbf{r};t)\,\hat{\rho}(\mathbf{r}) \tag{3.1}$$

where $\hat{\rho}(\mathbf{r})$ is the density operator. The correlated wave function for the perturbed state is chosen to be

$$\begin{aligned} \Big|\Psi(t)\Big\rangle &= \exp[-{\rm i}H_{\mathbf{o},\mathbf{o}}t/\hbar]\,\Big|\Psi_0(t)\Big\rangle\,, \\ \Big|\Psi_0(t)\Big\rangle &= \frac{1}{I^{1/2}(t)}\exp\Big[\tfrac{1}{2}U(t)\Big]\,\Big|\Psi_{\mathbf{o}}\Big\rangle \\ I(t) &= \Big\langle\Psi_{\mathbf{o}}\Big|\,\exp\Big[\tfrac{1}{2}U^\dagger(t)\Big]\exp\Big[\tfrac{1}{2}U(t)\Big]\,\Big|\,\Psi_{\mathbf{o}}\Big\rangle\,, \end{aligned} \tag{3.2}$$

with the excitation operator

$$\begin{aligned} U(t) &\equiv \sum_{ph}\delta u^{(1)}_{ph}(t)\;\alpha^\dagger_p\alpha_h + \frac{1}{2}\sum_{pp'hh'}\delta u^{(2)}_{pp'hh'}(t)\;\alpha^\dagger_p\alpha^\dagger_{p'}\alpha_{h'}\alpha_h \\ &\equiv U_1(t)+U_2(t)\,. \end{aligned} \tag{3.3}$$

The particle–hole amplitudes $\delta u^{(1)}_{ph}(t)$ and $\delta u^{(2)}_{pp'hh'}(t)$ are determined by the stationarity principle for the action

$$\mathcal{S}\left[\delta u^{(1)}_{ph}(t),\delta u^{(1)*}_{ph}(t),\delta u^{(2)}_{pp'hh'}(t),\delta u^{(2)*}_{pp'hh'}(t)\right] = \int dt\;\mathcal{L}(t)\;, \tag{3.4}$$

with the Lagrangian [1, 2, 4, 5]

$$\begin{aligned} \mathcal{L}(t) &= \Big\langle\Psi(t)\Big|\;H + H_{\rm ext}(t) - {\rm i}\,\hbar\frac{\partial}{\partial t}\;\Big|\Psi(t)\Big\rangle \\ &= \Big\langle\Psi_0(t)\Big|\;H' + H_{\rm ext}(t) - {\rm i}\,\hbar\frac{\partial}{\partial t}\;\Big|\Psi_0(t)\Big\rangle\,. \end{aligned} \tag{3.5}$$

A "boson" version of the theory is recovered when the particle-hole amplitudes $\delta u^{(1)}_{ph}(t)$ and $\delta u^{(2)}_{pp'hh'}(t)$ are restricted to *local* functions that depend only on the momentum transfers $\mathbf{q}^{(\prime)} = \mathbf{p}^{(\prime)} - \mathbf{h}^{(\prime)}$.

B. Brillouin conditions

To derive linear equations of motion, the Lagrangian (3.5) must be expanded to second order in the excitation operator $U(t)$. For the procedure to be meaningful, one should require that the first order terms vanish. This is, in principle, a necessary condition, however, in practice it is not always possible to satisfy it rigorously.

The first variation of the energy with respect to $\delta u^{(1)}_{ph}(t)$ and $\delta u^{(1)*}_{ph}(t)$ is

$$\left.\frac{\delta \langle\Psi(t)|\, H' \,|\Psi(t)\rangle}{\delta(\delta u^{(1)}_{ph}(t))}\right|_{\delta u^{(1)}(t)=\delta u^{(2)}(t)=0} = H'_{0,ph} \tag{3.6}$$

and its complex conjugate. This term vanishes in the homogeneous liquid due to momentum conservation.

The variation with respect to $\delta u^{(2)}_{pp'hh'}$ leads to a similar condition

$$\left.\frac{\delta \langle\Psi(t)|\, H' \,|\Psi(t)\rangle}{\delta(\delta u^{(2)}_{pp'hh'}(t))}\right|_{\delta u^{(1)}(t)=\delta u^{(2)}(t)=0} = H'_{0,pp'hh'} = 0 \tag{3.7}$$

and its complex conjugate. This condition is not rigorously satisfied by a Jastrow-Feenberg ground state. Recall, however, that the optimization condition (2.5) for pair correlations can be written in terms of off-diagonal matrix elements of H' in the form (2.19). If the correlation operator F is chosen optimally, *i.e.* satisfying Eq. (2.5) for all n, the weighted averages of $H_{\mathbf{o},\mathbf{n}}$ vanish. This shows precisely what an optimized ground state does: The Jastrow correlation function does not have enough flexibility to guarantee the Brillouin condition (3.7), because $H'_{0,pp'hh'}$ depends non–trivially on four momenta, whereas the two–body Jastrow–Feenberg function depends only on the momentum transfer. Optimization has the effect that the Brillouin conditions are satisfied in the Fermi-sea average.

To make progress we must assume that in the Lagrangian terms that are linear in the pair fluctuations are sufficiently small and can be omitted. Likewise, we also shall assume that the ground state wave function (2.3) is well enough optimized such that three- and four-body Brillouin conditions are satisfied. In momentum space, these are

$$\langle\Psi_0|H'\rho_{\mathbf{q}_1},\cdots,\rho_{\mathbf{q}_n}|\Psi_0\rangle = 0\,. \tag{3.8}$$

C. Transition density

The quantity of primary interest is the linear density fluctuation induced by the external field $H_{\rm ext}(t)$. We regard this density as a *complex* quantity; it is understood that the physical density fluctuation is its real part. Assuming the excitation operator (3.3), it is

$$\begin{aligned}\delta\rho(\mathbf{r};t) &= \sum_{ph}\left\langle\Psi_{\mathbf{o}}\right|\hat{\rho}(\mathbf{r})-\rho\left|\Psi_{ph}\right\rangle\delta u^{(1)}_{ph}(t)\\ &+\frac{1}{2}\sum_{pp'hh'}\left\langle\Psi_{\mathbf{o}}\right|\hat{\rho}(\mathbf{r})-\rho\left|\Psi_{pp'h'h}\right\rangle\delta u^{(2)}_{pp'hh'}(t)\\ &\equiv\sum_{ph}\rho_{0,ph}(\mathbf{r})\,\delta u^{(1)}_{ph}(t)+\frac{1}{2}\sum_{pp'hh'}\rho_{0,pp'hh'}(\mathbf{r})\,\delta u^{(2)}_{pp'hh'}(t)\,. \end{aligned}\tag{3.9}$$

The matrix elements of the density, $\rho_{0,ph}(\mathbf{r})$ and $\rho_{0,pp'hh'}(\mathbf{r})$ with respect to the correlated states can also be written as linear combinations of the matrix elements $\rho^{\rm F}_{0,ph}(\mathbf{r})$ with respect to uncorrelated states, and one-, two-, and three-body matrix elements of the unit operator. For the sake of discussion, let us briefly neglect the pair amplitudes. Since the density operator is local, we can commute $\hat{\rho}(\mathbf{r})$ to the right or to the left of the correlation operator F. The form obtained by commuting $\hat{\rho}(\mathbf{r})$ to the left is

$$\rho_{0,ph}(\mathbf{r})=\sum_{p'h'}\tilde{\rho}^{\rm F}_{0,p'h'}(\mathbf{r})\,M_{p'h',ph}=\rho^{\rm F}_{0,ph}(\mathbf{r})+\sum_{p'h'}\tilde{\rho}^{\rm F}_{0,p'h'}(\mathbf{r})\,N_{p'h',ph}\ ,\tag{3.10}$$

where $\tilde{\rho}^{F}_{0,ph}(\mathbf{r})\equiv z_{ph}\,\langle\Phi_{\mathbf{o}}|\,\hat{\rho}(\mathbf{r})-\rho\,|a^{\dagger}_{p}a_{h}\Phi_{\mathbf{o}}\rangle\equiv z_{ph}\,\langle h|\delta\hat{\rho}(\mathbf{r})|p\rangle$ are, apart from the normalization factors z_{ph}, the matrix elements of the density operator in a non-interacting system.

The second form is obtained by commuting $\hat{\rho}(\mathbf{r})$ to the right of F:

$$\rho_{0,ph}(\mathbf{r})=\frac{1}{z^2_{ph}}\tilde{\rho}^{\rm F}_{0,ph}(\mathbf{r})+\sum_{p'h'}N_{0,pp'hh'}\tilde{\rho}^{\rm F}_{p'h',0}(\mathbf{r})\,.\tag{3.11}$$

These two seemingly different expressions are identical, the different analytic forms appear only because the second quantized formulation hides the fact that the density operator is local. We will see below that both forms are useful.

Including pair fluctuations, the fluctuating density (3.9) can generally be written as

$$\delta\rho(\mathbf{r};t)\ =\ \sum_{ph}\tilde{\rho}^{\rm F}_{0,ph}(\mathbf{r})\left[\sum_{p'h'}M_{ph,p'h'}\delta u^{(1)}_{p'h'}(t)+\frac{1}{2}\sum_{p'p''h'h''}M_{ph,p'p''h'h''}\delta u^{(2)}_{p'p''h'h''}(t)\right]\,.\tag{3.12}$$

A key step that simplifies the structure of the equations of motion significantly is to introduce a new one-body function. In analogy to the boson theory [7], we define new

particle-hole amplitudes $\delta v^{(1)}_{ph}(t)$ through

$$\delta\rho(\mathbf{r};t) \equiv \sum_{ph} \rho_{0,ph}(\mathbf{r})\, \delta v^{(1)}_{ph}(t) \tag{3.13}$$

such that

$$\delta\rho(\mathbf{r};t) = \sum_{php'h'} \tilde{\rho}^{\mathrm{F}}_{0,ph}(\mathbf{r}) M_{ph,p'h'}\, \delta v^{(1)}_{p'h'}(t)\,. \tag{3.14}$$

This implies

$$\sum_{p'h'} M_{ph,p'h'}\, \delta v^{(1)}_{p'h'}(t) = \sum_{p'h'} M_{ph,p'h'}\, \delta u^{(1)}_{p'h'}(t) + \frac{1}{2} \sum_{p'p''h'h''} M_{ph,p'p''h'h''}\, \delta u^{(2)}_{p'p''h'h''}(t)\,. \tag{3.15}$$

Defining $M^{(\mathrm{I})}_{ph,p'p''h'h''}$ via

$$M_{ph,p'p''h'h''} \equiv \sum_{p_1h_1} M_{ph,p_1h_1} M^{(\mathrm{I})}_{p_1h_1,p'p''h'h''} \tag{3.16}$$

we can formally solve for $\delta v^{(1)}_{ph}(t)$:

$$\delta v^{(1)}_{ph}(t) = \delta u^{(1)}_{ph}(t) + \frac{1}{2} \sum_{p'p''h'h''} M^{(\mathrm{I})}_{ph,p'p''h'h''}\, \delta u^{(2)}_{p'p''h'h''}(t)\,. \tag{3.17}$$

For this operation, the inverse of $M_{ph,p'h'}$ seems to be needed. As its calculation is not immediately obvious, we hasten to note that $M^{(\mathrm{I})}_{ph,p'p''h'h''}$ is, in terms of Jastrow-Feenberg diagrams [31], a *proper subset* of the diagrams contributing to $M_{ph,p'p''h'h''}$. We will discuss the diagrammatic analysis of $\rho_{0,ph}(\mathbf{r})$ in App. B 1. The diagrammatic construction of $M^{(\mathrm{I})}_{ph,p'p''h'h''}$ in the spirit of Eq. (3.16) is carried out in App. B 2.

D. The Lagrangian

We split the Lagrangian (3.5) as $\mathcal{L}(t) = \mathcal{L}_{\mathrm{ext}}(t) + \mathcal{L}_{\mathrm{t}}(t) + \mathcal{L}_{\mathrm{int}}(t)$, with

$$\mathcal{L}_{\mathrm{ext}}(t) \;=\; \left\langle \Psi_0(t) \,\middle|\, H_{\mathrm{ext}} \,\middle|\, \Psi_0(t) \right\rangle , \tag{3.18}$$

$$\mathcal{L}_{\mathrm{t}}(t) \;=\; \left\langle \Psi_0(t) \middle| -\mathrm{i}\,\hbar \frac{\partial}{\partial t} \middle| \Psi_0(t) \right\rangle , \tag{3.19}$$

$$\mathcal{L}_{\mathrm{int}}(t) \;=\; \left\langle \Psi_0(t) \,\middle|\, H' \,\middle|\, \Psi_0(t) \right\rangle . \tag{3.20}$$

$\mathcal{L}_{\mathrm{ext}}(t)$ is obtained directly from the transition density:

$$\mathcal{L}_{\mathrm{ext}}(t) \;=\; \int d^3r\, h_{\mathrm{ext}}(\mathbf{r};t)\, \delta\rho(\mathbf{r};t)$$

$$= \int d^3r\, h_{\rm ext}(\mathbf{r};t)\, \Re e \left[\sum_{ph} \rho_{0,ph}(\mathbf{r})\, \delta u^{(1)}_{ph}(t) + \frac{1}{2} \sum_{pp'hh'} \rho_{0,pp'hh'}(\mathbf{r})\, \delta u^{(2)}_{pp'hh'}(t) \right]$$

$$= \Re e \sum_{ph} \int d^3r\, h_{\rm ext}(\mathbf{r};t)\, \rho_{0,ph}(\mathbf{r})\, \delta v^{(1)}_{ph}(t)\,. \tag{3.21}$$

The time-derivative term $\mathcal{L}_t(t)$ is, to second order in the fluctuations,

$$\begin{aligned}
\mathcal{L}_{\rm t}(t) &= \frac{\hbar}{2\langle\Psi_0(t)|\Psi_0(t)\rangle}\, \Im{\rm m} \sum \Big[\delta\dot{u}^{(1)}_{ph}(t)\, \langle\psi(t)|\alpha^\dagger_p\alpha_h\psi(t)\rangle \\
&\qquad + \frac{1}{2}\sum \delta\dot{u}^{(2)}_{pp'hh'}(t)\, \langle\Psi_0(t)|\alpha^\dagger_p\alpha^\dagger_{p'}\alpha_{h'}\alpha_h\Psi_0(t)\rangle \Big] \\
&= \frac{\hbar}{4}\, \Im{\rm m} \left[\sum \delta u^{(1)*}_{ph}(t) M_{ph,p'h'} \delta\dot{u}^{(1)}_{p'h'}(t) + \frac{1}{2}\sum \delta u^{(1)*}_{ph}(t) M_{ph,p'p''h'h''} \delta\dot{u}^{(2)}_{p'p''h'h''}(t) \right. \\
&+ \left. \frac{1}{2}\sum \delta u^{(2)*}_{pp'hh'}(t) M_{pp'hh',p''h''} \delta\dot{u}^{(1)}_{p''h''}(t) + \frac{1}{4}\sum \delta u^{(2)*}_{pp'hh'}(t) M_{pp'hh',p''p'''h''h'''} \delta\dot{u}^{(2)}_{p''p'''h''h'''}(t) \right].
\end{aligned} \tag{3.22}$$

Introducing the new amplitudes $\delta v^{(1)}_{ph}(t)$ defined in Eq. (3.13) eliminates the terms that couple the one- and the two-body amplitudes:

$$\mathcal{L}_{\rm t}(t) = \frac{\hbar}{4}\, \Im{\rm m} \left[\sum \delta v^{(1)*}_{ph}(t) M_{ph,p'h'} \delta\dot{v}^{(1)}_{p'h'}(t) + \frac{1}{4}\sum \delta u^{(2)*}_{pp'hh'}(t) M^{\rm (I)}_{pp'hh',p''p'''h''h'''} \delta\dot{u}^{(2)}_{p''p'''h''h'''}(t) \right], \tag{3.23}$$

where

$$M^{\rm (I)}_{pp'hh',p''p'''h''h'''} = M_{pp'hh',p''p'''h''h'''} - \sum_{p_1p_2h_1h_2} M^{\rm (I)}_{pp'hh',p_1h_1} M_{p_1h_1,p_2h_2} M^{\rm (I)}_{p_2h_2,p''p'''h''h'''}\,. \tag{3.24}$$

The second term in Eq. (3.24) cancels, in a diagrammatic expansion, some terms from the first one (*cf*. App. B 1). From Eqs. (3.21) and (3.23), the advantage of introducing the new particle-hole amplitudes $\delta v^{(1)}_{ph}(t)$ becomes obvious.

The contributions to the interaction term are classified according to the involved $n-$body fluctuations U_n as defined in (3.3),

$$\mathcal{L}_{\rm int}(t) = \mathcal{L}^{(11)}_{\rm int}(t) + \mathcal{L}^{(12)}_{\rm int}(t) + \mathcal{L}^{(22)}_{\rm int}(t)\,, \tag{3.25}$$

with

$$\begin{aligned}
\mathcal{L}^{(11)}_{\rm int}(t) &= \frac{1}{8}\langle\Psi_{\mathbf{o}}| \left[U^\dagger_1(t)U^\dagger_1(t)H' + 2U^\dagger_1(t)H'U_1(t) + H'U_1(t)U_1(t) \right] |\Psi_{\mathbf{o}}\rangle\,, \\
\mathcal{L}^{(12)}_{\rm int}(t) &= \frac{1}{4}\langle\Psi_{\mathbf{o}}| \left[U^\dagger_1(t)U^\dagger_2(t)H' + U^\dagger_1(t)H'U_2(t) + U^\dagger_2(t)H'U_1(t) + H'U_1(t)U_2(t) \right] |\Psi_{\mathbf{o}}\rangle\,, \\
\mathcal{L}^{(22)}_{\rm int}(t) &= \frac{1}{8}\langle\Psi_{\mathbf{o}}| \left[U^\dagger_2(t)U^\dagger_2(t)H' + 2U^\dagger_2(t)H'U_2(t) + H'U_2(t)U_2(t) \right] |\Psi_{\mathbf{o}}\rangle\,.
\end{aligned} \tag{3.26}$$

If the Brillouin conditions (3.6)–(3.7) as well as their generalizations to higher order fluctuations were satisfied exactly, all contributions to $\mathcal{L}_{\rm int}^{(ij)}(t)$ containing $U_i^\dagger(t)U_j^\dagger(t)$ and $U_i(t)U_j(t)$ would be zero. For fermions with optimized Jastrow–Feenberg wave functions it is only true in the averaged sense (2.19). These terms are nevertheless expected to be small in $\mathcal{L}_{\rm int}^{(22)}(t)$ since neglecting these terms is equivalent to negligible four-body correlations. Such a simplifying assumption is not necessary in $\mathcal{L}_{\rm int}^{(12)}(t)$ and $\mathcal{L}_{\rm int}^{(11)}(t)$ although we will see that the terms containing $U_1(t)U_2(t)$ and $U_1^\dagger(t)U_2^\dagger(t)$ in $\mathcal{L}_{\rm int}^{(12)}(t)$ are indeed negligible. We keep these terms for the time being since it will turn out that their omission will suggest, for consistency reasons, further simplifications.

The next step is to express the interaction term (3.26) in terms of the CBF matrix elements introduced on section II B. In the following it is understood that we sum over all quantum numbers when no summation subscripts are spelled out.

$$\mathcal{L}_{\rm int}^{(11)}(t) = \frac{1}{8}\sum \delta u_{ph}^{(1)*}(t)\delta u_{p'h'}^{(1)*}(t)H'_{pp'hh',0} + \text{c.c.} + \frac{1}{4}\sum \delta u_{ph}^{(1)*}(t)H'_{ph,p'h'}\delta u_{p'h'}^{(1)}(t)\ , \tag{3.27}$$

$$\begin{aligned}\mathcal{L}_{\rm int}^{(12)}(t) &= \frac{1}{8}\sum \delta u_{ph}^{(1)*}(t)\delta u_{p'p''h'h''}^{(2)*}(t)H'_{pp'p''hh'h'',0} + \text{c.c.} \\ &+ \frac{1}{8}\sum \delta u_{ph}^{(1)*}(t)H'_{ph,p'p''h'h''}\delta u_{p'p''h'h''}^{(2)}(t) + \text{c.c.}\ ,\end{aligned} \tag{3.28}$$

$$\begin{aligned}\mathcal{L}_{\rm int}^{(22)}(t) &= \frac{1}{32}\sum \delta u_{pp'hh'}^{(2)*}(t)\delta u_{p''p'''h''h'''}^{(2)*}(t)H'_{pp'p''p'''hh'h''h''',0} + \text{c.c.} \\ &+ \frac{1}{16}\sum \delta u_{pp'hh'}^{(2)*}(t)H'_{pp'hh',p''p'''h''h'''}\delta u_{p''p'''h''h'''}^{(2)}(t)\,.\end{aligned} \tag{3.29}$$

Substituting $\delta v_{ph}^{(1)}(t)$ for $\delta u_{ph}^{(1)}(t)$ leads to new coefficient functions in the interaction part of the Lagrangian:

$$\mathcal{L}_{\rm int}(t) = \mathcal{L}_{\rm int}^{\prime(11)}(t) + \mathcal{L}_{\rm int}^{\prime(12)}(t) + \mathcal{L}_{\rm int}^{\prime(22)}(t) \tag{3.30}$$

with

$$\mathcal{L}_{\rm int}^{\prime(11)}(t) = \frac{1}{8}\sum \delta v_{ph}^{(1)*}(t)\,\delta v_{p'h'}^{(1)*}(t)\,H'_{pp'hh',0} + \text{c.c.} + \frac{1}{4}\sum \delta v_{ph}^{(1)*}(t)\,H'_{ph,\,p'h'}\,\delta v_{p'h'}^{(1)}(t) \tag{3.31}$$

$$\begin{aligned}\mathcal{L}_{\rm int}^{\prime(12)}(t) &= \frac{1}{8}\sum \delta v_{ph}^{(1)*}(t)\,\delta u_{p'p''h'h''}^{(2)*}(t)\,K_{p'p''h'h'',0}^{(ph)} + \text{c.c.} \\ &+ \frac{1}{8}\sum \delta v_{ph}^{(1)*}(t)K_{ph,p'p''h'h''}\delta u_{p'p''h'h''}^{(2)}(t) + \text{c.c.}\end{aligned} \tag{3.32}$$

$$\begin{aligned}\mathcal{L}_{\rm int}^{\prime(22)}(t) &= \frac{1}{32}\sum \delta u_{pp'hh'}^{(2)*}(t)\,\delta u_{p''p'''h''h'''}^{(2)*}(t)\,K_{p''p'''h''h''',0}^{(pp'hh')} + \text{c.c.} \\ &+ \frac{1}{16}\sum \delta u_{pp'hh'}^{(2)*}(t)\,K_{pp'hh',\,p''p'''h''h'''}\,\delta u_{p''p'''h''h'''}^{(2)}(t)\,.\end{aligned} \tag{3.33}$$

The new coefficients $K_{\mathbf{m},\mathbf{n}}$ are

$$K_{ph,\,p'p''h'h''} \;\equiv\; H'_{ph,\,p'p''h'h''} - \sum_{p_1h_1} H'_{ph,\,p_1h_1}\, M^{(\mathrm{I})}_{p_1h_1,\,p'p''h'h''} \;, \tag{3.34}$$

$$K^{(ph)}_{p'p''h'h'',0} \;\equiv\; H'_{pp'p''hh'h'',0} - \sum_{p_1h_1} H'_{ph\,p_1h_1,0}\, M^{(\mathrm{I})}_{p'p''h'h'',\,p_1h_1} \;, \tag{3.35}$$

$$\begin{aligned} K_{pp'hh',\,p''p'''h''h'''} \;\equiv\;& H'_{pp'hh',\,p''p'''h''h'''} \\ &- \sum_{p_1h_1} \Big(M^{(\mathrm{I})}_{pp'hh',\,p_1h_1} H'_{p_1h_1,\,p''p'''h''h'''} + H'_{pp'hh',\,p_1h_1} M^{(\mathrm{I})}_{p_1h_1,\,p''p'''h''h'''} \Big) \\ &+ \sum_{p_1h_1p_2h_2} M^{(\mathrm{I})}_{pp'hh',\,p_1h_1} H'_{p_1h_1,\,p_2h_2} M^{(\mathrm{I})}_{p_2h_2,\,p''p'''h''h'''} \;, \end{aligned} \tag{3.36}$$

and an analogous term for $K^{(pp'hh')}_{p''p'''h''h''',0}$.

E. Equations of motion

With the sole approximation to neglect the terms proportional to $U_2(t)U_2(t)$ and $U_2^\dagger(t)U_2^\dagger(t)$, the Euler equations become

$$\sum \Big[\mathrm{i}\hbar M_{ph,p'h'} \frac{\partial}{\partial t} - H'_{ph,p'h'} \Big] \delta v^{(1)}_{p'h'}(t) \;-\; \sum H'_{pp'hh',0}\, \delta v^{(1)*}_{p'h'}(t) \tag{3.37}$$

$$-\frac{1}{2} \sum \Big[K_{ph,p'p''h'h''}\, \delta u^{(2)}_{p'p''h'h''}(t) \;+\; K^{(ph)}_{p'p''h'h'',0}\, \delta u^{(2)*}_{p'p''h'h''}(t) \Big] \;=\; 2 \int d^3r\, \rho_{ph,0}(\mathbf{r})\, h_{\mathrm{ext}}(\mathbf{r};t) \;,$$

$$\begin{aligned} &\frac{1}{2} \sum \Big[\mathrm{i}\hbar M^{(\mathrm{I})}_{pp'hh',\,p''p'''h''h'''} \frac{\partial}{\partial t} - K_{pp'hh',\,p''p'''h''h'''} \Big] \delta u^{(2)}_{p''p'''h''h'''}(t) \\ &\qquad - \sum \Big[K_{pp'hh',\,p''h''}\, \delta v^{(1)}_{p''h''}(t) + K^{(p''h'')}_{pp'hh',0}\, \delta v^{(1)*}_{p''h''}(t) \Big] \;=\; 0 \;. \end{aligned} \tag{3.38}$$

The time dependence of the external field can be assumed to be harmonic, with an infinitesimal turn-on component that determines the sign of the imaginary part

$$h_{\mathrm{ext}}(\mathbf{r};t) = h_{\mathrm{ext}}(\mathbf{r};\omega) \left[e^{\mathrm{i}\omega t} + e^{-\mathrm{i}\omega t} \right] e^{\eta t/\hbar} \,. \tag{3.39}$$

This imposes the time dependence

$$\begin{aligned} \delta v^{(1)}_{ph}(t) \;&=\; \delta v^{(1+)}_{ph}(\omega)\, e^{-\mathrm{i}(\omega+\mathrm{i}\eta/\hbar)t} \;+\; \Big[\delta v^{(1-)}_{ph}(\omega)\, e^{-\mathrm{i}(\omega+\mathrm{i}\eta/\hbar)t} \Big]^* , \\ \delta u^{(2)}_{pp'hh'}(t) \;&=\; \delta u^{(2+)}_{pp'hh'}(\omega)\, e^{-\mathrm{i}(\omega+\mathrm{i}\eta/\hbar)t} + \Big[\delta u^{(2-)}_{pp'hh'}(\omega)\, e^{-\mathrm{i}(\omega+\mathrm{i}\eta/\hbar)t} \Big]^* . \end{aligned} \tag{3.40}$$

Defining

$$E_{pp'hh',\,p''p'''h''h'''}(\omega) \equiv (\hbar\omega + \mathrm{i}\eta) M^{(\mathrm{I})}_{pp'hh',\,p''p'''h''h'''} - K_{pp'hh',\,p''p'''h''h'''} \tag{3.41}$$

the equations of motion for the pair fluctuations are

$$\frac{1}{2}\sum E_{pp'hh',p''p'''h''h'''}(\quad\omega)\,\delta u^{(2+)}_{p''p'''h''h'''}(\omega) = \sum\Big[K_{pp'hh',p''h''}\,\delta v^{(1+)}_{p''h''}(\omega) + K^{(p''h'')}_{pp'hh',0}\,\delta v^{(1-)}_{p''h''}(\omega)\Big]\,,$$
$$\frac{1}{2}\sum E^{*}_{pp'hh',p''p'''h''h'''}(-\omega)\,\delta u^{(2-)}_{p''p'''h''h'''}(\omega) = \sum\Big[K^{*}_{pp'hh',p''h''}\,\delta v^{(1-)}_{p''h''}(\omega) + K^{(p''h'')*}_{pp'hh',0}\,\delta v^{(1+)}_{p''h''}(\omega)\Big]\,. \tag{3.42}$$

All pair quantities are symmetric under the interchange of the involved pair variables, *e.g.* $(pp',hh') \leftrightarrow (p'p,h'h)$. We can utilize this feature to replace the fully symmetric $E_{pp'hh',p''p'''h''h'''}(\omega)$ by an asymmetric form, e.g. (C1) which removes the factor 1/2 in Eq. (3.42).

The pair equations (3.42) are now solved for the $\delta u^{(2\pm)}_{pp'hh'}(\omega)$ and the solutions are inserted into the one-body equation. The latter retains the structure of a TDHF equation, but with the matrix elements of H' supplemented by frequency-dependent terms. We adapt the definition of $W_{\mathbf{m},\mathbf{n}}$ in (2.11) by adding these corrections:

$$\begin{aligned} W_{ph,p'h'}(\omega) = W_{ph,p'h'} \;&+\; \sum K_{ph,p_1p_2h_1h_2}\,E^{-1}_{p_1p_2h_1h_2,p'_1p'_2h'_1h'_2}(\omega)K_{p'_1p'_2h'_1h'_2,p'h'} \\ &+\; \sum K^{(ph)}_{p_1p_2h_1h_2,0}E^{*-1}_{p_1p_2h_1h_2,p'_1p'_2h'_1h'_2}(-\omega)K^{(p'h')*}_{p'_1p'_2h'_1h'_2,0}\,, \qquad (3.43) \\ W_{pp'hh',0}(\omega) = W_{pp'hh',0} \;&+\; \sum K_{ph,p_1p_2h_1h_2}\,E^{-1}_{p_1p_2h_1h_2,p'_1p'_2h'_1h'_2}(\omega)K^{(p'h')}_{p'_1p'_2h'_1h'_2,0} \\ &+\; \sum K^{(ph)}_{p_1p_2h_1h_2,0}E^{*-1}_{p_1p_2h_1h_2,p'_1p'_2h'_1h'_2}(-\omega)K^{*}_{p'_1p'_2h'_1h'_2,p'h'}\,. \qquad (3.44) \end{aligned}$$

This TDHF form results also if the terms containing $U_2(t)U_2(t)$ are retained, but the expressions for the dynamic parts of the W-matrices become lengthier.

The equations of motion for the particle-hole amplitudes are then

$$\begin{aligned} 2\int d^3r\; h_{\rm ext}(\mathbf{r};\omega)\,\rho_{0,ph}(\mathbf{r}) \;&=\; \sum_{p'h'}\Big[(\hbar\omega{+}\mathrm{i}\eta)\,M_{ph,p'h'} - \delta_{p,p'}\delta_{h,h'}\,e_{ph}\Big]\,v^{(1+)}_{p'h'}(\omega) \\ &-\; \sum_{p'h'}\left[W_{ph,p'h'}(\omega) \;+\frac{1}{2}\,(e_{ph}+e_{p'h'})\,N_{ph,p'h'}\right]\delta v^{(1+)}_{p'h'}(\omega) \\ &-\; \sum_{p'h'}\left[W_{pp'hh',0}(\omega) + \frac{1}{2}\,(e_{ph}+e_{p'h'})\,N_{pp'hh',0}\right]\delta v^{(1-)}_{p'h'}(\omega)\,. \qquad (3.45) \end{aligned}$$

F. Supermatrix representation

We can now carry out exactly the same manipulations as in previous work [5] and reduce these equations (3.45) to the form of TDHF equations with energy-dependent effective interactions.

Equations (3.10) and (3.11) express the density in terms of CBF matrix elements in two different forms. For the present purpose, it is convenient to use these two representations symmetrically,

$$\delta\rho_{0,ph}(\mathbf{r}) = \frac{1}{2}\left[1+\frac{1}{z_{ph}^2}\right]\tilde{\rho}^{\rm F}_{0,ph}(\mathbf{r}) + \frac{1}{2}\sum_{p'h'}\left[\tilde{\rho}^{\rm F}_{0,p'h'}N_{p'h',ph} + \tilde{\rho}^{\rm F\,*}_{0,p'h'}(\mathbf{r})N_{0,pp'hh'}\right] \ . \tag{3.46}$$

Using Eqs. (3.13) and (3.40), the density fluctuations can then be written as

$$\begin{aligned}\delta\rho(\mathbf{r};\omega) \ &= \ \frac{1}{2}\sum_{ph}\left[\rho_{0,ph}(\mathbf{r})\,\delta v_{ph}^{(1+)}(\omega) + \rho^*_{0,ph}(\mathbf{r})\,\delta v_{ph}^{(1-)}(\omega)\right] \\ &\equiv \ \frac{1}{2}\sum_{ph}\left[\tilde{\rho}^{\rm F}_{0,ph}(\mathbf{r})\,\delta c_{ph}^{(1+)}(\omega) + \tilde{\rho}^{\rm F*}_{0,ph}(\mathbf{r})\,\delta c_{ph}^{(1-)}(\omega)\right] \ ,\end{aligned} \tag{3.47}$$

(*cf.* (3.10) for the definition of $\tilde{\rho}^{\rm F}_{0,ph}(\mathbf{r})$). This defines new amplitudes $\delta c_{ph}^{(1\pm)}(\omega)$. These relate, apart from the normalization factors, the observed density to the matrix elements of the density operator in the non-interacting system. The equations of motion can now be simplified by introducing a "supermatrix" notation. Particle-hole matrix elements together with their complex conjugate are combined into vectors, *e.g.*

$$\tilde{\boldsymbol{\rho}}^{\rm F} \equiv \begin{pmatrix} \tilde{\rho}^{\rm F}_{0,ph} \\ \tilde{\rho}^{F*}_{0,ph} \end{pmatrix} \quad ; \quad \delta\mathbf{c} \equiv \begin{pmatrix} \delta c_{ph}^{(1+)} \\ \delta c_{ph}^{(1-)} \end{pmatrix} \tag{3.48}$$

(and analogously for $\delta v_{ph}^{(1\pm)}$). Equation (3.47) then simply reads

$$\delta\rho(\mathbf{r};\omega) = \tfrac{1}{2}\,\delta\mathbf{c}(\omega)\cdot\tilde{\boldsymbol{\rho}}^{\rm F}(\mathbf{r}) \ . \tag{3.49}$$

The matrices

$$\mathbf{N} = \begin{pmatrix} N_{ph,p'h'} & N_{pp'hh',0} \\ N_{0,pp'hh'} & N_{p'h',ph} \end{pmatrix} \tag{3.50}$$

and

$$\mathbf{C} = \frac{1}{2}\begin{pmatrix} 1+\dfrac{1}{z_{ph}^2} & 0 \\ 0 & 1+\dfrac{1}{z_{ph}^2} \end{pmatrix}\delta_{p,p'}\delta_{h,h'} + \frac{1}{2}\mathbf{N} \tag{3.51}$$

relate the amplitude functions:

$$\delta\mathbf{c} = \mathbf{C}\cdot\delta\mathbf{v} \ . \tag{3.52}$$

In the driving term on the l.h.s. of (3.45) we use $\rho_{0,ph} = (\mathbf{C}\cdot\tilde{\boldsymbol{\rho}}^{\rm F})_{0,ph}$ to obtain

$$2\int d^3r\ h_{\rm ext}(\mathbf{r};\omega)\,\rho_{0,ph}(\mathbf{r}) = 2\,\mathbf{C}\cdot\mathbf{h}^{\rm ext} \ , \tag{3.53}$$

where the vector $\mathbf{h}^{\rm ext}$ is built with the non-interacting states (*cf*. $\tilde{\rho}^F_{0,ph}$ in (3.10))

$$\tilde{h}^F_{0,ph}(\omega) = z_{ph}\,\langle h|\,h_{\rm ext}(\mathbf{r};\omega)\,|p\rangle\,. \tag{3.54}$$

Defining the $\omega-$dependent matrices

$$\begin{aligned}
\mathbf{\Omega} &= \begin{pmatrix} (\hbar\omega+{\rm i}\eta - e_{ph})\delta_{p,p'}\delta_{h,h'} & 0 \\ 0 & -(\hbar\omega+{\rm i}\eta + e_{ph})\delta_{p,p'}\delta_{h,h'} \end{pmatrix}\,, \\
\mathbf{W} &= \begin{pmatrix} W^{(+)}_{ph,p'h'}(\omega) & W^{(-)}_{pp'hh',0}(\omega) \\ W^{(+)}_{0,pp'hh'}(\omega) & W^{(-)}_{p'h',ph}(\omega) \end{pmatrix}\,,
\end{aligned} \tag{3.55}$$

the equations of motion assume supermatrix form [5]

$$\left[\mathbf{\Omega} + \frac{1}{2}\mathbf{\Omega N} + \frac{1}{2}\mathbf{N\Omega} - \mathbf{W}(\omega)\right]\cdot\delta\mathbf{v} \;=\; 2\mathbf{C}\cdot\mathbf{h}^{\rm ext}\,. \tag{3.56}$$

We now formally define a new, energy–dependent interaction matrix $\mathbf{V}_{\rm p-h}(\omega)$ by

$$\left[\mathbf{\Omega} + \frac{1}{2}\mathbf{\Omega N} + \frac{1}{2}\mathbf{N\Omega} - \mathbf{W}\right] \;\equiv\; \mathbf{C}\cdot\left[\mathbf{\Omega} - \mathbf{V}_{\rm p-h}(\omega)\right]\cdot\mathbf{C}\,. \tag{3.57}$$

Thus the response equations take the simple TDHF form

$$\left[\mathbf{\Omega} - \mathbf{V}_{\rm p-h}(\omega)\right]\cdot\delta\mathbf{c} \;=\; 2\mathbf{h}^{\rm ext}\,. \tag{3.58}$$

With this, we have reformulated the theory for a strongly interacting system in the TDHF form (3.58) but with an energy dependent effective interaction. Our derivation has led to a clear definition of this effective particle-hole interaction and to a prescription on how to calculate this from the underlying bare Hamiltonian.

The formal derivation appears to involve the calculation of the inverse of a huge matrix. The key point, however, is that the manipulation (3.57) can be carried out diagrammatically. Then it becomes obvious that many terms occurring in the combination of matrices in (3.56) are *not* part of $\mathbf{V}_{\rm p-h}(\omega)$. Specifically, these are the chain diagrams in the direct channel [5].

IV. DIAGRAMMATIC ANALYSIS AND LOCAL INTERACTIONS

A. General strategy

Generally, the non-local operators $\mathcal{N}(1,2)$ and $\mathcal{W}(1,2)$ in (2.17) consists of up to 4-point functions. Cluster expansions and resummations have been carried out in Ref. 31 and led to

reasonably compact representations in terms of the compound-diagrammmatic quantities of the FHNC summation method. Nevertheless, due to their non-locality, it is difficult to deal with these quantities exactly. The simplest approximation for the operator is to keep just the local terms. These are given by the "direct-direct" correlation function $\Gamma_{\rm dd}(|\mathbf{r}_1-\mathbf{r}_2|)$ of FHNC theory. This approximation is adequate but not optimal.

On the other hand, summing $N_{0,pp'hh'}$ over the hole states, Eq. (2.18), relates $\mathcal{N}(1,2)$ to the static structure function. Accurate results are available for $S(q)$, either from simulations [33, 34] or from the FHNC-EL summation technique [28, 35]. An alternative strategy to deal with non-local operators is therefore to demand that these results are reproduced in whatever approximate form one chooses to use. In this sense, by *choosing* $\mathcal{N}(1,2)$ to be local, *naming* the corresponding function $\Gamma_{\rm dd}(r)$, and demanding that this operator in (2.18) gives the known static structure function, we obtain the relationship

$$S(q) = S_{\rm F}(q)\left[1+\tilde{\Gamma}_{\rm dd}(q)\,S_{\rm F}(q)\right] \tag{4.1}$$

as a *definition* of $\tilde{\Gamma}_{\rm dd}(q)$ in terms of $S(q)$. We adopt this view here and define the "best" local approximation for $\mathcal{N}(1,2)$ such that it reproduces the best known $S(q)$. Since the exact $S(q)$ contains a summation of exchange terms, this implies that their contribution to $S(q)$ is mimicked by a local contribution to $\tilde{\Gamma}_{\rm dd}(q)$.

An "optimal" local approximation for the effective interaction $\mathcal{W}(1,2)$ can be obtained along similar lines. From Eqs. (2.14) and (2.11) we have

$$H'_{0,pp'hh'} = W_{0,pp'hh'} + \frac{1}{2}\,(e_{ph}+e_{p'h'})\,N_{0,pp'hh'}\ . \tag{4.2}$$

The ground state Euler equation for pair correlations (2.19) implies that the Fermi sea average of $H'_{0,pp'hh'}$ vanishes. Postulating a local $\mathcal{W}(1,2)\approx W(r_{12})$, consistency relates this quantity to the local approximation of $\mathcal{N}(1,2)$. This leads to [28]

$$\widetilde{W}(q) = -\frac{t(q)}{S_{\rm F}(q)}\,\tilde{\Gamma}_{\rm dd}(q)\ . \tag{4.3}$$

Our procedure of using the relationships (2.18) and (2.19) to construct local approximations for $N_{0,pp'hh'}$ and $W_{0,pp'hh'}$ can be generalized to a systematic definition of optimal local approximations for the matrix elements of any non-local $d-$body operator: Averaging the matrix elements, which depend on d particle and d hole momenta, over the Fermi sea, generates functions of the momentum transfers $\mathbf{q}_i\equiv\mathbf{p}_i-\mathbf{h}_i$ only. Spelling out Fermi occupation

functions $n_{\mathbf{h}}$ and $\bar{n}_{\mathbf{p}} \equiv 1 - n_{\mathbf{p}}$ explicitly, this reads for a one-body quantity

$$O_{\mathbf{q}} \equiv \frac{\sum_h \bar{n}_{\mathbf{p}} n_{\mathbf{h}}\, O_{0,ph}}{\sum_h \bar{n}_{\mathbf{p}} n_{\mathbf{h}}\, 1} = \frac{1}{N S_{\rm F}(q)} \sum_h \bar{n}_{\mathbf{h}+\mathbf{q}} n_{\mathbf{h}}\, O_{0,\,ph} \ . \tag{4.4}$$

The extension to d variables is obvious,

$$O_{\mathbf{q}_1,\ldots,\mathbf{q}_d} = \sum_{h_1 \ldots h_d} \prod_{i=1}^{d} \frac{\bar{n}_{\mathbf{p}_i} n_{\mathbf{h}_i}}{N S_{\rm F}(q_i)}\, O_{0,\,p_1 \ldots p_d\, h_1 \ldots h_d} \ , \tag{4.5}$$

as is the extension to matrix elements $O_{\mathbf{m},\mathbf{n}\neq\mathbf{o}}$.

We emphasize again that the quantities $O_{\mathbf{q}_1,\ldots,\mathbf{q}_d}$ contain all exchange and correlation effects in a localized manner. Therefore, effects related to the z_{ph}, as well as CBF corrections to the e_{ph} , are already part of $\widetilde{W}(q)$ and $\tilde{\Gamma}_{\rm dd}(q)$. This implies, amongst others,

$$M_{p'h',ph} \approx \delta_{p,p'}\delta_{h,h'} + \langle hp'|\Gamma_{\rm dd}|ph'\rangle \ , \tag{4.6}$$

and the relationship (3.51) between the supermatrices $\mathbf{C}$ and $\mathbf{N}$ simplifies to

$$\mathbf{C} = \mathbf{1} + \frac{1}{2}\mathbf{N} \ . \tag{4.7}$$

B. Matrix elements

The localization procedure discussed above for $\mathcal{N}(1,2)$ implies

$$\mathbf{N} = \frac{1}{N}\tilde{\Gamma}_{\rm dd}(q) \begin{pmatrix} \delta_{\mathbf{q},+\mathbf{q}'} & \delta_{\mathbf{q},-\mathbf{q}'} \\ \delta_{\mathbf{q},-\mathbf{q}'} & \delta_{\mathbf{q},+\mathbf{q}'} \end{pmatrix} \bar{n}_{\mathbf{p}}\, \bar{n}_{\mathbf{p}'} n_{\mathbf{h}}\, n_{\mathbf{h}'} \ . \tag{4.8}$$

To simplify the notation, the $\delta_{\mathbf{q},\pm\mathbf{q}'}$ functions, together with the Fermi occupation numbers, are understood to be implicit in all the matrices from now on. Matrix products, *i.e.* sums over particle–hole labels, reduce to factors $S_{\rm F}(q)$. The inverse of $\mathbf{C}$ is readily obtained from (4.7) as

$$\mathbf{C}^{-1} = \mathbf{1} - \frac{1}{2N}\tilde{X}_{\rm dd}(q) \begin{pmatrix} 1 & 1 \\ 1 & 1 \end{pmatrix} \ . \tag{4.9}$$

with

$$\tilde{X}_{\rm dd}(q) = \frac{\tilde{\Gamma}_{\rm dd}(q)}{1 + S_{\rm F}(q)\,\tilde{\Gamma}_{\rm dd}(q)} \ . \tag{4.10}$$

In the spirit of the discussion in Sec. IV A, this is our definition of $\tilde{X}_{\rm dd}(q)$. According to (A13), it can also be identified with the sum of all non-nodal diagrams.

Multiplying $\mathbf{C}^{-1}$ from both sides to (3.57) yields the ω dependent effective interactions,

$$\mathbf{V}_{\rm p-h}(\omega) = \frac{1}{N}\begin{pmatrix} \tilde{V}_{\rm A}\,(q;\quad \omega) & \tilde{V}_{\rm B}\,(q;\quad \omega) \\ \tilde{V}_{\rm B}^{*}(q;-\omega) & \tilde{V}_{\rm A}^{*}(q;-\omega)\,. \end{pmatrix}\,. \tag{4.11}$$

To summarize, the localization of $\mathcal{N}(1,2)$ in an $S(q)$ conserving manner has *uniquely* fixed the functions $\tilde{\Gamma}_{\rm dd}(q)$ and $\tilde{X}_{\rm dd}(q)$ and, consequently, the corresponding matrices $\mathbf{N}$ and $\mathbf{C}^{-1}$. Calculating $\mathbf{V}_{\rm p-h}(\omega)$ from (3.57) has thus been reduced to calculating $V_{\rm A,B}(q;\omega)$ from $\mathbf{W}$.

In order to derive the explicit expressions, we need the optimal local form of (3.43). This involves two steps, calculating the localized versions of the three-body vertices $K_{ph,p'p''h'h''}$ and $K^{(ph)}_{p'p''h'h'',0}$, and deriving the inverse of the four-body energy matrix $[E(\omega)]^{-1}$. We expect these quantities to be sufficiently accurate within the convolution approximation, since improving on this only marginally changes the results [7] for bosons.

The details of the derivation of the local three-body vertices $\tilde{K}_{q,q'q''}$ and $\tilde{K}^{(q)}_{q'q'',0}$ defined in (3.34)-(3.36) can be found in App. B 3. These are

$$\begin{aligned}\tilde{K}_{q,q'q''} \;=\; & \frac{\hbar^2}{2m}\,\frac{S(q')S(q'')}{S_{\rm F}(q)S_{\rm F}(q')S_{\rm F}(q'')}\left[\mathbf{q}\cdot\,\mathbf{q}'\,\tilde{X}_{\rm dd}(q') + \mathbf{q}\cdot\,\mathbf{q}''\,\tilde{X}_{\rm dd}(q'') - q^2\tilde{u}_3(q,q',q'')\right] \\ & + \left[1 - \frac{S_{\rm F}(q')S_{\rm F}(q'')}{S(q')S(q'')}\right]^{-1}\tilde{K}^{(q)}_{q'q'',0}\,,\end{aligned} \tag{4.12}$$

$$\tilde{K}^{(q)}_{q'q'',0} \;=\; \frac{\hbar^2}{4m}\,\tilde{\Gamma}_{\rm dd}(q)\;\left[\frac{S(q')S(q'')}{S_{\rm F}(q')S_{\rm F}(q'')} - 1\right]\left\{\frac{q^2\,S^{(3)}_{\rm F}(q,q',q'')}{S_{\rm F}(q)S_{\rm F}(q')S_{\rm F}(q'')} \;+\; \left[\frac{\mathbf{q}\cdot\mathbf{q}'}{S_{\rm F}(q')} + \frac{\mathbf{q}\cdot\mathbf{q}''}{S_{\rm F}(q'')}\right]\right\} \tag{4.13}$$

Here, $S^{(3)}_{\rm F}(q,q',q'')$ is the three-body static structure function of non-interacting fermions, defined in Eq. (B8), and $\tilde{u}_3(q,q',q'')$ is the ground-state triplet correlation function [28]. The implicit momentum conservation functions $\delta_{\pm\mathbf{q},\mathbf{q}'+\mathbf{q}''}$ ensure that both vertices depend on the magnitudes of the three arguments only.

Going back to the Lagrangian, we realize that the term $\tilde{K}^{(q)}_{q'q'',0}$ is the coefficient function of the contributions to $\mathcal{L}'^{(12)}(t)$ containing $U_1(t)U_2(t)$ which we expect to be small. Our numerical applications to be discussed below will support this expectation. However, the vertex $\tilde{K}_{q,q'q''}$ contains a term of the same form. Neglecting $\tilde{K}^{(q)}_{q'q'',0}$ should, for consistency, also mean neglecting the same term in $\tilde{K}_{q,q'q''}$ which is then given by the very simple first

part of Eq. (4.12). In this term we recover, apart from $S_F(q)$ factors, also the Bose version of the three-body vertex.

C. Effective interactions

Next, the matrix elements (4.12) and (4.13) are used in (3.43) to calculate the dynamic parts of **W**,

$$\begin{aligned} W_{ph,p'h'}(\omega) &= \frac{\delta_{\mathbf{q},\mathbf{q}'}}{N}\left[\widetilde{W}(q) + \widetilde{W}_{\rm A}(q;\omega)\right] \\ W_{php'h',0}(\omega) &= \frac{\delta_{\mathbf{q},-\mathbf{q}'}}{N}\left[\widetilde{W}(q) + \widetilde{W}_{\rm B}(q;\omega)\right], \end{aligned} \tag{4.14}$$

where the energy independent part $\widetilde{W}(q)$ has been defined in Eq. (4.3). Because of the locality of the three-body matrix elements, we can write for the first dynamic contribution to (3.43),

$$\begin{aligned} &\sum_{p_1p_2h_1h_2}\sum_{p_1'p_2'h_1'h_2'} K_{ph,\,p_1p_2h_1h_2}\left[E(\omega)^{-1}\right]_{p_1p_2h_1h_2,p_1'p_2'h_1'h_2'} K_{p_1'p_2'h_1'h_2',\,p'h'} \\ &= \frac{1}{N^2}\sum_{q_1q_1'}\tilde{K}_{q,\,q_1q_2}\,\tilde{K}_{q_1'q_2',\,q}\,\frac{1}{N^2}\sum_{h_1h_2h_1'h_2'}\left[E(\omega)^{-1}\right]_{p_1p_2h_1h_2,p_1'p_2'h_1'h_2'} \\ &= \frac{1}{N^2}\sum_{q_1q_2}\tilde{K}_{q,\,q_1q_2}\,\tilde{E}^{-1}(q_1,q_2;\omega)\tilde{K}_{q_1q_2,\,q} \end{aligned} \tag{4.15}$$

with implicit factors $\delta_{\mathbf{q},\mathbf{q}_1+\mathbf{q}_2}\,\delta_{\mathbf{q},\mathbf{q}_1'+\mathbf{q}_2'}$ for momentum conservation. The other contributions to (3.43) are calculated analogously. The inverse four body energy matrix and the pair propagator

$$\frac{1}{N^2}\sum_{hh'h''h'''}\left[E(\omega)^{-1}\right]_{pp'hh',p''p'''h''h'''} \equiv \delta_{q,q''}\delta_{q',q'''}\,\tilde{E}^{-1}(q,q';\omega)\,. \tag{4.16}$$

are calculated and discussed in App. C. Basically, the pair spectrum is built from two particle-hole spectra. These are, however, not centered around free particle spectra but around the Feynman dispersion relation. Consequently, our pair propagator also includes *two-phonon* intermediate states.

The resulting expressions for the energy-dependent $\widetilde{W}_{\rm A,B}(q;\omega)$ are then

$$\widetilde{W}_{\rm A}(q;\omega) = \frac{1}{2N}\sum_{\mathbf{q}'\mathbf{q}''}\left[|\tilde{K}_{q,q'q''}|^2\,\tilde{E}^{-1}(q',q'';\omega) + |\tilde{K}^{(q)}_{q'q'',0}|^2\,\tilde{E}^{-1*}(q',q'';-\omega)\right], \tag{4.17}$$

$$\widetilde{W}_{\rm B}(q;\omega) = \frac{1}{2N}\sum_{\mathbf{q}'\mathbf{q}''}\left[\tilde{K}^{(q)}_{q'q'',0}\tilde{K}_{q,q'q''}\left(\tilde{E}^{-1}(q',q'';\omega) + \tilde{E}^{-1*}(q',q'';-\omega)\right)\right]. \tag{4.18}$$

Similar to the boson theory, the dynamic parts of the interactions are expressed in terms of three-body vertices and an energy denominator, the latter now being "spread" over the whole width of a two-particle-two-hole band.

The last step in our formal derivations is the calculation of $\mathbf{V}_{\mathrm{p-h}}(\omega)$. Carrying out the operations (3.57) yields the energy-dependent, but local functions

$$\begin{aligned}\tilde{V}_{\mathrm{A}}(q;\omega) = \tilde{V}_{\mathrm{p-h}}(q) \;&+\; [\sigma_q^+]^2\,\widetilde{W}_{\mathrm{A}}(q;\omega) + [\sigma_q^-]^2\,\widetilde{W}^*_{\mathrm{A}}(q;-\omega) \\ &+\; \sigma_q^+\sigma_q^-\,\left(\widetilde{W}_{\mathrm{B}}(q;\omega) + \widetilde{W}^*_{\mathrm{B}}(q;-\omega)\right)\,, \qquad (4.19)\\ \tilde{V}_{\mathrm{B}}(q;\omega) = \tilde{V}_{\mathrm{p-h}}(q) \;&+\; [\sigma_q^+]^2\,\widetilde{W}_{\mathrm{B}}(q;\omega) + [\sigma_q^-]^2\,\widetilde{W}^*_{\mathrm{B}}(q;-\omega) \\ &+\; \sigma_q^+\sigma_q^-\,\left(\widetilde{W}_{\mathrm{A}}(q;\omega) + \widetilde{W}^*_{\mathrm{A}}(q;-\omega)\right)\,, \qquad (4.20)\end{aligned}$$

with $\sigma_q^\pm \equiv [S_{\mathrm{F}}(q) \pm S(q)]/2S(q)$.

V. DENSITY-DENSITY RESPONSE FUNCTION

A. General form

We now derive the density-density response function $\chi(q;\omega)$. The final result for the dynamic effective interactions, (4.19), (4.20), is inserted into (3.58), which is solved for $\delta\mathbf{c}$. The induced density is then obtained from Eq. (3.47). Using $\rho^{\mathrm{F}}_{0,ph}(\mathbf{r}) = \frac{\rho}{N} e^{-\mathrm{i}(\mathbf{p}-\mathbf{h})\mathbf{r}}$ we obtain

$$\begin{aligned}\delta\rho(q;\omega) \;&=\; \frac{\rho}{2}\sum_h \left[z_{\mathbf{h+q},\mathbf{h}}\,\delta c^{(1+)}_{\mathbf{h+q},\mathbf{h}}(\omega)\,\bar{n}_{\mathbf{h-q}} + z_{\mathbf{h-q},\mathbf{h}}\,\delta c^{(1-)}_{\mathbf{h-q},\mathbf{h}}(\omega)\,\bar{n}_{\mathbf{h+q}}\right] \\ &\approx\; \frac{NS_{\mathrm{F}}(k)\,\rho}{2}\left[\delta c^{(1+)}(q;\omega) + \delta c^{(1-)}(q;\omega)\right]\,, \qquad (5.1)\end{aligned}$$

where we abbreviate in the second line $\delta c^{(1\pm)}(q;\omega) \;\equiv\; \frac{1}{N}\sum_h \delta c^{(1\pm)}_{ph}(\omega)$. Spelling out Eqs. (3.58) explicitly,

$$\begin{aligned}2\tilde{h}^F_{0,ph}(\omega) \;&=\; (\pm(\hbar\omega{+}\mathrm{i}\eta) - e_{ph})\,\delta c^{(\pm)}_{ph}(\omega) \\ &-\; \tilde{V}_{\mathrm{A}}\,(q;\omega)\,\delta c^{(\pm)}(q;\omega) - \tilde{V}^*_{\mathrm{B}}(q;-\omega)\,\delta c^{(\mp)}(q;\omega)\,, \qquad (5.2)\end{aligned}$$

dividing by $(\pm(\hbar\omega{+}\mathrm{i}\eta) - e_{ph})$ and summing over h yields

$$\delta c^{(1\pm)}(q;\omega) \;=\; \left[\frac{2}{N}\,\tilde{h}_{\mathrm{ext}}(q;\omega) + \tilde{V}_{\mathrm{A}}(q;\omega)\,\delta c^{(1\pm)}(q;\omega) + \tilde{V}^*_{\mathrm{B}}(q;-\omega)\,\delta c^{(1\mp)}(q;\omega)\right]\begin{cases}\kappa_0(q;\,\omega)\\ \kappa_0^*(q;-\omega)\end{cases} \qquad (5.3)$$

with the positive-energy Lindhard function

$$\kappa_0(q;\omega) \equiv \frac{1}{N}\sum_h \frac{\bar{n}_{\mathbf{p}} n_{\mathbf{h}}}{\hbar\omega - e_{ph} + \mathrm{i}\eta} \tag{5.4}$$

which is related to the full Lindhard function by

$$\chi_0(q;\omega) = \kappa_0(q;\omega) + \kappa_0^*(q;-\omega)\,. \tag{5.5}$$

Solving for $\delta c^{(1\pm)}(q;\omega)$ and inserting into (5.1) we obtain for $\chi(q;\omega)$

$$\begin{aligned}
\chi(q;\omega) &= N(q;\omega)/D(q;\omega) \\
N(q;\omega) &= \kappa_0(q;\omega) + \kappa_0^*(q;-\omega) \\
&- \kappa_0(q;\omega)\kappa_0^*(q;-\omega)\left[\tilde{V}_{\mathrm{A}}(q;\omega) + \tilde{V}_{\mathrm{A}}^*(q;-\omega) - \tilde{V}_{\mathrm{B}}(q;\omega) - \tilde{V}_{\mathrm{B}}^*(q;-\omega)\right] \\
D(q;\omega) &= 1 - \kappa_0(q;\omega)\tilde{V}_{\mathrm{A}}(q;\omega) - \kappa_0^*(q;-\omega)\tilde{V}_{\mathrm{A}}^*(q;-\omega) \\
&+ \kappa_0(q;\omega)\kappa_0^*(q;-\omega)\left[\tilde{V}_{\mathrm{A}}(q;\omega)\tilde{V}_{\mathrm{A}}^*(q;-\omega) - \tilde{V}_{\mathrm{B}}(q;\omega)\tilde{V}_{\mathrm{B}}^*(q;-\omega)\right]\,.
\end{aligned} \tag{5.6}$$

Eq. (5.6) is the TDHF response function for local and energy dependent interactions. Evidently, the conventional RPA form (1.7) can only be recovered if the interactions $\tilde{V}_{\mathrm{A}}(q;\omega)$ and $\tilde{V}_{\mathrm{B}}(q;\omega)$ are *energy independent* and *equal.* Clearly, our result (5.6) significantly differs from (1.7) with $\widetilde{V}_{\text{p-h}}(q)$ simply replaced by some energy dependent $\widetilde{V}_{\text{p-h}}(q;\omega)$. Such an RPA-like form for the density-density response function lacks microscopic justification.

B. Long wavelength limit

In the limit $q \to 0$, the spectrum is dominated by collective excitations, *e.g.* zero sound or plasmons. Both vertices (4.12) and (4.13) vanish linearly in q, hence $\widetilde{W}_{\mathrm{A}}(q;\omega)$ and $\widetilde{W}_{\mathrm{B}}(q;\omega)$ are quadratic in q as $q \to 0$.

For neutral systems, the dynamic corrections to the effective interactions $\tilde{V}_{\mathrm{A,B}}(q;\omega)$ in (4.19), (4.20) are therefore negligible in the long wavelength limit. The long wavelengths density-density response function is then given by its RPA form (1.7), with the static particle-hole interaction $\widetilde{V}_{\text{p-h}}(q)$. The zero sound speed c_0 is determined by the long wavelength solution of the RPA equation.

For charged quantum fluids, $\sigma_q^{\pm} \approx S_{\mathrm{F}}(q)/2S(q)$, hence $\tilde{V}_{\mathrm{A}}(q,\omega) = \tilde{V}_{\mathrm{B}}(q,\omega)$, which again implies the RPA form (1.7)

$$\chi(q;\omega) \;=\; \frac{\chi_0(q;\omega)}{1 - \chi_0(q;\omega)\,\tilde{V}_{\mathrm{A}}(q;\omega)} \quad \text{as} \quad q \to 0\,. \tag{5.7}$$

However, now the effective interaction is

$$\tilde{V}_{\rm A}(q;\omega) \;=\; \widetilde{V}_{\text{p-h}}(q) + \frac{S_F^2(q)}{4S^2(q)}\left[\widetilde{W}_{\rm A}(q;\omega) + \widetilde{W}_{\rm A}(q;-\omega) + \widetilde{W}_{\rm B}(q;\omega) + \widetilde{W}_{\rm B}(q;-\omega)\right] \quad \text{as} \quad q\to 0\,. \tag{5.8}$$

The static particle-hole interaction approaches the Coulomb potential $\tilde{v}_{\rm c}(q) = 4\pi e^2/q^2$

$$\widetilde{V}_{\text{p-h}}(q) = \tilde{v}_{\rm c}(q) + V_0 \quad \text{as} \quad q\to 0\,. \tag{5.9}$$

We can therefore write (5.8) as

$$\tilde{V}_{\rm A}(q;\omega) \;=\; \tilde{V}_{\rm B}(q;\omega) \;=\; \tilde{v}_{\rm c}(q) + V_0(\omega) \quad \text{as} \quad q\to 0\,. \tag{5.10}$$

As for charged bosons [36], the two-pair fluctuations modify the RPA result. The static potential $\widetilde{V}_{\text{p-h}}(q)$ and $\widetilde{W}_{\rm A,B}(q;\omega)$ contribute for $q\to 0$ at the same level.

C. Static response function

$\tilde{E}^{-1}(q,q';\omega=0)$ is real and negative, this is most easily seen from the representation (C9). Therefore, all interactions $\widetilde{W}_{\rm A,B}(q;0)$ in (4.17)-(4.18) and $\tilde{V}_{\rm A,B}(q;0)$ in (4.19)-(4.20) are real. The response function (5.6) can again be cast into the RPA form

$$\chi(q;0) = \frac{\chi_0(q;0)}{1 - \tilde{V}_{\rm stat}(q)\,\chi_0(q;0)}\,, \tag{5.11}$$

with a static effective interaction

$$\tilde{V}_{\rm stat}(q) \;\equiv\; \widetilde{V}_{\text{p-h}}(q) + \frac{S_{\rm F}^2(q)}{2S^2(q)}\left[\widetilde{W}_{\rm A}(q;0) + \widetilde{W}_{\rm B}(q;0)\right]. \tag{5.12}$$

Unlike Eq. (5.8), this form holds for all wavelengths.

For *short wavelengths* the static response function has the asymptotic form [37, 38]

$$\chi(q\to\infty;0) = -\frac{2}{t(q)} - \frac{8}{3t^2(q)}\frac{\langle\hat{T}\rangle}{N} + \mathcal{O}(q^{-5})\,, \tag{5.13}$$

where $\langle\hat{T}\rangle$ is the kinetic energy. In the RPA, one obtains in Eq. (5.13) only the kinetic energy of the non-interacting system. To obtain the correct asymptotic form, it is therefore necessary to include pair and, possibly, higher order fluctuations.

Again, we know the result for bosons as a guide: treating pair fluctuations in the "convolution" approximation leads to the correct asymptotic behavior with $\langle\hat{T}\rangle$ in (5.13) given in that approximation [18].

We show in App. D that

$$\tilde{V}_{\rm stat}(q\to\infty) = \frac{1}{2}\widetilde{W}_{\rm A}(q\to\infty;0) \;=\; -\frac{2}{3}\frac{\langle T\rangle^{\rm CA} - T_{\rm F}}{N}\,, \tag{5.14}$$

where $\langle T\rangle^{\rm CA}$ is the kinetic energy in "uniform limit" or "convolution" approximation (A12). Hence, inserting the short wavelength expansion of the Lindhard function, the static response function (5.11) indeed assumes the form (5.13)

$$\chi(q;0) \;=\; -\frac{2}{t(q)} - \frac{8}{3t^2(q)}\frac{\langle T\rangle^{\rm CA}}{N} \quad \text{as} \quad q\to\infty\,, \tag{5.15}$$

with the kinetic energy being calculated in the uniform limit approximation (A12).

VI. APPLICATIONS

A. Dynamic structure of ^{3}He

1. Motivation

The helium fluids are the prime examples of strongly correlated quantum many-body systems. They have been studied for decades, and still offer surprises leading to new insight. It is fair to say that understanding the helium fluids lies at the core of understanding other strongly correlated systems. The most important and most interesting field of application of our theory is therefore liquid ^{3}He.

Recent developments [7, 39] have brought manifestly microscopic theories of ^{4}He to a level where quantitative predictions of the excitation spectrum are possible far beyond the roton minimum without any information other than the underlying microscopic Hamiltonian (2.1). ^{3}He is the more challenging substance for both, theoretical and experimental investigations. Experimentally, the dynamic structure function $S(q;\omega)$ of ^{3}He is mostly determined by neutron scattering. The results are well documented in a book [40], the theoretical and experimental understanding a decade ago has been summarized in Ref. 25. Recent inelastic X-ray scattering experiments have led to a controversy on the evolution of the zero sound mode at intermediate wave-vectors [41–43], we will comment on this issue below.

The RPA (1.7) suggests that $S(q;\omega)$ can be characterized as a superposition of a collective mode similar to the phonon-maxon-roton in ^{4}He, *plus* an incoherent particle-hole band which strongly dampens this mode [44]. The picture is *qualitatively* adequate but misses

some important *quantitative* physics: In ^{3}He the RPA, when defined through the form (1.7) and such that the sum rules (1.4)–(1.5) are satisfied, predicts a zero-sound mode that is significantly too high. This is consistent with the same deficiency of the Feynman spectrum (1.6) in ^{4}He. Drawing on the analogy to ^{4}He [44], the cure for the problem is, as pointed out above, to include pair fluctuations $\delta u^{(2)}_{pp'hh'}(t)$ in the excitation operator.

An alternative, namely to lower the collective mode's energy by introduction of an effective mass in the Lindhard function, leads to various difficulties: First, one violates the sum rules (1.4)–(1.5), *i.e.* one disregards well established information on the system. Second, the effective mass is far from constant; it has a strong peak around the Fermi momentum [45–48], a secondary maximum around $2k_{\rm F}$, and then quickly falls off to the value of the bare mass. In fact, it is not even clear if the notion of a "single (quasi-)particle spectrum" that is characterized by a momentum is adequate at these wave numbers.

The localization procedure of Sec. IV implies that the only input needed for the application of our theory is the static structure function $S(q)$, whereas the single-particle spectrum is that of a free particle. We hasten to state that we do *not* claim that the precise location of the single-particle spectrum is completely irrelevant for the energetics of the zero sound; we only claim that the *dominant mechanism* in Bose and Fermi fluids is the same, namely pair-fluctuations. In order to maintain the sum rules (1.4)–(1.5), any modification of the particle-hole spectrum must go along with an inclusion of exchange effects. At the level of single-particle fluctuations [4, 5], such a calculation is quite feasible [49, 50]. However, to describe the dynamics of ^{3}He correctly, it is insufficient to include only the CBF single particle energies (2.14). These suggest a smooth spectrum with an effective mass slightly less than the bare mass, in contradiction to the highly structured spectrum mentioned already above.

2. Collective mode

For our calculations we have used input from the FHNC-EL calculations of Ref. 28 that utilizes the Aziz-II potential [51] and includes optimized triplet correlations as well as four- and five-body elementary diagrams. An overview of our results for bulk ^{3}He and a comparison with both the RPA and experimental data is shown in Figs. 1 for four different densities. The most prominent consequence of pair fluctuations is a change in energy and strength of

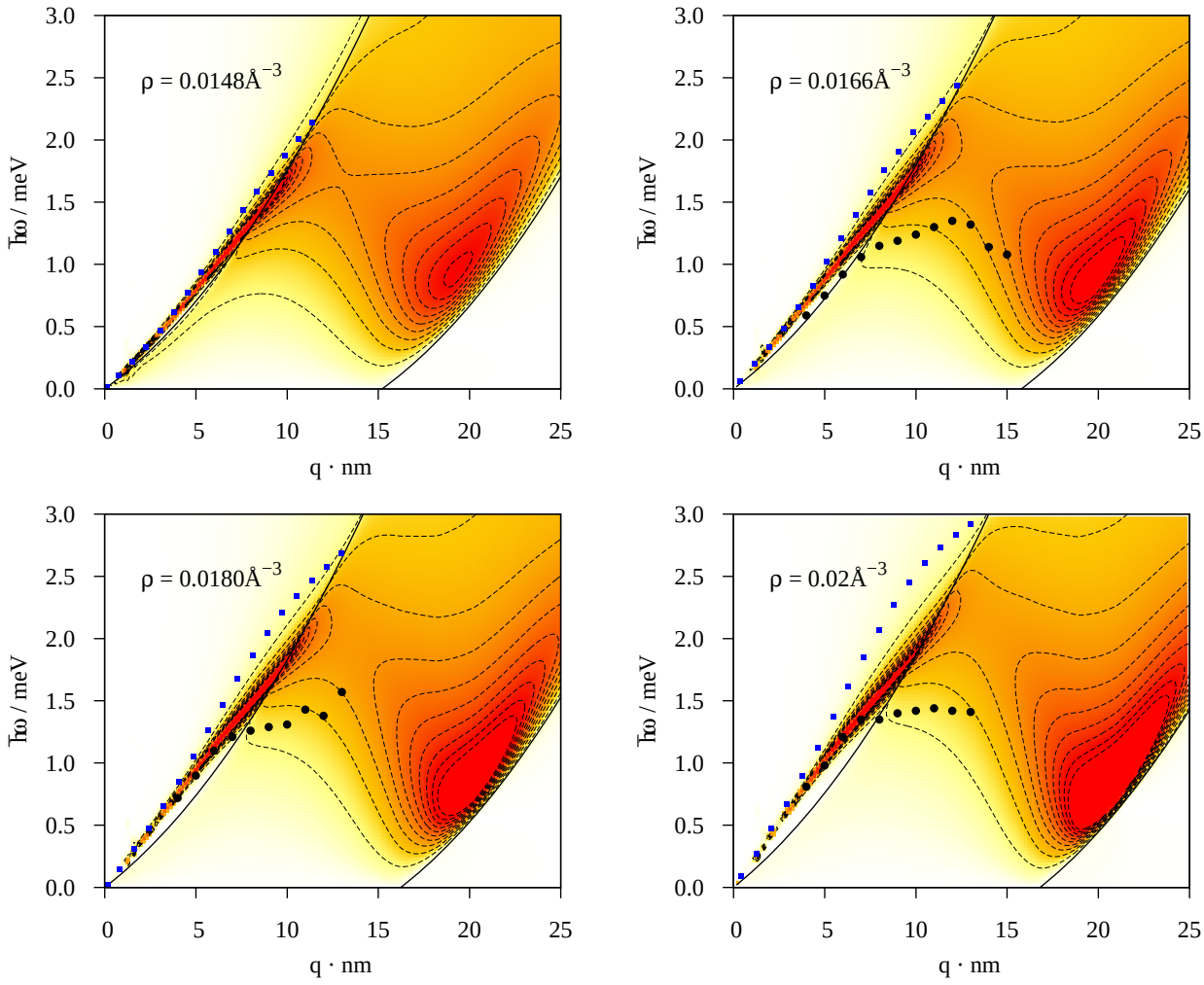

FIG. 1: (Color online) $S(q;\omega)$ of ^{3}He, for the densities $\rho = 0.0148,\ 0.0166,\ 0.018,\ 0.02\text{Å}^{-3}$. The experimental results for the collective mode (dots) are from inelastic neutron scattering experiments at the ILL (Ref. 24). The densities 0.0166, 0.0180 and 0.0200 Å^{-3} correspond in good approximation to the pressures $p = 0,\ 5,\ 10$ bar [52, 53]. Dashed lines are equidistant contours marking the same absolute value in all plots. Solid lines are the boundaries of the particle-hole continuum for $m^* = m$. The blue boxes show the RPA result for the collective mode.

the collective mode and its continuation into the particle-hole band. Pair fluctuations also contribute a continuum background outside the particle-hole continuum.

At long wavelengths, the collective mode is sharp and well defined above the particle-hole band, exhausting most of the sum rules (1.4) and (1.5). In this regime, the RPA provides a faithful description of the physics. This is in accordance with the observation that the dynamic correction to the effective interactions vanish, for neutral systems, in the long-

wavelength limit. With increasing density, the speed of sound increases and the phonon becomes farther separated from the particle-hole band.

Further details are shown in Fig. 2. At intermediate wavelengths the collective mode bends down due to the attractiveness of the effective interaction. This is where the dynamic theory starts to deviate visibly from the RPA. Evidently, pair fluctuations are the major cause for lowering the energy of the collective mode, although they do not completely bridge the discrepancy between the RPA and experiments [24, 25]. This is expected because, for bosons, pair fluctuations bridge only about two thirds of the gap between the Feynman and the experimental roton energy [7, 17]. Three-body and higher-order fluctuations are also important [18]. We expect that these corrections are smaller in ^{3}He due to its lower density, yet not negligible.

When the collective mode enters the particle-hole band, a slight kink in the position of the maximum in $S(q;\omega)$ is expected, as well as an abrupt broadening of the mode. At saturated vacuum pressure, shown in the left part of Fig. 2, these effects are difficult to identify in the experiments [25]. A possible reason is that the observed mode stays always very close to the particle-hole band. The measured mode width in Fig. 2 gives no clear indication of the upper boundary of the particle-hole band other than that it is determined by a spectrum with an average effective mass of $m^* \lessapprox m$.

The situation is much clearer at higher pressure: With increasing density, the speed of sound increases, separating the collective mode farther from the particle-hole band. For $\rho = 0.02\,\text{Å}^{-3}$ a clear kink is identified at $q \approx 5\,\text{nm}^{-1}$ (Fig. 2 right part). The broadening is also more abrupt and, in particular, does not increase for larger values of q. Similar to SVP, explaining these data requires a boundary of the particle-hole band that is even above that of the non-interacting Fermi fluid. Damping due to multiparticle excitations is, on the other hand, for both densities far too small to account for the experimentally seen broadening of the zero sound mode.

3. Frequency dependence of $S(q;\omega)$

For a quantitative discussion we show in Fig. 3 the dynamic structure factor as a function of frequency at a sequence of wave vectors. We conclude that the RPA quantitatively and even qualitatively differs from our theory and the experiment. Including pair fluctuations

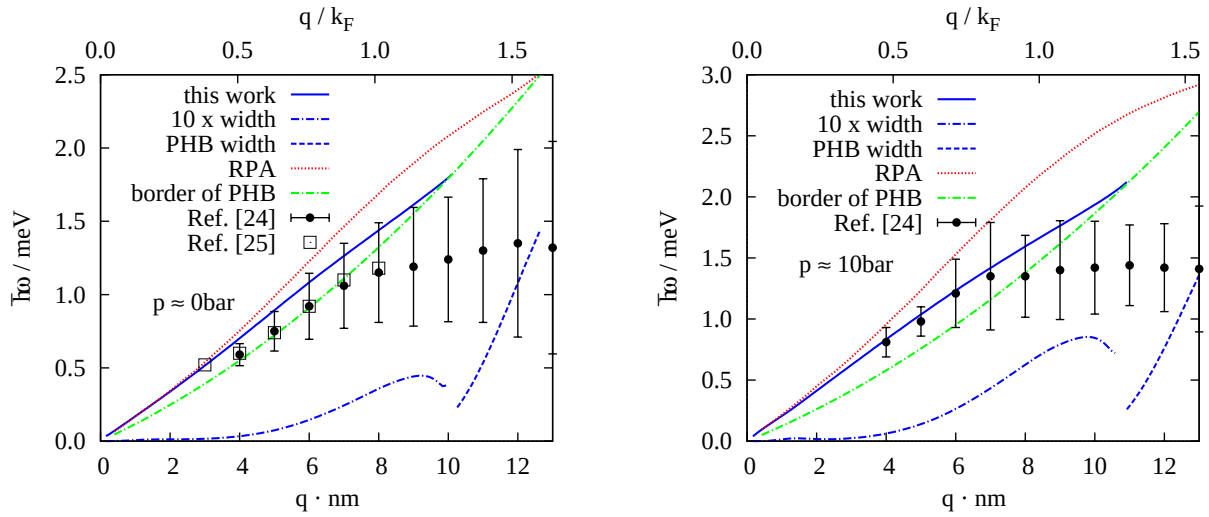

FIG. 2: Zero sound mode calculated within the pair fluctuation theory (full blue line), RPA (red chained line) and experimental data by the ILL group [25] (square symbols) and [24] (circles). The bars indicate the width of the fit to the data, the line at the bottom of the figure gives the width due to pair fluctuations enhanced by a factor of 10 to make it visible. The dashed blue line gives the FWHM of the mode within the particle hole continuum. Left part: $\rho = 0.0166\text{Å}^{-3}$, right part: $\rho = 0.02\text{Å}^{-3}$.

improves the agreement with experiment significantly. The arrows in panes (c) and (d) indicate the maximum of the experimentally observed dynamic structure function.

In Fig. 3(b) we also show the consequence of the plausible simplification of our theory discussed already in connection with Eqs. (4.12) and (4.13): We neglect all terms that vanish for bosons as well as for large momentum transfers $q, q', q'' \geq 2k_F$. This is $\tilde{K}^{(q)}_{q'q'',0}$ and, consequently, the second term in $K_{q,q'q''}$, Eq. (4.12). The three-body vertex is then given by the first term in Eq. (4.12), see also (D1). This simplifies the effective interactions significantly: Only the first term of Eq. (4.17) for $\widetilde{W}_{\rm A}(q;\omega)$ contributes, and $\widetilde{W}_{\rm B}(q;\omega)$ is neglected. Fig. 3(b) shows that these simplifications modify our results only marginally, the form (D1) can therefore be considered a practical and useful simplification of our theory.

Figs. 3(c) and 3(d) show our results for the two momentum transfers $q = 2.4\,k_{\rm F} = 1.89\,\text{Å}^{-1}$ and $q = 3.2\,k_{\rm F} = 2.52\,\text{Å}^{-1}$. Recent X-ray scattering experiments in that momentum range [41–43] appeared to support the notion of a high-momentum collective mode without visible damping by incoherent particle-hole excitations. Figs. 3(c) and 3(d) show that pair fluctuations lead to a narrowing of the strength of $S(q;\omega)$ compared to the RPA. To facilitate

the comparison with experiments, we have convoluted our result with the instrumental resolution of 1.58 meV, the results are also shown in Figs. 3(c) and 3(d). After this, our results agree quite well with the experimental spectrum. Also, the location of the observed peak intensity for $q = 2.4\,k_{\rm F}$ appears to be consistent with our calculation. The RPA is, on the other hand, too broad to explain the data. We also point out that a value of the effective mass close to $m^* \approx m$ is consistent with our theoretical calculations [48]. We have to conclude therefore that the observed width of the X-ray data are also consistent with our picture.

After a regime of strong damping we see in Figs. 1 an intensity peak at momentum transfer of $q \approx 2.5 k_{\rm F}$. With increasing density, this peak moves towards the lower edge of the particle-hole band and becomes sharper. Such a peak should be identified with the remnant of the roton excitation in ^{4}He, broadened by the particle-hole continuum. The overall agreement with the experiment is quite good, see Fig. 1 of Ref. 24. Our theory predicts a "roton minimum" that is slightly above the observed energy; this is expected because for bosons a similar effect is observed. To obtain a higher accuracy, triplet- and higher order fluctuations must be included [18].

4. Static response

For completeness, and because the quantity should be obtainable by experiments and simulations similar to those for ^{4}He [54, 55] and on bulk jellium [56], we show in Fig. 4 the static response function $\chi(q, 0)$ of ^{3}He at $\rho = 0.0166 \text{Å}^{-3}$. The main peak, which is a result of the local symmetry in the fluid, is visibly raised compared to the RPA result. We suspect, form experience with the boson theory, that this peak is still a bit underestimated.

The comparison also lets us assess the validity of an energy independent particle hole interaction. Fig. 5 shows a comparison between the FHNC $\widetilde{V}_{\text{p-h}}(q)$ and the static effective interaction (5.12). Evidently, the qualitative structure is very similar, in particular $\widetilde{V}_{\text{p-h}}(q \to 0) = \tilde{V}_{\rm stat}(q \to 0)$ as discussed in Sec. V B. The most visible difference is that $\tilde{V}_{\rm stat}(q)$ approaches a constant for large q, see Eqs. (5.13) and (5.14).

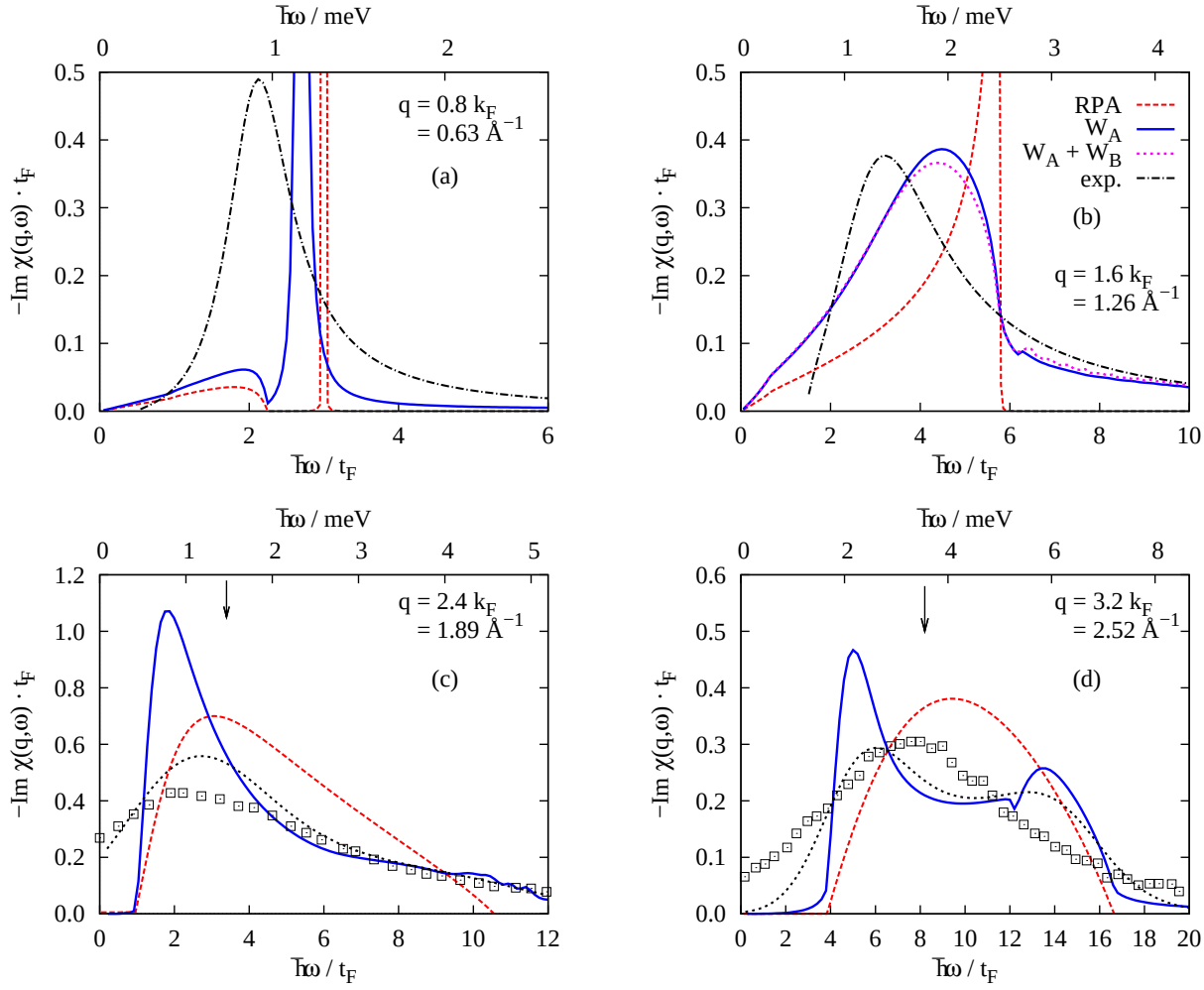

FIG. 3: (Color online) $S(q;\omega)$ for ^{3}He as a function of energy at $\rho = 0.0166\text{Å}^{-3}$ for a sequence of momentum transfers $q = 0.8,\ 1.6,\ 2.4,\ 3.2\ k_\mathrm{F}$ (a)-(d). Also shown is the RPA (dashed, red). The solid blue line is the result of this work with the simplified $\widetilde{W}_\mathrm{A}(q;\omega)$ and $\widetilde{W}_\mathrm{B}(q,\omega) = 0$ as discussed in the text. In pane (b), we also show the results when the full $\widetilde{W}_\mathrm{A}(q;\omega)$ and $\widetilde{W}_\mathrm{B}(q;\omega)$ of Eqs. (4.17) and (4.18) are retained (short dashed magenta line). The results from the different approximations are almost indistinguishable in panes (a),(c) and (d) and therefore not shown. The black dash-dotted line in panes (a) and (b) are fits to the experimental results of Ref. 24. In panes (c) and (d) we indicate the maximum of the experimentally observed dynamic structure function by an arrow. We also plot in panes (c) and (d) recent inelastic X-ray diffraction data obtained by Albergamo *et al.* [41] (boxes) as well as our theoretical results folded with the experimental resolution (dashed line).

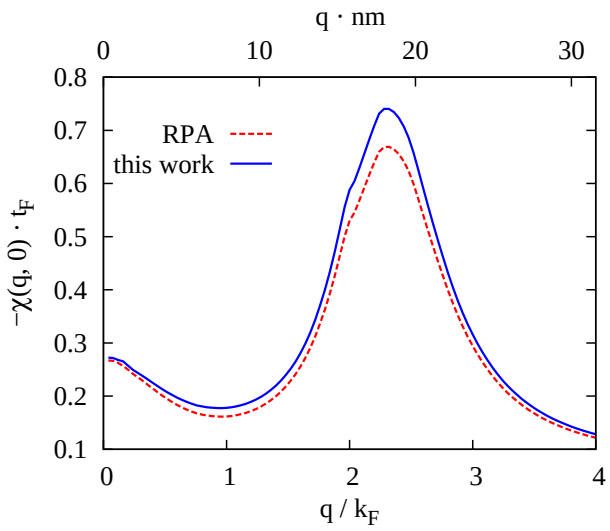

FIG. 4: (color online) Static response of ^{3}He at $\rho = 0.0166\text{Å}^{-3}$. The red curve shows the RPA result whereas the blue line is the result of this work.

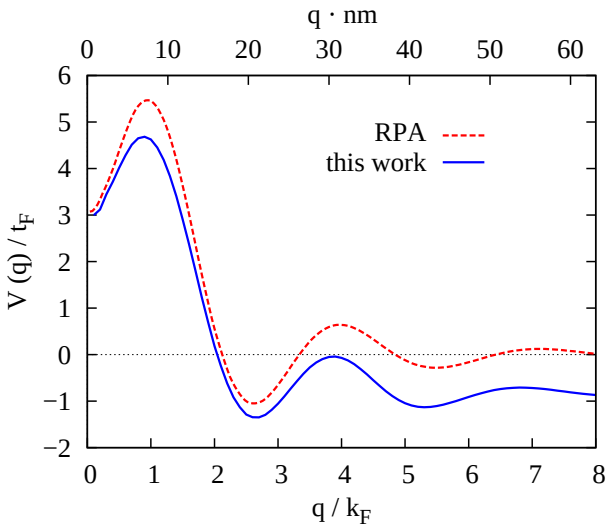

FIG. 5: (color online) Effective interaction of ^{3}He at $\rho = 0.0166\text{Å}^{-3}$. The red curve shows the static effective interaction $\widetilde{V}_{\text{p-h}}(q)$ whereas the blue line is $\tilde{V}_{\text{stat}}(q)$.

B. Electron liquid

The second typical area of application of microscopic many-body methods is the electron liquid [38, 57]. It provides the basic understanding of valence electron correlations in simple metals. In its two-component version it has proved useful for describing the electron-hole

liquid in semiconductors.

Compared to the helium fluids, the soft repulsion of the Coulomb interaction induces substantially weaker correlations. Therefore, electrons are much less challenging than ^{3}He and the RPA (or slightly modified versions) contain much of the relevant physics.

Correlations are somewhat more pronounced in layered realizations of the electron liquid, such as Si- and GaAs-AlGaAs hetero-structures. For electrons on He surfaces preliminary results show [58] that at very low densities, again, a roton-like structure evolves for intermediate wave vectors.

We have seen that pair fluctuations contribute, already at long wave lengths, to the static response function, see our discussion in Secs. V B-V C. Most important are, of course, those effects that are *qualitatively* new consequences of multiparticle fluctuations. These are the short–wavelength behavior of the static response function and the appearance of a new feature in the dynamics structure function, namely the "double plasmon" excitation. The latter has raised new interest [26, 27] in studying the dynamics of electrons at metallic densities in this $(q;\omega)$ region.

1. Double Plasmon

Figure 6 shows the dynamic structure factor $S(q;\omega)$ obtained from the pair fluctuation theory. We have chosen two different densities $\rho \equiv 3/(4\pi r_s^3 a_{\rm B}^3)$, corresponding to Al, $r_s = 2.06$, and Na, $r_s = 3.99$. Immediately obvious are the finite width (*i.e.* lifetime) of the plasmon above the particle-hole band, and a second peak-like structure around twice the plasma frequency $\omega_{\rm p}$.

Characteristic cuts at constant wave vectors q are shown in Fig. 7 for Na. In parts (a) and (b) the plasmon is outside the particle-hole band and rather sharp; the second peak slightly above $2\hbar\omega_{\rm p} = 4.5\, t_{\rm F}$ is clearly visible. We identify this feature, which has also been observed experimentally [27], with the "double-plasmon".

The "double-plasmon" excitation is due to the emergence of an imaginary part in $\tilde{V}_{\rm A}(a,\omega)$ at $\omega = 2\omega_{\rm p}$, caused by the appearance of an imaginary part of the pair propagator $\tilde{E}^{-1}(q',q'';\omega)$. It is therefore a genuine multipair effect. The properties of the pair propagator are discussed in in App. C 2. From (C19) we obtain for the double-pole part of the

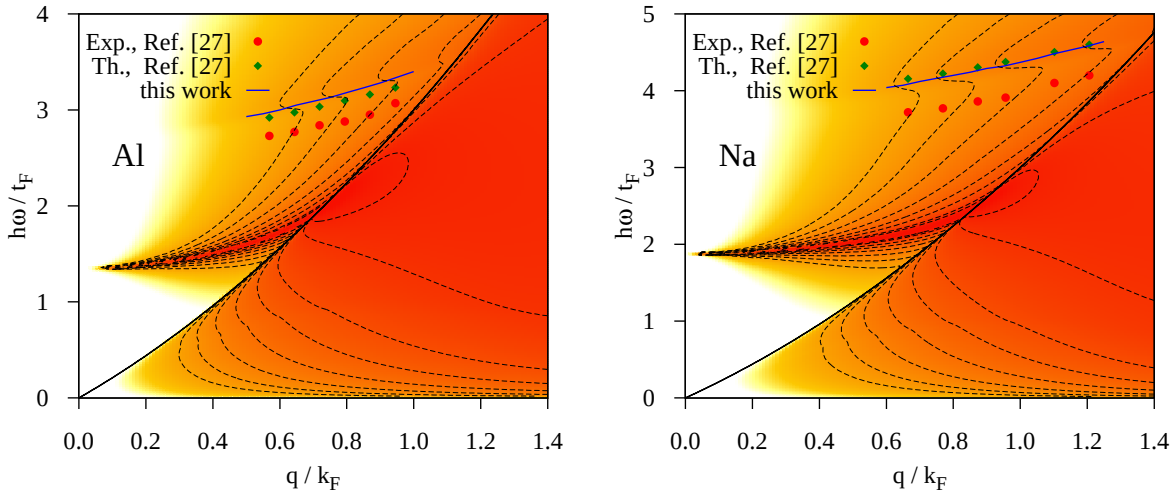

FIG. 6: (Color online) The figure shows $S(q;\omega)$ of an electron liquid with density parameters $r_s = 2.06$ and $r_s = 3.99$ appropriate for Al and Na, respectively. As in Figs. 1, dark red regions correspond to high intensity (logarithmic scale). The blue line is the position of the double-plasmon peak obtained in the present work, red dots are experimental results [27] from inelastic X-ray scattering and green diamonds results from Green's functions calculations [27, 59].

dynamic interaction (5.8)

$$\Im m\, \tilde{V}_{\rm A}(q\to 0;\omega) \;=\; \frac{9\hbar^2\omega_{\rm p}^2}{16 t_{\rm F}^2}\,\frac{\pi}{8N}\sum_{\mathbf{q}'}\left[\frac{k_{\rm F}}{q}K_{q,q'q''}\right]^2 \times \\ z^2(q')\;\left[\delta(2\hbar\omega_{\rm c}(q')-\hbar\omega)+\delta(2\hbar\omega_{\rm c}(q')+\hbar\omega)\right]\,. \qquad (6.1)$$

In Fig. 7(c), the plasmon is broad and Landau-damped, while the double-plasmon still shows a clear structure, even at the brink of entering the particle-hole continuum. Some structure in the spectrum persists to even higher momentum transfers: At $q = 2.0\,k_{\rm F}$ in Fig. 7(d), traces of the ordinary as well as the double plasmon show up as a faint double-peak structure, with its minimum where the RPA yields a single maximum.

We now investigate the nature of the slight but measurable [27] peak in the loss function at approximately twice the plasmon frequency $\omega_{\rm p}$. Fig. 8 shows $S(q,\omega)$ for $r_s = 3.99$ for three different momentum transfers, the position of the double plasmon is marked with arrows.

We have already shown in Figs. 6 the location of the double plasmon excitation and a comparison with the experimental inelastic X-ray scattering data [26, 27]. The double-plasmon is also accessible by Green's function methods [59]. These results are very close to

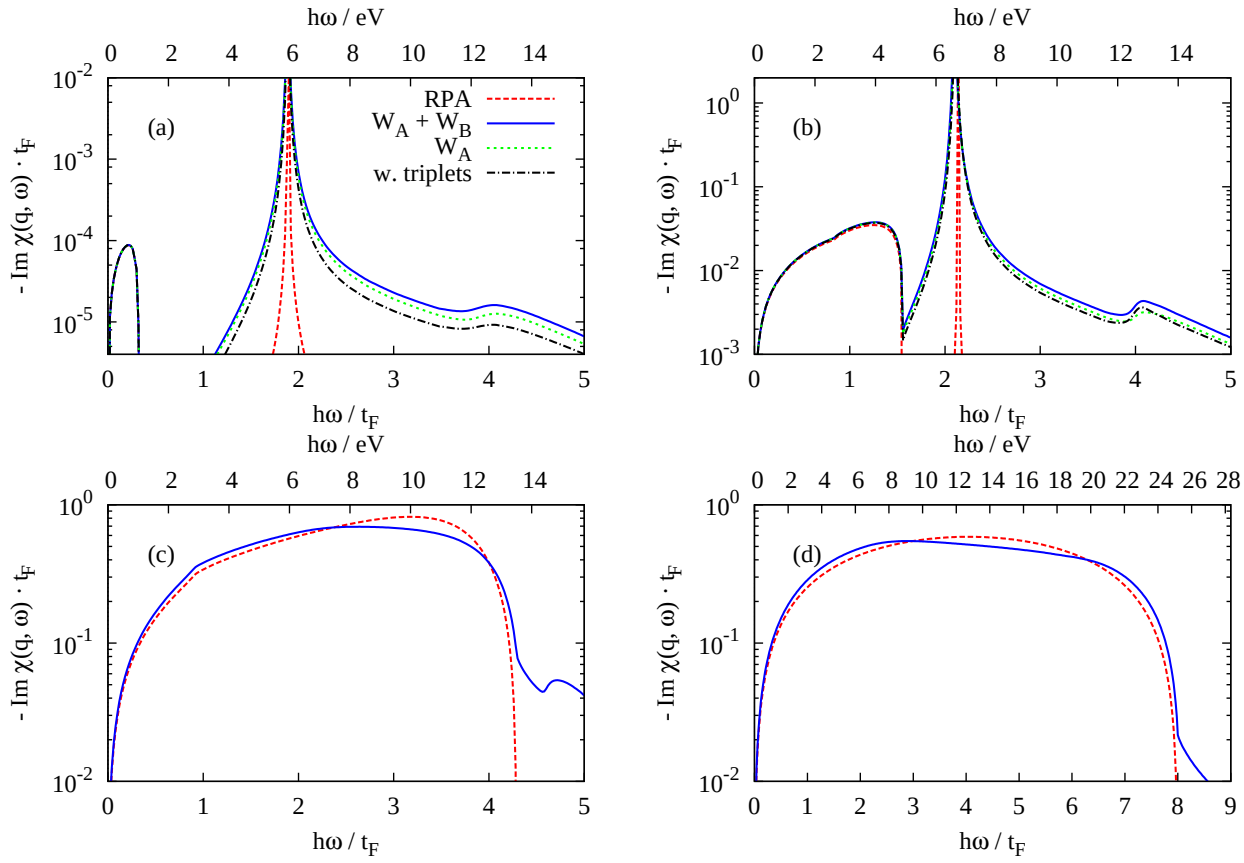

FIG. 7: (Color online) $S(q_0;\omega)$ for Na ($r_s = 3.99$), at wave vectors q_0 (a) $0.15\,k_{\rm F}$, (b) $0.6\,k_{\rm F}$, (c) $1.3\,k_{\rm F}$, and (d) $2.0\,k_{\rm F}$. The full (blue) lines are our pair fluctuation theory, dashed (red) lines are the RPA results using $\widetilde{V}_{\rm p\text{-}h}(q)$. To make the plasmon visible, the RPA data have been broadened artificially by adding an imaginary frequency of 10^{-5}eV/$\hbar$. The dotted (green) lines in (a) and (b) refer to neglecting $K^{(q)}_{q'q'',0}$ in Eqs. (4.12)-(4.13), and the dash-dotted (black) lines include ground state triplet correlations. At larger momentum transfers these effects are too small to be visible.

those of our pair fluctuation theory. This can be understood from the fact that the leading terms of the long-wavelength part of the pair propagator actually contain no correlation effects, see Eq. C29. Hence, theories that are less well suited than CBF for the description of strong correlations should, similar to the single plasmon, give the right answer. The remaining discrepancy with experiments must therefore be attributed to lattice effects. Fig. 8 shows more details of $S(q,\omega)$ at a sequence of three different momentum transfers for $r_s = 3.99$ (the position of the double-plasmon is marked with arrows), in particular in order to assess the relative strength of the double-plasmon excitation compared to the underlying continuum.

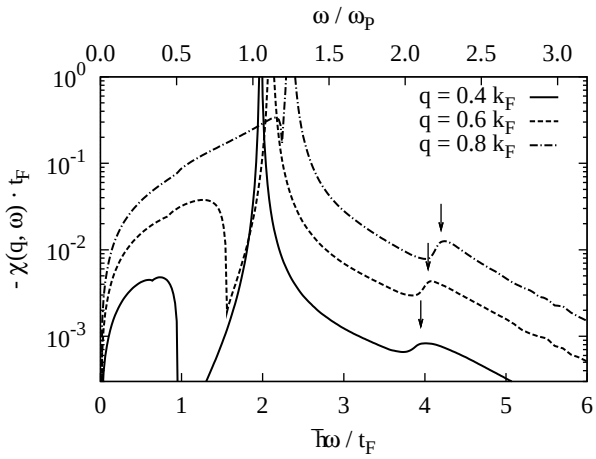

FIG. 8: Cuts of the density-density response function at Na-density ($r_s = 3.99$), for constant momentum transfer $q = 0.4\,k_\mathrm{F}$ (solid line), $q = 0.6\,k_\mathrm{F}$ (dashed line) and $q = 0.4\,k_\mathrm{F}$ (dash-dotted line). The arrows mark the position of the double-plasmon.

2. Static Response

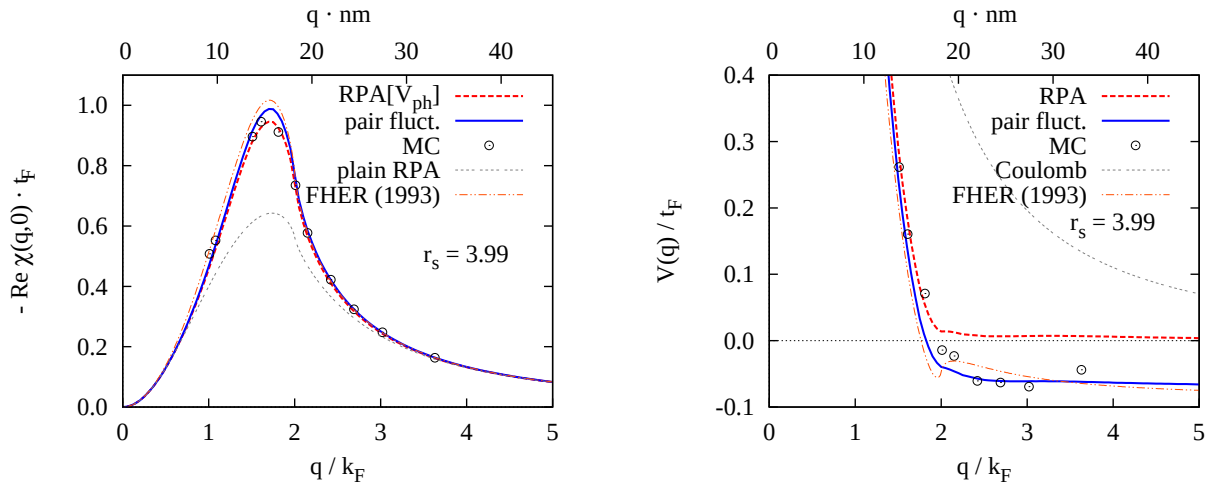

FIG. 9: Static response function (left), and static effective interaction (right) of the electron liquid at $r_s = 3.99$. Full blue lines are our results, black dash-dotted lines a fit based on the simulations [56, 60]. Dotted red and thin broken lines show the RPA with $\widetilde{V}_{\text{p-h}}(q)$ and $\tilde{v}_\mathrm{c}(q)$, respectively.

Monte Carlo studies of the static response function $\chi(q;0)$ were performed for two- and three-dimensional ^{4}He [54, 55] and on bulk jellium [56] for $r_s = 2$, 5 and 10. While $\chi(q;\omega)$ is accessible experimentally, for electron liquids it is popular to define a *static local field*

correction to the Coulomb interaction $\tilde{v}_{\rm c}(q)$ via [38]

$$\tilde{V}_{\rm stat}(q) \;\equiv\; \tilde{v}_{\rm c}(q)\,(1-G(q))\;. \tag{6.2}$$

From our analysis it is clear that a response function in the RPA form can be defined only for $q \to 0$ and at $\omega = 0$. Therefore, only in these two cases such a function is a physically meaningful quantity.

In the $q \to \infty$ limit, our theory yields a finite value for $V_{\rm stat}(q)$, resulting in $G(q) \propto q^2$, whereas $\widetilde{V}_{\rm p\text{-}h}(q)$ falls off like the bare potential. This correct $q-$dependence arises *solely* from multiparticle fluctuations. In Fig. 9 we compare our results with the Monte Carlo data, and with curves calculated from an analytic analytic fit for $-v_{\rm c}(q)\,G(q)$ obtained from the latter [60]. The agreement is remarkably good.

No trace of a possible "hump" in $G(q)$ around $2k_{\rm F}$ as a remnant of some charge- or spin-density wave instability was found in the simulations, but it also was not fully conclusively ruled out. Our results, clearly, do not yield any such peak structure at $2k_{\rm F}$ either.

VII. SUMMARY

We have presented the fermion version of theories of the dynamic response of Bose fluids that have been developed in the past successfully by Jackson, Feenberg, and Campbell. These methods form the basis of our present understanding of the dynamics of Bose fluids. Our derivations were admittedly lengthy but eventually led to a reasonably compact formulation of the dynamic response of correlated Fermi fluids. Our final result could be formulated as a set of TDHF equations in terms of dynamic and non-local effective interactions.

For the first applications we have reduced the theory to a practical level capturing the relevant physics, while avoiding many of the technical complications. In particular the version of the equations of motion spelled out in Appendix F has proved to be adequate for systems as different as ^{3}He and homogeneous electrons. It is hardly more complicated than TDHF. The sole required input is the static structure function $S(q)$ which can, in principle, also be obtained from simulations. Our developments have led to *quantitative* improvements of our understanding of ^{3}He and electrons as well as to the description of *qualitatively new* effects like mode-mode coupling, multiparticle spectra, and damping.

We have, at various places, commented on the role of the particle-hole spectrum. In

the homogeneous electron liquid, the interaction corrections to the single-particle spectrum are relatively small [35, 61], the theory formulated here should therefore suffice for many purposes. The situation is more difficult in ^{3}He: As is seen from our results, good agreement with experiments can be reached by assuming a spectrum of non-interacting fermions. In particular looking at the zero-sound damping suggests that, at $q \approx k_F$, the boundary of the single-particle continuum should be close (perhaps even above) to the one given by a non-interacting spectrum, *cf.* Fig. 2. This is not in contradiction to experiments [52, 62] suggesting an effective mass ratio $m^*/m \approx 3$ at the Fermi surface. One reason is that the effective mass ratio drops rapidly with distance from the Fermi surface. The more fundamental reason however, is that the concept of describing the particle-hole excitations by a spectrum that depends on momentum only is questionable at elevated wave numbers. More precisely, the single-particle motion is described by a non-local, energy dependent self-energy. Upon closer examination it becomes clear that exchange effects are intimately related to self-energy corrections and exchange effects must therefore be included simultaneously.

In independent work, we have used the ideas of CBF theory as well as the Aldrich-Pines pseudopotential theory to calculate the single-particle propagator in ^{3}He. In both three and two dimensions, we found good agreement between the theoretical effective mass near the Fermi surface, and that obtained experimentally from specific heat measurements [47, 48, 63]. However, the somewhat *ad-hoc* use of the effective interactions in that work is still awaiting rigorous justification. This is the subject of future work.

Acknowledgments

A part of this work was done while one of us (EK) visited the Physics Department at the University at Buffalo, SUNY. Discussions with C. E. Campbell, H. Godfrin and R. E. Zillich are gratefully acknowledged. This work was supported, in part, by the Austrian Science Fund FWF under project P21264.

Appendix A: Ground state theory

1. The essence of FHNC-EL

For the sake of the discussions of this work we here briefly review the essence of variational FHNC theory. The diagram expansion and summation procedure that is used to derive, for the variational wave function (2.2) a set of equation for the calculation and optimization of physical observables has been described at length in review articles [21] and pedagogical literature [22]. Details on the specific implementation for ^{3}He are given in Ref. 28.

Here, we spell out a reduced set of equations. These do not provide the quantitatively best implementation [28] of the FHNC-EL theory, but they contain the relevant physics: They provide, in the language of perturbation theory, a self-consistent approximate summation of ring– and ladder diagrams [29], thereby capturing both, long- as well as short-ranged features.

In the simplest approximation [64], which contains, as we shall see momentarily, the "RPA" expression (1.7), the Euler equation (2.5) can be written in the form [28]

$$S(q) = \frac{S_{\rm F}(q)}{\sqrt{1 + 2\frac{S_{\rm F}^2(q)}{t(q)}\widetilde{V}_{\rm p\text{-}h}(q)}}\,, \tag{A1}$$

where $t(q) = \hbar^2 q^2/2m$ is the kinetic energy of a free particle, and

$$V_{\rm p\text{-}h}(r) = \left[1 + \Gamma_{\rm dd}(r)\right] v(r) + \frac{\hbar^2}{m}\left|\nabla\sqrt{1+\Gamma_{\rm dd}(r)}\right|^2 + \Gamma_{\rm dd}(r) w_{\rm I}(r) \tag{A2}$$

is what we call the "particle-hole interaction". Auxiliary quantities are the "induced interaction"

$$\tilde{w}_{\rm I}(q) = -t(q)\left[\frac{1}{S_{\rm F}(q)} - \frac{1}{S(q)}\right]^2\left[\frac{S(q)}{S_{\rm F}(q)} + \frac{1}{2}\right]. \tag{A3}$$

and the "direct-direct correlation function"

$$\tilde{\Gamma}_{\rm dd}(q) = (S(k) - S_{\rm F}(q))/S_{\rm F}^2(q) \tag{A4}$$

(see also Eq. (4.1)). Eqs. (A1)–(A4) form a closed set which can be solved by iteration. Note that the Jastrow correlation function has been eliminated entirely.

The relationship (A1) between the static structure function $S(q)$ and the particle-hole interaction $\widetilde{V}_{\rm p\text{-}h}(q)$ can also be derived from Eq. (1.7), if the Lindhard function is replaced

with its "mean spherical" or "collective" approximation (CA),

$$\chi_0^{\rm CA}(q;\omega) = \frac{2t(q)}{(\hbar\omega + {\rm i}\eta)^2 - t^2(q)/S_{\rm F}^2(q)} \; . \tag{A5}$$

The essence of this approximation is to replace the branch cut in $\chi_0(q;\omega)$ by a single pole; its strength chosen such that the first two sum rules agree when evaluated with the full Lindhard function $\chi_0(q;\omega)$ or in the collective approximation $\chi_0^{\rm CA}(q;\omega)$, *i.e.*

$$\begin{aligned} \Im m \int d\omega \; \chi_0^{\rm CA}(q;\omega) &= \Im m \int d\omega \; \chi_0(q;\omega) \\ \Im m \int d\omega \; \omega \, \chi_0^{\rm CA}(q;\omega) &= \Im m \int d\omega \; \omega \, \chi_0(q;\omega) \; . \end{aligned} \tag{A6}$$

In fact, (1.7) together with (A5) or, alternatively,

$$\widetilde{V}_{\rm p\text{-}h}(q) = \frac{t(q)}{2} \left(\frac{1}{S^2(q)} - \frac{1}{S_{\rm F}^2(q)} \right) \tag{A7}$$

can be used [28] to *define* the particle-hole interaction from an accurately known $S(q)$.

The energy, consisting of kinetic and potential energy $\langle T \rangle + \langle V \rangle$, is [28]

$$E \; = \; \frac{3}{5} N t_{\rm F} + E_{\rm R} + E_{\rm Q} \, , \tag{A8}$$

$$E_{\rm R} \; = \; \frac{\rho N}{2} \int d^3r \; \left[g(r) \, v(r) + \frac{\hbar^2}{m} (1 + C(r)) \left| \nabla \sqrt{1 + \Gamma_{\rm dd}(r)} \right|^2 \right] \, , \tag{A9}$$

$$E_{\rm Q} \; = \; \frac{N}{4} \int \frac{d^3q}{(2\pi)^2 \rho} \, t(q) \left[S_{\rm F}^2(q) - 1 - S^2(q) + S(q) \right] \, \tilde{\Gamma}_{\rm dd}^2(q) \, . \tag{A10}$$

Here, $t_{\rm F}$ is the Fermi energy, and, in this approximation,

$$\tilde{C}(q) = S_{\rm F}(q) - 1 + (S_{\rm F}^2(q) - 1) \tilde{\Gamma}_{\rm dd}(q) \, . \tag{A11}$$

To make the connection with the limiting behavior of $\chi(q,0)$ in Sec. V C, we next spell out what is known as the "uniform limit" or "collective" approximation (CA). Products of functions which *in coordinate space* vanish for $r \to \infty$ are considered small. This implies to expand $\nabla \sqrt{1 + \Gamma_{\rm dd}(r)} \approx \frac{1}{2} \nabla \Gamma_{\rm dd}(r)$ and to neglect $C(r)$. The kinetic energy then is

$$\langle T \rangle^{\rm CA} \; = \; T_{\rm F} + \frac{1}{4} \sum_{\mathbf{q}} t(q) \, S(q) \, \tilde{X}_{\rm dd}^2(q) \, . \tag{A12}$$

Here, $T_{\rm F} = 3Nt_{\rm F}/5$, and $\tilde{X}_{\rm dd}(q)$ is the "non-nodal" function. In our reduced FHNC approximation, $\tilde{X}_{\rm dd}(q)$ is related to the static structure factor by

$$\tilde{X}_{\rm dd}(q) = \frac{1}{S_{\rm F}(q)} - \frac{1}{S(q)} \; . \tag{A13}$$

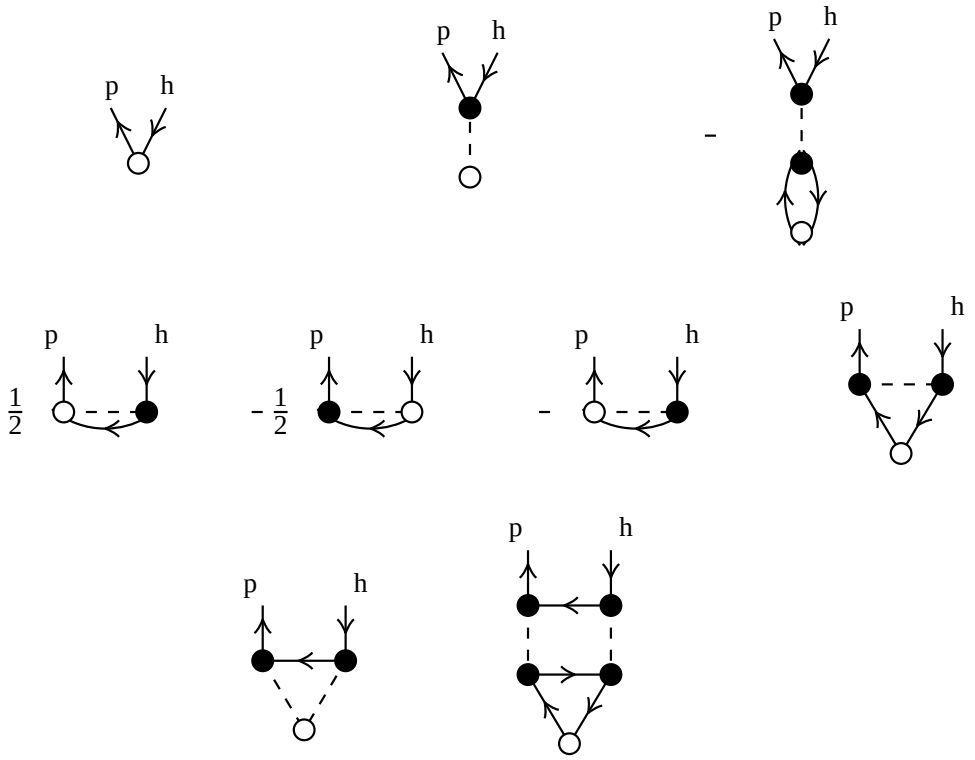

FIG. 10: Diagrammatic representation of some contributions to $\rho_{0,ph}(\mathbf{r})$. The upper row shows the diagrams defining the local approximation. The second row are the leading exchange diagrams and the third row shows two corrections due to the non-locality of $\mathcal{N}(1,2)$.

Appendix B: Diagrammatic analysis

1. Transition density

We first examine the diagrammatic structure of CBF matrix elements $\rho_{0,ph}(\mathbf{r})$ of the density operator, (3.10, 3.11). The simplest approximation for $M_{ph,p'h'}$ has been spelled out in Eq. (4.6), the corresponding approximation for $\rho_{0,ph}(\mathbf{r})$ is

$$\rho_{0,ph}(\mathbf{r}) \;=\; \rho^{\rm F}_{0,ph}(\mathbf{r}) + \rho\int d^3r' \int d^3r'' \left[\delta(\mathbf{r}-\mathbf{r}') - \frac{\rho}{\nu}\ell^2(|\mathbf{r}-\mathbf{r}'|k_{\rm F})\right] \Gamma_{\rm dd}(\mathbf{r}'-\mathbf{r}'')\, \rho^{\rm F}_{0,ph}(\mathbf{r}'')\,. \quad \text{(B1)}$$

The diagrammatic representation of some leading diagrams contributing to $\rho_{0,ph}(\mathbf{r})$ is shown in Fig. 10. As usual, open points represent particle coordinates $\mathbf{r}_i$, while filled points indicate an integration over the associate coordinate space and a density factor. Dashed lines connecting points $\mathbf{r}_i$ and $\mathbf{r}_j$ represent a function $\Gamma_{\rm dd}(r_{ij})$, and oriented solid lines an exchange function $\ell(r_{ij}k_{\rm F})$. New elements are particle- and hole-states, depicted as upward

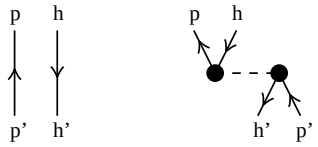

FIG. 11: Diagrammatic representation of the local approximation for $M_{ph,p'h'}$.

(particles) or downward (holes) lines entering or leaving the diagram.

The three leading terms (B1) are shown in the upper row of Fig. 10. In the second row of Fig. 10 we show the leading exchange diagrams. In the representation (3.10), these originate from the factors z_{ph} in the definition of the $\tilde{\rho}_{0,ph}(\mathbf{r})$, these are shown as the first two diagrams. Exchange terms also originate from the matrix element $\langle ph'|\Gamma_{\rm dd}|hp'\rangle_a$, these are shown as third and fourth diagram in that row. Evidently there is a partial cancellation. The diagrams shown in that row also serve as an example for how the representations (3.10) and (3.11) are equal: Starting from the form (3.11), the diagrams originating from the z_{ph}-factors (*i.e.* the first two diagrams in the second row), have opposite signs; and the exchange term of $\langle pp'|\Gamma_{\rm dd}|hh'\rangle_a$ yields the third diagram with interchanged particle- and hole labels. The sum of all three diagrams is the same.

2. The $M^{(\rm I)}$ matrix

Our next task is to show that the diagrams representing $M^{(\rm I)}_{ph,p'p''h'h''}$ are a proper subset of those contributing to $M_{ph,p'p''h'h''}$. We restrict ourselves here to the simplest case, which is the numerically implemented version. We start with the two-body matrix $M_{ph,p'h'}$. As spelled out in Eq. (4.6), besides the δ-function, the leading contribution is the *local* term in the two-body operator

$$\mathcal{N}_{\rm loc}(1,2) = \Gamma_{\rm dd}(r_{12})\,. \tag{B2}$$

The diagrammatic representation of this approximation for $M_{ph,p'h'}$ is shown in Fig. 11.

A diagrammatic expansion of the matrix elements $M_{ph,p'p''h'h''}$ can be derived in exactly the same way as the corresponding expansions of the two-body matrix elements [31]. Generally, the $M_{ph,p'p''h'h''}$ are matrix elements of a non-local three-body operator, which can be expressed in terms of FHNC diagrams. Restricting ourselves again to the numerically

implemented level, we need these quantities in an approximation equivalent to the "uniform limit approximation" [17] for bosons. We generalize this approach to fermions by keeping all diagrams contained in the Bose case plus those, where the end points of the correlation functions are linked by exchange paths (the bosonic $g(r_{ij})-1$ is identified with the direct-direct correlation function $\Gamma_{\rm dd}(r_{ij})$). This procedure has already been used for deriving the optimal triplet correlations for the fermion ground state [28]. The diagrammatic representation of this approximation is shown in Fig. 12, the analytic form is

$$\begin{aligned}
M^{\rm CA}_{ph,p'p''h'h''} \;=\; & \delta_{h,h'}\,\langle ph''|\Gamma_{\rm dd}(1,2)|p'p''\rangle - \delta_{p,p'}\,\langle h'h''|\Gamma_{\rm dd}(1,2)|hp''\rangle \\
& +\frac{1}{2}\,\langle ph'h''|\Gamma_{\rm dd}(3,1)\,\Gamma_{\rm dd}(1,2)|hp'p''\rangle \\
& -\frac{1}{2}\,\sum_{h_1}\langle ph''|\Gamma_{\rm dd}|h_1p''\rangle\,\langle h'h_1|\Gamma_{\rm dd}|p'h\rangle - \frac{1}{2}\,\sum_{h_1}\langle ph'|\Gamma_{\rm dd}|h_1p'\rangle\,\langle h''h_1|\Gamma_{\rm dd}|p''h\rangle \\
& +\langle ph'h''|\Gamma_{\rm dd}(1,2)\,\Gamma_{\rm dd}(2,3)|hp'p''\rangle \\
& -\sum_{h_1}\langle ph'|\Gamma_{\rm dd}|hh_1\rangle\,\langle h''h_1|\Gamma_{\rm dd}|p''p'\rangle - \sum_{h_1}\langle ph_1|\Gamma_{\rm dd}|hp'\rangle\,\langle h'h''|\Gamma_{\rm dd}|h_1p''\rangle \\
& +\langle ph'h''|\Gamma^{\rm CA}_{\rm ddd}(1,2,3)|hp'p''\rangle \\
& +\{(p'h')\leftrightarrow(p''h'')\}\;. \qquad \text{(B3)}
\end{aligned}$$

Here, in convolution approximation,

$$\begin{aligned}
\Gamma^{\rm CA}_{\rm ddd}(\mathbf{r}_1,\mathbf{r}_2,\mathbf{r}_3) = \quad & \frac{\rho}{2}\int d^3r_4\,\Gamma_{\rm dd}(\mathbf{r}_1-\mathbf{r}_4)\Gamma_{\rm dd}(\mathbf{r}_2-\mathbf{r}_4)\Gamma_{\rm dd}(\mathbf{r}_3-\mathbf{r}_4) \\
& +\;\frac{\rho^2}{2\nu}\int d^3r_4\,d^3r_5\,\ell^2(|\mathbf{r}_4-\mathbf{r}_5|k_{\rm F})\Gamma_{\rm dd}(\mathbf{r}_1-\mathbf{r}_4)\Gamma_{\rm dd}(\mathbf{r}_2-\mathbf{r}_5)\Gamma_{\rm dd}(\mathbf{r}_3-\mathbf{r}_5) \\
& +\;\frac{\rho^2}{\nu}\int d^3r_4\,d^3r_5\,\ell^2(|\mathbf{r}_4-\mathbf{r}_5|k_{\rm F})\Gamma_{\rm dd}(\mathbf{r}_1-\mathbf{r}_4)\Gamma_{\rm dd}(\mathbf{r}_3-\mathbf{r}_4)\Gamma_{\rm dd}(\mathbf{r}_2-\mathbf{r}_5) \\
& +\;\frac{\rho^3}{\nu^2}\int d^3r_4\,d^3r_5\,d^3r_6\,\ell(|\mathbf{r}_4-\mathbf{r}_5|k_{\rm F})\ell(|\mathbf{r}_5-\mathbf{r}_6|k_{\rm F})\ell(|\mathbf{r}_6-\mathbf{r}_4|k_{\rm F}) \\
& \quad\times\Gamma_{\rm dd}(\mathbf{r}_1-\mathbf{r}_4)\Gamma_{\rm dd}(\mathbf{r}_2-\mathbf{r}_5)\Gamma_{\rm dd}(\mathbf{r}_3-\mathbf{r}_6)\,. \qquad \text{(B4)}
\end{aligned}$$

The first two lines are invariant under exchanging $\mathbf{r}_2\leftrightarrow\mathbf{r}_3$, equivalent to exchanging $(p'h')\leftrightarrow(p''h'')$ in (B3).

Optimized triplet correlations improve the description of the ground-state structure, in particular in the area of the peak of the static structure function and also improve, for bosons, the density dependence of the spectrum [17]. These correlations add another term to the three-body function $\Gamma^{\rm CA}_{\rm ddd}(\mathbf{r}_1,\mathbf{r}_2,\mathbf{r}_3)$. The expressions are lengthy [28], we refrain from

spelling them out here and just show the diagrammatic representation of some typical terms in the last row of Fig. 12.

Per definition in (3.16), $M^{(\mathrm{I})}_{ph,p'p''h'h''}$ is to be constructed such that its matrix product with $M_{ph,p'h'}$ reproduces $M_{ph,p'p''h'h''}$. A low-order manifestation of this is easily verified with choosing for $M^{(\mathrm{I})}_{ph,p'p''h'h''}$ the uniform limit diagrams shown in the first row of Fig. 12,

$$\begin{aligned} M^{(\mathrm{I})\,\mathrm{CA}}_{ph,p'p''h'h''} &= \Big\{\delta_{h,h'}\langle ph''|\Gamma_{\mathrm{dd}}|p'p''\rangle - \delta_{p,p'}\langle h'h''|\Gamma_{\mathrm{dd}}|hp''\rangle + (p'h') \leftrightarrow (p''h'')\Big\} \\ &+ \sum_{p_1}\langle ph''|\Gamma_{\mathrm{dd}}|p_1p''\rangle\langle p_1h'|\Gamma_{\mathrm{dd}}|hp'\rangle - \sum_{h_1}\langle ph'|\Gamma_{\mathrm{dd}}|h_1p'\rangle\langle h_1h''|\Gamma_{\mathrm{dd}}|hp''\rangle \quad \text{(B5)} \\ &= \frac{1}{N}\delta_{\mathbf{q},\mathbf{q}'+\mathbf{q}''}\,\bar{n}_{\mathbf{p}}\bar{n}_{\mathbf{p}'}\bar{n}_{\mathbf{p}''}n_{\mathbf{h}}n_{\mathbf{h}'}n_{\mathbf{h}''}\times \\ &\quad \Big[\Big\{\tilde{\Gamma}_{\mathrm{dd}}(q'')\,(\delta_{h,h'}-\delta_{p,p'}) + (p'h') \leftrightarrow (p''h'')\Big\} \\ &\quad + \frac{1}{N}\tilde{\Gamma}_{\mathrm{dd}}(q'')\tilde{\Gamma}_{\mathrm{dd}}(q')\,(\bar{n}_{\mathbf{h}+\mathbf{q}'} - n_{\mathbf{h}+\mathbf{q}''})\Big] \quad \text{(B6)} \end{aligned}$$

where the term originating from triplet correlations has not been spelled out.

Generally, $M^{(\mathrm{I})}_{ph,p'p''h'h''}$ is represented by the subset of $M_{ph,p'p''h'h''}$ diagrams that can *not* be cut into two pieces, one connected to the labels ph and the other to $p'p''h'h''$, by cutting either two exchange lines, or cutting the diagram in an internal point. The third row of Fig. 12 shows such contributions.

$M^{(\mathrm{I})\,\mathrm{CA}}_{ph,p'p''h'h''}$ depends non-trivially on three particle and three hole quantum numbers. We define the localized version as its Fermi sea average, Eq. (4.5),

$$\begin{aligned} \tilde{M}^{(\mathrm{I})\,\mathrm{CA}}_{q,\,q'q''} &\equiv \frac{1}{S_{\mathrm{F}}(q)S_{\mathrm{F}}(q')S_{\mathrm{F}}(q'')}\,\frac{1}{N}\sum_{hh'h''} M^{(\mathrm{I})\,\mathrm{CA}}_{ph,p'p''h'h''} \\ &= \delta_{\mathbf{q},\mathbf{q}'+\mathbf{q}''}\left[\left[\frac{S(q')S(q'')}{S_{\mathrm{F}}(q')S_{\mathrm{F}}(q'')} - 1\right]\frac{S^{(3)}_{\mathrm{F}}(q,q',q'')}{S_{\mathrm{F}}(q)S_{\mathrm{F}}(q')S_{\mathrm{F}}(q'')} + \frac{S(q')S(q'')}{S_{\mathrm{F}}(q')S_{\mathrm{F}}(q'')}\tilde{u}_3(q,q',q'')\right]. \quad \text{(B7)} \end{aligned}$$

Here, the relationship (A4) was used for the connection between $\tilde{\Gamma}_{\mathrm{dd}}(q)$ and $S(q)$, and

$$S^{(3)}_{\mathrm{F}}(q,q',q'') \equiv \frac{1}{N}\sum_{h} n_{\mathbf{h}}\bar{n}_{\mathbf{h}-\mathbf{q}}\,[\bar{n}_{\mathbf{h}+\mathbf{q}'} - n_{\mathbf{h}+\mathbf{q}''}] \quad \text{(B8)}$$

is the three-body static structure function of non-interacting fermions.

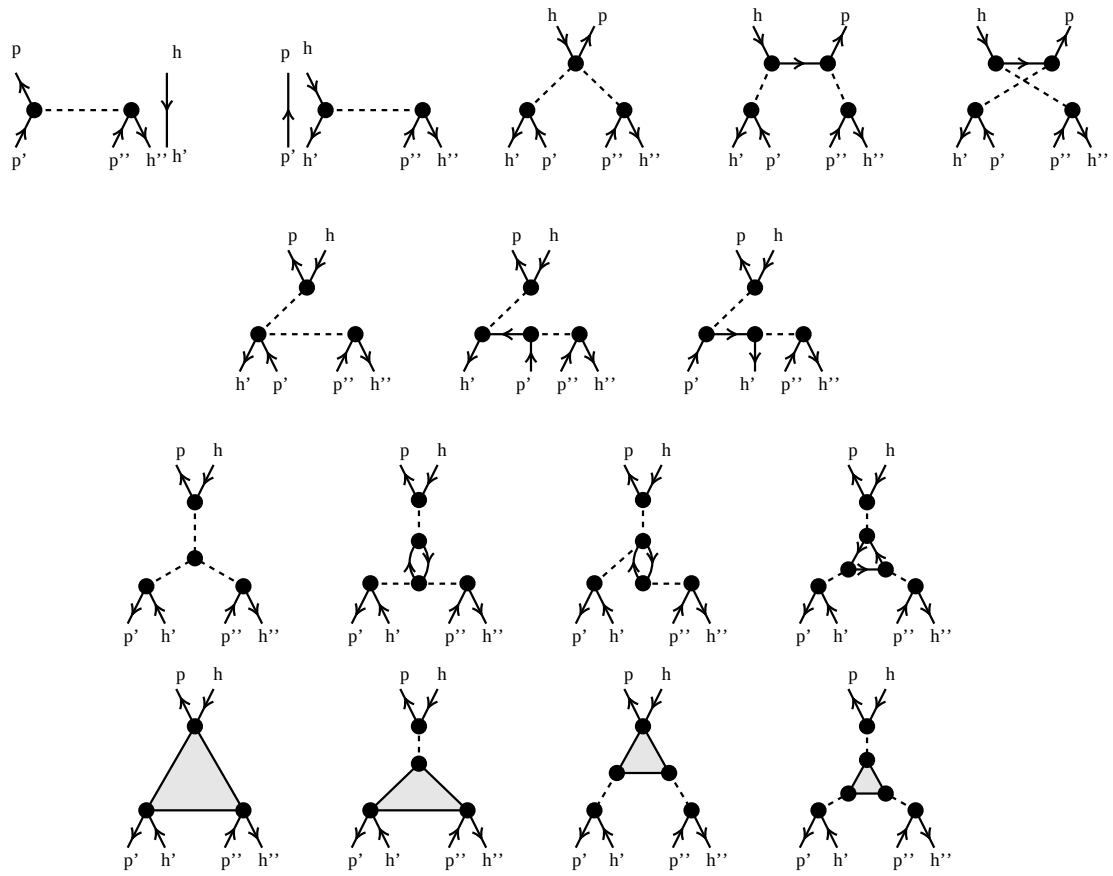

FIG. 12: Diagrams of $M_{ph,p'p''h'h''}$ in the convolution approximation (B3). Graphs obtained by exchanging the pairs $(p'h')$ and $(p''h'')$ are to be added. The last row shows some diagrams containing ground state triplet correlations (shaded triangle), all of these contribute to $M^{(I)}_{ph,p'p''h'h''}$.

3. Three-body vertices

We now apply the localization procedure (4.5) to the three-body vertices. Starting with (3.35), we have

$$\tilde{K}^{(q)}_{q'q'',0} \equiv N^2\, K^{(q)}_{q'q'',0} = \frac{1}{N\, S_{\rm F}(q) S_{\rm F}(q') S_{\rm F}(q'')} \sum_{hh'h''} \left[H'_{pp'p''hh'h'',0} - \sum_{p_1h_1} H'_{ph\,p_1h_1,0}\, M^{(\rm I)}_{p'p''h'h'',\,p_1h_1} \right] . \tag{B9}$$

As discussed in Sec. III B, the Euler equations (2.5) for the ground state optimizations ensure that the Fermi sea average (3.7) of $H'_{pp'p''hh'h'',0}$ vanishes. For the matrix elements $H'_{php'h',0}$

Eqs. (4.1)-(4.3) yield

$$H'_{php'h',0} = \frac{1}{2N}\delta_{\mathbf{q}+\mathbf{q}',\mathbf{0}}\Big[e_{ph} + e_{p'h'} - 2\frac{t(q)}{S_{\rm F}(q)}\Big]\,\tilde{\Gamma}_{\rm dd}(q). \tag{B10}$$

Therefore, using (B6) for $M^{(\rm I)}_{ph,p'p''h'h''}$

$$\begin{aligned}
\frac{1}{N^3}\sum_{hh'h''} K^{(ph)}_{p'p''h'h'',0} &= -\frac{1}{N^3}\sum_{hh'h''}\sum_{p_1h_1} H'_{ph\,p_1h_1,0}\,M^{(\rm I)}_{p'p''h'h'',p_1h_1} \\
&= -\frac{1}{2N^3}\,\tilde{\Gamma}_{\rm dd}(q)\,S_{\rm F}(q)\sum_{h'h''h_1}\Big(e_{h_1-q,h_1} - \frac{t(q)}{S_{\rm F}(q)}\Big)\,M^{(\rm I)}_{p'p''h'h'',(h_1-q)h_1} \\
&= \frac{\delta_{\mathbf{q}+\mathbf{q}'+\mathbf{q}'',\mathbf{0}}}{N^2}\,\frac{\hbar^2}{4m}\,\tilde{\Gamma}_{\rm dd}(q)\left[\frac{S(q')S(q'')}{S_{\rm F}(q')S_{\rm F}(q'')} - 1\right] \\
&\quad\times\Big[q^2\,S^{(3)}_{\rm F}(q,q',q'') + \mathbf{q}\cdot[\mathbf{q}''\,S_{\rm F}(q') + \mathbf{q}'\,S_{\rm F}(q'')]\,S_{\rm F}(q)\Big].
\end{aligned} \tag{B11}$$

This term vanishes when q and q' are larger than $2\,k_{\rm F}$. It is also zero if the matrix element $H'_{ph\,p_1h_1,0}$ in Eq. (B11) is replaced by its Fermi sea average. We therefore expect this term to be small, in particular since it has no analog in the Bose limit. Note also that triplet ground state correlations do not contribute to this term. Dividing by the normalization factors $S_{\rm F}(q)S_{\rm F}(q')S_{\rm F}(q'')$ leads to the result (4.13).

To calculate a localized version of the vertex $K_{ph,p'p''h'h''}$, Eq. (3.34), we need

$$\tilde{K}_{q,q'q''} \equiv N^2\,K_{q,q'q''} = \frac{1}{N\,S_{\rm F}(q)S_{\rm F}(q')S_{\rm F}(q'')}\sum_{hh'h''}\left[H'_{ph,\,p'p''h'h''} - \sum_{p_1h_1} H'_{ph,\,p_1h_1}\,M^{(\rm I)}_{p_1h_1,\,p'p''h'h''}\right] \tag{B12}$$

with

$$H'_{ph,p'h'} = \delta_{\mathbf{q}\,,\,\mathbf{q}'}\Big\{\delta_{h,h'}\,e_{ph} + \frac{1}{2N}\Big[e_{ph} + e_{p'h'} - 2\frac{t(q)}{S_{\rm F}(q)}\Big]\,\tilde{\Gamma}_{\rm dd}(q)\Big\}. \tag{B13}$$

We first separate the contribution that survives in the boson limit. Starting with the identity

$$\sum_{h'h''}|\Psi_{p'p''h'h''}\rangle = F\left[\hat{\rho}_{\mathbf{q}'}\hat{\rho}_{\mathbf{q}''} - \sum_{h'} a^\dagger_{h'+q'+q''}a_{h'}\,(\bar{n}_{\mathbf{h}'+\mathbf{q}''} - n_{\mathbf{h}'+\mathbf{q}'})\right]|\Phi_{\mathbf{o}}\rangle \tag{B14}$$

we have

$$\sum_{hh'h"} H'_{ph,\,p'p''h'h''} = \langle\Psi_{\mathbf{o}}\,|\,\hat{\rho}_{\mathbf{q}}H'\hat{\rho}_{\mathbf{q}'}\hat{\rho}_{\mathbf{q}''}\,|\,\Psi_{\mathbf{o}}\rangle - \sum_{hh'}(\bar{n}_{\mathbf{h}'+\mathbf{q}''} - n_{\mathbf{h}'+\mathbf{q}'})\,H_{ph,\,h'+q\,h'}\,. \tag{B15}$$

Postulating that three-body correlations have been optimized we can simplify the first term

$$\frac{1}{2N}\left\langle\Psi_{\mathbf{o}}\,\middle|\,\Big[[\hat{\rho}_{\mathbf{q}},H'],\hat{\rho}_{\mathbf{q}'}\hat{\rho}_{\mathbf{q}''}\Big]\,\middle|\,\Psi_{\mathbf{o}}\right\rangle = -\frac{\hbar^2}{2m}\mathbf{q}\cdot\Big[\mathbf{q}''\,S(q') + \mathbf{q}'\,S(q'')\Big]. \tag{B16}$$

For the form (B13), the second term in (B15) is

$$
\begin{aligned}
- \; \frac{1}{N} \sum_{hh'} H_{ph,\, h'+q\, h'} \, (\bar{n}_{\mathbf{h}'+\mathbf{q}''} - n_{\mathbf{h}'+\mathbf{q}'}) &= \frac{\hbar^2}{2m} \mathbf{q} \cdot \Big[\mathbf{q}'' \, S_{\rm F}(q') + \mathbf{q}' \, S_{\rm F}(q'') \Big] \\
+ \; \frac{\hbar^2}{4m} \tilde{\Gamma}_{\rm dd}(q) \Big[q^2 \, S_{\rm F}^{(3)}(q, q', q'') + \mathbf{q} \cdot \Big[\mathbf{q}'' \, S_{\rm F}(q') + \mathbf{q}' \, S_{\rm F}(q'') \Big] S_{\rm F}(q) \Big] \, . & \qquad \text{(B17)}
\end{aligned}
$$

The remaining term of $\tilde{K}_{q,q'q''}$ in (3.35), $-\sum_{p_1 h_1} H'_{ph,\, p_1 h_1} \, M^{(\rm I)}_{p_1 h_1, p'p''h'h''}$, contains contributions originating from the diagonal and the off-diagonal parts of H'_{ph,p_1h_1}, Eq. (B13). The off-diagonal part is identical to the expression (B11), whereas the contribution from the diagonal term gives

$$
\begin{aligned}
- \frac{1}{N} \sum_{h,h',h''} e_{ph} \, M^{(\rm I)}_{ph,p'p''h'h''} \; &= \; \frac{\hbar^2}{2m} \mathbf{q} \cdot \Big[\mathbf{q}'' \, S_{\rm F}(q') + \mathbf{q}' \, S_{\rm F}(q'') \Big] \left[\frac{S(q') S(q'')}{S_{\rm F}(q') S_{\rm F}(q'')} - 1 \right] \\
&- \; \frac{\hbar^2 q^2}{2m} S(q') S(q'') \tilde{u}_3(q, q', q'') . \qquad \text{(B18)}
\end{aligned}
$$

Collecting the individual contributions we obtain Eq. (4.12).

4. Four-body coupling matrix element

In Eq. (3.24) we have defined the irreducible four-body coupling matrix element $M^{(\rm I)}_{pp'hh',p''p'''h''h'''}$. Again, "irreducible" means that in the diagrammatic representation left and right arguments can not be separated by cutting a particle and a hole line. In analogy to the Bose case the "convolution" ("uniform limit") approximation is obtained by retaining the leading order diagrams

$$
M^{(\rm I)\,\rm CA}_{pp'hh',p''p'''h''h'''} \; \equiv \; M_{ph,p''h''} \, M_{p'h',p'''h'''} \; + \; M_{ph,p'''h'''} \, M_{p'h',p''h''} \, . \qquad \text{(B19)}
$$

This contains all diagrams with up to two correlations. A consistent improvement of the convolution approximation involves an infinite resummation. For bosons [7] this had only a marginal effect. We expect a similarly small improvement for fermions.

The approximation for $K_{pp'hh',p''p'''h''h'''}$ consistent with (B19) is to keep all diagrams containing only one correlation function $\Gamma_{\rm dd}(r)$,

$$
\begin{aligned}
K^{\rm CA}_{pp'hh',p''p'''h''h'''} \; &\equiv \; \delta_{p,p''} \delta_{h,h''} \, e_{ph} \, M_{p'h',p'''h'''} \; + \; \delta_{p',p'''} \delta_{h',h'''} \, e_{p'h'} \, M_{ph,p''h''} \\
&+ \; \{ p''h'' \leftrightarrow p'''h''' \} \, . \qquad \text{(B20)}
\end{aligned}
$$

Note that both $M^{(\mathrm{I})\,\mathrm{CA}}_{pp'hh',p''p'''h''h'''}$ and $K^{\mathrm{CA}}_{pp'hh',p''p'''h''h'''}$ contain explicit particle- and hole-labels. Again, we no longer spell out the superscript "CA" in the following.

A word is in order about the symmetry of both quantities. Eqs. (B19) and (B20) show that both operators are the sum of two term that differ from each other merely by the interchanging $\{p''h'' \leftrightarrow p'''h'''\}$. We have discussed in connection with Eq. (3.42) that it is legitimate to replace $M^{(\mathrm{I})}_{pp'hh',p''p'''h''h'''}$ and $K_{pp'hh',p''p'''h''h'''}$ by their asymmetric form.

Appendix C: Pair propagator

1. Pair energy matrix

A priori, $E_{pp'hh',p''p'''h''h'''}(\omega)$ is a function of four hole and four particle momenta as well as the energy. In the uniform limit approximation we can, however, express the inverse in terms of two-body quantities. From (B19) and (B20) we obtain the pair energy matrix

$$\begin{aligned} E_{pp'hh',p''p'''h''h'''}(\omega) \;=\; & (\hbar\omega{+}\mathrm{i}\eta) M_{ph,p''h''}\, M_{p'h',p'''h'''} \\ & - (\delta_{p,p''}\delta_{h,h''}\, e_{ph})\, M_{p'h',p'''h'''} \;-\; M_{ph,p''h''}\, (\delta_{p',p'''}\delta_{h',h'''}\, e_{p'h'})\,. \end{aligned} \tag{C1}$$

To calculate its inverse, write (C1) as

$$\begin{aligned} \sum_{p_1h_1p_2h_2} M^{-1}_{ph,p_1h_1} M^{-1}_{p'h',p_2h_2} E_{p_1p_2h_1h_2,p''p'''h''h'''}(\omega) \;=\; & (\hbar\omega{+}\mathrm{i}\eta)\delta_{p,p''}\delta_{h,h''}\,\delta_{p',p'''}\delta_{h,h'''} \\ & - (M^{-1}_{ph,p''h''}\, e_{p''h''})\,\delta_{p',p'''}\delta_{h,h'''} \;-\; \delta_{p,p''}\delta_{h,h''}\,(M^{-1}_{p'h',p'''h'''}\, e_{p'''h'''}) \end{aligned} \tag{C2}$$

Use now, for two commuting operators A, B

$$\Big[(\hbar\omega{+}\mathrm{i}\eta) - \mathrm{A} - \mathrm{B}\Big]^{-1} \;=\; -\int_{-\infty}^{\infty} \frac{d\hbar\omega'}{2\pi\mathrm{i}} \Big[(\hbar\omega'{+}\mathrm{i}\eta) - \mathrm{A}\Big]^{-1} \Big[\hbar(\omega{-}\omega'{+}\mathrm{i}\eta) - \mathrm{B}\Big]^{-1}, \tag{C3}$$

which can be proved by series expansion. Consequently, we have

$$E^{-1}_{pp'hh',p''p'''h''h'''}(\omega) \;=\; -\int_{-\infty}^{\infty} \frac{d\hbar\omega'}{2\pi\mathrm{i}}\, \kappa_{ph,p''h''}(\omega')\, \kappa_{p'h',p'''h'''}(\omega{-}\omega') \tag{C4}$$

with

$$\kappa_{ph,p'h'}(\omega) \;\equiv\; [(\hbar\omega{+}\mathrm{i}\eta) M_{ph,p'h'} \;-\; \delta_{pp'}\delta_{hh'}\, e_{ph}]^{-1}\,. \tag{C5}$$

For our choice (4.6) of $M_{p'h',ph}$, we can calculate $\kappa_{ph,p'h'}(\omega)$ analytically,

$$\begin{aligned}\kappa_{ph,p'h'}(\omega) \;&=\; \frac{\delta_{p,p'}\delta_{h,h'}}{\hbar\omega - e_{ph} + \mathrm{i}\eta} \\ &-\; \frac{1}{\hbar\omega - e_{ph} + \mathrm{i}\eta}\,\frac{\hbar\omega\,\tilde{\Gamma}_{\rm dd}(q)/N}{1 + \hbar\omega\,\tilde{\Gamma}_{\rm dd}(q)\,\kappa^0(q;\omega)}\,\frac{1}{\hbar\omega - e_{p'h'} + \mathrm{i}\eta}\,,\end{aligned} \tag{C6}$$

where $\kappa^0(q;\omega)$ has been defined in Eq. (5.4).

According to Eqs. (3.43) and (4.14), the dynamic parts of the interactions are obtained from matrix products of $E^{-1}_{pp'hh',p''p'''h''h'''}(\omega)$ as given in (C4) with the three-body vertices (4.12) and (4.13). The latter being local functions, only sums over the hole states enter $V_{\rm A,B}(q;\omega)$.

$$\tilde{E}^{-1}(q_1,q_2;\omega) \equiv \frac{1}{N^2}\sum_{h_1h_2h_1'h_2'} E^{-1}_{p_1p_2h_1h_2,p_1'p_2'h_1'h_2'}(\omega) \;=\; -\int_{-\infty}^{\infty}\frac{d\hbar\omega'}{2\pi\mathrm{i}}\,\kappa(q_1;\omega')\,\kappa(q_2;\omega-\omega') \tag{C7}$$

with

$$\kappa(q;\omega) \;\equiv\; \frac{1}{N}\sum_{hh'}\kappa_{ph,p'h'}(\omega) \;=\; \frac{\kappa_0(q;\omega)}{1+\hbar\omega\tilde{\Gamma}_{\rm dd}(q)\kappa_0(q;\omega)}\,. \tag{C8}$$

Using Kramers-Kronig relations, we obtain the useful alternative representation

$$\tilde{E}^{-1}(q_1,q_2;\omega) \;=\; \int_{-\infty}^{\infty}\frac{d(\hbar\omega_1)d(\hbar\omega_2)}{\pi^2}\,\frac{\Im m\kappa(q_1;\omega_1)\,\Im m\kappa(q_2;\omega_2)}{\hbar\omega_1+\hbar\omega_2-\hbar\omega-\mathrm{i}\eta}\,. \tag{C9}$$

2. Properties of the pair propagator

a. Properties of $\kappa(q;\omega)$

The structure of $\kappa(q;\omega)$ resembles that of $\chi(q;\omega)$ in the RPA. It features a particle-hole continuum $\kappa_{\rm cont}(q;\omega)$, and, possibly, a "collective mode" with a dispersion relation given by

$$1+\kappa_0(q;\omega_{\rm c}(q))\,\hbar\omega_{\rm c}(q)\,\tilde{\Gamma}_{\rm dd}(q) = 0\,. \tag{C10}$$

We can therefore write

$$\begin{aligned}\Im m\,\kappa(q,\omega) \;&=\; z(q)\pi\,\delta(\hbar\omega-\hbar\omega_c(q)) + \Im m\,\kappa_{\rm cont}(q;\omega)\,, \\ z(q) \;&=\; \frac{\kappa_0(q;\omega)}{\tilde{\Gamma}_{dd}(q)\,\frac{d}{d\omega}\,\omega\kappa_0(q;\omega)}\Big|_{\omega_{\rm c}(q)}\,.\end{aligned} \tag{C11}$$

$\kappa(q,\omega)$ satisfies the following sum rules which we write in the suggestive way

$$\frac{S^2(q)}{S_{\rm F}^2(q)}\int_0^\infty \frac{d(\hbar\omega)}{\pi}\,\Im m\kappa(q;\omega) \;=\; -S(q) \tag{C12}$$

$$\frac{S^2(q)}{S_{\rm F}^2(q)}\int_0^\infty \frac{d(\hbar\omega)}{\pi}\,\hbar\omega\,\Im m\kappa(q;\omega) \;=\; -t(q)\,. \tag{C13}$$

Eq. (C12) is proved by extending the integration to $-\infty$, noting that $\kappa_0(q;\omega)$ is real on the negative ω axis. Since $\kappa_0(q;\omega)$ has no poles in the upper complex plane, we can evaluate the integral along a circle, using the asymptotic expansion

$$\kappa_0(q;\omega\to\infty) \;=\; \frac{S_{\rm F}(q)}{\hbar\omega}+\frac{t(q)}{\hbar^2\omega^2}+\mathcal{O}(\hbar\omega)^{-3}\,. \tag{C14}$$

The proof of Eq. (C13) proceeds along the same line, subtracting the asymptotic expansion of $\kappa(q;\omega)$ beforehand. From Eqs. (C12), (C13) it is clear that the analytic properties of $S^2(q)\,\kappa(q;\omega)/S_{\rm F}^2(q)$ are similar to those of the density-density response function $\chi^{\rm RPA}(q;\omega)$. For bosons, the two functions coincide exactly: Identifying $\tilde{\Gamma}_{\rm dd}(q)=S(q)-1$ and $S_{\rm F}(q)=1$, $\kappa^0(q;\omega)$ consists of a single mode, so that

$$\kappa_0(q;\omega)=\frac{1}{\hbar\omega+{\rm i}\eta-t(q)}\,,\qquad \kappa(q;\omega)=\frac{1}{S(q)}\frac{1}{\hbar\omega+{\rm i}\eta-\varepsilon(q)}\,. \tag{C15}$$

Figure 13 further confirms this similarity for ^{3}He at saturation density. Expectedly, a solution of Eq. (C10) is found to lie within a few percent of the RPA zero sound mode.

b. Properties of $\tilde{E}^{-1}(q,q';\omega)$

Equations (C12) and (C13) lead to the sum rules for the pair propagator,

$$\int_{-\infty}^\infty \frac{d(\hbar\omega)}{\pi}\,\Im m E^{-1}(q,q';\omega) \;=\; -\frac{S_F^2(q)}{S(q)}\frac{S_F^2(q')}{S(q')}\,. \tag{C16}$$

$$\int_{-\infty}^\infty \frac{d(\hbar\omega)}{\pi}\,\hbar\omega\,\Im m E^{-1}(q,q';\omega) \;=\; -\frac{S_F^2(q)}{S(q)}\frac{S_F^2(q')}{S(q')}\,(\varepsilon(q)+\varepsilon(q'))\,. \tag{C17}$$

The proof of (C16) is best carried out starting from the representation (C9),

$$\int_0^\infty \frac{d(\hbar\omega)}{\pi}\Im m E^{-1}(q_1,q_2;\omega) \;=\; -\int_0^\infty \frac{d\hbar\omega_1}{\pi}\,\Im m\kappa(q_1;\omega_1)\int_0^\infty \frac{d(\hbar\omega)}{\pi}\,\Im m\kappa(q_2;\omega-\omega_1)\,. \tag{C18}$$

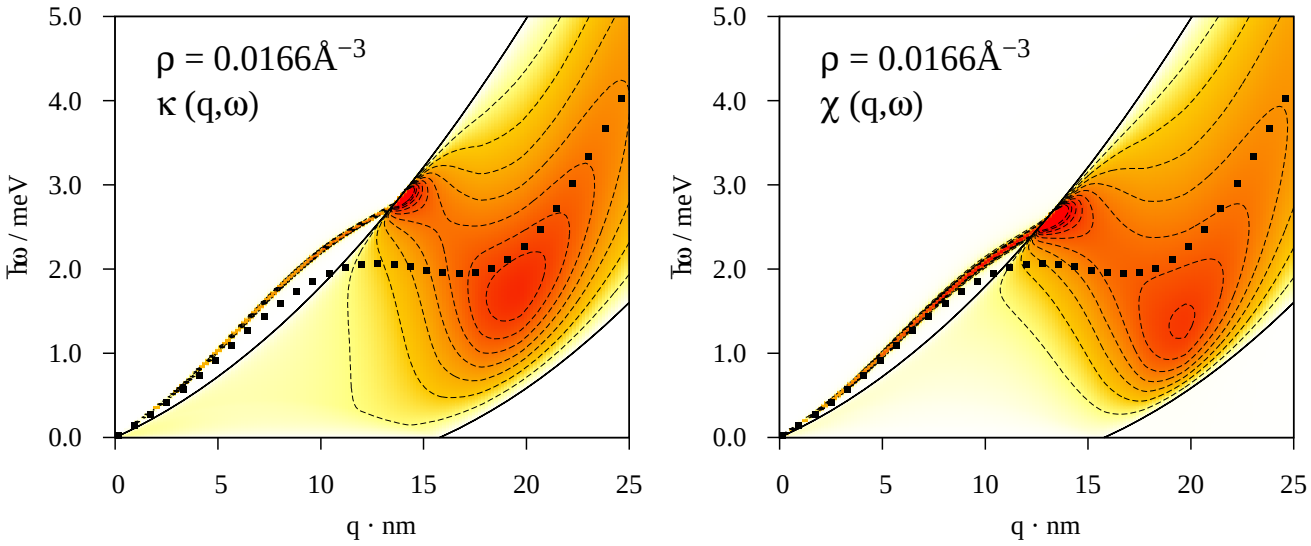

FIG. 13: Imaginary part of the scaled propagator $S^2(q)\,\kappa(q,\omega)/S_F^2(q)$ (left) and of $\chi^{\rm RPA}(q,\omega)$ (right) at the density $\rho = 0.0166\,\text{Å}^{-3}$. The black squares show, for reference, the Feynman dispersion relation $\varepsilon(q)$.

The $\hbar\omega$ integral in the last term can be extended to $-\infty$ since $\Im m\kappa(q;\omega)$ is real on the negative ω-axis.

If Eq. (C10) has a solution, the pair propagator has a collective mode. From (C11) we obtain

$$\Im m\,\tilde{E}^{-1}(q_1,q_2;\omega) = \pi\, z(q_1)\, z(q_2)\, \delta(\hbar\omega_{\rm c}(q_1) + \hbar\omega_{\rm c}(q_2) - \hbar\omega)\,. \tag{C19}$$

This is the origin of two-phonon excitations, or the double-plasmon in charged systems.

The two-particle-two-hole band consists of three parts which may overlap. The first one is the continuum–continuum (c-c) coupling, where the contribution of each $\kappa(q,\omega)$ in (C7) comes from its particle hole band. This defines the two-particle-two-hole "tube" in $(q,q';\omega)$ space. Its boundaries are

$$e_{\rm min}(q) + e_{\rm min}(q') \;\le\; \hbar\omega \;\le\; e_{\rm max}(q) + e_{\rm max}(q')\,, \tag{C20}$$

where $e_{\rm min}$ and $e_{\rm max}$ denote the upper and lower border of each single-particle-hole band, respectively.

The other two parts of $E^{-1}(q,q';\omega)$ arise from continuum–mode (c-m) coupling, they are identical apart from interchanging q and q'. Their boundaries are

$$e_{\rm min}(q) + \hbar\omega_{\rm cm}(q') \;\le\; \hbar\omega \;\le\; e_{\rm max}(q) + \hbar\omega_{\rm cm}(q')\,. \tag{C21}$$

Finally, we consider three limits of the pair propagator. First, in the non-interacting case, $\tilde{\Gamma}_{\rm dd}(q) = 0$, we simply obtain a sum over two-pair energy denominators

$$\tilde{E}^{-1}_{\rm F}(q,q';\omega) = -\int \frac{d\hbar\omega'}{2\pi{\rm i}} \kappa_0(q';\omega-\omega')\kappa_0(q;\omega') = \frac{1}{N^2}\sum_{hh'} \frac{1}{\hbar\omega+{\rm i}\eta - e_{ph} - e_{p'h'}}\,, \qquad \text{(C22)}$$

i.e. the two-particle energy denominator appropriate for perturbation theory in a weakly interacting Fermi system.

Second, (C15) reproduces the energy denominator appearing in the boson theory,

$$\tilde{E}^{-1}_{\rm bos}(q,q';\omega) = \frac{1}{S(q)S(q')}\,\frac{1}{\varepsilon(q)+\varepsilon(q')-\hbar\omega-{\rm i}\eta}\,. \qquad \text{(C23)}$$

Finally, we consider the "collective" or "uniform limit" approximation. Following (A6) we replace $\kappa_0(q;\omega)$ by that single-pole approximation which ensures its correct ω^0 and ω^1 sum rules. This gives

$$\kappa^{\rm CA}_0(q;\omega) = \frac{S_{\rm F}(q)}{\hbar\omega+{\rm i}\eta - t(q)/S_{\rm F}(q)}\,, \qquad \text{(C24)}$$

$$\kappa^{\rm CA}(q;\omega) = \frac{S^2_{\rm F}(q)}{S(q)}\,\frac{1}{\hbar\omega+{\rm i}\eta-\varepsilon(q)}\,, \qquad \text{(C25)}$$

and

$$E^{-1}_{\rm CA}(q,q';\omega) = \frac{S^2_F(q)}{S(q)}\frac{S^2_F(q')}{S(q')}\frac{1}{\varepsilon(q)+\varepsilon(q')-\hbar\omega-{\rm i}\eta}\,. \qquad \text{(C26)}$$

The boson limit as well as the collective approximation demonstrate the effect of correlations: The single-particle energies get shifted and form a band around the "Feynman-spectrum". Note that the collective approximation satisfies the sum rules (C16)-(C17) exactly.

c. Pair propagator for charged systems

For charged systems, the dispersion of the solution of Eq. (C10) has, unlike the plasmon, a term that is linear in the wave number:

$$\hbar\omega_{\rm c}(q) = \omega_{\rm p} + \frac{t_{\rm F}}{6}\,\frac{q}{k_{\rm F}} - \frac{9t^2_{\rm F}}{4\hbar\omega_{\rm p}}\left(\frac{q}{k_{\rm F}}\right)^2 + \mathcal{O}(q^3)\,. \qquad \text{(C27)}$$

For the strength of this mode we obtain

$$z(q,\omega_{\rm c}(q)) = \frac{9\hbar\omega_{\rm p}}{16t_{\rm F}} - \frac{3}{32}\frac{q}{k_{\rm F}}\,. \qquad \text{(C28)}$$

Hence, to leading order, for the pole of $E^{-1}(q_1, q_2; \omega)$ in (C19) we obtain

$$\Im m\, \tilde{E}^{-1}(q', q'; \omega) = -\pi \left(\frac{9}{16} \frac{\hbar\omega_{\rm p}}{t_{\rm F}} - \frac{3}{32} \frac{q'}{k_{\rm F}} \right)^2 \delta \left(\hbar\omega - 2\hbar\omega_{\rm p} - \frac{t_{\rm F}}{3} \frac{q'}{k_{\rm F}} \right) \text{ as } q' \to 0. \quad \text{(C29)}$$

Note that the location of double-plasmon pole contains, in leading order in the momentum transfer, no information on many-body correlations.

Appendix D: Large momentum limit

For large momenta, $S(q)-1$ falls off at least as q^{-4}. The vertices (4.12) and (4.13) fall off as q^{-1} and as q^{-2}, respectively, hence we have

$$\begin{aligned} \tilde{K}_{q,q'q''} &\approx \frac{S(q')\, S(q'')}{S_{\rm F}(q')\, S_{\rm F}(q'')} \frac{\hbar^2}{2m} \left[\mathbf{q} \cdot \mathbf{q}'\, \tilde{X}_{\rm dd}(q') + \mathbf{q} \cdot \mathbf{q}''\, \tilde{X}_{\rm dd}(q'') \right], \quad \text{(D1)} \\ \tilde{K}^{(q)}_{q'q'',0} &\approx 0\,. \end{aligned}$$

As a consequence, $\widetilde{W}_{\rm B}(q;0)$ is negligible for large momenta, and only the first term in Eq. (4.17)) contributes to $\widetilde{W}_{\rm A}(q;0)$.

For large q either q' or q'' (or both) must be large. (let $q'' \geq q'$, the symmetry in $\mathbf{q}' \leftrightarrow \mathbf{q}''$ just yielding a factor of two). Since $\tilde{X}_{\rm dd}(q)$ falls off for large q, the dominant contribution of (D1) then arises from small q' and we can write

$$\begin{aligned} \tilde{W}_A(q \to \infty, 0) &= \left(\frac{\hbar^2}{2m} \right)^2 \frac{1}{N} \sum_{\mathbf{q}'} \left(\frac{S(q')}{S_{\rm F}(q')} \right)^2 \left[\mathbf{q} \cdot \mathbf{q}'\, \tilde{X}_{\rm dd}(q') \right]^2 \tilde{E}^{-1}(q', q''; 0) \\ &= \frac{t(q)}{3} \frac{1}{N} \sum_{\mathbf{q}'} t(q') \left[\frac{S(q')}{S_{\rm F}(q')} \tilde{X}_{\rm dd}(q') \right]^2 \tilde{E}^{-1}(q', q; 0)\,. \quad \text{(D2)} \end{aligned}$$

We now use the representation (C7) for the pair propagator

$$\tilde{E}^{-1}(q', q; 0) = -\int_{-\infty}^{\infty} \frac{d\hbar\omega'}{\pi}\, \Re e\, \kappa(q', \omega')\, \Im m\, \kappa(q, -\omega')\,. \quad \text{(D3)}$$

Since $\kappa^0(q \gg k_{\rm F}; \omega) = 1/(\hbar\omega - t(q) + {\rm i}\eta)$ we have

$$\kappa(q \to \infty; \omega) = \frac{1}{S(q)} \frac{1}{\hbar\omega - \varepsilon(q) + {\rm i}\eta}\,. \quad \text{(D4)}$$

Consequently,

$$\begin{aligned} \tilde{E}^{-1}(q', q \to \infty; 0) &= \frac{1}{S(q)}\, \Re e\, \kappa(q', -\tfrac{1}{\hbar}\varepsilon(q)) \\ &= -\frac{1}{t(q)} \frac{{S_{\rm F}}^2(q')}{S(q')}\,, \quad \text{(D5)} \end{aligned}$$

where the last equality follows from the high-frequency limit $\kappa^0(q';\omega) \to S_{\rm F}(q')/\omega$. Insertion into (D2) yields

$$\tilde{W}_A(q\to\infty,0) \;=\; -\frac{1}{3N}\sum_{\mathbf{q}'} t(q')S(q')\left[\tilde{X}_{\rm dd}(q')\right]^2 , \tag{D6}$$

which together with Eq. (A12) gives the result (5.14).

Appendix E: Sum rules

For bosons, the ω^0 and ω^1 sum rules (1.4) and (1.5) are satisfied exactly [16] in the sense that the result of the frequency integration is independent of the level at which pair fluctuations are treated. This feature provides an unambiguous method to determine the static particle-hole interaction $\widetilde{V}_{\rm p\text{-}h}(q)$ through the sum rule (1.4) from the static structure function.

The proof of the m_1 sum rule is identical to the one for bosons: Due to the symmetry

$$\chi(q;\omega) = \chi^*(q,-\omega)$$

we can write

$$m_1 = -\frac{1}{2\pi}\Im m\int_{-\infty}^{\infty} d(\hbar\omega)\,\hbar\omega\,\chi(q;\omega)\,. \tag{E1}$$

All poles of $\chi(q;\omega)$ are in the lower half plane, allowing to close the integral in the upper half plane. For large ω we have, however,

$$\chi_0(q;\omega) - \chi^{\rm RPA}(q;\omega) \propto \omega^{-4} \qquad \chi_0(q;\omega) - \chi(q;\omega) \propto \omega^{-4} \tag{E2}$$

since

$$\widetilde{V}_{A,B}(q;\omega) = \tilde{V}_{\rm ph}(q) + \frac{\text{const.}}{\omega} \qquad \text{as} \qquad \omega\to\infty. \tag{E3}$$

We have therefore

$$\Im m\int_{-\infty}^{\infty} d(\hbar\omega)\,\hbar\omega\,\chi(q;\omega) = \Im m\int_{-\infty}^{\infty} d(\hbar\omega)\,\hbar\omega\,\chi^{\rm RPA}(q;\omega) = \Im m\int_{-\infty}^{\infty} d(\hbar\omega)\;\hbar\omega\,\chi(q;\omega)\,. \tag{E4}$$

For fermions, the frequency integration in (1.4) must be carried out numerically, which is best done by Wick rotation along the imaginary axis. The result of the integration is no longer rigorously independent of the approximation used for the response function.

Fig. 14 compares the m_0 sum rule calculated within the RPA and the pair excitation theory. Evidently, the discrepancy is very small. One can understand by comparing with the

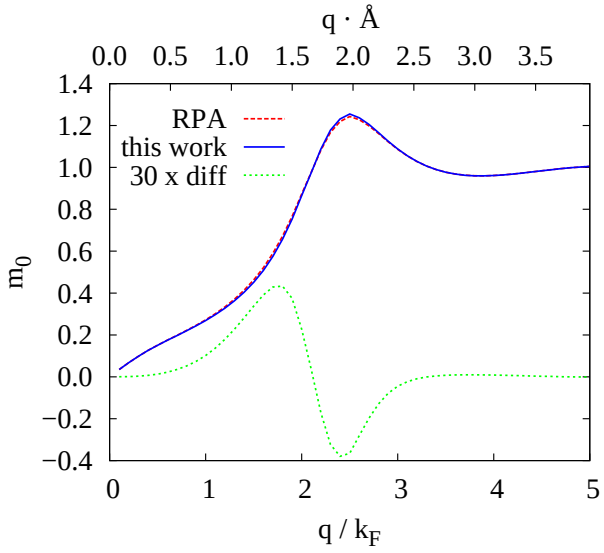

FIG. 14: Result of the m_0 sum rule for ^{3}He at saturated vapor pressure. The purple dashed line shows the FHNC $S(q)$ and the blue short dashed line the result from the pair fluctuation theory; the dashed green line shows the difference, magnified by a factor of 30 to make it visible.

boson theory: If we restricted the fluctuation operators $\delta u^{(1)}_{ph}(t)$ and $\delta u^{(2)}_{pp'hh'}(t)$ to be functions of momentum transfers $\mathbf{q} = \mathbf{p} - \mathbf{h}$ and $\mathbf{q}' = \mathbf{p}' - \mathbf{h}'$, we would end up with a density-density response function that is formally identical to that of bosons and would, hence, lead to an $S(q)$ that is independent of the treatment of the pair fluctuations. The expectation that the inclusion of the particle-hole structure of the two-pair energy denominator makes only a small difference is verified in Fig. 14. Thus, it is also legitimate in the pair-excitation theory to obtain the static particle-hole interaction $\tilde{V}_{\mathrm{p-h}}(q)$ from the static structure function $S(q)$ through Eqs. (1.4) and (1.7).

Appendix F: Implementation Recipe

This section provides, for the convenience of the reader and easy further reference, a compilation of all necessary ingredients to implement the theory. Mostly a summary of sections IV and V A, we deliberately refrain from any explanation to avoid redundancy and keep it as compact as possible.

We have shown in our applications to ^{3}He and the electron liquid that for practical

purposes, only one of the local three-body vertices is necessary:

$$\tilde{K}_{q,q'q''} \;=\; \frac{\hbar^2}{2m}\,\frac{S(q')S(q'')}{S_{\rm F}(q)S_{\rm F}(q')S_{\rm F}(q'')}\left[\mathbf{q}\cdot\mathbf{q}'\,\tilde{X}_{\rm dd}(q')+\mathbf{q}\cdot\mathbf{q}''\,\tilde{X}_{\rm dd}(q'')-q^2\tilde{u}_3(q,q',q'')\right]\,, \quad \text{(F1)}$$

where $u_3(q,q',q'')$ is the three-body ground state correlation [28]. The effective interaction $\widetilde{W}_{\rm A}(q,\omega)$ is then

$$\widetilde{W}_{\rm A}(q;\omega)=\frac{1}{2N}\sum_{\mathbf{q}'}|\tilde{K}_{q,q'q''}|^2\,\tilde{E}^{-1}(q',q'';\omega) \quad \text{(F2)}$$

whereas $\widetilde{W}_{\rm B}(q,\omega)$ vanishes. Consequently, the components of the (energy–dependent) interaction matrix $\mathbf{V}_{\rm p-h}(\omega)$ are

$$\tilde{V}_{\rm A}(q;\omega)=\tilde{V}_{\rm p-h}(q)\;+\;[\sigma_q^+]^2\,\widetilde{W}_{\rm A}(q;\omega)+[\sigma_q^-]^2\,\widetilde{W}^*_{\rm A}(q;-\omega)\,, \quad \text{(F3)}$$

$$\tilde{V}_{\rm B}(q;\omega)=\tilde{V}_{\rm p-h}(q)\;+\;\sigma_q^+\sigma_q^-\,\left(\widetilde{W}_{\rm A}(q;\omega)+\widetilde{W}^*_{\rm A}(q;-\omega)\right)\,, \quad \text{(F4)}$$

with $\sigma_q^\pm\equiv[S_{\rm F}(q)\pm S(q)]/2S(q)$.

Finally we need the pair propagator:

$$\tilde{E}^{-1}(q_1,q_2;\omega)\;=\;-\int_{-\infty}^{\infty}\frac{d\hbar\omega'}{2\pi{\rm i}}\,\kappa(q_1;\omega')\,\kappa(q_2;\omega-\omega') \quad \text{(F5)}$$

$$\kappa(q;\omega)\;=\;\frac{\kappa_0(q;\omega)}{1+\hbar\omega\tilde{\Gamma}_{\rm dd}(q)\kappa_0(q;\omega)} \quad \text{(F6)}$$

with the partial Lindhard functions:

$$\kappa_0(q;\omega)\equiv\frac{1}{N}\sum_h\frac{\bar{n}_{\mathbf{p}}n_{\mathbf{h}}}{\hbar\omega-e_{ph}+{\rm i}\eta} \quad \text{(F7)}$$

The simplifications of the interactions do not significantly simplify the form (5.6) of the density-density response function.

---

[1] A. K. Kerman and S. E. Koonin, Ann. Phys. (NY) **100**, 332 (1976).

[2] P. Kramer and M. Saraceno, *Geometry of the time-dependent variational principle in quantum mechanics*, Vol. 140 of *Lecture Notes in Physics* (Springer, Berlin, Heidelberg, and New York, 1981).

[3] D. J. Thouless, *The quantum mechanics of many-body systems*, 2 ed. (Academic Press, New York, 1972).

[4] J. M. C. Chen, J. W. Clark, and D. G. Sandler, Z. Physik A **305**, 223 (1982).

[5] E. Krotscheck, Phys. Rev. A **26**, 3536 (1982).

[6] H. W. Jackson and E. Feenberg, Ann. Phys. (NY) **15**, 266 (1961).

[7] C. E. Campbell and E. Krotscheck, Phys. Rev. B **80**, 174501/1 (2009).

[8] L. D. Landau, Sov. Phys. JETP **3**, 920 (1957).

[9] L. D. Landau, Sov. Phys. JETP **5**, 101 (1957).

[10] R. P. Feynman, Phys. Rev. **94**, 262 (1954).

[11] R. P. Feynman and M. Cohen, Phys. Rev. **102**, 1189 (1956).

[12] H. W. Jackson and E. Feenberg, Rev. Mod. Phys. **34**, 686 (1962).

[13] E. Feenberg, *Theory of Quantum Fluids* (Academic, New York, 1969).

[14] H. W. Jackson, Phys. Rev. A **4**, 2386 (1971).

[15] H. W. Jackson, Phys. Rev. A **8**, 1529 (1973).

[16] H. W. Jackson, Phys. Rev. A **9**, 964 (1974).

[17] C. C. Chang and C. E. Campbell, Phys. Rev. B **13**, 3779 (1976).

[18] C. E. Campbell and E. Krotscheck, Dymanic Many Body Theory III: Multi-particle fluctuations in bulk ^{4}He, 2010, in preparation.

[19] C. H. Aldrich III and D. Pines, J. Low Temp. Phys. **31**, 689 (1978).

[20] N. Iwamoto and D. Pines, Phys. Rev. B **29**, 3924 (1984).

[21] J. W. Clark, in *Progress in Particle and Nuclear Physics*, edited by D. H. Wilkinson (Pergamon Press Ltd., Oxford, 1979), Vol. 2, pp. 89–199.

[22] A. Fabrocini, S. Fantoni, and E. Krotscheck, *Introduction to Modern Methods of Quantum Many–Body Theory and their Applications*, Vol. 7 of *Advances in Quantum Many–Body Theory* (World Scientific, Singapore, 2002).

[23] R. Scherm *et al.*, Phys. Rev. Lett. **59**, 217 (1987).

[24] B. Fåk, K. Guckelsberger, R. Scherm, and A. Stunault, J. Low Temp. Phys. **97**, 445 (1994).

[25] H. R. Glyde *et al.*, Phys. Rev. B **61**, 1421 (2000).

[26] C. Sternemann *et al.*, Phys. Rev. Lett. **95**, 157401 (2005).

[27] S. Huotari *et al.*, Phys. Rev. B **77**, in press (2008).

[28] E. Krotscheck, J. Low Temp. Phys. **119**, 103 (2000).

[29] A. D. Jackson, A. Lande, and R. A. Smith, Physics Reports **86**, 55 (1982).

[30] P. M. Morse and H. Feshbach, *Methods of Theoretical Physics* (McGraw-Hill, New York -

Toronto - London, 1953), Vol. I.

[31] E. Krotscheck and J. W. Clark, Nucl. Phys. A **328**, 73 (1979).

[32] E. Krotscheck, in *Introduction to Modern Methods of Quantum Many–Body Theory and their Applications*, Vol. 7 of *Advances in Quantum Many–Body Theory*, edited by A. Fabrocini, S. Fantoni, and E. Krotscheck (World Scientific, Singapore, 2002), pp. 267–330.

[33] D. M. Ceperley and B. J. Alder, Phys. Rev. Lett. **45**, 566 (1980).

[34] J. Casulleras and J. Boronat, Phys. Rev. Lett. **84**, 3121 (2000).

[35] E. Krotscheck, Ann. Phys. (NY) **155**, 1 (1984).

[36] V. Apaja *et al.*, Phys. Rev. B **55**, 12925 (1997).

[37] A. Holas, in *Strongly Coupled Plasma Physics*, edited by F. J. Rogers and H. E. DeWitt (Plenum Press, New York, 1986), Vol. 154, pp. 463–482.

[38] G. Giuliani and G. Vignale, *Quantum Theory of the Electron Liquid* (Cambridge University Press, Cambridge, 2005).

[39] C. E. Campbell and E. Krotscheck, J. Low Temp. Phys. **158**, 226 (2010).

[40] H. Glyde, *Excitations in liquid and solid helium* (Oxford University Press, Oxford, 1994).

[41] F. Albergamo *et al.*, Phys. Rev. Lett. **99**, 205301/1 (2007).

[42] A. J. M. Schmets and W. Montfrooij, Phys. Rev. Lett. **100**, 239601 (2008).

[43] F. Albergamo *et al.*, Phys. Rev. Lett. **100**, 239602 (2008).

[44] D. Pines, Physics Today **34**, 106 (Nov. 1981).

[45] V. K. Mishra, G. E. Brown, and C. J. Pethick, J. Low Temp. Phys. **52**, 379 (1983).

[46] G. E. Brown, C. J. Pethick, and A. Zaringhalam, J. Low Temp. Phys. **48**, 349 (1982).

[47] B. L. Friman and E. Krotscheck, Phys. Rev. Lett. **49**, 1705 (1982).

[48] E. Krotscheck and J. Springer, J. Low Temp. Phys. **132**, 281 (2003).

[49] N.-H. Kwong, Ph.D. thesis, California Institute of Technology, 1982.

[50] M. Panholzer, H. M. Böhm, R. Holler, and E. Krotscheck, J. Low Temp. Phys. **158**, 135 (2010).

[51] R. A. Aziz, F. R. W. McCourt, and C. C. K. Wong, Molec. Phys. **61**, 1487 (1987).

[52] D. S. Greywall, Phys. Rev. B **33**, 7520 (1986).

[53] R. de Bruyn Ouboter and C. N. Yang, Physica **144B**, 127 (1986).

[54] S. Moroni, D. M. Ceperley, and G. Senatore, Phys. Rev. Lett. **69**, 1837 (1992).

[55] F. Caupin, J. Boronat, and K. H. Andersen, J. Low Temp. Phys. **152**, 108 (2008).

[56] S. Moroni, D. M. Ceperley, and G. Senatore, Phys. Rev. Lett. **75**, 689 (1995).

[57] K. S. Singwi and M. P. Tosi, Solid State Phys. **36**, 177 (1981).

[58] H. M. Böhm, R. Holler, E. Krotscheck, and M. Panholzer, Journal of Physics A: Mathematical and Theoretical **42**, 214037 (2009).

[59] K. Sturm and A. Gusarov, Phys. Rev. B **62**, 16474 (2000).

[60] M. Corradini *et al.*, Phys. Rev. B **57**, 14569 (1998).

[61] N. Iwamoto, E. Krotscheck, and D. Pines, Phys. Rev. B **29**, 3936 (1984).

[62] D. S. Greywall, Phys. Rev. B **27**, 2747 (1983).

[63] J. Boronat *et al.*, Phys. Rev. Lett. **91**, 085302 (2003).

[64] E. Krotscheck and M. L. Ristig, Phys. Lett. A **48**, 17 (1974).

J Low Temp Phys (2010) 158: 135–140
DOI 10.1007/s10909-009-9986-8

Exchange Effects and the Dynamics of ^{3}He

M. Panholzer · H.M. Böhm · R. Holler · E. Krotscheck

Received: 16 June 2009 / Accepted: 21 September 2009 / Published online: 1 October 2009

Abstract The ground state of strongly interacting Fermi fluids, specifically ^{3}He, is well understood, using either simulation or correlated basis function techniques. However, the manifestly microscopic determination of the *dynamics* of such systems still poses a number of open problems. One of these is the importance of exchange effects in the density channel. The subject of this work is to clarify this question.

We demonstrate here that exchange effects are, even in the density channel, not negligible. The main consequence is a lowering of the collective mode toward the particle-hole continuum in agreement with recent measurements on ^{3}He. In the experiment also a strong damping of the collective mode is observed. Our results show that we should, by including self-energy corrections and multipair-fluctuations, be able to determine conclusively the many-particle aspects of that effect.

Keywords Fermi fluid · Linear response · Exchange · Helium 3

PACS 67.30.Em · 67.10.Db

1 Introduction

A popular paradigm for discussing the dynamics of Fermi fluids is the random phase approximation (RPA). The approach implies a number of crucial approximations. These are

(i) The strong, bare interaction has to be replaced by a static, weak, effective interaction. This can be done phenomenologically as in the Aldrich-Pines pseudopotential model [1], or from microscopic many-body theory [2].

M. Panholzer (✉) · H.M. Böhm · R. Holler · E. Krotscheck
Institute of Theoretical Physics, Johannes Kepler University, Altenbergerstr. 69, 4040 Linz, Austria
e-mail: martin.panholzer@jku.at

(ii) The excited states are described in a space restricted to "one-particle-one-hole" excitations of the ground state, and
(iii) Exchange effects are neglected. Since the importance of exchange effects for the ground state is well established, such an approximation can be argued only by computational convenience.

The first two assumptions are indeed related, a theory that includes multi-pair-excitations can be re-formulated in terms of a "one-particle-one-hole" excitation theory with a dynamic, *energy dependent effective interaction*. The fact that such an effective interaction must be dynamic has been known, for ^{4}He, since the sixties [3], and there is no reason that effects that are dramatic in ^{4}He should be negligible in ^{3}He.

In this contribution we concentrate on the other important simplification of the RPA, namely the omission of exchange terms. When exchange effects are included, the appropriate language is the time-dependent (correlated) Hartree-Fock theory [4, 5]. Correlated Basis Functions (CBF) theory provides an unambiguous method for calculating an effective interaction in the exchange channel [2]. This approach is robust in the sense that it can, without modifications, also be applied to other system such as nuclear matter [6] or electrons [7].

2 Formalism

The starting point of the time-dependent CBF theory [2, 5] is the *ansatz* for the dynamic wave function

$$|\Psi(t)\rangle = \frac{1}{\mathcal{N}} e^{-\mathrm{i}E_0 t/\hbar} F \exp\left\{\frac{1}{2}\sum_{ph} u_{ph}(t) a_p^\dagger a_h\right\} |\Phi_0\rangle, \tag{1}$$

where $|\Phi_0\rangle$ is a Slater determinant of single-particle orbitals, which are plane waves for an infinite homogeneous system. F is a Jastrow correlation factor, E_0 the ground state energy and $\mathcal{N}$ the normalization integral. The p- and h-indices denote particle and hole states, respectively and $u_{ph}(t)$ are called "particle–hole excitation amplitudes". These amplitudes are determined by the stationarity principle [8]

$$\delta \int dt\, \mathcal{L}(t) = \delta \int dt \langle \Psi(t)| H + H_{\mathrm{ext}} - \mathrm{i}\hbar \frac{\partial}{\partial t} |\Psi(t)\rangle, \tag{2}$$

where H is the many body Hamiltonian and H_{ext} a scalar external perturbation. The algebraic manipulations to turn the equations of motion following from the stationarity principle (2) into a form that is suitable for numerical analysis are somewhat tedious since they involve the diagrammatic analysis of effective interactions of CBF theory. It suffices here to state that the above effective interactions are obtainable from the ground state theory.

The density response equations are formally solved by the "supermatrix" equation [2]

$$\chi(q,\omega) = \begin{pmatrix}\rho_{ph,0} & \rho_{0,ph}\end{pmatrix} \left[\Omega + \mathbf{V}_{\mathrm{p-h}}(\omega)\right]^{-1} \begin{pmatrix}\rho_{ph,0} \\ \rho_{0,ph}\end{pmatrix}, \tag{3}$$

where $\rho_{0,ph} = \langle \Phi_0 | \hat{\rho} a_p^\dagger a_h | \Phi_0 \rangle$ are the matrix elements of the density operator $\hat{\rho}$. Further we have introduced

$$\Omega = \begin{pmatrix} e_{ph} - \hbar\omega - \mathrm{i}\eta & 0 \\ 0 & e_{ph} + \hbar\omega + \mathrm{i}\eta \end{pmatrix} \tag{4}$$

with the particle hole energy difference e_{ph} predicted by CBF theory [2]. It is essential to include the full CBF spectrum together with the exchange diagrams, whereas a free spectrum is normally used in conventional RPA. The interaction matrix is defined as

$$\mathbf{V}_{\mathrm{p-h}}(\omega) = \begin{pmatrix} V^{\mathrm{A}}_{ph,p'h'} & V^{\mathrm{B}}_{pp'hh',0} \\ V^{\mathrm{B}}_{0,pp'hh'} & V^{\mathrm{A}}_{p'h',ph} \end{pmatrix} \tag{5}$$

with

$$V^{\mathrm{A}}_{ph,p'h'} = \langle ph' | V^{\mathrm{A}}_{\mathrm{p-h}} | hp' \rangle - \langle ph' | V^{\mathrm{A}}_{\mathrm{X}} | p'h \rangle \tag{6}$$

and

$$V^{\mathrm{B}}_{pp'hh',0} = \langle pp' | V^{\mathrm{B}}_{\mathrm{p-h}} | hh' \rangle - \langle pp' | V^{\mathrm{B}}_{\mathrm{X}} | h'h \rangle. \tag{7}$$

All interactions can, in principle, be energy dependent, see Ref. [9]. In the present implementation of the theory, which is restricted to correlated one-particle-one-hole fluctuations, they are energy independent.

A few words are in order concerning the interpretation of these effective interactions. Both, the "direct" interactions $V^{\mathrm{A,B}}_{\mathrm{p-h}}$ and the "exchange" interactions $V^{\mathrm{A,B}}_{\mathrm{X}}$ are normally non-local and different. The "direct" interactions $V^{\mathrm{A,B}}_{\mathrm{p-h}}$ are, in the language of the diagrammatic analysis of Jastrow-Feenberg theory, represented by "non-nodal" diagrams. In the language of diagrammatic perturbation theory, these correspond to "particle-hole irreducible" diagrams. The exchange interactions, on the other hand, $V^{\mathrm{A,B}}_{\mathrm{X}}$ contain nodal diagrams which correspond to "particle-hole reducible" diagrams.

In the present study we have only kept the dominant, local parts of the interactions. These are the same in the "A" and the "B" channel, they are shown in Fig. 1. Their features show the qualitative effects discussed by Aldrich and Pines [10], namely

- Short-ranged screening. This is just the purpose of using correlated wave functions.
- A repulsive core or barrier that is somewhat larger than the repulsive core of the bare potential. This enhanced core repulsion is due to the fact that the wave function has to go to zero at the hard core. The "curvature" of the wave function leads to increased repulsion.
- An attractive part that is slightly stronger than the attraction of the bare potential. This is due to the fact that the effective potential, being a pure pair quantity, must effectively simulate the presence of the other particles.
- The "exchange" interaction $V_{\mathrm{X}}(r)$ shows a slight over-screening. This is due to "single-phonon exchanges" which are present in the exchange interaction but not in the direct interaction.

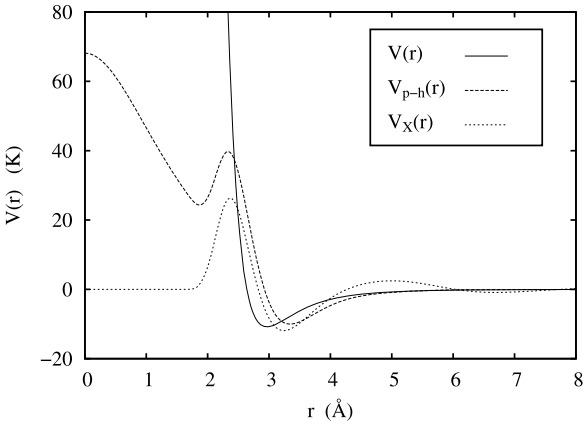

Fig. 1 The figure shows a comparison between the bare Aziz potential [11] (*solid line*), the local "direct" particle hole interaction (*long-dashed line*) and the local exchange interaction (*short-dashed line*)

In the simplest possible approximation, one also neglects exchange effects. In that case, one can indeed identify $V^{\mathrm{A}}_{\mathrm{p-h}} \equiv V^{\mathrm{B}}_{\mathrm{p-h}} \equiv V_{\mathrm{p-h}}$ with a local "particle–hole interaction" in the sense of the RPA. One can then derive a density-density response function in the usual RPA form

$$\chi^{(\mathrm{RPA})}(q,\omega) = \frac{\chi_0(q,\omega)}{1 - V_{\mathrm{p-h}}(q)\chi_0(q,\omega)}, \tag{8}$$

where $\chi_0(q,\omega)$ is the Lindhard function. However, even if exchange terms are omitted, but the effective interactions are different in the "A" and the "B" channels, such a form can not be justified.

3 Results

We have applied the theory formulated above to bulk ^{3}He at saturated vapor pressure and zero temperature. The results are compared with the experiments of Glyde et al. [12] and Fåk et al. [13]. As pointed out in an accompanying paper [9], *pair* excitations also play a crucial role in the dynamics, the present results are therefore meant to illustrate the importance of exchange effects. In Fig. 2 we compare the result of our theory with the RPA and the experiment for different wave-numbers. For collective modes, which correspond to δ-functions, the result of the theoretical calculations have been artificially broadened. We here define "RPA" as follows: *Assume* a density–density response function of the form (8). Then *define* the particle–hole interaction $V_{\mathrm{p-h}}(q)$ through the m_0 sum rule

$$S(q) = -\int_0^\infty \frac{d(\hbar\omega)}{\pi}\, \Im m\chi^{(\mathrm{RPA})}(q,\omega). \tag{9}$$

We start with low values $q = 0.4$ Å^{-1} and $q = 0.6$ Å^{-1}. At these small wave numbers, multipair excitations are expected to be negligible [3, 14]; and a theory based on one-particle-one-hole excitations should be adequate. Indeed, the theoretically predicted energy of the collective mode agrees quite well with the experimental

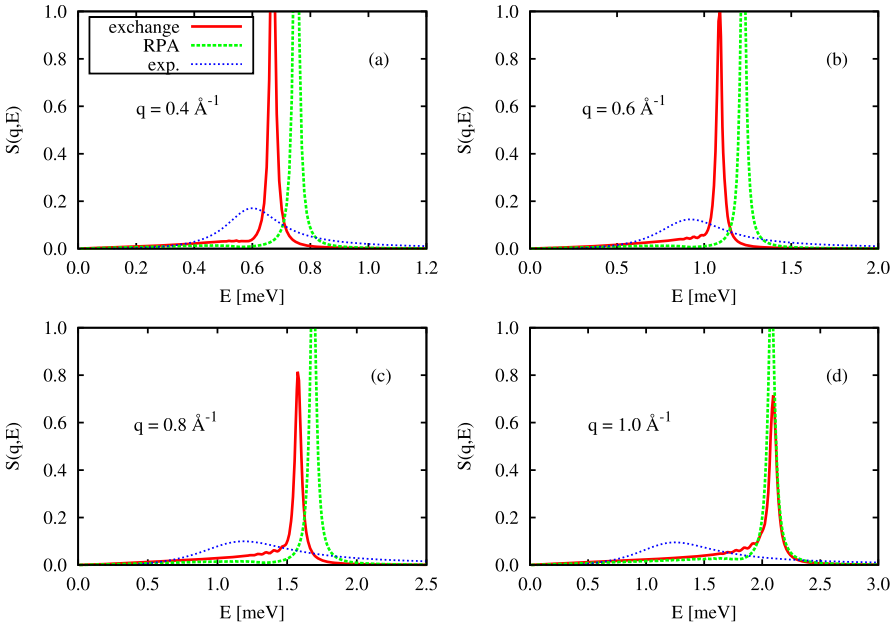

Fig. 2 (Color online) Comparison of our theory (*red, solid line*) with RPA (*green, dashed*) and experiment (*blue, short dashed*) at wave-numbers q =0.4, 0.6, 0.8 and 1.0 Å^{-1}. The experimental data are from Glyde et al. [12] (plots (**a**)–(**c**)) and Fåk et al. [13] (plot (**d**))

one, whereas the RPA predicts the collective mode at a significantly higher energy. This effect is expected: At long wave lengths, the collective mode is basically determined by the speed of sound, and exchange contributions are for the speed of sound just as important as for the ground state energetics.

At higher momentum transfers $q = 0.8$ A^{-1} and $q = 1.0$ Å^{-1} the agreement between theory and experiment is expectedly less satisfactory. When the wave length of the excitation becomes comparable to the interparticle distance, multi-particle fluctuations that describe fluctuations on this scale become important. This is well known from ^{4}He [3] and there is no reason that the effect should not be similarly important in ^{3}He. In fact, an accompanying paper [9] demonstrates precisely this fact. Another reason for the discrepancy is the naïve assumption of a static CBF spectrum. This spectrum could be fitted by introducing an effective mass $m^* = 0.87m$ whereas specific heat measurements suggest an effective mass of approximately $m^* \approx 3m$. The discrepancy has been reconciled by more realistic calculations of the ^{3}He self energy [15]. To include such effects one must, however, also include dynamic exchange effects which will be the topic of future work.

We have seen in this work that exchange effects are indeed quite visible in the dynamics of ^{3}He. In particular, they lead to a lowering of the collective mode at low momentum transfers, which is often attributed to a downward shift of the single-particle spectrum by self-energy corrections. While we have in this work not included self-energy corrections of the kind discussed in Ref. [15], we do, at this point, of

course *not* claim that these corrections are negligible. Work in this direction is in progress.

Acknowledgements This work was supported, in part, by the Austrian Science Fund FWF under project P21264 and the "Amadeus" program under Project 17306PG. We thank H. Godfrin for useful discussions.

References

1. C.H. Aldrich III, D. Pines, J. Low Temp. Phys. **31**(5/6), 689 (1978)
2. E. Krotscheck, Phys. Rev. A **26**, 3536 (1982)
3. H.W. Jackson, Phys. Rev. A **8**, 1529 (1973)
4. D.J. Thouless, *The Quantum Mechanics of Many-Body Systems*, 2nd edn. (Academic Press, New York, 1972)
5. J.M.C. Chen, J.W. Clark, D.G. Sandler, Z. Phys. A **305**, 223 (1982)
6. N.H. Kwong, Realistic calculations of excitations in nuclear matter. Ph.D. thesis, California Institute of Technology (1982)
7. H.M. Böhm, R. Holler, E. Krotscheck, M. Panholzer, Int. J. Mod. Phys. B **22**, 4655 (2008)
8. A.K. Kerman, S.E. Koonin, Ann. Phys. (NY) **100**, 332 (1976)
9. H.M. Böhm, E. Krotscheck, M. Panholzer, H. Godfrin, H.J. Lauter, M. Meschke, Two-dimensional ^{3}He: A crucial system for understanding fermion dynamics (2009). These proceedings
10. C.H. Aldrich, D. Pines, J. Low Temp. Phys. **25**, 677 (1976)
11. R.A. Aziz, F.R.W. McCourt, C.C.K. Wong, Mol. Phys. **61**, 1487 (1987)
12. H.R. Glyde, B. Fåk, N.H. van Dijk, H. Godfrin, K. Guckelsberger, R. Scherm, Phys. Rev. B **61**, 1421 (2000)
13. B. Fåk, K. Guckelsberger, R. Scherm, A. Stunault, J. Low Temp. Phys. **97**, 445 (1994)
14. D. Pines, P. Nozieres, *The Theory of Quantum Liquids*, vol. I (Benjamin, New York, 1966)
15. B.L. Friman, E. Krotscheck, Phys. Rev. Lett. **49**, 1705 (1982)